

Monoamine oxidase inhibition properties of quinolinone analogues

L Meiring
21069565

Thesis submitted for the degree *Doctor Philosophiae* in
Pharmaceutical Chemistry at the Potchefstroom Campus of the
North-West University

Promoter: Prof A Petzer
Co-Promoter: Prof JP Petzer
Co-Promoter: Dr LJ Legoabe

Nov 2016

It all starts here™



This work is based on the research supported by the National Research Foundation of South Africa (Grant specific unique reference numbers (UID) 85642 and 80647). The Grantholders acknowledge that opinions, findings and conclusions or recommendations expressed in any publication generated by the NRF supported research are that of the authors, and that the NRF accepts no liability whatsoever in this regard.

PREFACE

This thesis is submitted in article format and consists of four research articles. One of the articles was submitted to the academic journal, *Mini-Reviews in Medicinal Chemistry*, while a second was submitted to *Drug Research*. The article and author guidelines for these two articles are also included. All scientific research for this thesis was conducted by L. Meiring at the North-West University, Potchefstroom campus. Letters of agreement from the co-authors of the research articles and the publishing agreements from the editors of the stated journals are included.

I would like to take this opportunity to thank the North-West University, especially the School of Pharmacy, for the financial support and for granting me the enormous opportunity to pursue doctoral studies. I would like to thank the following people for supporting and assisting me throughout the completion of this study:

- André Joubert, for the numerous NMR and MS spectra.
- The NRF (National Research Foundation of South Africa) for their financial support.
- My promoter, A. Petzer, and co-promoters, J.P. Petzer and L.J. Legoabe for all the guidance, knowledge, patience, advice and inputs during the whole study period.
- My family and parents for their motivation and support.
- Finally, my husband for the love and support, especially during the hardships.

DECLARATION

This thesis is submitted in fulfillment of the requirements for the degree of the Philosophiae Doctor in Pharmaceutical Chemistry, at the School of Pharmacy, North-West University.

I, Letitia Meiring hereby declare that the dissertation with the title: **MONOAMINE OXIDASE INHIBITION PROPERTIES OF QUINOLINONE ANALOGUES** is my own work and has not been submitted at any other university either whole or in part.

L. Meiring

LETTER OF AGREEMENT



Privaatsak X6001, Potchefstroom
Suid-Afrika, 2520

Tel: (018) 299-1111/2222

Web: <http://www.nwu.ac.za>

November 2016

To whom it may concern,

Dear Sir/Madam

CO-AUTHORSHIP ON RESEARCH PAPERS

The undersigned as co-authors of the research articles listed below, hereby give permission to L. Meiring to submit these articles as part of the degree PhD in Pharmaceutical Chemistry at the North-West University, Potchefstroom campus.

- A review of the pharmacological properties of 3,4-dihydro-2(1*H*)-quinolinones
- C6- and C7-Substituted 3,4-dihydro-2(1*H*)-quinolinones as inhibitors of monoamine oxidase.
- The evaluation of 2-phenoxyethoxy-substituted tetralones as inhibitors of monoamine oxidase
- The evaluation of N-propargylamine-2-aminotetralin as an irreversible inhibitor of monoamine oxidase

Yours sincerely,

Prof. A. Petzer

Prof. J.P. Petzer

Dr. L.J. Legoabe

TABLE OF CONTENTS

ABSTRACT	ix
UITTREKSEL	xi
LIST OF TABLES, FIGURES AND SCHEMES	xiii
LIST OF ABBREVIATIONS	xxi
CHAPTER 1 – Introduction	
1.1 Background	1
1.2 Rationale	3
1.3 Hypotheses of this study	8
1.4 Aim and objectives of this study	9
1.5 References	10
CHAPTER 2 - Literature Background	
2.1 Monoamine oxidase	16
2.1.1 General background	16
2.1.2 The therapeutic applications of MAO-A and MAO-B	17
2.1.3 Adverse effects of MAO-A and MAO-B	20
2.1.4 Catalytic mechanism of MAO-A and MAO-B	21
2.1.5 The three dimensional structure of MAO	24
2.1.6 Inhibitors of MAO	27
2.1.7 Conclusion	31
2.2 References	32
CHAPTER 3 – Manuscript A	
A REVIEW OF THE PHARMACOLOGICAL PROPERTIES OF 3,4-DIHYDRO-2(1<i>H</i>)- QUINOLINONES	
Abstract	41
1. Introduction	42
2. Chemistry of 3,4-dihydro-2(1 <i>H</i>)-quinolinone	43
3. The pharmacology of 3,4-dihydro-2(1 <i>H</i>)-quinolinones	44
Phosphodiesterase inhibition	44
Blocking of β -adrenergic receptors	45

Interaction with serotonin and dopamine receptors	45
Antagonism of vasopressin receptors	47
Sigma receptor antagonism and agonism	48
Muscarinic acetylcholine receptor agonism	49
N-Methyl-D-aspartate (NMDA) antagonism	49
Monoamine oxidase inhibition	50
Oxytocin receptor antagonism	51
Anticonvulsant activities	51
3,4-Dihydro-2(1 <i>H</i>)-quinolinones as contraceptives	52
Positive inotropic action	53
4. Natural products containing 3,4-dihydro-2(1 <i>H</i>)-quinolinones	54
5. Metabolism of 3,4-dihydro-2(1 <i>H</i>)-quinolinones	54
6. Conclusion	57
References	59

CHAPTER 4 – Manuscript B

C6- AND C7-SUBSTITUTED 3,4-DIHYDRO-2(1*H*)-QUINOLINONES AS INHIBITORS OF MONOAMINE OXIDASE

Abstract	66
Introduction	67
Materials and methods	70
Chemicals and instrumentation	70
Chemistry	71
Enzymology	77
Computer modelling	79
Results and Discussion	80
Chemistry	80
IC ₅₀ values and SARs for MAO inhibition	81
Reversibility of MAO-B inhibition	85
Lineweaver-Burk plots and competitive inhibition	86
Docking studies	87
Conclusion	90
References	92
Supplementary Material	96

CHAPTER 5 – Manuscript C

THE EVALUATION OF 2-PHENOXYETHOXY-SUBSTITUTED TETRALONES AS INHIBITORS OF MONOAMINE OXIDASE

Abstract	112
Acknowledgements	128
Conflict of Interest	128
References	129
Supplementary Material	133
1. Materials and methods	133
2. Synthesis of 7-(2-phenoxyethoxy)-3,4-dihydronaphthalen-2(1 <i>H</i>)-one (17)	134
3. Synthesis of compounds 18 and 19	135
4. Measurement of IC ₅₀ values for the inhibition of MAO	136
5. Investigation of reversibility of inhibition by dialysis	137
6. Construction of Lineweaver-Burk plots	139
7. Protocol for docking with CDOCKER	139
8. References	141

CHAPTER 6 – Manuscript D

THE EVALUATION OF N-PROPARGYLAMINE-2-AMINOTETRALIN AS AN IRREVERSIBLE INHIBITOR OF MONOAMINE OXIDASE

Abstract	147
Acknowledgements	163
Conflict of Interest	163
References	164
Supplementary Material	170
1. Materials and methods	170
2. Synthesis of hydrochloric acid salt of N-propargylamine-2-aminotetralin (2-PAT)	171
3. Procedure of the measurement of IC ₅₀ values	172
4. Recovery of enzyme activity after dialysis	173
5. The construction of Lineweaver-Burk plots and calculation of K _i value	173

6. Procedure for molecular docking and dynamics simulations	174
7. References	175
CHAPTER 7 – Conclusion	178
ADDENDUM A - Author guidelines:	187
<u>Mini-Reviews in Medicinal Chemistry</u>	
ADDENDUM B - Author guidelines:	192
<u>Drug Research</u>	

ABSTRACT

Parkinson's disease (PD) is an age-related neurodegenerative disorder characterised by selective loss of dopaminergic neurons in the substantia nigra pars compacta (SNpc) of the brain. This leads to the loss of dopamine from the striatum, which is responsible for the motor symptoms of PD. Monoamine oxidase (MAO) plays an important role in the neurodegenerative processes and therapy of PD since dopamine is oxidised by MAO in the basal ganglia. Inhibitors, of the MAO-B isoform conserve the depleted supply of dopamine and are thus used in the therapy of PD. MAO-B inhibitors may also enhance the therapeutic efficacy of L-dopa, the metabolic precursor of dopamine, by enhancing dopamine levels derived from administered L-dopa.

In this study, three chemical classes were synthesised and evaluated as potential recombinant human MAO-A and MAO-B inhibitors. These include (1) C6- and C7-substituted 3,4-dihydro-2(1*H*)-quinolinones, (2) 2-phenoxyethoxy-substituted tetralones and (3) N-propargylamine-2-aminotetralin (2-PAT). The quinolinone and tetralone derivatives are structurally related to chemical classes that have been reported to inhibit the MAO enzymes, including α -tetralone, 1-indanone and 3-coumaranone derivatives. 2-PAT is structurally similar to rasagiline, an irreversible MAO-B inhibitor currently used in clinic.

C6- and C7-substituted 3,4-dihydro-2(1*H*)-quinolinone and 2-phenoxyethoxy tetralone derivatives were synthesised by reacting 6- or 7-hydroxy-3,4-dihydro-2(1*H*)-quinolinone and 6- or 7-hydroxytetralone, respectively, with an appropriately substituted alkyl bromide in the presence of base. 2-PAT was synthesised in low yield by dehydrating β -tetralone and propargylamine (commercially available) in the presence of sodium cyanoborohydride (NaCNBH₄).

To evaluate the MAO inhibitory properties (IC₅₀ values) of the synthesised derivatives the recombinant human MAO-A and MAO-B enzymes were used. The reversibility of inhibition of selected derivatives was examined by employing dialysis, while the mode of MAO inhibition was determined by constructing Lineweaver-Burk plots.

To determine possible binding modes and key interactions of selected inhibitors with the MAO enzymes, the inhibitors were docked into the MAO active sites.

The results document that the 3,4-dihydro-2(1*H*)-quinolinone derivatives are highly potent and selective MAO-B inhibitors with the most potent inhibitor displaying an IC_{50} value of 0.0014 μ M. Based on dialysis experiments it was concluded that a selected quinolinone derivative is a reversible MAO-B inhibitor. The Lineweaver-Burk plots constructed for the inhibition of MAO-B by the selected quinolinone derivative were linear and intersected on the y-axis. These data indicated that this compound is a competitive MAO-B inhibitor with a K_i value of 2.8 nM.

The results further document that 7-(2-phenoxyethoxy)-3,4-dihydronaphthalen-2(1*H*)-one from the second series is a highly potent MAO-B inhibitor with an IC_{50} value of 0.033 μ M. Based on dialysis experiments it was concluded that this β -tetralone derivative is a reversible and competitive MAO-B inhibitor. An analysis of the Lineweaver-Burk plots indicated that this compound inhibit MAO-B with a K_i value of 0.128 μ M. This is the first report of the MAO inhibition properties of a β -tetralone.

Finally, 2-PAT was found to be a reversible MAO-A ($IC_{50} = 0.721\mu$ M) inhibitor, while acting as an inactivator of MAO-B ($IC_{50} = 14.6 \mu$ M). 2-PAT is also approximately fivefold more potent than toloxatone ($IC_{50} = 3.92 \mu$ M), a clinically used antidepressant and reversible MAO-A inhibitor.

It may thus be concluded that the synthesised compounds are promising potent MAO-B inhibitors, and thus leads for the design of therapeutic agents for PD.

UITTREKSEL

Parkinson se siekte (PS) is 'n ouderdomsverwante neurodegeneratiewe siekte wat deur die degenerasie van die neurone van die substantia nigra in die brein en die verlies van dopamien in die striatum gekenmerk word. Die gevolglike tekort aan dopamien in die striatum is verantwoordelik vir die simptome van PS. Die ensiem, monoamienoksidase (MAO), speel moontlik 'n rol in die neurodegeneratiewe prosesse van PS aangesien dopamien deur MAO geoksideer word. MAO-inhibeerders blokkeer die katabolisme van dopamien en word dus gebruik om die siekteverloop van PS te vertraag. MAO-inhibeerders kan ook in kombinasie met L-dopa gebruik word en verbeter so die terapeutiese effek van L-dopa.

In hierdie studie is drie reekse verbindings gesintetiseer en geëvalueer as inhibeerders van rekombinante menslike MAO-A en MAO-B. Hierdie reekse sluit die volgende in (1) C6- en C7-gesubstitueerde 3,4-dihidro-2(1*H*)-kinolinoonderivate, (2) 2-fenoksie-etoksie-gesubstitueerde tetraloon derivate en (3) N-propargielamien-2-aminotetralien (2-PAT). Hierdie kinolinoon- en tetraloonderivate is struktureel verwant aan verbindings wat in vorige studies as potente MAO-inhibeerders geïdentifiseer is, insluitend α -tetraloon-, 1-indanoon- en 3-kumarienoonderivate. 2-PAT is struktureel verwant aan rasagilien, 'n onomkeerbare MAO-B-inhibeerder wat tans klinies gebruik word.

C6- en C7-gesubstitueerde 3,4-dihidro-2(1*H*)-kinolinoon- en 2-fenoksie-etoksie-gesubstitueerde tetraloonderivate is gesintetiseer deur 6- of 7-hidroksie-3,4-dihidro-2(1*H*)-kinolinoon en 6- of 7-hidroksietetraloon, onderskeidelik, met 'n toepaslike alkielbromied in die teenwoordigheid van 'n basis te laat reageer. 2-PAT is met 'n lae opbrengs gesintetiseer deur β -tetraloon en propargielamien in die teenwoordigheid van natriumsianoborohidried (NaCNBH_4) te dehidreer. Die produk is met HCl aangesuur, gewas met diëtleter en met dichloormetaan geëkstraheer, om die soutsuursout van 2-PAT te lewer.

Rekombinante menslike MAO-A en MAO-B is gebruik om die MAO-inhibisie eienskappe (IC_{50} -waardes) van die derivate te evalueer. Die omkeerbaarheid van inhibisie van 'n geselekteerde derivaat is deur dialise geëvalueer, terwyl die meganisme van inhibisie ondersoek is deur Lineweaver-Burk-grafieke op te stel.

Moontlike bindingsoriëntasies en interaksies van geselekteerde inhibeerders met die MAO-ensiem is geëvalueer deur die inhibeerders in die MAO aktiewe setel te pas.

Die resultate toon dat die 3,4-dihidro-2(1*H*)-kinolinoonderivate hoogs potente en selektiewe MAO-B-inhibeerders is. Die mees potente MAO-B-inhibeerder het 'n IC_{50} -waarde van 0.0014 μ M getoon. Op grond van dialise-eksperimente en Lineweaver-Burk-grafieke is tot die gevolgtrekking gekom dat 'n geselekteerde derivaat as 'n omkeerbare MAO-B-inhibeerder optree. Die resultate toon ook dat die Lineweaver-Burk-grafieke op een punt op die y-as sny. Dit dui daarop dat die spesifieke kinoloon derivaat 'n kompeterende inhibeerder van MAO-B is. Verdere analise van die Lineweaver-Burk-grafieke dui daarop dat MAO-B met 'n K_i -waarde van 2.8 nM inhibeer word.

Die resultate toon verder dat 7-(2-fenoksi-etoksie)-3,4-dihidro-2(1*H*)-naftalenoen, 'n verbinding uit die tweede reeks, 'n hoogs potente MAO-B-inhibeerder is, met 'n IC_{50} -waarde van 0.033 μ M. Op grond van dialise eksperimente en Lineweaver-Burk-grafieke is tot die gevolgtrekking gekom dat hierdie verbinding 'n kompeterende en omkeerbare MAO-B-inhibeerder is. Verdere analise van die Lineweaver-Burk-grafieke dui daarop dat MAO-B met 'n K_i -waarde van 0.128 μ M inhibeer word. Hierdie is die eerste berig van die MAO-inhiberende eienskappe van β -tetraloon derivate.

Laastens is gevind dat 2-PAT 'n omkeerbare MAO-A-inhibeerder ($IC_{50} = 0.721 \mu$ M) is, maar optree as 'n inaktiveerder van MAO-B ($IC_{50} = 14.6 \mu$ M). 2-PAT is ongeveer 2750-voudig meer potent as toloksatoon ($IC_{50} = 3.92 \mu$ M), 'n omkeerbare MAO-A inhibeerder wat tans gebruik word.

Uit hierdie studie kan afgelei word dat die gesintetiseerde verbindings belowende, hoogs potente MAO-B-inhibeerders is, wat as moontlike geneesmiddelkandidate vir die behandeling van PS kan dien.

LIST OF FIGURES, SCHEMES AND TABLES

Chapter 1

Figure 1.1	The structure of dopamine.	1
Figure 1.2	The structures of α -tetralone (3 and 4), 1-indanone (5 and 6), 3-coumaranone (7) and 3,4-dihydro-2(1 <i>H</i>)-quinolinone derivatives (8 and 9) (R = alkyl/arylalkyl substituent).	5
Figure 1.3	The structure of β -tetralone.	5
Figure 1.4	The structures of 6-(2-phenoxyethoxy)-3,4-dihydronaphthalen-1(2 <i>H</i>)-one (10), 7-(2-phenoxyethoxy)-3,4-dihydronaphthalen-1(2 <i>H</i>)-one (11) and 7-(2-phenoxyethoxy)-3,4-dihydronaphthalen-2(1 <i>H</i>)-one (12).	6
Figure 1.5	The structures of 8-(2)-phenoxyethoxycaffeine derivatives (R = H, Cl, Br, F, CF ₃ , CH ₃ , OCH ₃ , I, CN, NO ₂) that have been shown to inhibit MAO.	7
Figure 1.6	The structures of the irreversible MAO-B inhibitors, selegiline and rasagiline.	7
Figure 1.7	The structures of N-propargylamine-2-aminotetralin (2-PAT) and N-methyl-N-propargylamine-2-aminotetralin (2-MPAT).	8
Table 1	The structures of the C6- and C7-substituted quinolinones (1a–g and 2a–g) that will be synthesised in this study.	4

Chapter 2

Figure 2.1	The structures of isoniazid (left) and iproniazid (right), respectively.	16
Figure 2.2	The structures of clorgyline (left) and selegiline (right), respectively.	17
Figure 2.3	The reaction pathway of monoamine metabolism by MAO.	18
Figure 2.4	The mechanism of neurotoxicity by hydrogen peroxide (H ₂ O ₂), induced by the Fenton reaction.	19
Figure 2.5	The mechanism of the 'cheese reaction'.	20
Figure 2.6	The structure of serotonin.	21
Figure 2.7	Single electron transfer (SET) mechanism of MAO catalysis.	22

Figure 2.8	Polar nucleophilic mechanism of MAO catalysis. The products of amine oxidation are the protonated imine and the flavin hydroquinone.	23
Figure 2.9	The hydride transfer mechanism of MAO catalysis.	23
Figure 2.10	The three dimensional structure of human MAO-B. The ball and stick model in yellow represents the covalent flavin moiety. The blue represents the flavin binding domain. The red is the substrate domain. The green represents the membrane binding domain.	24
Figure 2.11	The partial structure of the FAD cofactor.	24
Figure 2.12	The two suggested conformations of C-terminal anchoring of MAO-B within the mitochondrial outer membrane. The first panel shows the C-terminal protruding on the same side of the enzyme and the second panel shows the C-terminal exiting the membrane on the other side.	25
Figure 2.13	The three dimensional structure of human MAO-A. The colouring is similar to those in figure 2.10.	26
Figure 2.14	The structures of phenelzine, pargyline, moclobemide and lazabemide.	27
Figure 2.15	The structures of reversible MAO-B inhibitors, 1,4-diphenyl-2-butene, trans,trans-farnesol, 8-(3-chlorostyryl)caffeine and safinamide.	28
Figure 2.16	The structures of irreversible MAO-B inhibitors, selegiline, rasagiline and PF-9601 N.	29
Figure 2.17	The structures of reversible MAO-A inhibitors, brofaromine, toloxatone, cimoxatone and befloxatone.	30
Figure 2.18	The structures of isocarboxazide and tranylcypromine.	31

Chapter 3

Figure 1	The structure of 3,4-dihydro-2(1 <i>H</i>)-quinolinone (1).	34
Figure 2	Two perspectives of a low energy conformer of 3,4-dihydro-2(1 <i>H</i>)-quinolinone (1), calculated by the MMFF94 force field.	34
Figure 3	The structure of cilostazol (2) and 3.	44
Figure 4	The structure of carteolol (4).	45

Figure 5	The structures of aripiprazole (5), OPC-14523(6) and compounds 7–9.	47
Figure 6	The structure of OPC-21268 (10).	48
Figure 7	The structure of compound 11.	48
Figure 8	The structure of 77-LH-28-1 (12).	49
Figure 9	The structures of compound 13 and L-698,544 (14).	50
Figure 10	The structure of compound 15.	51
Figure 11	The structure of compound 16.	51
Figure 12	The structure of compound 17.	52
Figure 13	The structure of 84-182 (18).	52
Figure 14	The structures of Y-20487 (19) and OPC-8212 (20).	53
Figure 15	The structures of compounds 21–24.	54
Figure 16	The metabolism of carteolol.	55
Figure 17	The metabolism of cilostazol.	56
Figure 18	The metabolism of aripiprazole to its major metabolite, dehydroaripiprazole (OPC-14857).	56
Figure 19	The metabolism of vesnarinone to its major metabolite, OPC-18692.	57

Chapter 4

Figure 1	The structures of 7-(3-bromobenzyloxy)-3,4-dihydro-2(1 <i>H</i>)-quinolinone (1a) and 7-(3-chlorobenzyloxy)-3,4-dihydro-2(1 <i>H</i>)-quinolinone (1b).	70
Figure 2	The synthesis of 3,4-dihydro-2(1 <i>H</i>)-quinolinone derivatives 2a–g and 3a–g. Reagents and conditions: (i) KOH, ethanol, reflux; (ii) recrystallization from ethanol.	81
Figure 3	Sigmoidal dose–response curves for the inhibition of human MAO-B by 2d.	82

Figure 4	Compound 2b inhibits MAO-B with a reversible mode. MAO-B and 2b (at $4 \times IC_{50}$) was preincubated for 15 min, dialyzed for 24 h and the residual enzyme activity was measured (2b dialyzed). Similar incubation and dialysis of MAO-B in the absence inhibitor (NI dialyzed) and presence of the irreversible inhibitor, (R)-deprenyl (depr dialyzed), were also carried out. The residual activity of undialyzed mixtures of MAO-B with 2b was also recorded (2b undialyzed).	86
Figure 5	Lineweaver-Burk plots for the inhibition of MAO-B by 2b . The inset is a graph of the slopes of the Lineweaver-Burk plots versus inhibitor concentration.	87
Figure 6	The proposed binding modes of 2c and 3c to MAO-B.	89
Figure 7	The proposed binding modes of 2c and 3c to MAO-A.	90
Table 1	The IC_{50} values for the inhibition of recombinant human MAO-A and MAO-B by compounds 2a-g and 3a-g .	83

Chapter 5

Figure 1	The structures of α -tetralone and β -tetralone.	117
Figure 2	Synthetic pathway to C6- or C7-substituted ethers of α -tetralone and β -tetralone. Reagents and conditions: (i) $AlCl_3$, toluene; reflux; (ii) acetone, K_2CO_3 , reflux.	118
Figure 3	The structures of tetralone derivatives 17-19 .	118
Figure 4	The sigmoidal dose-response curves for the inhibition of MAO-B by 17 . Data were measured in triplicate and data points are given as mean \pm standard deviation (SD).	120

Figure 5	Compounds 17–19 inhibit MAO-B reversibly. MAO-B and the test inhibitors (at $4 \times IC_{50}$) were preincubated for 15 min, dialysed for 24 h and the residual enzyme activity was measured (17–19 dialysed). Similar incubation and dialysis of MAO-B in the absence inhibitor (NI dialysed) and presence of the irreversible inhibitor, (R)-deprenyl (depr dialysed), were also carried out. The residual activities of undialysed mixtures of MAO-B with the test inhibitors were also recorded (17–19 undialysed).	123
Figure 6	Lineweaver-Burk plots for the inhibition of MAO-B by 17 . The inset is a graph of the slopes of the Lineweaver-Burk plots versus inhibitor concentration.	124
Figure 7	The docked binding orientations of 17–19 in MAO-B. Key: 17 (light green); 18 (dark green); 19 (magenta).	125
Figure 8	The structure of 7-(3-chlorobenzyloxy)-4-formylcoumarin (22).	125
Figure 9	The docked binding orientations of 17–19 in MAO-A. Key: 17 (light green); 18 (dark green); 19 (magenta).	127
Table 1	The reported IC_{50} values for the inhibition of recombinant human MAO-A and MAO-B by α -tetralone (1 and 2), 1-indanone (3 and 4), 3-coumaranone (5) and 3,4-dihydro-2(1 <i>H</i>)-quinolinone (6 and 7) derivatives (R = alkyl/arylalkyl substituent).	115
Table 2	The reported IC_{50} values for the inhibition of recombinant human MAO-A and MAO-B by hydroxy-substituted α -tetralones, 1-indanones, 3-coumaranone and 3,4-dihydro-2(1 <i>H</i>)-quinolinones.	116
Table 3	The measured IC_{50} values for the inhibition of recombinant human MAO-A and MAO-B by tetralone derivatives 17–19 as well as by 7-methoxy-2-tetralone (15) and 7-hydroxy-2-tetralone (16).	120

Chapter 6

Figure 1	The structures of the irreversible MAO-B inhibitors, selegiline and rasagiline.	149
Figure 2	The structures of the irreversible MAO inhibitors, phenelzine, isocarboxazid, tranylcyproamine and iproniazid.	150
Figure 3	Functional groups responsible for mechanism-based inhibition of the MAOs: propargylamine, cyclopropylamine, hydrazine, haloallylamine and N-(2-aminoethyl)carboxamide.	152
Figure 4	The structures of N-propargylamine-2-aminotetralin (2-PAT) and N-methyl-N-propargylamine-2-aminotetralin (2-MPAT).	152
Figure 5	The sigmoidal dose-response curves for the inhibition of MAO-A and MAO-B by 2-PAT. Rates were measured in triplicate and are shown as mean \pm standard deviation (SD).	155
Figure 6	2-PAT is a reversible MAO-A inhibitor and an irreversible MAO-B inhibitor. The MAO enzymes and 2-PAT (at a concentration of $4 \times IC_{50}$) were incubated for 15 min, dialysed for 24 h and the residual enzyme activity was measured (2-PAT dialysed). Similar incubation and dialysis of the MAOs in the absence (NI dialysed) and presence of the irreversible inhibitors, pargyline (parg dialysed) and selegiline (seleg dialysed) were also carried out. The residual MAO activity of undialysed mixtures of the MAOs with 2-PAT was also recorded (2-PAT undialysed).	157
Figure 7	Lineweaver-Burk plots for the inhibition of human MAO-A by 2-PAT. The inset is a graph of the slopes of the Lineweaver-Burk plots versus inhibitor concentration.	158
Figure 8	The proposed reversible interactions between 2-PAT and the MAOs.	159
Figure 9	The proposed reversible interactions of rasagiline and its S-enantiomer with the MAOs.	161
Table 1	The reported IC_{50} values for the inhibition of rat brain MAO-A and MAO-B by 2-MPAT.	152
Table 2	The IC_{50} values for the inhibition of recombinant human MAO-A and MAO-B by 2-PAT and reference inhibitors.	155

Scheme 1	Synthetic pathway to 2-PAT. Reagents and conditions:	
	(i) p-toluenesulfonic acid, benzene, Dean-Stark trap;	
	(ii) (ii) NaCNBH ₄ , methanol, N ₂ , rt; (iii) 10% HCl.	154

Chapter 7

Figure 7.1	The structures of 6-(2-phenoxyethoxy)-3,4-dihydronaphthalen-1(2 <i>H</i>)-one (10), 7-(2-phenoxyethoxy)-3,4-dihydronaphthalen-1(2 <i>H</i>)-one (11) and 7-(2-phenoxyethoxy)-3,4-dihydronaphthalen-2(1 <i>H</i>)-one (12).	180
Figure 7.2	The structures of N-propargylamine-2-aminotetralin (2-PAT) and N-methyl-N-propargylamine-2-aminotetralin (2-MPAT).	180
Figure 7.3	The synthesis of 3,4-dihydro-2(1 <i>H</i>)-quinolinone derivatives 1a–g and 2a–g . Reagents and conditions: (i) KOH, ethanol, reflux; (ii) recrystallisation from ethanol.	181
Figure 7.4	The synthesis of C6- or C7-substituted ethers of β-tetralone. Reagents and conditions: (i) AlCl ₃ , toluene; reflux; (ii) acetone, K ₂ CO ₃ , reflux.	181
Figure 7.5	The synthesis of 2-PAT. Reagents and conditions: (i) p-toluenesulfonic acid, benzene, Dean-Stark trap; (ii) (ii) NaCNBH ₄ , methanol, N ₂ , rt; (iii) 10% HCl.	182
Table 7.1	The structures of the C6- and C7-substituted quinolinones (1a–g and 2a–g) that were synthesised in this study.	179

LIST OF ABBREVIATIONS

A

ADH	Aldehyde dehydrogenase
AlCl ₃	Aluminum trichloride
APCI	Atmospheric-pressure chemical ionization
AVP	Arginine vasopressin
AVPR1A	Arginine vasopressin receptor 1A

C

CNS	Central nervous system
CSC	8-(3-Chlorostyryl)caffeine

D

DA	Dopamine
----	----------

F

FAD	Flavin adenine dinucleotide
-----	-----------------------------

G

GPO	Glutathione peroxidase
GSH	Glutathione

H

12-HETE	12(S)-Hydroxyeicosatetraenoic acid
H ₂ O ₂	Hydrogen peroxide
5-HT	Serotonin

I

IC ₅₀	Inhibitor concentration at 50% inhibition
ISA	Intrinsic sympathomimetic activity

M

MAO	Monoamine oxidase
MPTP	1-Methyl-4-phenyl-1,2,3,6-tetrahydropyridine
MPP ⁺	1-Methyl-4-phenylpyridinium
MP	Melting points
2-MPAT	N-Methyl-N-propargylamine-2-aminotetralin

N

NA Noradrenaline

NaCNBH₄ Sodium cyanoborohydride

NMDA N-Methyl-D-aspartate

P

2-PAT N-propargylamine-2-aminotetralin

PD Parkinson's disease

PDE Phosphodiesterase

S

SAR Structure-activity relationships

SerT Serotonin transporter

SNpc Substantia nigra pars compacta

CHAPTER 1

INTRODUCTION

1.1 Background

Parkinson's disease: James Parkinson discovered an unrecognised disorder, Parkinson's disease (PD), in the 1800's. PD is regarded as the second most common neurodegenerative disease and is characterised by the loss of dopaminergic neurons in the substantia nigra pars compacta (SNpc) of the brain (Parkinson, 2002; Dauer & Przedborski, 2003). The clinical manifestations encountered with this disease are mostly motor dysfunctions such as tremors, rigidity, postural instability, slowness or absence of voluntary movement and freezing (Dauer & Przedborski, 2003; Lees, 2005; Prediger *et al.*, 2012; Nagatsu & Sawada, 2006; Henderson *et al.*, 2003; Yazdani *et al.*, 2006). The debilitating movement disorders observed in PD patients is a result of the degeneration of dopaminergic neurons, which leads to depletion of dopamine (DA) in the striatum (Figure 1.1) (Przedborski, 2005). Approximately 1% of the world population is affected by PD today and the incidence of this disease rises steeply with age, with a mean duration of 15 years from diagnoses to death (Lees *et al.*, 2009; Dorsey *et al.*, 2007; Von Campenhausen *et al.*, 2005; Dluzen & McDermott, 2000).

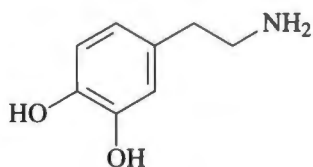


Figure 2.1: The structure of dopamine.

The prevention of degeneration of dopaminergic neurons is the ultimate goal of PD treatment (Dauer & Przedborski, 2003), but at present no such neuroprotective strategies exist (Bové *et al.*, 2005). Treatment of PD is symptomatic and involves mainly DA replacement therapy with agents such as L-dopa and DA agonists, drugs which either replace DA or stimulate DA receptors in the brain (Schapira & Olanow, 2008; Jenner *et al.*, 2009).

Monoamine oxidase: Another treatment option for PD is to inhibit the metabolism of DA in the brain. Monoamine oxidase (MAO) type B is an enzyme that is involved in the catabolism of DA in the brain. MAO-B inhibitors thus conserve the depleted supply of DA in PD and are used as adjuvants to L-dopa therapy (Nagatsu & Sawada, 2006; Youdim *et al.*, 2006; Yamada & Yasuhara, 2004).

MAO consists of two isoenzymes, MAO-A and MAO-B. The MAOs are flavin adenine dinucleotide (FAD) containing enzymes, which are tightly anchored to the mitochondrial outer membrane. DA is oxidised by mainly MAO-B within the basal ganglia. This oxidation is associated with the formation of by-products such as hydrogen peroxide and aldehydes, which may lead to oxidative stress and neurotoxicity if not inactivated by cellular protective systems (Fernandez & Chen, 2007). It has been suggested that the hydrogen peroxide and aldehydes produced by the MAO catalytic cycle may contribute to neurodegeneration in PD. By preventing the formation of these potentially neurotoxic metabolic by-products, MAO-B inhibitors may act as neuroprotective agents (Youdim *et al.*, 2006). This analysis shows that MAO-B inhibitors may be useful as symptomatic and potentially neuroprotective agents for the treatment of PD.

Two types of MAO-B inhibitors are currently available in the clinic for the treatment of PD, irreversible and reversible inhibitors. Irreversible MAO-B inhibitors, which include (R)-deprenyl (also known as selegiline) and rasagiline, are the most often used MAO inhibitors for the treatment of PD (Youdim *et al.*, 2006). These inhibitors contain the propargylamine functional group. Reversible MAO-B inhibitors, such as safinamide which has completed phase III development for the management of PD, are also under consideration as future medications (Borghain *et al.*, 2014; Dézsi & Vécsei, 2014).

While the irreversible MAO-B inhibitors are well tolerated and exhibit good safety profiles, they may have potential disadvantages. For example, a slow enzyme recovery rate after drug withdrawal occurs with the irreversible inhibition of MAO, since *de novo* synthesis of the enzyme is required for activity to recover. The recovery of enzyme activity with reversible inhibitors is almost immediate after drug withdrawal and clearance from the tissues (Riederer *et al.*, 2004; Tipton *et al.*, 2004). This makes reversible MAO inhibitors more desirable than irreversible inhibitors (Binda *et al.*, 2003).

In spite of the risks associated with the use of irreversible inhibitors of the MAOs, they are an important class of therapeutic agents (Yamada & Yasuhara, 2004; Tipton *et al.*, 2004).

Another factor to consider when designing MAO inhibitors are adverse effects that may occur with MAO-A inhibition. Irreversible inhibition of MAO-A is associated with a dangerous elevation in blood pressure, termed the “cheese reaction”. The cheese reaction occurs when MAO-A inhibitors are used in combination with tyramine and other dietary amines usually present in foods (most commonly in cheeses). Dietary amines are normally metabolised by MAO-A in the gut wall and liver, preventing them from entering the systemic circulation. When used in combination with irreversible MAO-A inhibitors, tyramine and other dietary amines are free to enter the systemic circulation where they release noradrenaline (NA) from peripheral adrenergic neurons, leading to a hypertensive response which can be fatal (Youdim & Bakhle, 2006; Youdim *et al.*, 2006; Youdim & Weinstock, 2004; Hasan *et al.*, 1988; Finberg & Tenne, 1982; Chen & Swope, 2005). Reversible MAO-A inhibitors do not cause the cheese reaction because dietary amines can displace the reversible inhibitor from MAO-A and can thus be normally metabolised in the intestine (Haefely *et al.*, 1992).

Based on the observation that MAO-B inhibitors are useful agents for the treatment of PD, the aim of this study is to discover inhibitors of MAO-B. Such compounds may enhance the levels of DA in the brain and therefore provide symptomatic relief for PD patients. MAO-B inhibitors may also represent potential neuroprotective treatment for PD.

1.2 Rationale

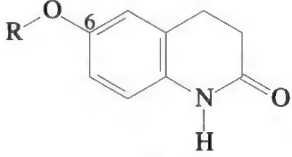
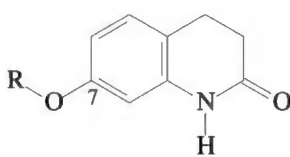
In this study three chemical classes were investigated as potential MAO-B inhibitors. These include (1) C6- and C7-substituted 3,4-dihydro-2(1*H*)-quinolinones, (2) 2-phenoxyethoxy-substituted tetralones and (3) N-propargylamine-2-aminotetralin.

1.2.1 C6- and C7-Substituted 3,4-dihydro-2(1*H*)-quinolinones as inhibitors of monoamine oxidase.

Based on our interest in the discovery of reversible inhibitors with specificity for MAO-B, we have recently reported that, among a series of ten 3,4-dihydro-2(1*H*)-quinolinone derivatives, are high potency MAO-B inhibitors, which possess specificity for the MAO-B isoform (Meiring *et al.*, 2013).

To expand on these results, a series of fourteen 3,4-dihydro-2(1*H*)-quinolinone derivatives will be synthesised (**1a–g** and **2a–g**) and substituted on C6 and C7 with a variety of substituents (Table 1). Substitution with the benzyloxy, phenylethoxy and 2-phenoxyethoxy moieties on both the C6 (compounds **1**) and C7 (compounds **2**) positions will be considered.

Table 1. The structures of the C6- and C7-substituted quinolinones (**1a–g** and **2a–g**) that will be synthesised in this study.

 1a-g		 2a-g	
R		R	
1a	4-ClC ₆ H ₄ CH ₂ -	2a	4-ClC ₆ H ₄ CH ₂ -
1b	4-BrC ₆ H ₄ CH ₂ -	2b	4-BrC ₆ H ₄ CH ₂ -
1c	3-CH ₃ C ₆ H ₄ CH ₂ -	2c	3-CH ₃ C ₆ H ₄ CH ₂ -
1d	4-CH ₃ C ₆ H ₄ CH ₂ -	2d	4-CH ₃ C ₆ H ₄ CH ₂ -
1e	3-CH ₃ C ₆ H ₄ (CH ₂) ₂ -	2e	4-CH ₃ C ₆ H ₄ (CH ₂) ₂ -
1f	4-CH ₃ C ₆ H ₄ (CH ₂) ₂ -	2f	C ₆ H ₅ O(CH ₂) ₂ -
1g	C ₆ H ₅ O(CH ₂) ₂ -	2g	4-ClC ₆ H ₄ O(CH ₂) ₂ -

It is expected that the synthesised compounds will act as reversible MAO-B inhibitors since the previously synthesised series of 3,4-dihydro-2(1*H*)-quinolinone derivatives were reported to interact reversibly with the MAO enzymes (Meiring *et al.*, 2013). As mentioned, with reversible MAO-B inhibitors enzyme activity is recovered as soon as the inhibitor is cleared, which is a major advantage over irreversible inhibitors (Tipton *et al.*, 2004; Binda *et al.*, 2003).

1.2.2 The evaluation of 2-phenoxyethoxy-substituted tetralones as inhibitors of monoamine oxidase.

Tetralones are often used as starting material for the synthesis of heterocyclic compounds, active pharmaceutical ingredients, natural products and their derivatives (Carreño *et al.*, 2006). The tetralone moiety is also frequently encountered in compounds displaying pharmacological activities (Manvar *et al.*, 2015).

Previous studies have shown that α -tetralone (3,4-dihydro-2H-naphthalen-1-one) derivatives are highly potent MAO inhibitors with substitution on both the C6- and C7-positions (**3** and **4**) (Legoabe *et al.*, 2014; Legoabe *et al.*, 2015).

Other chemical classes closely related to α -tetralone, including 1-indanone (**5** and **6**), 3-coumaranone (**7**) and 3,4-dihydro-2(1H)-quinolinone derivatives (**8** and **9**) have also been reported to inhibit the MAOs (Figure 1.2) (Meiring *et al.*, 2013; Mostert *et al.*, 2015; Van Dyk *et al.*, 2015)

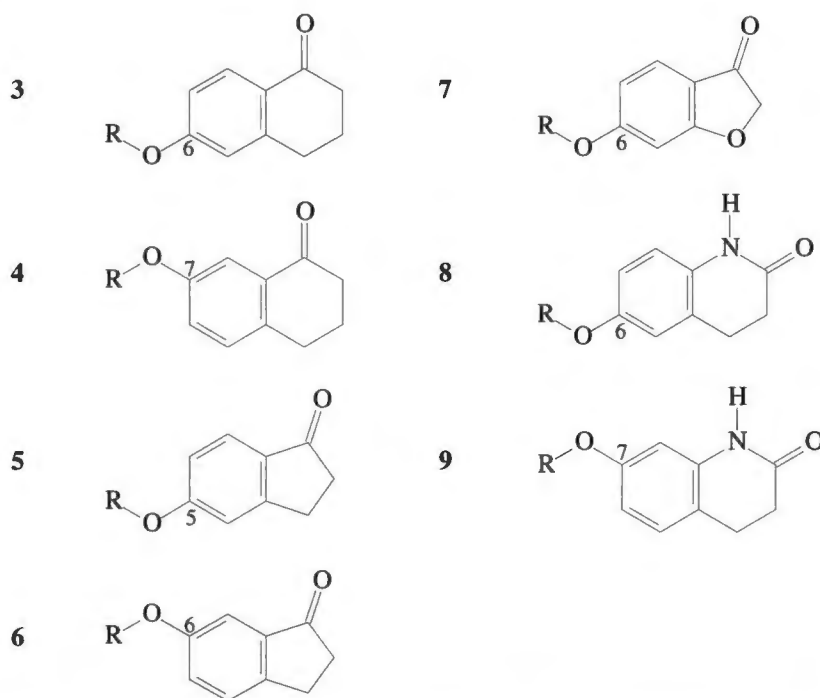


Figure 1.2: The structures of α -tetralone (**3** and **4**), 1-indanone (**5** and **6**), 3-coumaranone (**7**) and 3,4-dihydro-2(1H)-quinolinone derivatives (**8** and **9**) (R = alkyl/arylalkyl substituent).

The present study will investigate the possibility that β -tetralone (3,4-dihydro-1H-naphthalen-2-one), the regioisomer of α -tetralone, may also represent a useful scaffold for the design of MAO inhibitors (Figure 1.3). β -Tetralone is structurally related to α -tetralone, 1-indanone, 3-coumaranone and 3,4-dihydro-2(1H)-quinolinone derivatives (figure 1.2) which, as mentioned above, have been used as scaffolds for MAO inhibitor design.

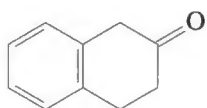


Figure 1.3: The structure of β -tetralone.

For the purpose of this study, three β -tetralone derivatives will be synthesised: 6-(2-phenoxyethoxy)-3,4-dihydronaphthalen-1(2*H*)-one (**10**), 7-(2-phenoxyethoxy)-3,4-dihydronaphthalen-1(2*H*)-one (**11**) and 7-(2-phenoxyethoxy)-3,4-dihydronaphthalen-2(1*H*)-one (**12**) (Figure 1.4).

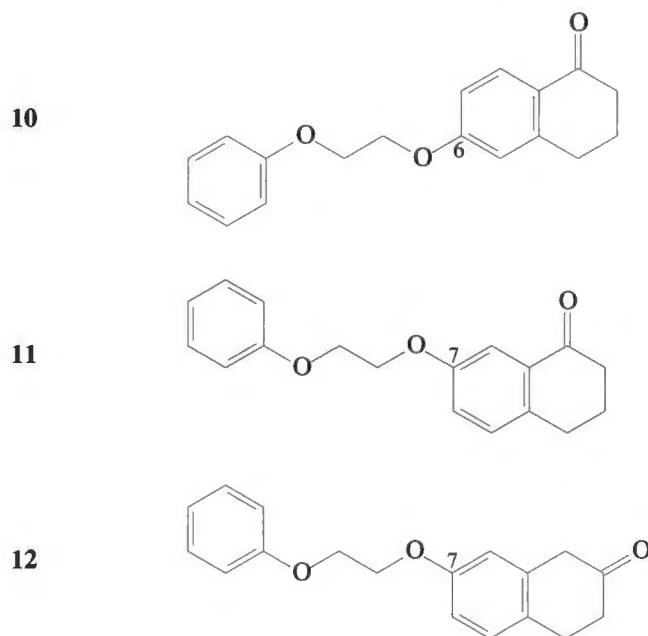


Figure 1.4: The structures of 6-(2-phenoxyethoxy)-3,4-dihydronaphthalen-1(2*H*)-one (**10**), 7-(2-phenoxyethoxy)-3,4 dihydronaphthalen-1(2*H*)-one (**11**) and 7-(2-phenoxyethoxy)-3,4-dihydronaphthalen-2(1*H*)-one (**12**).

It is also expected that these synthesised compounds will act as reversible MAO-B inhibitors since the previously synthesised and closely related α -tetralone derivatives were reported to interact reversibly with the MAO enzymes (Legoabe *et al.*, 2014; Legoabe *et al.*, 2015). As will be shown in this thesis, the selection of the phenoxyethoxy side chain was based, in part, on synthetic feasibility.

The phenoxyethoxy side chain is also found in experimental MAO inhibitors. In particular, a series of 8-(2)-phenoxyethoxycaffeine derivatives (Figure 1.5) have been shown to act as high potency MAO-B inhibitors (Strydom *et al.*, 2012).

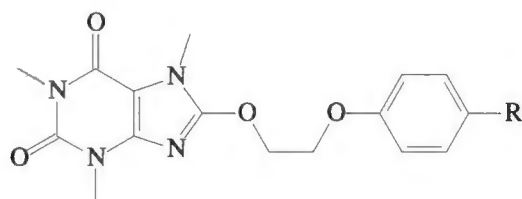


Figure 1.5: The structures of 8-(2)-phenoxyethoxycaffeine derivatives (R = H, Cl, Br, F, CF₃, CH₃, OCH₃, I, CN, NO₂) that have been shown to inhibit MAO.

1.2.3 The evaluation of N-propargylamine-2-aminotetralin as an irreversible inhibitor of monoamine oxidase.

Irreversible inhibitors of the MAOs are an important class of therapeutic agents, in spite of the risks associated with their use. These include the slow recovery of enzyme activity after the inhibitor is withdrawn, and loss of isoform selectivity with repeated administration of the drug (Tipton *et al.*, 2004). Irreversible MAO inhibitors that are currently used in clinic include (R)-deprenyl, rasagiline, tranlycypromine, phenelzine, isocarboxazid, mofegiline and lazabemide (Figure 1.6) (Edmondson *et al.*, 2004a; Edmondson *et al.*, 2004b; Binda *et al.*, 2004; Binda *et al.*, 2005; Milczek *et al.*, 2008). A transdermal delivery system of selegiline [(R)-deprenyl] has also been developed and reported to be effective for the treatment of major depressive disorder (Pae *et al.*, 2014).

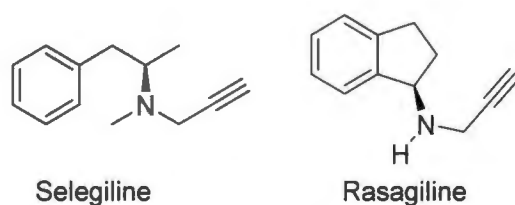


Figure 1.6: The structures of the irreversible MAO-B inhibitors, selegiline and rasagiline.

Motivated by the academic challenge of designing and discovering high potency and isoform-specific MAO inhibitors that may be useful therapeutic agents, the final study of this thesis synthesises a rasagiline related structure, N-propargylamine-2-aminotetralin (2-PAT) (Figure 1.7). 2-PAT is structurally very similar to rasagiline, and also contains the propargylamine functional group. The MAO inhibition properties of 2-PAT may, however, be very different from that of rasagiline. According to literature, N-methylation of rasagiline significantly affects the inactivation kinetics, inhibition potency and isoform selectivity (Hubálek *et al.*, 2004) and the MAOs are much less sensitive to inhibition by the *S*-enantiomer of rasagiline.

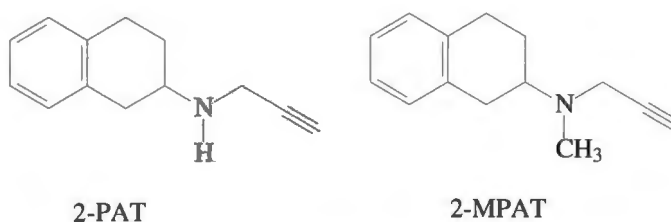


Figure 1.7: The structures of N-propargylamine-2-aminotetralin (2-PAT) and N-methyl-N-propargylamine-2-aminotetralin (2-MPAT).

N-Methyl-N-propargylamine-2-aminotetralin (2-MPAT), the N-methyl analogue of 2-PAT, has previously been studied. *In vitro* studies have shown that 2-MPAT displays potent inhibition of both MAO isoforms (Hazelhoff *et al.*, 1985), however the (+)-enantiomer displayed the highest MAO-B inhibition as well as superior isoform selectivity (for MAO-B over MAO-A) compared to the (-)-enantiomer. The present study will therefore investigate the human MAO inhibition properties of 2-PAT and compare it with those reported for 2-MPAT. As with rasagiline and its N-methyl analogue, the MAO inhibition properties of 2-PAT and 2-MPAT may be very different.

1.3 Hypotheses of this study

Based on literature it is postulated that highly potent and MAO-B specific inhibitors may be designed using 3,4-dihydro-2(1*H*)-quinolinone and β -tetralone as scaffolds. In fact, previous studies have already demonstrated the MAO inhibition potential of the 3,4-dihydro-2(1*H*)-quinolinone and α -tetralone classes of compounds (Meiring *et al.*, 2013; Legoabe *et al.*, 2014; Legoabe *et al.*, 2015).

It is further postulated that 2-PAT will act as an irreversible MAO inhibitor. Although 2-PAT is structurally very similar to rasagiline and the previously studied 2-MPAT, the MAO inhibition properties of 2-PAT may be very different. Based on motivation by the academic challenge of designing and discovering high potency and isoform-specific MAO inhibitors that may be useful therapeutic agents, 2-PAT will thus be synthesised and evaluated as a MAO inhibitor.

1.4 Aim and objectives of this study

The aim of this study is to discover new MAO inhibitors with specificity for the MAO-B isoform. Such compounds may represent useful adjuvants to L-dopa in the treatment of PD. In this study a series of substituted 3,4-dihydro-2(1*H*)-quinolinones and 2-phenoxyethoxy-substituted tetralones will be examined as potential MAO inhibitors. N-propargylamine-2-aminotetralin will also be synthesised and its MAO inhibition properties will be determined.

The objectives of this study are:

- This study will synthesise (1) a series of C6- and C7-substituted 3,4-dihydro-2(1*H*)-quinolinones, (2) a series of 2-phenoxyethoxy-substituted tetralones and (3) N-propargylamine-2-aminotetralin.
- The synthesised analogues will be investigated as potential MAO-A and MAO-B inhibitors using the recombinant human MAO enzymes. IC₅₀ values (concentration of the inhibitor that produces 50% inhibition) will be used to express the inhibition potencies of the analogues.
- The reversibility of inhibition of MAO by selected derivatives will be assessed by employing dialysis.
- For reversible inhibition, sets of Lineweaver-Burk plots will be constructed to determine the modes of inhibition of selected inhibitors.
- Finally, the inhibitors will be docked into the MAO active sites using the CDOCKER docking algorithm of Discovery Studio 3.1. This will be done to gain insight into the interactions between the enzyme and selected inhibitors.

1.5 References

Binda, C., Hubálek, F., Li, M., Herzig, Y., Sterling, J., Edmondson, D.E. & Mattevi, A. (2005) 'Binding of rasagiline-related inhibitors to human monoamine oxidases: a kinetic and crystallographic analysis', *Journal of medicinal chemistry*, 48(26), pp. 8148–8154.

Binda, C., Li, M., Hubalek, F., Restelli, N., Edmondson, D.E. & Mattevi, A. (2003) 'Insights into the mode of inhibition of human mitochondrial monoamine oxidase B from high-resolution crystal structures', *Proceedings of the national academy of sciences of the United States of America*, 100(17), pp. 9750–9755.

Binda, C., Hubálek, F., Li, M., Herzig, Y., Sterling, J., Edmondson, D.E. & Mattevi, A. (2004) 'Crystal structures of monoamine oxidase B in complex with four inhibitors of the N-propargylaminoindan class', *Journal of medicinal chemistry*, 47(7), pp. 1767–1774.

Binda, C., Mattevi, A. & Edmondson, D.E. (2002) 'Structure-function relationships in flavoenzyme-dependent amine oxidations: a comparison of polyamine oxidase and monoamine oxidase', *Journal of biological chemistry*, 277(27), pp. 23973–23976.

Borghain, R., Szasz, J., Stanzione, P., Meshram, C., Bhatt, M., Chirilineau, D., Stocchi, F., Lucini, V., Giuliani, R., Forrest, E., Rice, P. & Anand, R. (2014) 'Randomized trial of safinamide add-on to levodopa in Parkinson's disease with motor fluctuations', *Movement disorders*, 29(2), pp. 229–237.

Bové, J., Prou, D., Perier, C. & Przedborski, S. (2005) 'Toxin induced models of Parkinson's disease', *The journal of the American society for experimental neurotherapeutics*, 2, pp. 484–494.

Carreño, M.C., Gonzalez-López, M., Latorre, A. & Urbano, A. (2006) 'General synthesis of 8-aryl-2-tetralones', *The journal of organic chemistry*, 71(13), pp. 4956–4964.

Chen, J.J. & Swope, D.M. (2005) 'Clinical pharmacology of rasagiline: a novel, second-generation propargylamine for the treatment of Parkinsons disease', *Journal of clinical pharmacology*, 45, pp. 878–894.

Dauer, W. & Przedborski, S. (2003) 'Parkinson's disease: Mechanisms and models', *Neuron*, 39, pp. 889–909.

Dézsi, L. & Vécsei, L. (2014) 'Safinamide for the treatment of Parkinson's disease', *Expert opinion on investigational drugs*, 23(5), pp. 729–742.

Dluzen, D.E., & McDermott, J.L. (2000) 'Gender differences in neurotoxicity of the nigrostriatal dopaminergic system: Implications for Parkinson's disease', *Journal of gender-specific medicine*, 3, pp. 36–42.

Dorsey, E.R., Constantinescu, R., Thompson, J.P., Biglan, K.M., Holloway, R.G. & Kieburtz, K. (2007) 'Projected number of people with Parkinson disease in the most populous nations', *Neurology*, 68, pp. 384–386.

Edmondson, D.E., Binda, C. & Mattevi, A. (2004a) 'The FAD binding sites of human monoamine oxidases A and B', *Neurotoxicology*, 25, pp. 63–72.

Edmondson, D.E., Mattevi, A., Binda, C., Li, M. & Hubálek, F. (2004b) 'Structure and mechanism of monoamine oxidase', *Current medicinal chemistry*, 11, pp. 1983–1993.

Fernandez, H.H. & Chen, J.J. (2007) 'Monoamine oxidase B inhibition in the treatment of Parkinson's disease', *Pharmacotherapy*, 27, pp. S174–S185.

Finberg, J.P. & Tenne, M. (1982) 'Relationship between tyramine potentiation and selective inhibition of monoamine oxidase types A and B in the rat vas deferens', *British journal of pharmacology*, 77, pp. 13–21.

Haefely, W., Bukard, W.P., Cesura, A.M., Kettler, R., Lorez, H.P., Martin, J.R., Richards, J.G., Scherschlicht, R. & Da Prada, M. (1992) 'Biochemistry and pharmacology of moclobemide, a prototype RIMA', *Psychopharmacology*, 106, pp. S6–S14.

Hasan, F., McCrodden, J.M., Kennedy, N.P. & Tipton, K.F. (1988) 'The involvement of intestinal monoamine oxidase in the transport and metabolism of tyramine', *Journal of neural transmission*, 26, pp. S1–S9.

Hazelhoff, B., De Vries, J.B., Dijkstra, D., de Jong, W. & Horn, A.S. (1985) 'The neuropharmacological profile of N-methyl-N-propargyl-2-aminotetralin: a potent monoamine oxidase inhibitor', *Naunyn-Schmiedeberg's archives of pharmacology*, 330(1), pp. 50–58.

Henderson, J.M., Lu, Y., Wang, S., Cartwright, H. & Halliday, G.M. (2003) 'Olfactory deficits and sleep disturbances in Parkinson's disease: a case-control survey', *Journal of neurology, neurosurgery and psychiatry*, 74, pp. 956–958.

Hubálek, F., Binda, C., Li, M., Herzig, Y., Sterling, J., Youdim, M.B., Mattevi, A. & Edmondson, D.E. (2004) 'Inactivation of purified human recombinant monoamine oxidases A and B by rasagiline and its analogues', *Journal of medicinal chemistry*, 47(7), pp. 1760–1766.

Jenner, P., Mori, A., Hauser, R., Morelli, M., Fredholm, B. & Chen, J.F. (2009) 'Adenosine, adenosine A_{2A} antagonists and Parkinson's disease', *Parkinsonism and related disorders*, 15, pp. 406–413.

Lees, A. (2005) 'Alternatives to levodopa in the initial treatment of early Parkinson's disease', *Drugs & aging*, 22, pp. 731–740.

Lees, A.J., Hardy, J. & Revesz, T. (2009) 'Parkinson's disease', *The lancet*, 373, pp. 2055–2066.

Legoabe, L.J., Petzer, A. & Petzer, J.P. (2014) 'α-Tetralone derivatives as inhibitors of monoamine oxidase', *Bioorganic & medicinal chemistry letters*, 24(12), pp. 2758–2763.

Legoabe, L.J., Petzer, A. & Petzer, J.P. (2015) 'The synthesis and evaluation of C7-substituted α-tetralone derivatives as inhibitors of monoamine oxidase', *Chemical biology & drug design*, 86(4), pp. 895–904.

Manvar, D., Fernandes Tde, A., Domingos, J.L., Baljinnyam, E., Basu, A., Junior, E.F., Costa, P.R. & Kaushik-Basu, N. (2015) 'Synthesis and biological evaluation of α -aryl- α -tetralone derivatives as hepatitis C virus inhibitors', *European journal of medicinal chemistry*, 93, pp. 51–54.

Meiring, L., Petzer, J.P. & Petzer, A. (2013) 'Inhibition of monoamine oxidase by 3,4-dihydro-2(1*H*)-quinolinone derivatives', *Bioorganic & medicinal chemistry letters*, 23(20), pp. 5498–5502.

Milczek, E.M., Bonivento, D., Binda, C., Mattevi, A., McDonald, I.A. & Edmondson, D.E. (2008) 'Structural and mechanistic studies of mofegiline inhibition of recombinant human monoamine oxidase B', *Journal of medicinal chemistry*, 51(24), pp. 8019–8026.

Mostert, S., Petzer, A. & Petzer, J.P. (2015) 'Indanones as high-potency reversible inhibitors of monoamine oxidase', *ChemMedChem*, 10(5), pp. 862–873.

Nagatsu, T. & Sawada, M. (2006) 'Molecular mechanism of the relation of monoamine oxidase B and its inhibitors to Parkinson's disease: possible implications of glial cells', *Journal of neural transmissions*, 71, pp. 53–65.

Pae, C.U., Patkar, A.A., Jang, S., Portland, K.B., Jung, S. & Nelson, J.C. (2014) 'Efficacy and safety of selegiline transdermal system (STS) for the atypical subtype of major depressive disorder: pooled analysis of 5 short-term, placebo-controlled trials', *CNS spectrums*, 19(4), pp. 324–329.

Parkinson, J. (2002) 'An essay on the shaking palsy', *Journal of neuropsychiatry and clinical neuroscience*, 14, pp. 223–236.

Prediger, R.D.S., Matheus, F.C., Schwarzbald, M.L., Lima, M.M.S. & Vital, M.A.B.F. (2012) 'Anxiety in Parkinson's disease: a critical review of experimental and clinical studies', *Neuropharmacology*, 62, pp. 115–124.

Przedborski, S. (2005) 'Pathogenesis of nigral cell death in Parkinson's disease', *Parkinsonism & related disorders*, 11, pp. S3–S7.

Riederer, P., Danielczyk, W. & Grunblatt, E. (2004) 'Monoamine oxidase-B inhibition in Alzheimer's disease', *Neurotoxicology*, 25, pp. 271–277.

Schapira, A.H.V. & Olanow, C.W. (2008) 'Drug selection and timing of initiation of treatment in early Parkinson's disease', *Annals of neurology*, 64(S2), pp. S47–S55.

Strydom, B., Bergh, J.J. & Petzer, J.P. (2012) '8-Aryl- and alkyloxycaffeine analogues as inhibitors of monoamine oxidase', *European journal of medicinal chemistry*, 46(8), pp. 3474–3485.

Tipton, K.F., Boyce, S., O'Sullivan, J., Davey, G.P. & Healy, J. (2004) 'Monoamine oxidases: certainties and uncertainties', *Current medicinal chemistry*, 11, pp. 1965–1982.

Van Dyk, A.S., Petzer, J.P., Petzer, A. & Legoabe, L.J. (2015) '3-Coumaranone derivatives as inhibitors of monoamine oxidase', *Journal of drug design, development and therapy*, 9, pp. 5479–5489.

Von Campenhausen, S., Bornschein, B., Wick, R., Botzel, K., Sampaio, C., Poewe, W., Oertel, W., Siebert, U., Berger, K. & Dodel, R. (2005) 'Prevalence and incidence of Parkinson's disease in Europe', *Neuropsychopharmacology*, 15, pp. 473–490.

Yamada, M. & Yasuhara, H. (2004) 'Clinical pharmacology of MAO inhibitors: safety and future', *Neurotoxicology*, 25, pp. 215–221.

Yazdani, U., German, D.C., Liang, C.L., Manzano, L., Sonsalla, P.K. & Zeevalk, G.D. (2006) 'Rat model of Parkinson's disease: chronic central delivery of 1-methyl-4-phenylpyridinium (MPP⁺)', *Experimental neurology*, 200, pp. 172–183.

Youdim, M.B.H., Edmondson, D. & Tipton, K.F. (2006), 'The therapeutic potential of monoamine oxidase inhibitors', *Nature reviews. Neuroscience*, 7, pp. 295–309.

Youdim, M.B.H. & Bakhle, Y.S. (2006) 'Monoamine oxidase: Isoforms and inhibitors in Parkinson's disease and depressive illness', *British journal of pharmacology*, 147(S1), pp. S287–S296.

Youdim, M.B.H. & Weinstock, M. (2004) 'Therapeutic applications of selective and non-selective inhibitors of monoamine oxidase A and B that do not cause significant tyraminepotentiation', *Neurotoxicology*, 25, pp. 243–250.

CHAPTER 2

LITERATURE BACKGROUND

2.1 Monoamine oxidase

2.1.1 General background

Over 50 years ago, MAO inhibitors were developed as antidepressant drugs by Zeller's laboratory. Patients receiving treatment for tuberculosis evoked further development of MAO inhibitors after experiments revealed that the antituberculosis drug, isoniazid, was also a potent MAO inhibitor. The first antidepressant to be developed was a MAO inhibitor related to isoniazid, iproniazid.

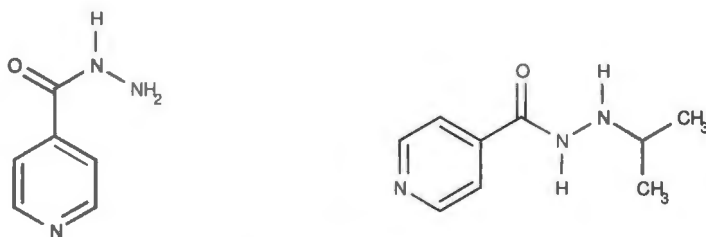


Figure 2.1: The structures of isoniazid (left) and iproniazid (right), respectively.

MAO-A and MAO-B have since received extensive attention, with more than 14 000 MAO related published papers (Youdim *et al.*, 1988). In 1928, MAO was first described by Mary Hare-Bernheim as catalysing the oxidative deamination of tyramine. Since coming to England in the 1930s, Hugh Blaschko's primary interest in research was MAO and he later discovered that tyramine oxidase, noradrenaline oxidase and aliphatic amine oxidase is the same enzyme, able to metabolise primary, secondary and tertiary amines, but not diamines. The enzyme, mitochondrial monoamine oxidase, was eventually named by Albert Zeller in 1938 (MAO; EC1.4.3.4) (Schnaitman *et al.*, 1967; Youdim *et al.*, 1988; Shih *et al.*, 1999; Tipton *et al.*, 2004).

MAO is present in most mammalian tissues and consists of two isoenzymes, MAO-A and MAO-B, varying in proportion from tissue to tissue (Shih *et al.*, 1999; Tipton *et al.*, 2004; Nicotra *et al.*, 2004; Tsang *et al.*, 1986; Strolin Benedetti *et al.*, 1992).

Gene cloning and sequencing for MAO-A and MAO-B was the breakthrough in demonstrating that MAO-A and MAO-B are two separate enzymes, sharing similar structures and possessing covalently attached flavin adenine dinucleotide (FAD) cofactors, with an amino acid sequence identity of ~70% (Bach *et al.*, 1988; Youdim *et al.*, 2006). Both MAO-A and MAO-B are associated with the mitochondrial outer membrane, with MAO-B being the main form in the basal ganglia, blood platelets and liver, and MAO-A being mostly present in the placenta and gastrointestinal tract (Youdim *et al.*, 2006). MAO-A and MAO-B have different substrate specificities, biological functions, pH optima and sensitivity to heat inactivation, as well as different specificities for inhibitors (Youdim *et al.*, 2006; Youdim *et al.*, 1988; Shih *et al.*, 1999; Nicotra & Parvez, 1999).

In 1968, JP Johnston distinguished between MAO-A and MAO-B in discovering that MAO-A is inhibited by low concentrations of clorgyline and preferably oxidises serotonin (5-HT) and noradrenaline (NA), while MAO-B is inhibited by low concentrations of selegiline [(R)-deprenyl] and preferably oxidises benzylamine and 2-phenylethylamine (Knoll, 1978). DA, tyramine and tryptamine are oxidised by both MAO-A and MAO-B.

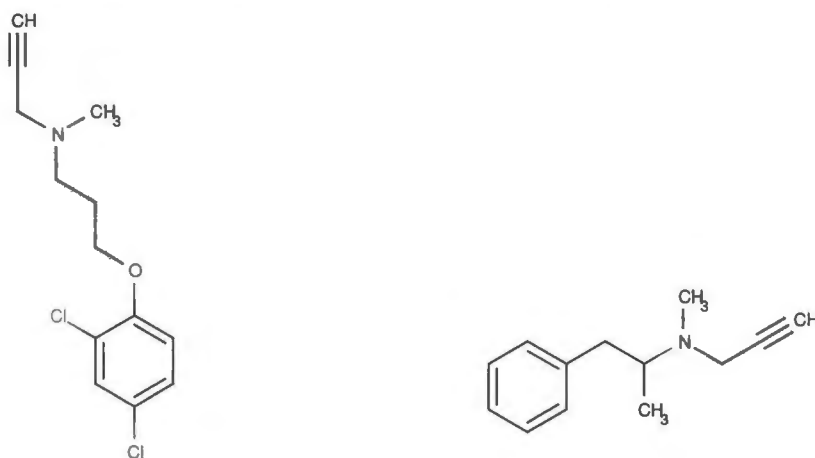


Figure 2.2: The structures of clorgyline (left) and selegiline (right), respectively.

2.1.2 The therapeutic applications of MAO-A and MAO-B

MAO inhibitors for the treatment of Parkinson's disease: MAO exerts a protective action and serves as metabolic barrier by oxidising potentially harmful amines already present in the blood and preventing exogenous amines from entering the systemic circulation. Besides acting as metabolic barriers, the MAOs also terminate the action of certain neurotransmitters (Youdim *et al.*, 2006). Since MAO-B is predominantly present in the basal ganglia, in the brain, the metabolism of DA in this region is largely due to MAO-B.

MAO-B thus participates in the degradation of DA and also deaminates β -phenylethylamine, an endogenous amine which stimulates DA release and inhibits neuronal DA uptake (Glover *et al.*, 1977; Fernandez & Chen, 2007). Because of MAO-B's role in the metabolism of DA in the brain, MAO-B inhibitors have been used for the treatment of Parkinson's disease. In Parkinson's disease the nigrostriatal neuronal pathway degenerates, which results in a deficiency of DA in the striatum. Symptomatic therapy is aimed at replacing DA in this brain region with the most effective therapy being L-dopa, the metabolic precursor of DA. To further enhance DA levels after L-dopa treatment, MAO-B inhibitors may be used. MAO-B inhibitors act by inhibiting DA metabolism in the brain. In early Parkinson's disease, MAO-B inhibitors may be used as monotherapy (Dauer & Przedborski, 2003; Carlsson, 1959; Rascol *et al.*, 2002a; Lees *et al.*, 2009)

The oxidative deamination of DA catalysed by MAO-B produces hydrogen peroxide (H_2O_2), the corresponding aldehyde (dopanal - RCHO), either ammonia or a substituted amine and the reduced FAD cofactor (Binda *et al.*, 2002a; Edmondson *et al.*, 2004).

In high concentrations these products can be harmful and may contribute to neurodegeneration (Riederer *et al.*, 2004). Dopanal has been implicated in α -synuclein aggregation, while increased H_2O_2 levels promote apoptotic cell death (Burke *et al.*, 2008). The aldehyde (RCHO) is oxidised by aldehyde dehydrogenase (ADH), releasing the final excreted metabolite, a carboxylic acid (RCOOH) (Youdim & Bakhle, 2006). ADH deficiency could result in accumulation of neurotoxic aldehydes derived from DA (Figure 2.3) (Grünblatt *et al.*, 2004).

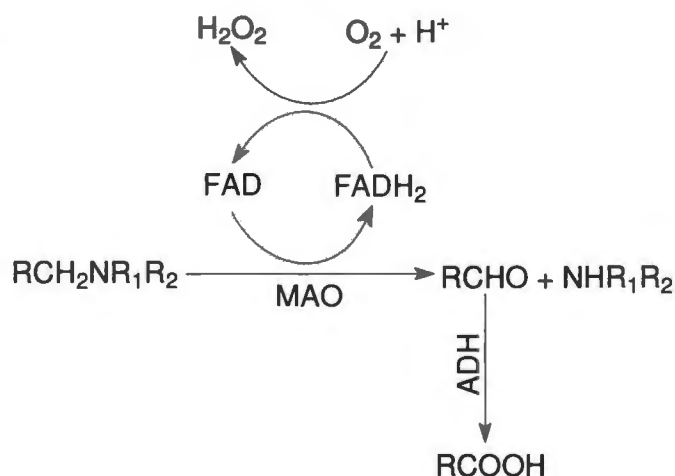


Figure 2.3: The reaction pathway of monoamine metabolism by MAO.

Metabolic products generated by MAO may react with iron in the brain (Symes *et al.*, 1969). H_2O_2 produced with the metabolism of monoamines, can either be converted into the hydroxyl radical (via reaction with iron) or be inactivated by glutathione peroxidase (GPO), which uses glutathione (GSH) as cofactor (Youdim & Bakhle, 2006). The hydroxyl radical formed in the Fenton reaction (Figure 2.4), diminishes cellular anti-oxidants and reacts with, and damages lipids, proteins and DNA. MAO-B activity increases with age, leading to increased concentrations of the components (H_2O_2) of the Fenton reaction and subsequently increased hydroxyl radical formation.

This analysis suggests that MAO-B inhibitors may be able to protect neuronal tissue against metabolic injury by reducing the formation of the toxic products produced by the MAO-B catalytic cycle. This reduces oxidative stress and slows neuronal cell death (Youdim *et al.*, 2006). Therefore, MAO inhibitors may likely be neuroprotective (Edmondson *et al.*, 2009). By acting as neuroprotective agents, MAO-B inhibitors may thus have further relevance in the treatment of Parkinson's disease.

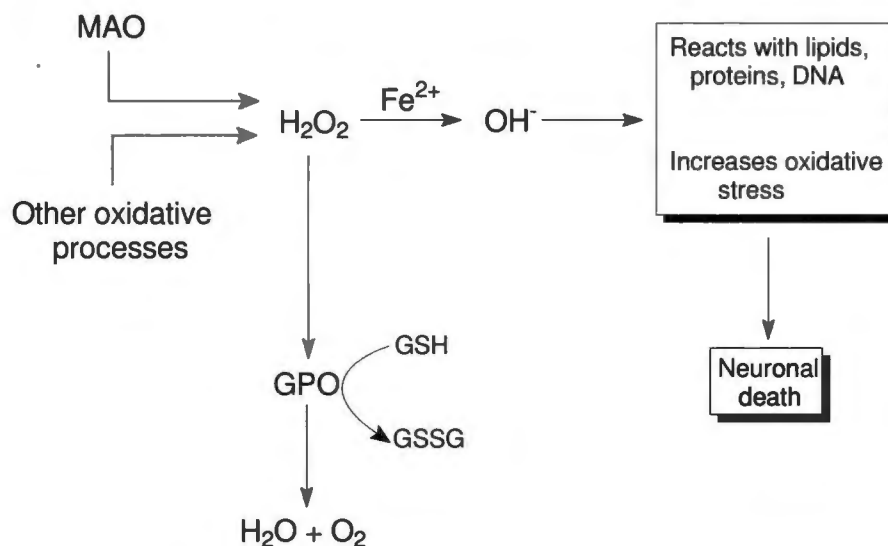


Figure 2.4: The mechanism of neurotoxicity by hydrogen peroxide (H_2O_2), induced by the Fenton reaction.

MAO inhibitors as antidepressants: As mentioned, MAO inhibitors were first marketed as antidepressants, with iproniazid being the first MAO inhibitor to be discovered. Initially used for the treatment of tuberculosis, it was subsequently discovered that iproniazid produced antidepressant effects in patients. Both noradrenaline and serotonin are substrates of MAO-A.

MAO-A is responsible for metabolising serotonin in the central nervous system (CNS) and deactivating circulatory catecholamines as well as vasopressors, such as tyramine in the intestine (Fernandez & Chen, 2007). Inhibition of MAO-A in the CNS, leads to elevated DA, NA and serotonin levels (Pletscher, 1991). MAO-A inhibitors thus demonstrate remarkable antidepressant action, but their clinical value is compromised by serious side effects, including liver toxicity, the ‘cheese reaction’ and the serotonin syndrome (Youdim *et al.*, 1988). The occurrence of the ‘cheese reaction’ prompted researchers to develop reversible MAO-A inhibitors such as moclobemide, which is an example of an active antidepressant (Youdim & Bakhle, 2006).

2.1.3 Adverse effects of MAO-A and MAO-B inhibition.

The ‘cheese reaction’ is induced by tyramine and other dietary amines usually present in foods (most commonly in cheeses). Under normal circumstances, this dietary amine is metabolised by MAO-A in the gut wall and liver, preventing it from entering the systemic circulation. With the use of MAO-A inhibitors, tyramine and other dietary amines are free to enter the systemic circulation. Here they release NA from peripheral adrenergic neurons, leading to a hypertensive response which can be fatal (Figure 2.5) (Youdim & Bakhle, 2006; Youdim *et al.*, 2006; Youdim & Weinstock, 2004; Hasan *et al.*, 1988; Finberg & Tenne, 1982; Chen & Swope, 2005). Reversible MAO-A inhibitors do not cause the ‘cheese reaction’ because dietary amines can displace the reversible inhibitor from MAO-A and thus be normally metabolised in the intestine (Haefely *et al.*, 1992).

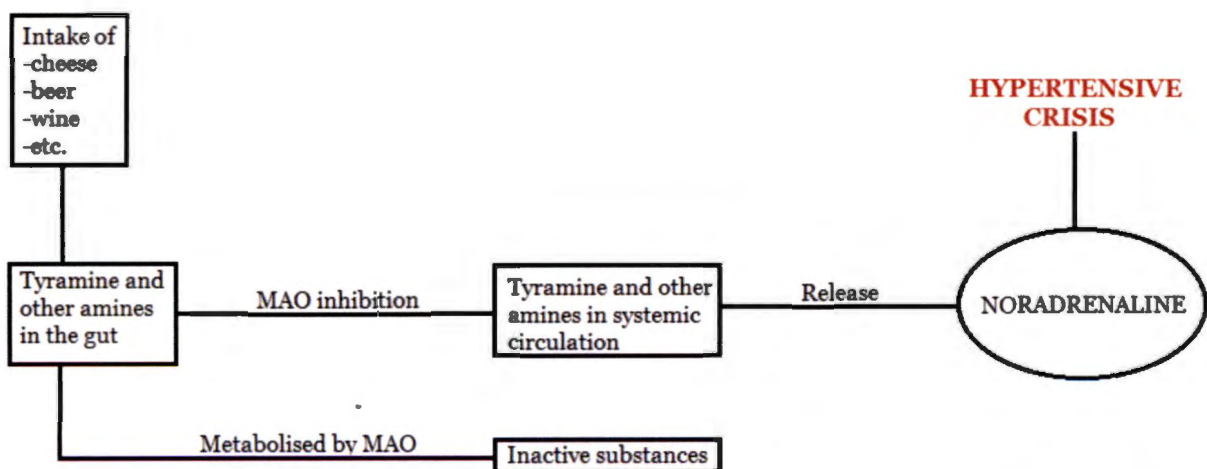


Figure 2.5: The mechanism of the ‘cheese reaction’.

The serotonin syndrome occurs with an over activity of serotonin in the CNS. Due to the role that MAO-A plays in metabolising serotonin, the use of MAO-A inhibitors in combination with other serotonin enhancing drugs such as selective serotonin reuptake inhibitors and tricyclic antidepressants, can lead to the serotonin syndrome. This is a serious condition which may be life-threatening (Boyer & Shannon, 2005). The serotonin syndrome is characterised by the following symptoms: restlessness, hallucination, rapid heartbeat, sudden blood pressure changes, overactive reflexes, elevated body temperature, nausea, vomiting and diarrhoea (Fernandez & Chen, 2007; Chen & Swope, 2005).

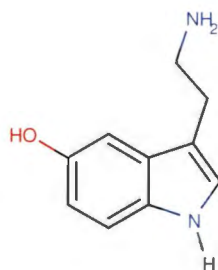


Figure 2.6: The structure of serotonin.

2.1.4 Catalytic mechanism of MAO-A and MAO-B

The exact mechanism of MAO catalysis is still unknown, but possible mechanisms proposed, include the single electron transfer mechanism suggested by Silverman and co-workers (1995), the polar nucleophilic mechanism and the hydride transfer mechanism.

The single electron transfer mechanism involves firstly the oxidation of the amine by one electron, producing an aminium cation radical and flavin radical intermediate. This results in the intermediary product with an acidic α -proton, allowing proton abstraction by a basic amino acid residue in the active site (Figure 2.7). A second single electron transfer yields the fully reduced flavin and the imine product. However, the MAO-A and MAO-B active sites do not contain basic amino acid residues and there exists no direct evidence to support the formation of a flavin radical intermediate (Silverman *et al.*, 1980).

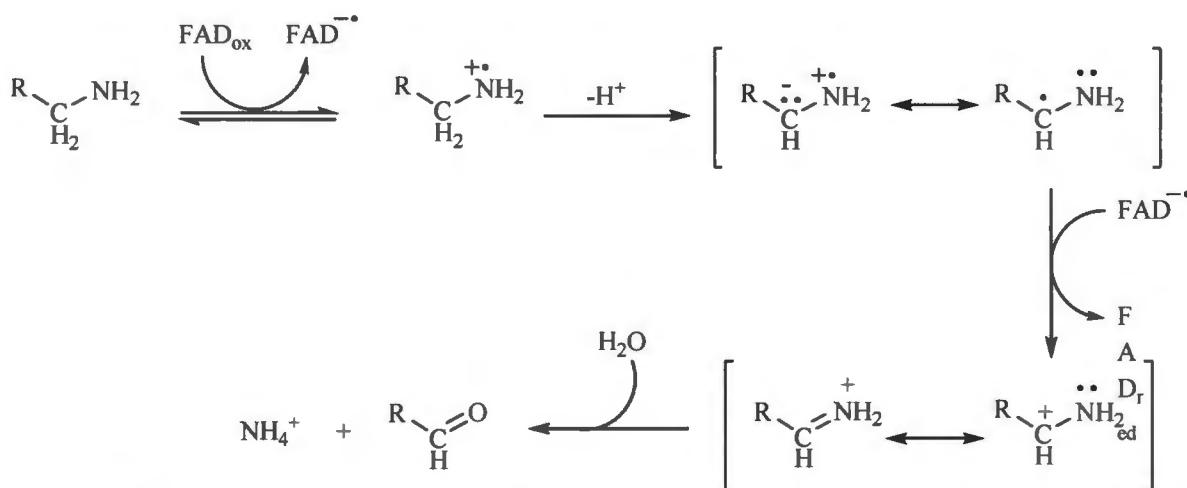


Figure 2.7: Single electron transfer (SET) mechanism of MAO catalysis (Edmondson *et al.*, 2007).

The polar nucleophilic mechanism first proposed by Miller & Edmondson (1999), is a more likely mechanism. The deprotonated amine substrate covalently binds to the 4a position of the flavin, in a nucleophilic manner. This results in a flavin-substrate adduct which enables position N5 to act as a strong active site base. Position N5 exhibits a pKa in the range of 25-27, which is sufficient for α -pro-R-H abstraction from the substrate (Edmondson *et al.*, 2004b). With formation of the reduced flavin, the imine product is released (Figure 2.8) (Binda *et al.*, 2002a; Edmondson *et al.*, 2004).

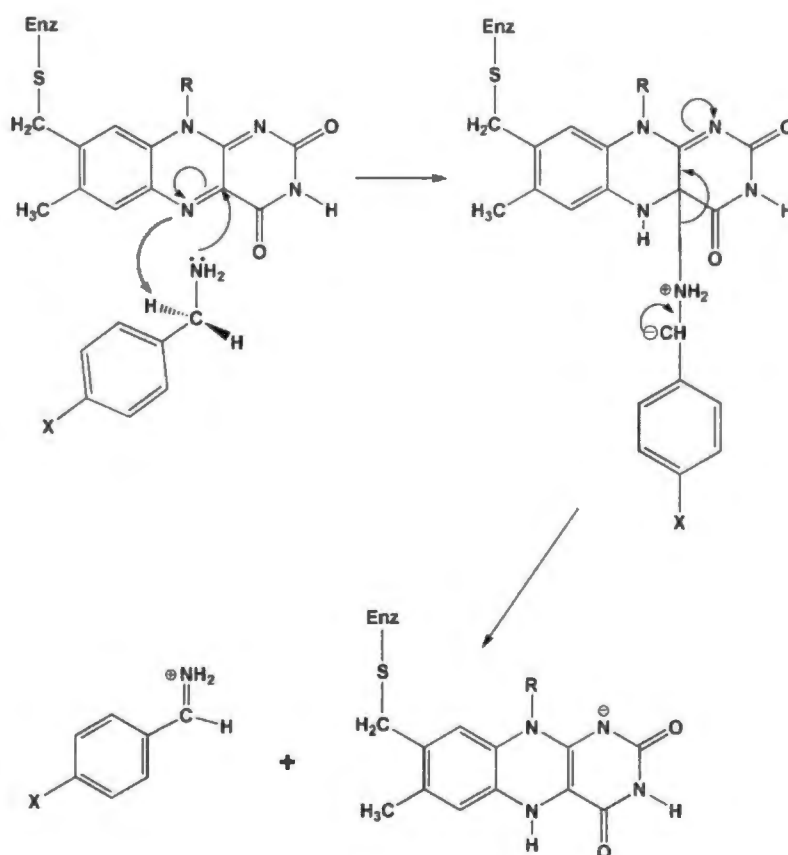


Figure 2.8: Polar nucleophilic mechanism of MAO catalysis. The products of amine oxidation are the protonated imine and the flavin hydroquinone (Edmondson *et al.*, 2007).

The hydride transfer mechanism was recently suggested since there is no direct evidence against this mechanism. Other amine oxidases such as the D-amino acid oxidases employ a single hydride transfer mechanism (Figure 2.9) (Fitzpatrick, 2010). In this mechanism a hydride is simply transferred from the α -carbon of the substrate to the N5 of the flavin to yield the reduced flavin and the imine product.

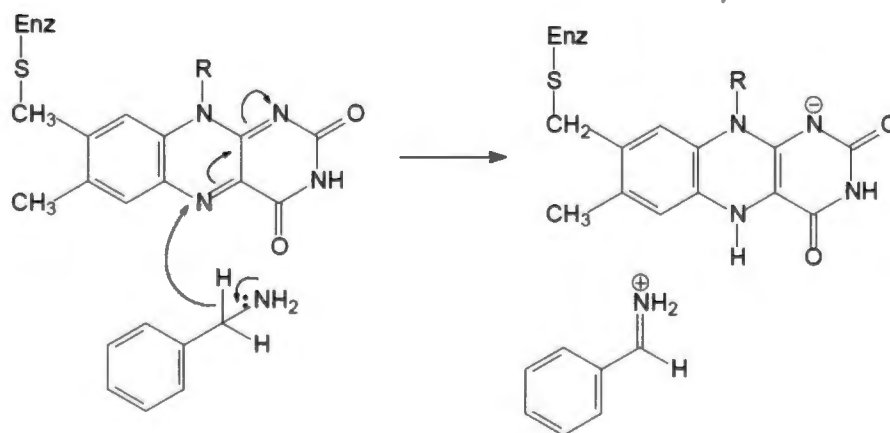


Figure 2.9: The hydride transfer mechanism of MAO catalysis (Fitzpatrick, 2010).

2.1.5 The three dimensional structure of MAO

MAO-B:

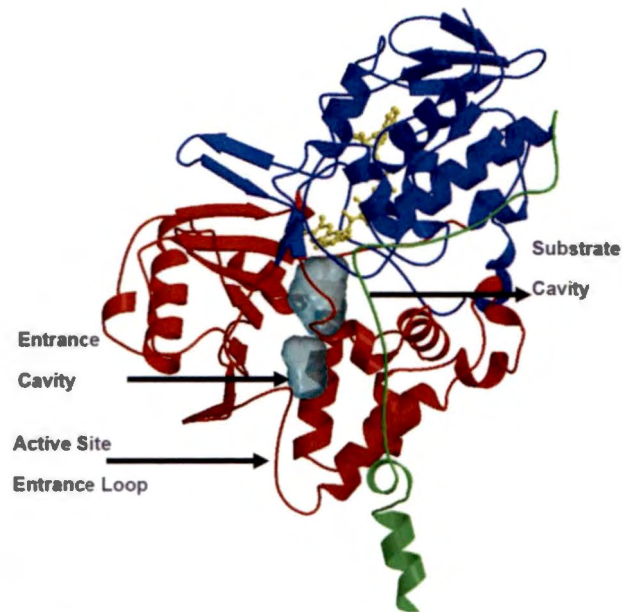


Figure 2.10: The three dimensional structure of human MAO-B. The ball and stick model in yellow represents the covalent flavin moiety. The blue represents the flavin binding domain. The red is the substrate domain. The green represents the membrane binding domain (Edmondson *et al.*, 2007).

An FAD cofactor is covalently bound to the MAO protein via an $\delta\alpha$ -thioether linkage to Cys397. Human MAO-B crystallises as a dimer and is tightly bound at the C-terminal of MAO, through a polypeptide segment (α -helix) to the mitochondrial outer membrane. The hydrophobic C-terminal consists of 32 amino acids. It protrudes perpendicularly into the phospholipid bilayer of the mitochondrial membrane, anchoring the enzyme (Binda *et al.*, 2002b; Edmondson *et al.*, 2004).

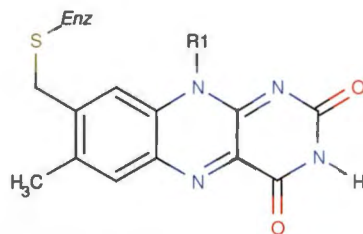


Figure 2.11: The partial structure of the FAD cofactor.

Two theories exist concerning the conformation of the C-terminal within the mitochondrial membrane. The first theory proposes that the C-terminal traverses the membrane with 5 amino acids protruding on the other side.

The second theory suggests that the C-terminal is folded within the membrane allowing the end of the helix to protrude on the same side as the enzyme (Figure 2.12) (Binda *et al.*, 2004). The C-terminal anchoring into the mitochondrial membrane might be crucial for MAO catalytic activity.

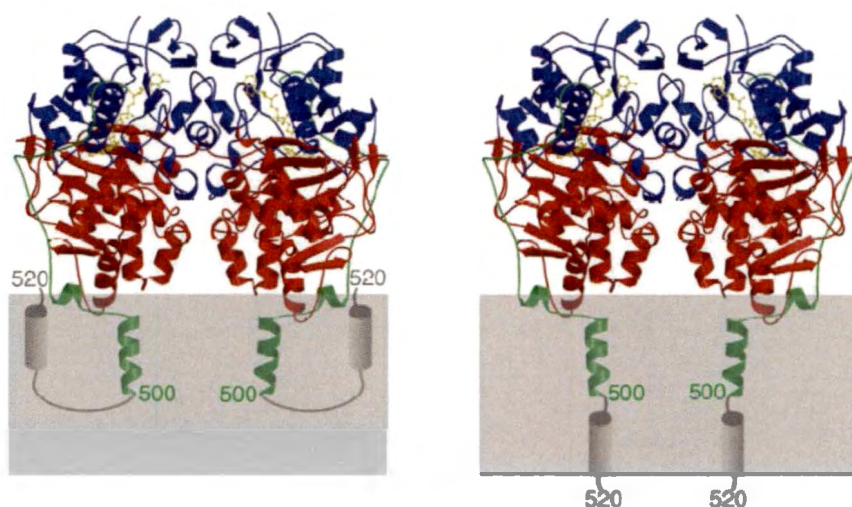


Figure 2.12: The two suggested conformations of C-terminal anchoring of MAO-B within the mitochondrial outer membrane. The first panel shows the C-terminal protruding on the same side of the enzyme and the second panel shows the C-terminal exiting the membrane on the other side (Binda *et al.*, 2004).

MAO-B has apolar groups at various positions in the sequence and consists of 520 amino acids (Fraaije & Mattevi, 2000; Binda *et al.*, 2002a, 2007). To reach the flavin coenzyme, a substrate molecule must negotiate a protein loop at the entrance to one of two cavities. These cavities include the “entrance cavity” and the “substrate cavity”, separated by the Ile199 side chain. This residue thus serves as a “gate” between the two cavities.

The active site of MAO-B consists of a 420 Å³ hydrophobic cavity and is connected to an entrance cavity of 290 Å³. An aromatic cage formed by residues Tyr 398 and Tyr 435 is the recognition site for the substrate amino group. These residues are orientated perpendicular to the plane of the flavin ring (Binda *et al.*, 2002a; 2003). The entrance cavity connects the surface of the protein to the substrate cavity in MAO-B. Besides Ile199, residues Leu171, Phe168 and Tyr326 also defines the border between the two cavities. The two cavities may fuse, forming a single larger cavity able to accommodate larger substrates and inhibitors (Binda *et al.*, 2002a; Edmondson *et al.*, 2007). This occurs when the side chain of Ile199 rotates from the cavity.

MAO-A:

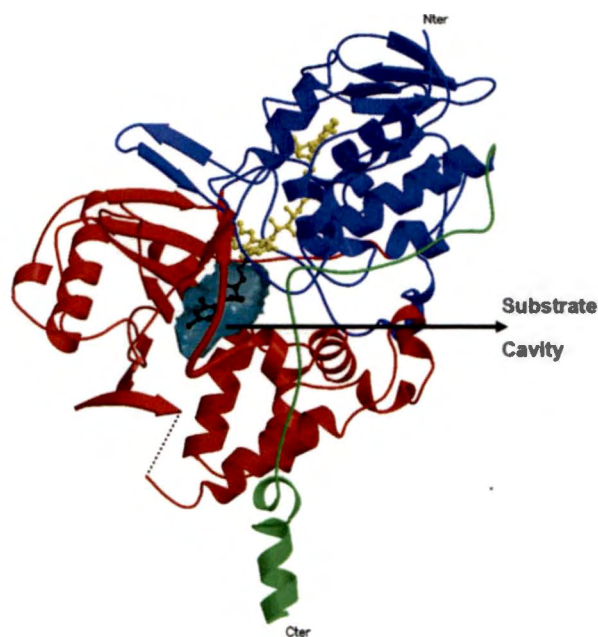


Figure 2.13: The three dimensional structure of human MAO-A. The colouring is similar to those in figure 2.10 (Edmondson *et al.*, 2007).

Human MAO-A crystallises as a monomer. The structure of MAO-A can be divided into two domains, the extra-membrane domain and the membrane binding domain. The extra-membrane domain is further divided into two regions, the FAD binding region and substrate/inhibitor binding region (Son *et al.*, 2008).

In contrast to human MAO-B, both human and rat MAO-A have single substrate binding cavities with protein loops at the entrances of the active site cavities. Compared to MAO-B, the active site cavity of MAO-A is much smaller, shorter and wider. Similar to MAO-B, human MAO-A is also hydrophobic, with a volume of 550 \AA^3 . The covalent attachment of the FAD cofactor in MAO-A and the tyrosine residues which form the “aromatic cage” in the active sites, are identical to those of MAO-B (Edmondson *et al.*, 2007; De Colibus *et al.*, 2005).

The difference in active site residues between MAO-A and MAO-B may contribute to the different substrate and inhibitor specificities of the two isoforms. For example, in MAO-A the Phe208 residue is in the homologous position to the MAO-B Ile199 residue. Ile 199 in MAO-B is able to rotate from the active site to allow larger inhibitors, including safinamide, to bind to the fused entrance and substrate cavities.

Phe208 in MAO-A on the other hand, is not able to rotate from the active site in order to accommodate larger inhibitors. This is due to the fact that the phenyl side chain of Phe208 is much larger than the side chain of Ile199. Also, in the position of Tyr326 in MAO-B, MAO-A has residue Ile335. Because of its larger size, Tyr326 in MAO-B would restrict the binding of certain inhibitors such as clorgyline, where Ile335 would allow such binding within MAO-A (De Colibus *et al.*, 2005; Son *et al.*, 2008).

2.1.6 Inhibitors of MAO

MAO inhibitors were used as antidepressants in the 1950s, with the first inhibitor being iproniazid, initially developed as tuberculosis treatment. Since iproniazid was found ineffective for tuberculosis treatment, other hydrazine derivatives such as phenelzine were developed. The severe liver toxicity caused by iproniazid, was overcome by the development of non-hydrazine derivatives, including pargyline and tranylcypromine. Hypertensive crises were still a major side effect of MAO-A inhibitors (Youdim *et al.*, 2006). However, selective MAO-B inhibitors and reversible MAO-A inhibitors, including moclobemide and lazabemide, did not lead to hypertensive crisis (Da Prada *et al.*, 1990).

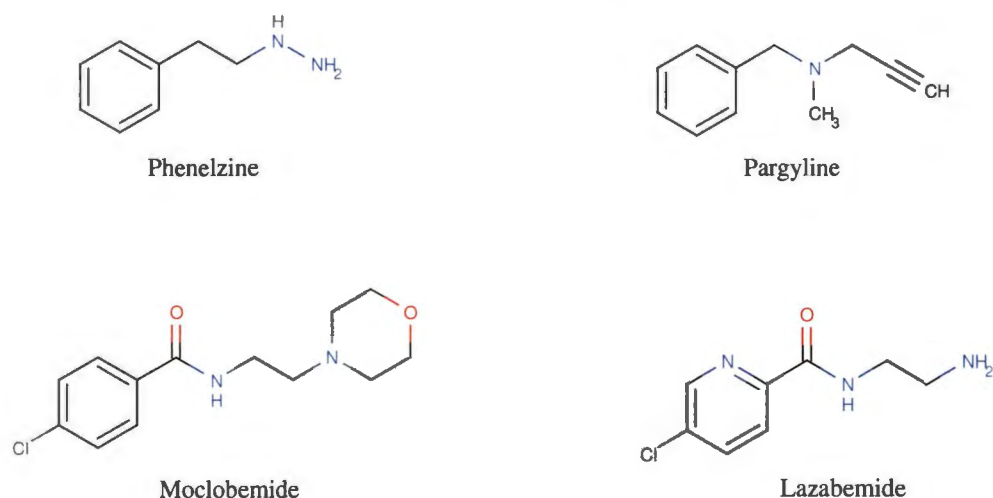


Figure 2.14: The structures of phenelzine, pargyline, moclobemide and lazabemide.

Inhibitors of MAO-A and MAO-B can be divided into two classes, namely reversible and irreversible inhibitors. Within these classes selective and non-selective inhibitors may be found.

Reversible inhibitors bind non-covalently to the active sites of MAO-A and MAO-B and an increase of the substrate concentration can overcome inhibition. Irreversible inhibitors bind in an irreversible manner. The irreversible inhibitor is oxidised to the active inhibitor which covalently binds, via interaction with the FAD cofactor, to the active site of the enzymes. Irreversible inhibition can only be overcome by *de novo* enzyme synthesis and do not allow competition with other substrates, hampering normal metabolism of certain substrates (Lees, 2005; Abeles & Maycock, 1976; Binda *et al.*, 2003).

Examples of reversible MAO-B inhibitors include 1,4-diphenyl-2-butene, discovered in MAO-B crystallisation experiments (Binda *et al.*, 2003); trans,trans-farnesol a component of tobacco smoke (Hubálek *et al.*, 2005); 8-(3-chlorostyryl)caffeine (CSC) also an A_{2A} adenosine receptor antagonist (Chen *et al.*, 2002) and safinamide, a DA modulator (Caccia *et al.*, 2006; Fernandez & Chen, 2007).

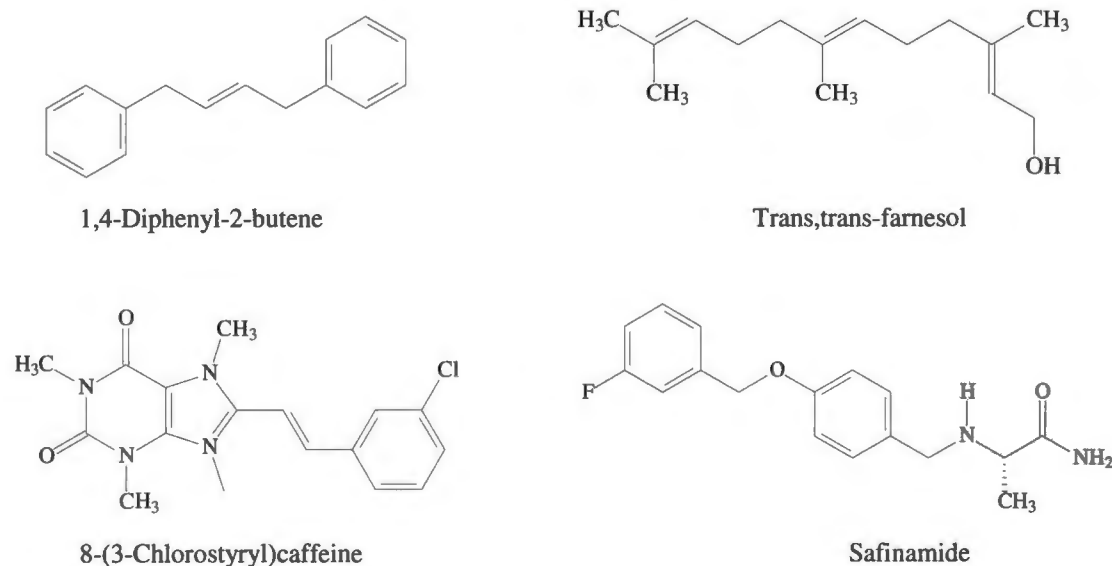


Figure 2.15: The structures of reversible MAO-B inhibitors, 1,4-diphenyl-2-butene, trans,trans-farnesol, 8-(3-chlorostyryl)caffeine and safinamide.

Examples of irreversible MAO-B inhibitors are the propargylamines, selegiline (Knoll & Magyar, 1972), rasagiline (Finberg *et al.*, 1981) and the experimental inhibitor PF-9601 N (Perez *et al.*, 2003). Selegiline undergoes first pass hepatic metabolism and forms three metabolites, desmethylselegiline, l-methamphetamine and l-amphetamine.

The amphetamine metabolites are potentially neurotoxic and are associated with cardiovascular and psychiatric adverse effects (Churchyard *et al.*, 1997).

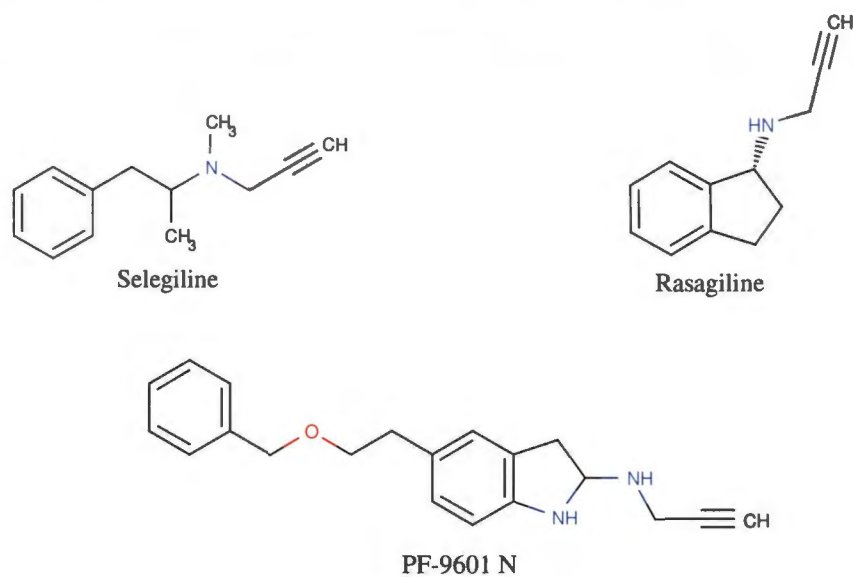


Figure 2.16: The structures of irreversible MAO-B inhibitors, selegiline, rasagiline and PF-9601 N.

Reversible selective MAO-A inhibitors are clinically used in the treatment of various depression states and include brofaromine, toloxatone, cimoxatone and befloxatone (Bortolato *et al.*, 2008).

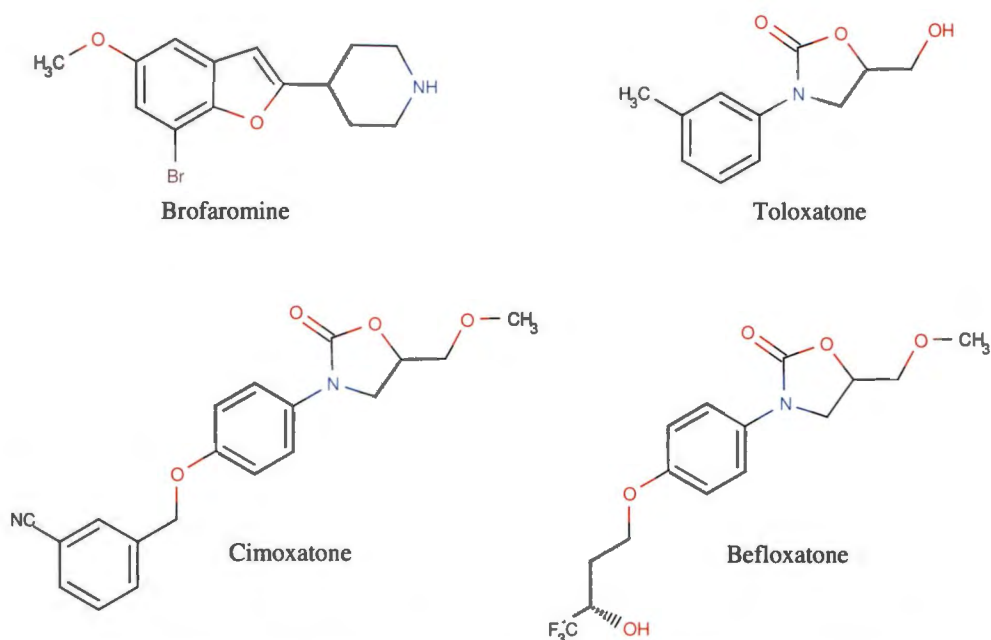


Figure 2.17: The structures of reversible MAO-A inhibitors, brofaromine, tolaxatone, cimoxatone and befloxatone.

An example of a selective, irreversible MAO-A inhibitor is clorgyline, and examples of nonselective irreversible MAO inhibitors include isocarboxazide and tranylcypromine (Riederer *et al.*, 2004). Although clorgyline and isocarboxazide are effective in the treatment of depressive disorders, their clinical use as antidepressants is prevented by the ‘cheese reaction’.

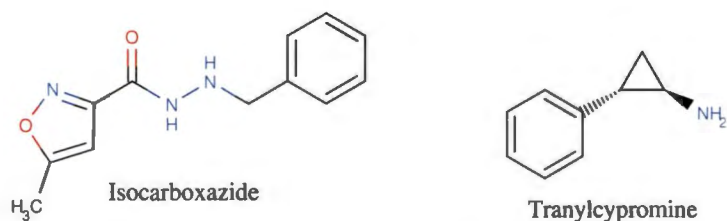


Figure 2.18: The structures of isocarboxazide and tranylcypromine.

2.1.7 Conclusion

This chapter discussed the general background of MAO, including the therapeutic applications of both MAO-A and MAO-B inhibitors. Furthermore, the three dimensional structures of MAO-A and MAO-B, as well as mechanistic proposals for MAO catalysis were discussed. MAO inhibitors were also briefly discussed. The main focus for this study is to synthesise new inhibitors, with specificity for MAO-B. The next chapter will provide additional background to this thesis in the form of a review of the pharmacological properties of 3,4-dihydro-2(1*H*)-quinolinones, one of the series of compounds studied in this thesis.

2.2 References

Abeles, R.H. & Maycock, A.L. (1976) 'Suicide enzyme inactivators', *Accounts of chemical research*, 9(9), pp. 313–319.

Bach, A.W., Lan, N.C., Johnson, D.L., Abell, C.W., Bembenek, M.E., Kwan, S.W., Seeburg, P.H. & Shih, J.C. (1988) 'cDNA cloning of human liver monoamine oxidase A and B: molecular basis of differences in enzymatic properties', *Proceedings of the national academy of sciences of the United States of America*, 85, pp. 4934–4938.

Binda, C., Hubalek, F., Li, M., Herzig, Y., Sterling, J., Edmondson, D.E. & Mattevi, A. (2004) 'Crystal structures of monoamine oxidase B in complex with four inhibitors of the N-propargylaminoindan class', *Journal of medicinal chemistry*, 47, pp. 1767–1774.

Binda, C., Li, M., Hubálek, F., Restelli, N., Edmondson, D.E. & Mattevi, A. (2003) 'Insights into the mode of inhibition of human mitochondrial monoamine oxidase B from high-resolution crystal structures', *Proceedings of the national academy of sciences of the United States of America*, 100, pp. 9750–9755.

Binda, C., Mattevi, A. & Edmondson, D.E. (2002a) 'Structure-function relationships in flavoenzyme-dependent amine oxidations: a comparison of polyamine oxidase and monoamine oxidase', *Journal of biological chemistry*, 277, pp. 23973–23976.

Binda, C., Newton-Vinson, P., Hubalek, F., Edmondson, D.E. & Mattevi, A. (2002b) 'Structure of human monoamine oxidase B, a drug target for the treatment of neurological disorders', *Nature structural biology*, 9, pp. 22–26.

Binda, C., Wang, J., Pisani, L., Caccia, C., Carotti, A., Salvati, P., Edmonson, D.E. & Mattevi, A. (2007) 'Structures of human monoamine oxidase B complexes with selective noncovalent inhibitors: safinamide and coumarin analogues', *Journal of medicinal chemistry*, 50, pp. 5848–5852.

Bortolato, M., Chen, K. & Shih, J.C. (2008) 'Monoamine oxidase inactivation: From pathophysiology to therapeutics', *Advanced drug delivery reviews*, 60, pp. 1527–1533.

Boyer, E.W. & Shannon, M. (2005) 'Current concepts: The serotonin syndrome', *New England journal of medicine*, 352, pp. 1112–1120.

Burke, W.J., Kumar, V.B., Pandey, N., Panneton, W.M., Gan, Q., Franko, M.W., O'Dell, M., Li, S.W., Pan, Y., Chung, H.D. & Galvin, J.E. (2008) 'Aggregation of α -synuclein by DOPAL, the monoamine oxidase metabolite of dopamine', *Acta neuropathologica*, 115, pp. 193–203.

Caccia, C., Maj, R., Calabresi, M., Maestroni, S., Faravelli, L., Curatolo, L., Salvati, P. & Fariello, R.G. (2006) 'Safinamide: From molecular targets to a new anti-parkinson drug', *Neurology*, 67(S2), pp. S18–S23.

Carlsson, A. (1959) 'The occurrence, distribution and physiological role of catecholamines in the nervous system', *Pharmacological reviews*, 11, pp. 490–493.

Chen, J.J. & Swope, D.M. (2005) 'Clinical pharmacology of rasagiline: a novel, second-generation propargylamine for the treatment of Parkinsons disease', *Journal of clinical pharmacology*, 45, pp. 878–894.

Chen, J.F., Steyn, S., Staal, R., Petzer, J.P., Xu, K., Van Der Schyf, C.J., Castagnoli, K., Sonsalla, P.K., Castagnoli Jr., N. & Schwarzschild, M.A. (2002) '8-(3-Chlorostyryl)caffeine may attenuate MPTP neurotoxicity through dual actions of monoamine oxidase inhibition and A_{2A} receptor antagonism', *Journal of biological chemistry*, 277, pp. 36040–36044.

Churchyard, A., Mathias, C.J., Boonkongchuen, P. & Lees, A.J. (1997) 'Autonomic effects of selegiline: Possible cardiovascular toxicity in Parkinson's disease', *Journal of neurology, neurosurgery and psychiatry*, 63, pp. 228–234.

Da Prada, M., Kettler, R., Keller, H.H., Cesura, A.M., Richards, J.G., Saura Marti, J., Muggli-Maniglio, D., Wyss, P.C., Kyburz, E. & Imhof, R. (1990) 'From moclobemide to ro 19-6327 and ro 41-1049: The development of a new class reversible, selective MAO-A and MAO-B inhibitors', *Journal of neural transmission*, 29, pp. S279–S292.

Dauer, W. & Przedborski, S. (2003) 'Parkinson's disease: Mechanisms and models', *Neuron*, 39, pp. 889–909.

De Colibus, L., Li, M., Binda, C., Lustig, A., Edmondson, D.E. & Mattevi, A. (2005) 'Three dimensional structure of human monoamine oxidase A (MAO-A): Relation to the structures of rat MAO-A and human MAO-B', *Proceedings of the national academy of sciences of the United States of America*, 102, pp. 12684–12689.

Edmondson, D.E., Binda, C. & Mattevi, A. (2004a) 'The FAD binding sites of human monoamine oxidases A and B', *Neurotoxicology*, 25, pp. 63–72.

Edmondson, D.E., Mattevi, A., Binda, C., Li, M. & Hubálek, F. (2004b) 'Structure and mechanism of monoamine oxidase', *Current medicinal chemistry*, 11, pp. 1983–1993.

Edmondson, D.E., Mattevi, A. & Binda, C. (2007) 'Structural insights into the mechanism of amine oxidation by monoamine oxidases A and B', *Archives of biochemistry and biophysics*, 464, pp. 269–276.

Edmondson, D.E., Binda, C., Wang, J., Upadhyay, A.K. & Mattevi, A. (2009) 'Molecular and mechanistic properties of the membrane-bound mitochondrial monoamine oxidases', *Biochemistry*, 48, pp. 4220–4230.

Finberg, J.P. & Tenne, M. (1982) 'Relationship between tyramine potentiation and selective inhibition of monoamine oxidase types A and B in the rat vas deferens', *British journal of pharmacology*, 77, pp. 13–21.

Finberg, J.P., Tenne, M. & Youdim, M.B. (1981) 'Tyramine antagonistic properties of AGN 1135, an irreversible inhibitor of monoamine oxidase type B', *British journal of pharmacology*, 73, pp. 65–74.

Fernandez, H.H. & Chen, J.J. (2007) 'Monoamine oxidase B inhibition in the treatment of Parkinson's disease', *Pharmacotherapy*, 27, pp. S174–S185.

Fitzpatrick, P.F. (2010) 'Oxidation of amines by flavoproteins', *Archives of biochemistry and biophysics*, 493, pp. 13–25.

Fraaije, M.W.A. & Mattevi, A. (2000) 'Flavoenzymes: Diverse catalysts with recurrent features', *Trends in biochemical sciences*, 25, pp. 126–132.

Glover, V., Sandler, M., Owen, F. & Riley, G.J. (1977) 'Dopamine is a monoamine oxidase B substrate in man', *Nature*, 265, pp. 80–81.

Grünblatt, E., Mandel, S., Jacob-Hirsch, J., Zeligson, S., Amariglio, N., Rechavi, G., Li, J., Ravid, R., Roggendorf, W., Riederer, P. & Youdim, M.B.H. (2004) 'Gene expression profiling of parkinsonian substantia nigra pars compacta; alterations in ubiquitin-proteasome, heat shock protein, iron and oxidative stress regulated proteins, cell adhesion/cellular matrix and vesicle trafficking genes', *Journal of neural transmission*, 111(12), pp. 1543–1573.

Haefely, W., Burkard, W.P., Cesura, A.M., Kettler, R., Lorez, H.P., Martin, J.R., Richards, J.G., Scherschlicht, R. & Da Prada, M. (1992) 'Biochemistry and pharmacology of moclobemide, a prototype RIMA', *Psychopharmacology*, 106, pp. S6–S14.

Hasan, F., McCrodden, J.M., Kennedy, N.P. & Tipton, K.F. (1988) 'The involvement of intestinal monoamine oxidase in the transport and metabolism of tyramine', *Journal of neural transmission*, 26, pp. S1–S9.

Hubálek, F., Binda, C., Khalil, A., Li, M., Mattevi, A., Castagnoli, N. & Edmondson, D.E. (2005) 'Demonstration of isoleucine 199 as a structural determinant for the selective inhibition of human monoamine oxidase B by specific reversible inhibitors', *Journal of biological chemistry*, 280, pp. 15761–15766.

Knoll, J. (1978) 'The possible mechanisms of action of (-)deprenyl in Parkinson's disease', *Journal of neural transmission*, 43, pp. 177–198.

Knoll, J. & Magyar, K. (1972) 'Some puzzling pharmacological effects of monoamine oxidase inhibitors', *Advances in biochemical psychopharmacology*, 5, pp. 393–408.

Lees, A. (2005) 'Alternatives to L-dopa in the initial treatment of early Parkinson's disease', *Drugs and aging*, 22, pp. 731–740.

Lees, A.J., Hardy, J. & Revesz, T. (2009) 'Parkinson's disease', *The lancet*, 373, pp. 2055–2066.

Miller, J.R. & Edmondson, D.E. (1999) 'Influence of flavin analogue structure on the catalytic activities and flavinylation reactions of recombinant human liver monoamine oxidase A and B', *The journal of biological chemistry*, 274, pp. 23515–23525.

Nicotra, A. & Parvez, S.H. (1999) Methods for assaying monoamine oxidase A and B activities: Recent developments', *Biogenic amines*, 15, pp. 307–320.

Nicotra, A., Pierucci, F., Parvez, H. & Senatori, O. (2004) 'Monoamine oxidase expression during development and aging', *Neurotoxicology*, 25, pp. 155–165.

Perez, V., Romera, M., Lizcano, J.M., Marco, J.L. & Unzeta, M. (2003) 'Protective effect of N-(2-propynyl)-2-(5-benzyloxy-indolyl) methylamine (PF 9601N), a novel MAO-B inhibitor, on dopamine-lesioned PC12 cultured cells', *Journal of pharmacy and pharmacology*, 55, pp. 713–716.

Pletscher, A. (1991) 'The discovery of antidepressants: A winding path', *Experientia*, 47, pp. 4–8.

Rascol, O., Goetz, C.G., Koller, W.C. & Poewe, W. (2002a) 'Physical and occupational therapy in Parkinson's disease', *Movement disorders*, 4, pp. 156–159.

Riederer, P., Danielczyk, W. & Grunblatt, E. (2004) 'Monoamine oxidase-B inhibition in Alzheimer's disease', *Neurotoxicology*, 25, pp. 271–277.

Schnaitman, C., Erwin, V.G. & Greenawalt, J.W. (1967) 'The submitochondrial localization of monoamine oxidase. An enzymatic marker for the outer membrane of rat liver mitochondria', *Journal of cell biology*, 32, pp. 719–735.

Shih, J.C., Chen, K., & Ridd, M.J. (1999) 'Monoamine oxidase: from genes to behavior', *Annual review of neuroscience*, 22, pp. 197–217.

Silverman, R.B., Hoffman, S.J. & Catus III, W.B. (1980) 'A mechanism for mitochondrial monoamine oxidase catalyzed amine oxidation', *Journal of the American chemical society*, 102, pp. 7126–7128.

Son, S., Ma, J., Kondou, Y., Yoshimura, M., Yamashita, E. & Tsukihara, T. (2008) 'Structure of human monoamine oxidase A at 2.2-Å resolution: The control of opening the entry for substrates/inhibitors', *The national academy of sciences of the United States of America*, 105, pp. 5739–5744.

Strolin Benedetti, M., Dostert, P. & Tipton, K.F. (1992) 'Developmental aspects of the monoamine-degrading enzyme monoamine oxidase', *Developmental pharmacology and therapeutics*, 18, pp. 191–200.

Symes, A.L., Sourkes, T.L., Youdim, M.B., Gregoriadis, G. & Birnbaum, H. (1969) 'Decreased monoamine oxidase activity in liver of iron-deficient rats', *Canadian journal of biochemistry*, 47(11), pp. 999–1002.

Tipton, K.F., Boyce, S., O'Sullivan, J., Davey, G.P. & Healy, J. (2004) 'Monoamine oxidases: certainties and uncertainties', *Current medicinal chemistry*, 11, pp. 1965–1982.

Tsang, D., Ho, K.P. & Wen, H.L. (1986) 'Ontogenesis of multiple forms of monoamine oxidase in rat brain regions and liver', *Developmental neuroscience*, 8(4), pp. 243–250.

Youdim, M.B.H., Edmondson, D. & Tipton, K.F. (2006), 'The therapeutic potential of monoamine oxidase inhibitors', *Nature reviews. Neuroscience*, 7, pp. 295–309.

Youdim, M.B.H. & Bakhle, Y.S. (2006) 'Monoamine oxidase: Isoforms and inhibitors in Parkinson's disease and depressive illness', *British journal of pharmacology*, 147(S1), pp. S287–S296.

Youdim, M.B.H., Finberg, J.P., & Tipton, K.F. (1988) 'Monoamine oxidase', *Advances in experimental pharmacology*, 2, pp. 119–199.

Youdim, M.B.H. & Weinstock, M. (2004) 'Therapeutic applications of selective and non-selective inhibitors of monoamine oxidase A and B that do not cause significant tyramine potentiation', *Neurotoxicology*, 25, pp. 243–250.

CHAPTER 3

MANUSCRIPT A

Article submitted to Mini-Reviews in Medicinal Chemistry:

A review of the pharmacological properties of 3,4-dihydro-2(1*H*)-quinolinones

The manuscript is written as a review article and is presented according to the author guidelines as stipulated in addendum A.

All co-authors provided permission to use this manuscript as part of L. Meiring's Ph.D thesis.

Letitia Meiring, ¹Jacobus P. Petzer,¹ and Anél Petzer^{1,*}

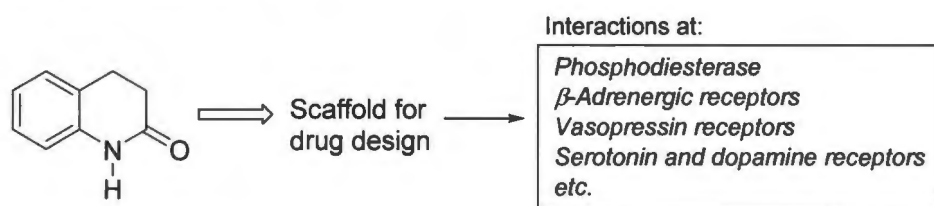
- ¹ *Pharmaceutical Chemistry, School of Pharmacy and Centre of Excellence for Pharmaceutical Sciences, North-West University, Private Bag X6001, Potchefstroom 2520, South Africa*

*Address correspondence to this author at Pharmaceutical Chemistry, School of Pharmacy and Centre of Excellence for Pharmaceutical Sciences, North-West University, Private Bag X6001, Potchefstroom 2520, South Africa; Tel: +27-18-2994464; Fax: +27-18-2994243, E-mail: 12264954@nwu.ac.za

Running title: 3,4-Dihydro-2(1*H*)-quinolinones

Keywords: aripiprazole; carteolol; cilostazol; 3,4-dihydro-2(1*H*)-quinolinone; pharmacology; drug design

Graphical abstract:



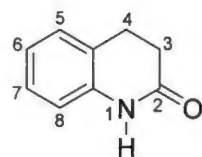
A review of the pharmacological actions of compounds containing the 3,4-dihydro-2(1H)-quinolinone scaffold concludes that the 3,4-dihydro-2(1H)-quinolinone moiety is a versatile and potentially useful scaffold in medicinal chemistry.

ABSTRACT

The 3,4-dihydro-2(1*H*)-quinolinone moiety is present in a number of pharmacologically active compounds. These include registered drugs such as cilostazol, carteolol and aripiprazole as well as numerous experimental compounds. Compounds containing the 3,4-dihydro-2(1*H*)-quinolinone moiety also exhibit a variety of activities in both the peripheral and central tissues, which includes phosphodiesterase inhibition, blocking of β -adrenergic receptors, antagonism of vasopressin receptors and interaction with serotonin and dopamine receptors. Based on its versatility in drug design and action, this paper reviews the pharmacological actions of compounds containing the 3,4-dihydro-2(1*H*)-quinolinone scaffold with emphasis being placed on the most important and significant members of each activity class.

1. INTRODUCTION

Small organic molecules are powerful tools in the medicinal sciences and function as therapeutic and diagnostic agents, as well as probes to elucidate biological processes. In modern medicine, small molecule therapeutics most often exerts pharmacological actions by binding to protein receptors and enzymes. It is therefore not surprising that compounds that bind to a specific protein target bear close structural resemblance and often share a common molecular scaffold. Molecular scaffolds are thus an important concept in medicinal chemistry and are ordinarily the starting point for the design and development of new therapeutics. Since compounds that share a specific molecular scaffold may possess dissimilar pharmacological activities, a specific scaffold may serve as point of departure for different drug design projects. The 3,4-dihydro-2(1*H*)-quinolinone moiety (**1**) is an example of this concept and is present in a variety of compounds exhibiting different biological activities (Fig. 1). Examples of well-known 3,4-dihydro-2(1*H*)-quinolinones are cilostazol (**2**), carteolol (**4**) and aripiprazole (**5**), compounds that have been registered for therapeutic use in humans. A number of experimental compounds also are 3,4-dihydro-2(1*H*)-quinolinones. Based on our interest in the design of quinolinone-derived monoamine oxidase (MAO) inhibitors, we review in this paper the pharmacological properties of compounds containing the 3,4-dihydro-2(1*H*)-quinolinone scaffold [1]. A Pubmed search with the term “3,4-dihydro-2(1*H*)-quinolinone” yields 97 results, which were for the most part considered in compiling this review. This paper will demonstrate the versatility of the 3,4-dihydro-2(1*H*)-quinolinone moiety as useful scaffold for future medicinal chemistry projects.



3,4-Dihydro-2(1*H*)-quinolinone

Fig. 1. The structure of 3,4-dihydro-2(1*H*)-quinolinone (**1**).

2. CHEMISTRY OF 3,4-DIHYDRO-2(1*H*)-QUINOLINONE

3,4-Dihydro-2(1*H*)-quinolinone(**1**) may be considered to be a bicyclic system of a δ -lactam fused to a phenyl ring. 3,4-Dihydro-2(1*H*)-quinolinone exhibits moderate lipophilicity with a calculated logP of 1.34 (ChemSketch) and a pKa of \sim 14, which makes it unionised at physiological pH. The amide may act as both hydrogen donor and acceptor with protein residues. Due to presence of two sp^3 hybridised carbons, the 3,4-dihydro-2(1*H*)-quinolinone moiety is nonplanar (Fig. 2). The amide function of 3,4-dihydro-2(1*H*)-quinolinone is stable towards acid and base catalysed hydrolysis.



Fig. 2. Two perspectives of a low energy conformer of 3,4-dihydro-2(1*H*)-quinolinone (**1**), calculated by the MMFF94 force field.

3. THE PHARMACOLOGY OF 3,4-DIHYDRO-2(1H)-QUINOLINONES

3.1. Phosphodiesterase inhibition

Cilostazol [6-[4-(1-cyclohexyl-1*H*-tetrazol-5-yl)butoxy]-3,4-dihydro-2(1*H*)-quinolinone, OPC-13013, **2**] is a medication approved for the alleviation of intermittent claudication (pain in the legs that occurs with walking and disappears with rest) in individuals with peripheral vascular disease (Fig. 3). In this respect cilostazol inhibits platelet activation but also induces vasodilation [2]. Although it is generally believed that cilostazol may mediate these effects by acting as a specific inhibitor of phosphodiesterase type 3 (PDE3) to elevate intracellular cAMP, the exact mechanism of action is not fully understood [3]. Based on its unique mechanisms of action cilostazol is under investigation as treatment for a variety of indications. For example cilostazol may protect the heart against ischemia/reperfusion injury [4] and exert neuroprotective effects against cerebral ischemia [5].

Cilostazol derivatives have been synthesised as potential inhibitors of 12(S)-hydroxyeicosatetraenoic acid (12-HETE) release from platelets, a process which plays an important role in the pathogenesis of various circulatory disorders and arteriosclerosis. 3,4-Dihydro-6-[3-(1-*o*-tolylimidazol-2-yl)sulfinylpropoxy]-2(1*H*)-quinolinone (**3**) was found to be one of the most potent inhibitors of 12-HETE release, and showed in vivo inhibitory activity on platelet adhesion in rats[6]. The S-(+)-enantiomer of this compound exhibited a superior potency and in vivo activity compared to the R-(-)-enantiomer.

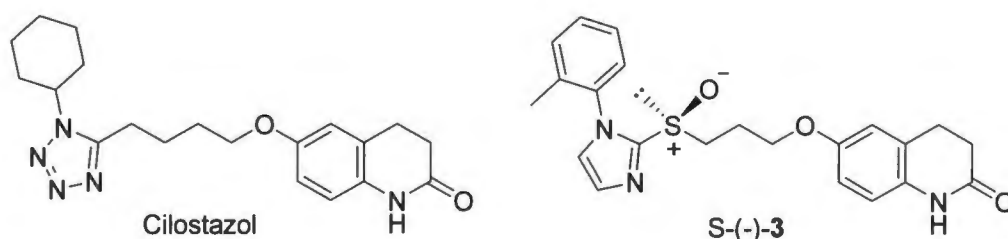


Fig. 3. The structure of cilostazol (**2**) and **3**.

3.2. Blocking of β -adrenergic receptors

3,4-Dihydro-2(1*H*)-quinolinones also may act as antagonists of β -adrenergic receptors. This is exemplified by carteolol [5-(3-tert-butylamino-2-hydroxy-propoxy)-3,4-dihydro-2(1*H*)-quinolinone, **4**], a non-selective β_1 - and β_2 -adrenergic receptor-blocking agent registered for the ophthalmic treatment of glaucoma (Fig. 4). Carteolol is active via the oral and intravenous routes and produces potent, long lasting adrenergic receptor blocking [7]. Carteolol has strong intrinsic sympathomimetic activity (ISA), up to 30-fold more powerful than that of propranolol.

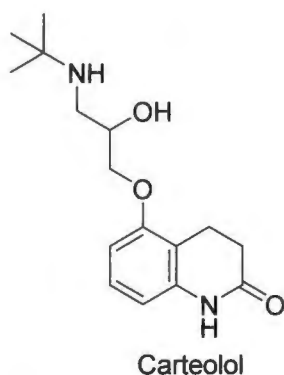


Fig. 4. The structure of carteolol (**4**).

3.3. Interaction with serotonin and dopamine receptors

Aripiprazole [7-(4-[4-(2,3-dichlorophenyl)-1-piperazinyl]butyloxy)-3,4-dihydro-2-(1*H*)-quinolinone, OPC-14597, **5**] is an antipsychotic with a mechanism of action that differs from typical and atypical antipsychotics (Fig. 5). Aripiprazole interacts with a range of receptors, including serotonin (5-HT) and dopamine receptors [8]. In this respect, aripiprazole possesses partial agonist activity at D_2 and 5-HT_{1A} receptors, antagonist activity at 5-HT_{2A} receptors and agonist activity at dopamine autoreceptors [8-10]. Aripiprazole is currently registered for use in schizophrenia and bipolar disorder.

A related compound, OPC-14523 [1-[3-[4-(3-chlorophenyl)-1-piperazinyl]propyl]-5-methoxy-3,4-dihydro-2(1*H*)-quinolinone, **6**] is an experimental antidepressant whose mechanism of action involves potent partial agonist activity at 5-HT_{1A} receptors [11], agonist activity at sigma receptors and possibly inhibition of serotonin reuptake [12,13].

In another study of interest, 3-piperazinyl-3,4-dihydro-2(1*H*)-quinolinone derivatives were designed to act as mixed dopamine D₂/D₄receptor antagonists, an activity profile that is similar to that of clozapine, a clinically used antipsychotic agent [14]. Examples of mixed antagonists are compounds **7** and **8** (Fig. 5). These have the advantage of possessing weak α_1 -affinities, which would minimise undesirable cardiovascular effects. 3,4-Dihydro-2(1*H*)-quinolinone derivatives have also been synthesised and shown to possess high 5-HT_{1A} and 5-HT_{1D} antagonist potencies, with some derivatives also possessing affinities for 5-HT_{1B} and the serotonin transporter (SerT). By acting at 5-HT₁ autoreceptors and the SerT, such compounds, exemplified by structure **9**, control synaptic 5-HT levels and thus represent useful pharmacological tools for animal behavioural and disease models [15].

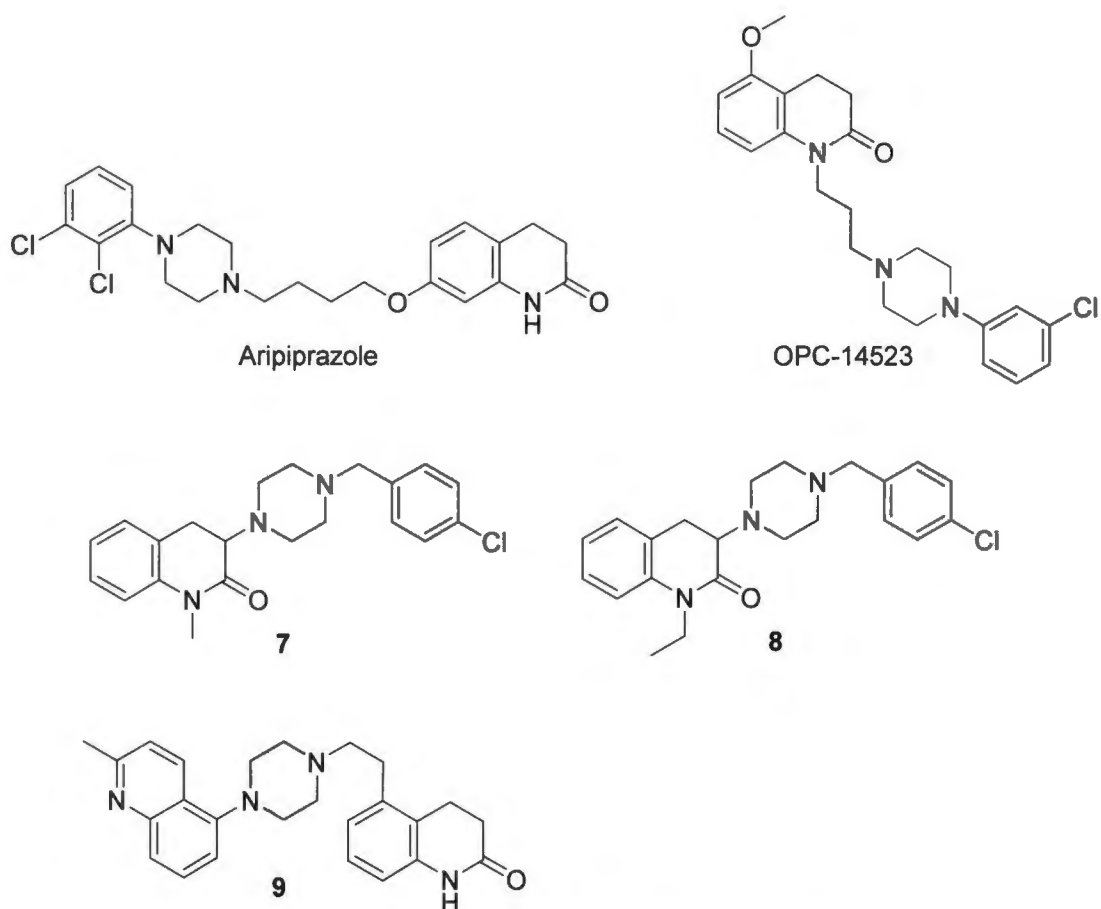


Fig. 5. The structures of aripiprazole (5), OPC-14523(6) and compounds 7–9.

3.4. Antagonism of vasopressin receptors

The arginine vasopressin receptor 1A (V1A receptor or AVPR1A) is one of the three major receptor types for arginine vasopressin (AVP). This receptor is found in the brain as well as in the periphery in the liver, kidney and vasculature [16]. OPC-21268 [1-[1-[4-(3-acetylamino-propoxy)benzoyl]-4-piperidyl]-3,4-dihydro-2(1H)-quinolinone, **10**] is a 3,4-dihydro-2(1H)-quinolinone compound that acts as a vasopressin V1A receptor-selective antagonist (Fig. 6). In vivo, this compound antagonises AVP-induced vasoconstriction and pressor responses. It has thus been suggested that OPC-21268 may be useful for the treatment of hypertension and congestive heart failure [17].

OPC-21268 also serves as a pharmacological tool to probe the physiological roles of V1A receptors and has entered clinical trials for a number of indications, for example for the treatment of albuminuria in patients with non-insulin dependent diabetes mellitus [18].

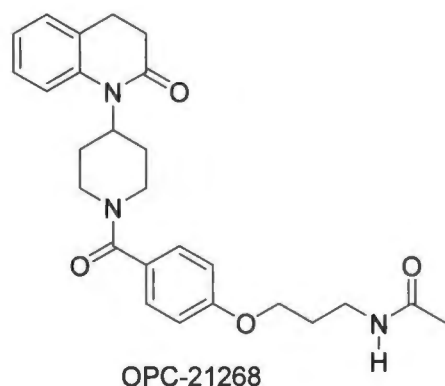


Fig. 6. The structure of OPC-21268 (10).

3.5. Sigma receptor antagonism and agonism

Sigma-1 (σ_1) receptor antagonists possess analgesic properties and may be useful for the management of pain. 3,4-Dihydro-2(1*H*)-quinolinone derivatives have been reported to antagonise σ_1 receptors with compound **11** exhibiting a K_i of 1.22 nM (Fig. 7) [19]. Sigma receptor agonists, in turn, exert antidepressant effects [20]. In this respect, a series of 3,4-dihydro-2(1*H*)-quinolinones have been shown to act as sigma receptor agonists with antidepressant-like activity in animal models [21]. This behaviour is exemplified by OPC-14523 (**6**) which reduces immobility time in the forced-swimming test in mice.

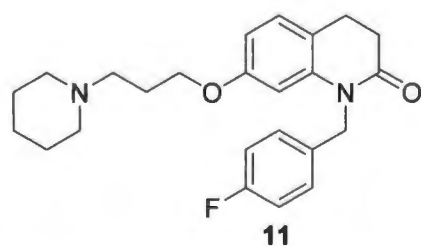


Fig. 7. The structure of compound **11**.

3.6. Muscarinic acetylcholine receptor agonism

77-LH-28-1 [1-[3-(4-butyl-1-piperidinyl)propyl]-3,4-dihydro-2(1*H*)-quinolinone, **12**] is a 3,4-dihydro-2(1*H*)-quinolinone derivative that acts as an allosteric agonist of M1 muscarinic acetylcholine receptors (Fig. 8). Experimental evidence has shown that 77-LH-28-1 is bioavailable and penetrates the blood-brain barrier, making it a suitable tool to study M1 receptor activation in vivo [22]. Selective M1 agonists may represent useful agents for a number of clinical conditions, including improving cognitive deficits and behavioural disturbances in Alzheimer's disease patients [23].

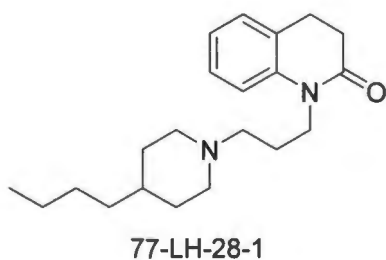


Fig. 8. The structure of 77-LH-28-1 (**12**).

3.7. N-Methyl-D-aspartate (NMDA) antagonism

NMDA receptors are glutamate-gated ion channel proteins that play important roles in many neuronal processes including learning, memory and pain transmission. NMDA receptors are heteromers, consisting of NR1, NR2A, NR2B, NR2C and NR2D subunits. Among these, NMDA receptors with the NR2B-subunits are involved in pain transmission and have thus been targeted for the treatment of pain. Compound **13** [(-)-6-[2-[4-(3-fluorophenyl)-4-hydroxy-1-piperidinyl]-1-hydroxyethyl]-3,4-dihydro-2(1*H*)-quinolinone], a 3,4-dihydro-2(1*H*)-quinolinone derivative, as an orally active and selective antagonist of the NR2B-subunit of NMDA receptors and a potential development candidate for the management of pain (Fig. 9) [24]. This compound exhibits an IC_{50} value of 5 nM for the NR2B-subunit.

3,4-Dihydro-2(1*H*)-quinolinone derivatives have also been designed for combined antagonist activity at the glycine site of the NMDA receptors as well as at AMPA receptors. An example of such a compound is L-698,544 (**14**), which has been found to be active in an anticonvulsant animal model [25].

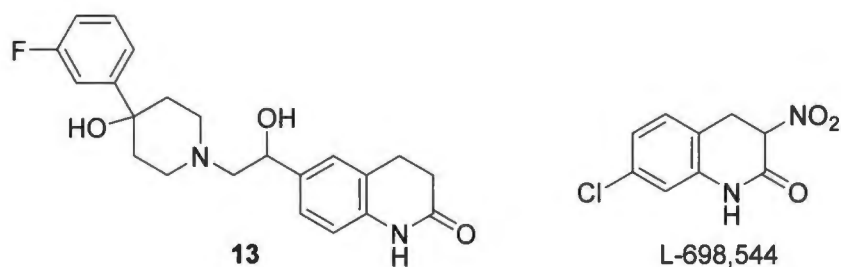


Fig. 9. The structures of compound **13** and L-698,544 (**14**).

3.8. Monoamine oxidase inhibition

The MAO enzymes consist of two genetically distinct isoforms, MAO-A and MAO-B, and are key role-players in the catabolism of neurotransmitters and dietary amines. Inhibitors of the MAOs are of considerable pharmacological importance with MAO-A inhibitors being used as antidepressant agents while MAO-B inhibitors are established therapy for Parkinson's disease [26]. Literature reports that a series of 3,4-dihydro-2(1*H*)-quinolinones acts as specific inhibitors of the MAO-B isoform with the most potent homologue, compound **15**, exhibiting an IC_{50} value of $0.0029 \mu\text{M}$ (Fig. 10) [1]. This compound is much less potent as a MAO-A inhibitor ($IC_{50} = 7.98 \mu\text{M}$). Interestingly, substitution on C7 of the 3,4-dihydro-2(1*H*)-quinolinone moiety yields higher potency inhibition compared to analogous substitution on C6.

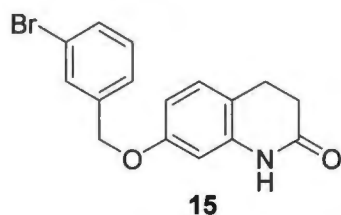


Fig. 10. The structure of compound 15.

3.9. Oxytocin receptor antagonism

3,4-Dihydro-2(1H)-quinolinones have also been considered as antagonists of human oxytocin receptors. Derivative **16** was labeled with [³⁵S] and shown to exhibit sub-nanomolar affinities for human oxytocin receptors, with good selectivity over vasopressin receptors (Fig. 11). Compound **16** therefore represents a potential tool for studying the pharmacology of oxytocin receptors in human and non human primate tissue [27].

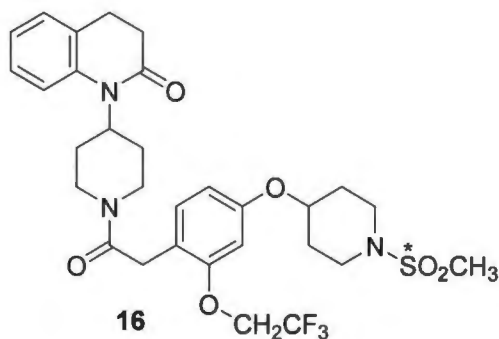


Fig. 11. The structure of compound 16.

3.10. Anticonvulsant activities

As mentioned above, by acting as combined antagonists of NMDA and AMPA receptors, simple 3,4-dihydro-2(1H)-quinolinones (e.g. L-698,544) exert anticonvulsant activity in animal models [25].

Another study reports that simple alkyloxy substitution on C6 of 3,4-dihydro-2(1*H*)-quinolinone also yields compounds with anticonvulsant activity in animals, although the mechanism of action is not clear [28]. This is exemplified by 6-benzyloxy-3,4-dihydro-2(1*H*)-quinolinone (**17**) (Fig. 12).

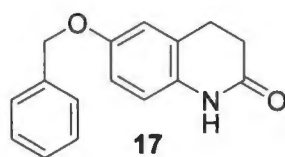


Fig. 12. The structure of compound **17**.

3.11. 3,4-Dihydro-2(1*H*)-quinolinones as contraceptives

A 3,4-dihydro-2(1*H*)-quinolinone compound, 84-182 (3-cyano-3,4-dihydro-2(1*H*)-quinolinone, **18**), has been shown to possess contraceptive activity in female hamsters, guinea pig and rhesus monkeys when administered during the peri-implantation period (the period that extends from the time the blastocyst is free in the uterus, through the processes of attachment, to the start of trophoblast differentiation) (Fig. 13). The compound, however, does not prevent implantation and does not interrupt an established pregnancy [29].

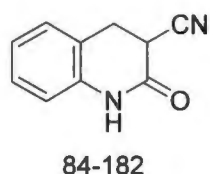


Fig. 13. The structure of 84-182 (**18**).

3.12. Positive inotropic action

Positive inotropic agents increase myocardial contractility, and are used to support cardiac function in various conditions including congestive heart failure, myocardial infarction and cardiomyopathy. Cilostazol (**2**), by acting as a specific inhibitor of PDE3, is a positive inotropic agent, useful for the treatment of congestive heart failure. Y-20487 [6-(3,6-dihydro-2-oxo-2*H*-1,3,4-thiadiazin-5-yl)-3,4-dihydro-2(1*H*)-quinolinone, **19**] is another example of such a cardiotoxic agent and acts by inhibition of both PDE3 and PDE4 isoenzymes (Fig. 14) [30]. In this regard, PDE4 inhibition may reduce the breakdown of cAMP generated by β -adrenergic receptor stimulation while inhibition of PDE3 may result in cAMP accumulation and thus a direct inotropic effect. Another positive inotropic agent, OPC-8212 [3,4-dihydro-6-[4-(3,4-dimethoxybenzoyl)-1-piperazinyl]-2(1*H*)-quinolinone, **20**], is a compound that produces bradycardia and antitachycardiac effects in animals and humans [31]. This compound may act by elevating intracellular cAMP levels, leading to activation of calcium currents. This compound, also known as vesnarinone, possesses unique and complex mechanisms of action and inhibits PDE3, which increases intracellular calcium, and also affects numerous myocardial ion channels. Vesnarinone has been used for the treatment of advanced congestive heart failure, but has been withdrawn from the market due to a narrow therapeutic window [32-34].

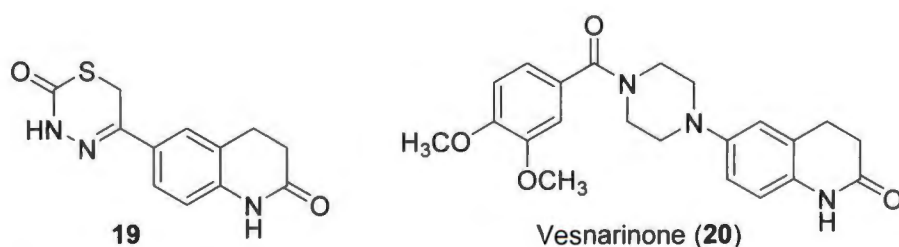


Fig. 14. The structures of Y-20487 (**19**) and OPC-8212 (vesnarinone, **20**).

4. NATURAL PRODUCTS CONTAINING 3,4-DIHYDRO-2(1H)-QUINOLINONES

It is interesting to note that 3,4-dihydro-2(1H)-quinolinones have been found as secondary metabolites in natural products. Microbial fungi isolated from marine sources have been considered for their potential of providing new natural products that are structurally unusual and biologically highly active. In this respect 3,4-dihydro-2(1H)-quinolinones **21–24** have been isolated from *Penicilliumjanczewskii* cultures and found to possess some degree of cytotoxicity towards mammalian tissue cultures (Fig. 15) [35].

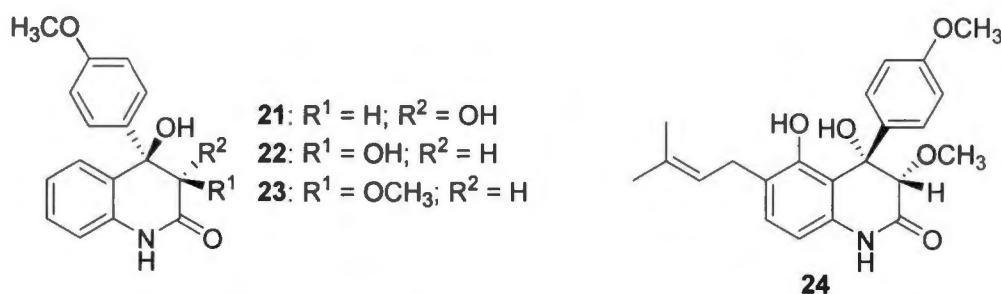


Fig. 15. The structures of compounds **21–24**.

5. METABOLISM OF 3,4-DIHYDRO-2(1H)-QUINOLINONES

In drug design, metabolism is an important consideration since this may, to a large extent, determine the bioavailability and toxicity profiles of a compound. Some knowledge of the metabolic transformation of 3,4-dihydro-2(1H)-quinolinone may be obtained from studies with drugs containing this moiety. For example, carteolol is converted, with species-specific differences, almost exclusively and to a relatively small extent into 8-hydroxycarteolol, a reaction catalysed by cytochrome P450 (CYP) 2D6 (Fig. 16) [7,36]. Glucuronides and oxidative O-dealkylation of carteolol and 8-hydroxycarteolol are also possible [37,38]. Cilostazol, in turn, undergoes hydroxylation to yield OPC-13326 as predominant metabolite and OPC-13217 as second most predominant metabolite (Fig. 17). These transformations are catalysed by CYP3A4 and CYP3A5, respectively [39].

Metabolism of aripiprazole occurs via CYP3A4 and CYP2D6 to yield dehydroaripiprazole (OPC-14857) as principal metabolite (Fig. 18) [40,41]. This transformation possibly occurs via dehydration of the 4-hydroxy metabolite. Vesnarinone, in turn, is metabolised by CYP2E1 and CYP3A4 to its primary metabolite OPC-18692 (Fig. 19) [42]. In this instance, metabolism occurs in the side chain and not the 3,4-dihydro-2(1*H*)-quinolinone moiety of vesnarinone[43]. From these examples, it may be concluded that the principal metabolic reaction of the 3,4-dihydro-2(1*H*)-quinolinone moiety is aliphatic hydroxylation on the C4 position, which may be followed by dehydration to yield the 2-oxoquinoline metabolite. Aromatic hydroxylation of the phenyl ring also is a possibility, which may be followed by phase 2 reactions such as glucuronidation.

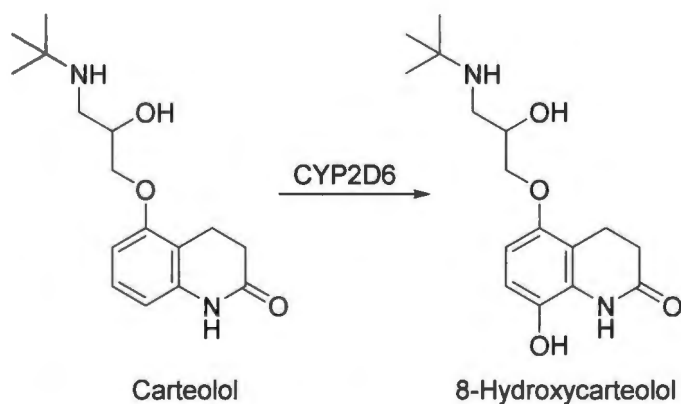


Fig. 16. The metabolism of carteolol.

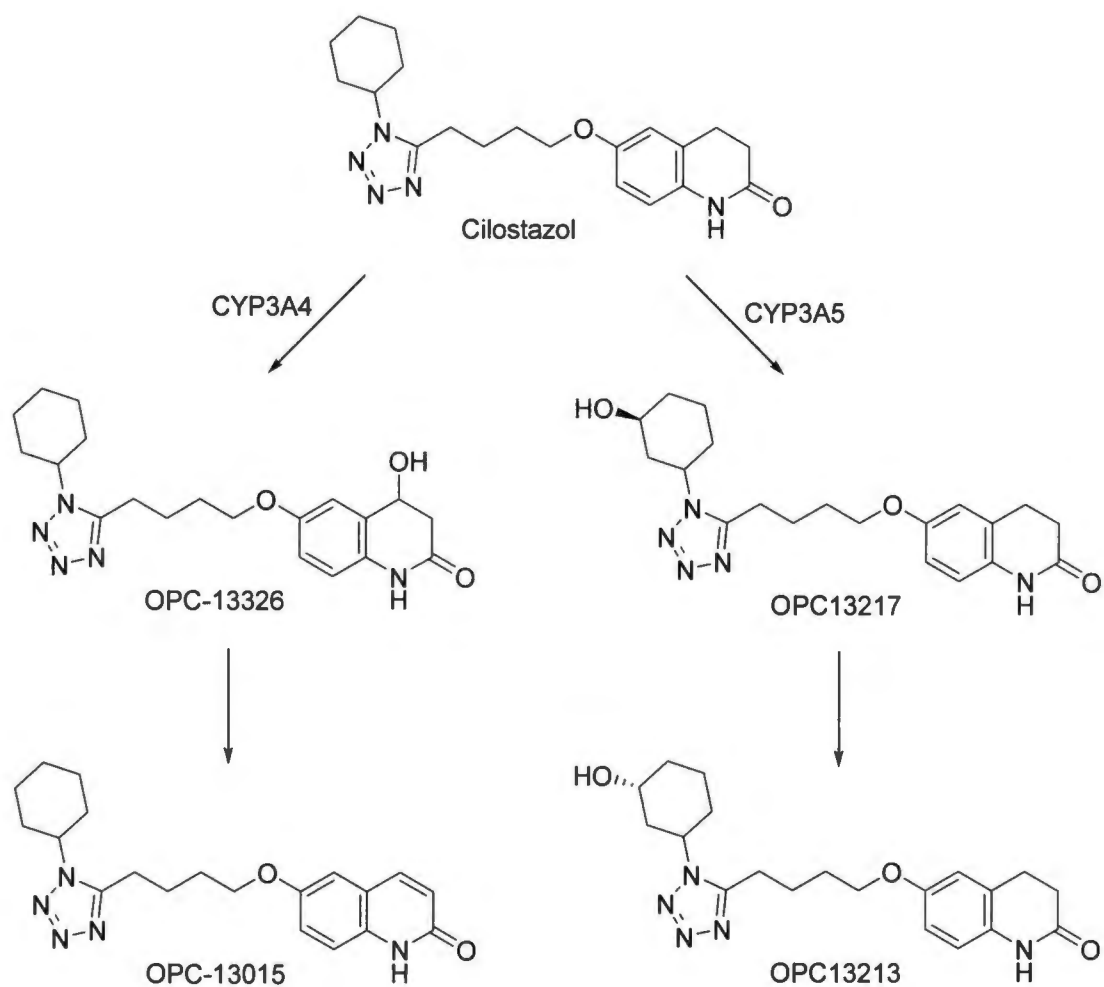


Fig. 17. The metabolism of cilostazol.

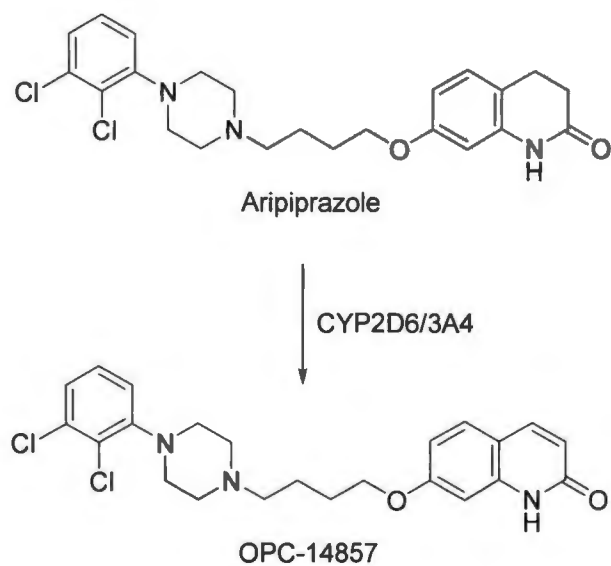


Fig. 18. The metabolism of aripiprazole to its major metabolite, dehydroaripiprazole (OPC-14857).

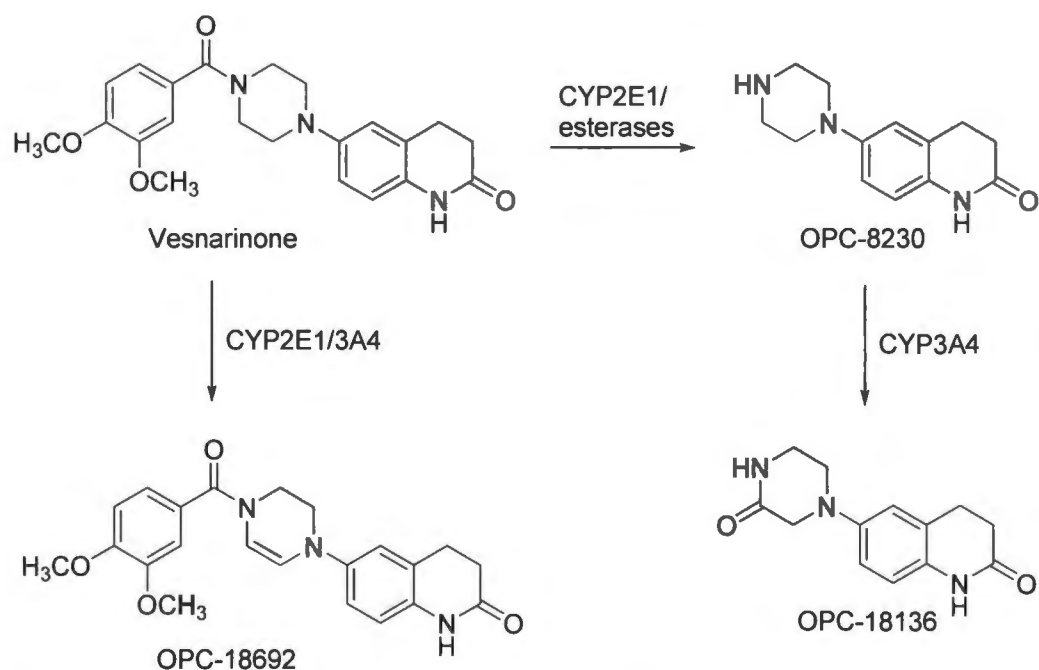


Fig. 19. The metabolism of vesnarinone to its major metabolite, OPC-18692.

6. CONCLUSION

This review shows that the 3,4-dihydro-2(1H)-quinolinone moiety is present in a number of pharmacologically active compounds, acting in the peripheral tissues as well as the central nervous system. Although it is not nearly as abundant in drug structures as many other scaffolds, 3,4-dihydro-2(1H)-quinolinone most likely would be an appropriate choice for many drug design projects. In this respect, an analysis of the metabolic routes of selected 3,4-dihydro-2(1H)-quinolinones does not alert to any potential liabilities. The 3,4-dihydro-2(1H)-quinolinone moiety has the distinct advantage of many points of attachment for functional groups and side chains, and with substitution on C3 and C4 chiral compounds can be generated. It may thus be concluded that the 3,4-dihydro-2(1H)-quinolinone moiety is a versatile and potentially useful scaffold in the medicinal chemist's toolkit.

CONFLICT OF INTEREST

The authors confirm that this article content has no conflict of interest.

ACKNOWLEDGEMENTS

This work is based on the research supported in part by the National Research Foundation of South Africa (Grant specific unique reference numbers (UID) 85642, 96180). The Grantholders acknowledge that opinions, findings and conclusions or recommendations expressed in any publication generated by the NRF supported research are that of the authors, and that the NRF accepts no liability whatsoever in this regard.

REFERENCES

- [1] Meiring, L.; Petzer, J.P.; Petzer, A. Inhibition of monoamine oxidase by 3,4-dihydro-2(1H)-quinolinone derivatives. *Bioorg. Med. Chem.Lett.*,**2013**,*23*(20), 5498-5502.
- [2] Schror, K. The pharmacology of cilostazol. *Diabetes Obes.Metab.*,**2002**,*4*(Suppl 2), S14-S19.
- [3] Sun, B.; Le, S.N.; Lin, S.; Fong, M.; Guertin, M.; Liu, Y.; Tandon, N.N.; Yoshitake, M.; Kambayashi, J. New mechanism of action for cilostazol: interplay between adenosine and cilostazol in inhibiting platelet activation. *J.Cardiovasc.Pharmacol.***2002**,*40*(4), 577-585.
- [4] Fukasawa, M.; Nishida, H.; Sato, T.; Miyazaki, M.; Nakaya, H. 6-[4-(1-Cyclohexyl-1H-tetrazol-5-yl)butoxy]-3,4-dihydro-2-(1H)quinolinone (cilostazol), a phosphodiesterase type 3 inhibitor, reduces infarct size via activation of mitochondrial Ca²⁺-activated K⁺ channels in rabbit hearts. *J.Pharmacol. Exp.Ther.*,**2008**,*326*(1), 100-104.
- [5] Nonaka, Y.; Koumura, A.; Hyakkoku, K.; Shimazawa, M.; Yoshimura, S.; Iwama, T.; Hara, H. Combination treatment with normobarichyperoxia and cilostazol protects mice against focal cerebral ischemia-induced neuronal damage better than each treatment alone. *J.Pharmacol. Exp.Ther.*,**2009**,*330*(1), 13-22.
- [6] Uno, T.; Ozeki, Y.; Koga, Y.; Chu, G.N.; Okada, M.; Tamura, K.; Igawa, T.; Unemi, F.; Kido, M.; Nishi, T. Synthesis of 2(1H)-quinolinone derivatives and their inhibitory activity on the release of 12(S)-hydroxyeicosatetraenoic acid (12-HETE) from platelets. *Chem. Pharm. Bull.*,**1995**,*43*(10), 1724-1733.
- [7] Odenthal, K.P.Pharmacodynamics of carteolol. *Arzneimittel-Forsch.*,**1983**,*33*(2a), 281-285.
- [8] Stark, A.D.; Jordan, S.; Allers, K.A.; Bertekap, R.L.; Chen, R.; MistryKannan, T.; Molski, T.F.; Yocca, F.D.; Sharp, T.; Kikuchi, T.; Burris, K.D. Interaction of the novel antipsychotic aripiprazole with 5-HT1A and 5-HT2A receptors: functional receptor-binding and in vivo electrophysiological studies. *Psychopharmacology*,**2007**,*190*(3), 373-382.
- [9] Tadori, Y.; Kitagawa, H.; Forbes, R.A.; McQuade, R.D.; Stark, A.; Kikuchi, T. Differences in agonist/antagonist properties at human dopamine D(2) receptors between aripiprazole, bifeprunox and SDZ 208-912. *Eur. J.Pharmacol.*,**2007**,*574*(2-3), 103-111.

- [10] Oshiro, Y.; Sato, S.; Kurahashi, N.; Tanaka, T.; Kikuchi, T.; Tottori, K.; Uwahodo, Y.; Nishi, T. Novel antipsychotic agents with dopamine autoreceptor agonist properties: synthesis and pharmacology of 7-[4-(4-phenyl-1-piperazinyl)butoxy]-3,4-dihydro-2(1H)-quinolinone derivatives. *J. Med. Chem.*, **1998**, *41*(5), 658-667.
- [11] Jordan, S.; Chen, R.; Koprivica, V.; Hamilton, R.; Whitehead, R.E.; Tottori, K.; Kikuchi, T. In vitro profile of the antidepressant candidate OPC-14523 at rat and human 5-HT_{1A} receptors. *Eur. J. Pharmacol.*, **2005**, *517*(3), 165-173.
- [12] Bermack, J.E.; Haddjeri, N.; Debonnel, G. Effects of the potential antidepressant OPC-14523 [1-[3-[4-(3-chlorophenyl)-1-piperazinyl]propyl]-5-methoxy-3,4-dihydro-2-quinolinone monomethanesulfonate] a combined sigma and 5-HT_{1A} ligand: modulation of neuronal activity in the dorsal raphe nucleus. *J. Pharmacol. Exp. Ther.*, **2004**, *310*(2), 578-583.
- [13] Tottori, K.; Miwa, T.; Uwahodo, Y.; Yamada, S.; Nakai, M.; Oshiro, Y.; Kikuchi, T.; Altar, C.A. Antidepressant-like responses to the combined sigma and 5-HT_{1A} receptor agonist OPC-14523. *Neuropharmacology*, **2001**, *41*(8), 976-988.
- [14] Zhao, H.; Thurkauf, A.; Braun, J.; Brodbeck, R.; Kieltyka, A. Design, synthesis, and discovery of 3-piperazinyl-3,4-dihydro-2(1H)-quinolinone derivatives: a novel series of mixed dopamine D₂/D₄ receptor antagonists. *Bioorg. Med. Chem. Lett.*, **2000**, *10*(18), 2119-2122.
- [15] Bromidge, S.M.; Arban, R.; Bertani, B.; Borriello, M.; Capelli, A.M.; Di-Fabio, R.; Faedo, S.; Gianotti, M.; Gordon, L.J.; Granci, E.; Pasquarello, A.; Spada, S.K.; Worby, A.; Zonzini, L.; Zucchelli, V. 5-{2-[4-(2-Methyl-5-quinolinyl)-1-piperazinyl]ethyl}-2(1H)-quinolinones and 3,4-dihydro-2(1H)-quinolinones: dual-acting 5-HT₁ receptor antagonists and serotonin reuptake inhibitors. Part 3. *Bioorg. Med. Chem. Lett.*, **2010**, *20*(23), 7092-7096.
- [16] Caldwell, H.K.; Lee, H.J.; Macbeth, A.H.; Young, W.S. Vasopressin: behavioral roles of an "original" neuropeptide. *Prog. Neurobiol.*, **2008**, *84*(1), 1-24.
- [17] Yamamura, Y.; Ogawa, H.; Chihara, T.; Kondo, K.; Onogawa, T.; Nakamura, S.; Mori, T.; Tominaga, M.; Yabuuchi, Y. OPC-21268, an orally effective, nonpeptide vasopressin V₁ receptor antagonist. *Science*, **1991**, *252*(5005), 572-574.

- [18] Nishikawa, T.; Omura, M.; Iizuka, T.; Saito, I.; Yoshida, S. Short-term clinical trial of 1-(1-[4-(3-acetylaminopropoxy)-benzoyl]-4-piperidyl)-3,4-dihydro-2(1H)-quinolinone in patients with diabetic nephropathy. Possible effectiveness of the specific vasopressin V1 receptor antagonist for reducing albuminuria in patients with non-insulin dependent diabetes mellitus. *Arzneimittel-Forsch.*, **1996**, *46*(9), 875-878.
- [19] Lan, Y.; Chen, Y.; Xu, X.; Qiu, Y.; Liu, S.; Liu, X.; Liu, B.F.; Zhang, G. Synthesis and biological evaluation of a novel sigma-1 receptor antagonist based on 3,4-dihydro-2(1H)-quinolinone scaffold as a potential analgesic. *Eur. J. Med. Chem.*, **2014**, *79*, 216-230.
- [20] Matsuno, K.; Kobayashi, T.; Tanaka, M.K.; Mita, S. Sigma 1 receptor subtype is involved in the relief of behavioral despair in the mouse forced swimming test. *Eur. J. Pharmacol.*, **1996**, *312*(3), 267-271.
- [21] Oshiro, Y.; Sakurai, Y.; Sato, S.; Kurahashi, N.; Tanaka, T.; Kikuchi, T.; Tottori, K.; Uwahodo, Y.; Miwa, T.; Nishi, T. 3,4-dihydro-2(1H)-quinolinone as a novel antidepressant drug: synthesis and pharmacology of 1-[3-[4-(3-chlorophenyl)-1-piperazinyl]propyl]-3,4-dihydro-5-methoxy-2(1H)-quinolinone and its derivatives. *J. Med. Chem.*, **2000**, *43*(2), 177-189.
- [22] Langmead, C.J.; Austin, N.E.; Branch, C.L.; Brown, J.T.; Buchanan, K.A.; Davies, C.H.; Forbes, I.T.; Fry, V.A.; Hagan, J.J.; Herdon, H.J.; Jones, G.A.; Jeggo, R.; Kew, J.N.; Mazzali, A.; Melarange, R.; Patel, N.; Pardoe, J.; Randall, A.D.; Roberts, C.; Roopun, A.; Starr, K.R.; Teriakidis, A.; Wood, M.D.; Whittington, M.; Wu, Z.; Watson, J. Characterization of a CNS penetrant, selective M1 muscarinic receptor agonist, 77-LH-28-1. *Br. J. Pharmacol.*, **2008**, *154*(5), 1104-1115.
- [23] Heinrich, J.N.; Butera, J.A.; Carrick, T.; Kramer, A.; Kowal, D.; Lock, T.; Marquis, K.L.; Pausch, M. H.; Popiolek, M.; Sun, S.C.; Tseng, E.; Uveges, A.J.; Mayer, S.C. Pharmacological comparison of muscarinic ligands: historical versus more recent muscarinic M1-preferring receptor agonists. *Eur. J. Pharmacol.*, **2009**, *605*(1-3), 53-56.
- [24] Kawai, M.; Ando, K.; Matsumoto, Y.; Sakurada, I.; Hirota, M.; Nakamura, H.; Ohta, A.; Sudo, M.; Hattori, K.; Takashima, T.; Hizue, M.; Watanabe, S.; Fujita, I.; Mizutani, M.; Kawamura, M. Discovery of (-)-6-[2-[4-(3-fluorophenyl)-4-hydroxy-1-piperidinyl]-1-hydroxyethyl]-3,4-dihydro-2(1H)-quinolinone - a potent NR2B-selective N-methyl D-aspartate (NMDA) antagonist for the treatment of pain. *Bioorg. Med. Chem. Lett.*, **2007**, *17*(20), 5558-5562.

- [25] Carling, R.W.; Leeson, P.D.; Moore, K.W.; Smith, J.D.; Moyes, C.R.; Mawer, I.M.; Thomas, S.; Chan, T.; Baker, R.; Foster, A.C.; Grimwood, S.; Kemp, J.A.; Marshall, G.R.; Tricklebank, M.D.; Saywell, K.L. 3-Nitro-3,4-dihydro-2(1H)-quinolones. Excitatory amino acid antagonists acting at glycine-site NMDA and (RS)-alpha-amino-3-hydroxy-5-methyl-4-isoxazolepropionic acid receptors. *J. Med. Chem.*, **1993**, *36*(22), 3397-3408.
- [26] Ramsay, R.R. Inhibitor design for monoamine oxidases. *Curr. Pharm. Des.*, **2013**, *19*(14), 2529-2539.
- [27] Lemaire, W.; O'Brien, J.A.; Burno, M.; Chaudhary, A.G.; Dean, D.C.; Williams, P.D.; Freidinger, R. M.; Pettibone, D.J.; Williams, D.L., Jr. A nonpeptide oxytocin receptor antagonist radioligand highly selective for human receptors. *Eur. J. Pharmacol.*, **2002**, *450*(1), 19-28.
- [28] Quan, Z.-S.; Wang, J.-M.; Rho, J.-R.; Kwak, K.-C.; Kang, H.-C.; Jun, C.-S.; Chai, K.-Y. Synthesis of 6-alkyloxyl-3,4-dihydro-2(1H)-quinolones and their anticonvulsant activities. *Bull. Korean Chem. Soc.*, **2005**, *26*(11), 1757-1760.
- [29] Singh, M.M.; Mehrotra, P.K.; Agnihotri, A.; Srivastava, R.P.; Seth, M.; Bhaduri, A.P.; Kamboj, V.P. Contraceptive and hormonal properties of a new 1,4-dihydro-2-oxoquinoline derivative (compound 84-182) in rodents and rhesus monkeys. *Contraception*, **1987**, *36*(2), 239-251.
- [30] Katano, Y.; Endoh, M. Effects of a cardiotonicquinolinone derivative Y-20487 on the isoproterenol-induced positive inotropic action and cyclic AMP accumulation in rat ventricular myocardium: comparison with rolipram, Ro 20-1724, milrinone, and isobutylmethylxanthine. *J. Cardiovasc. Pharmacol.*, **1992**, *20*(5), 715-722.
- [31] Yatani, A.; Imoto, Y.; Schwartz, A.; Brown, A.M. New positive inotropic agent OPC-8212 modulates single Ca^{2+} channels in ventricular myocytes of guinea pig. *J. Cardiovasc. Pharmacol.*, **1989**, *13*(6), 812-819.
- [32] Cavusoglu, E.; Frishman, W.H.; Klapholz, M. Vesnarinone: a new inotropic agent for treating congestive heart failure. *J. Card. Fail.*, **1995**, *1*(3), 249-257.
- [33] Feldman, A.M. Clinical characteristics of vesnarinone. *Drug Saf.*, **2004**, *27*(Suppl 1), 1-9.
- [34] Wu, Y.; Piao, H.R. The progress towards the development of DHQO derivatives and related analogues with inotropic effects. *Mini Rev. Med. Chem.*, **2013**, *13*(12), 1801-1811.

- [35] He, J.; Lion, U.; Sattler, I.; Gollmick, F.A.; Grabley, S.; Cai, J.; Meiners, M.; Schunke, H.; Schaumann, K.; Dechert, U.; Krohn, M. Diastereomericquinolinone alkaloids from the marine-derived fungus *Penicilliumjanczewskii*. *J. Nat. Prod.*,**2005**, *68*(9), 1397-1399.
- [36] Umehara, K.; Kudo, S.; Odomi, M. Involvement of CYP2D1 in the metabolism of carteolol by male rat liver microsomes. *Xenobiotica*,**1997**,*27*(11), 1121-1129.
- [37] Lang, W. Animal experimental studies on the pharmacokinetics of carteolol. *Arzneimittel-Forsch.*,**1983**,*33*(2a), 286-289.
- [38] Kudo, S.; Uchida, M.; Odomi, M. Metabolism of carteolol by cDNA-expressed human cytochrome P450. *Eur. J.Clin.Pharmacol.*,**1997**,*52*(6), 479-485.
- [39] Hiratsuka, M.; Hinai, Y.; Sasaki, T.; Konno, Y.; Imagawa, K.; Ishikawa, M.; Mizugaki, M. Characterization of human cytochrome p450 enzymes involved in the metabolism of cilostazol. *Drug Metab. Dispos.*,**2007**,*35*(10), 1730-1732.
- [40] Kubo, M.; Mizooku, Y.; Hirao, Y.; Osumi, T. Development and validation of an LC-MS/MS method for the quantitative determination of aripiprazole and its main metabolite, OPC-14857, in human plasma. *J. Chromatogr. B*, **2005**, *822*(1-2), 294-299.
- [41] Molden, E.; Lunde, H.; Lunder, N.; Refsum, H. Pharmacokinetic variability of aripiprazole and the active metabolite dehydroaripiprazole in psychiatric patients. *Ther. Drug Monit.*,**2006**, *28*(6), 744-749.
- [42] Wandel, C.; Lang, C.C.; Cowart, D.C.; Girard, A.F.; Bramer, S.; Flockhart, D.A.; Wood, A.J. Effect of CYP3A inhibition on vesnarinone metabolism in humans. *Clin. Pharmacol. Ther.*,**1998**,*63*(5), 506-511.
- [43] Frye, R.F.; Tammara, B.; Cowart, T.D.; Bramer, S.L. Effect of disulfiram-mediated CYP2E1 inhibition on the disposition of vesnarinone. *J.Clin.Pharmacol.*,**1999**,*39*(11), 1177-1183.

CHAPTER 4

MANUSCRIPT B

Article submitted to Drug Research:

C6- and C7-Substituted 3,4-dihydro-2(1*H*)-quinolinones as inhibitors of monoamine oxidase.

The manuscript is written as a research article and is presented according to the author guidelines as stipulated in addendum B.

Authors' contributions:

- The experimental work, interpretation of results and documentation of this study was carried out by L. Meiring.
- This study was conceptualised and documented with the assistance of J.P Petzer.
- The enzymology section of this study was conducted under the supervision of A. Petzer.

All co-authors provided permission to use this manuscript as part of L. Meiring's Ph.D thesis.

C6- and C7-Substituted 3,4-dihydro-2(1H)-quinolinones as inhibitors of monoamine oxidase

Letitia Meiring,¹ Jacobus P. Petzer,¹ Anél Petzer¹

¹ *Pharmaceutical Chemistry, School of Pharmacy and Centre of Excellence for Pharmaceutical Sciences, North-West University, Private Bag X6001, Potchefstroom 2520, South Africa*

Correspondence to: Prof. A. Petzer, PhD, Pharmaceutical Chemistry, School of Pharmacy, North-West University, Private Bag X6001, Potchefstroom 2520, South Africa; Tel.: +27 18 2994464; Fax: +27 18 2994243
E-mail: 12264954@nwu.ac.za

Running title: Quinolinones as inhibitors of MAO

Abstract

Purpose: Monoamine oxidase (MAO) inhibitors are considered to be useful therapeutic agents and isoform specific inhibitors are employed for the treatment of depression and Parkinson's disease. MAO inhibitors are also under investigation for the treatment of disorders ranging from Alzheimer's disease, prostate cancer and certain cardiomyopathies. While a number of irreversible MAO inhibitors are available in the clinic, reversible inhibitors, particularly of the MAO-B isoform are still being developed. Based on our interest in discovering reversible inhibitors with specificity for MAO-B, we have recently reported that, among a series of ten 3,4-dihydro-2(1*H*)-quinolinone derivatives, are high potency MAO-B inhibitors, with a number of homologues displaying good selectivities for MAO-B over the MAO-A isoform.

Methods and findings: To expand on these promising findings and to derive structure-activity relationships, the current study synthesizes a series of fourteen 3,4-dihydro-2(1*H*)-quinolinone derivatives. An evaluation of their MAO inhibition properties shows that all derivatives are MAO-B specific with the most potent inhibitor (**3a**) displaying an IC₅₀ value of 0.0014 μM. Selectivities for MAO-B ranged from 99 to 40,000-fold.

Conclusions: It may thus be concluded that substitution of 3,4-dihydro-2(1*H*)-quinolinone on C6 and C7 with a variety of side chains yields highly potent and selective MAO-B inhibitors, compounds with existing and prospective therapeutic applications.

Keywords: monoamine oxidase, MAO, reversible inhibition, 3,4-dihydro-2(1*H*)-quinolinone, structure-activity relationship.

Introduction

The monoamine oxidases (MAOs) are key metabolic enzymes that are expressed in most mammalian tissues. The two isoforms, MAO-A and MAO-B, metabolize neurotransmitter amines such as serotonin, noradrenaline, adrenaline and dopamine, thereby terminating their physiological actions in the peripheral tissues and central nervous system [1]. Since the MAOs modulate the levels of key neurotransmitters, inhibitors of these enzymes have been used in the clinic for the treatment of neuropsychiatric and neurodegenerative disorders such as depression and Parkinson's disease [1]. In the central nervous system, serotonin is mostly metabolized by the MAO-A isoform, and MAO-A inhibitors are considered effective treatment of major depression [2,3]. MAO-B inhibitors are used for the treatment of Parkinson's disease where they prevent the metabolic degradation (by MAO-B) of dopamine in the brain. In this regard, MAO-B inhibitors are often combined with L-dopa, the direct metabolic precursor of dopamine and treatment of choice [4–6]. MAO-B inhibitors thus enhance the therapeutic efficacy of L-dopa and allow for a reduction of the effective L-dopa dosage.

The MAOs also are metabolic barriers, preventing dietary amines from entering the systemic circulation and brain. Thus intestinal (and peripheral) MAO-A metabolizes the sympathomimetic amine, tyramine (present in cheese, wine etc.), and prevents it from entering the systemic circulation in excessive amounts, which could lead to a potentially severe rise in blood pressure. This response, termed the “cheese effect”, is often observed when irreversible MAO-A inhibitors are combined with tyramine-containing food, and imposes the restrictive use of these drugs in the clinic [7–9]. MAO-B in the brain microvasculature, in turn, represents a metabolic barrier for β -phenethylamine entry into the brain.

β -Phenethylamine is a false neurotransmitter which releases neuronal dopamine and inhibits its active uptake [10,11]. MAO-B inhibitors drastically increase the brain levels of β -phenethylamine and the resulting enhancement of extracellular dopamine concentrations may, at least in part, be responsible for the symptomatic benefit of these drugs in Parkinson's disease [12].

Paradoxically, the MAOs may also activate xenobiotics to yield metabolites which may be extremely harmful, as exemplified by the activation of 1-methyl-4-phenyl-1,2,3,6-tetrahydropyridine (MPTP) by MAO-B to yield 1-methyl-4-phenylpyridinium (MPP⁺), a compound that induces a parkinsonian syndrome in experimental animals and humans [13].

The by-products of the MAO catalytic cycle also is of pharmacological and toxicological interest. Hydrogen peroxide and aldehyde intermediates formed by the MAOs may be injurious if not effectively cleared. In the brain these species may damage neuronal cells and contribute to neurodegeneration in disorders such as Parkinson's disease [14,15]. The MAO-B isoform seems to be of relevance in this regard since MAO-B activity increases as the human brain ages, while MAO-A activity remains largely unchanged [16]. Based on these considerations it has been suggested that inhibitors of MAO-B may be neuroprotective in age-related diseases such as Parkinson's disease. Hydrogen peroxide formed by MAO-A in the heart, in turn, has been implicated in age-related cardiac cellular degeneration in rats [17], thus establishing a rationale for MAO-A inhibitors as treatment for certain cardiomyopathies. Recently the role of MAO-A inhibitors in cancer treatment has been investigated. MAO-A levels are found to be elevated in certain types of cancer tissue such as prostate cancer, and MAO-A inhibition may, in synergism with survivin suppressants, inhibit cancer cell growth, migration and invasion [18,19].

Based on the pharmacological importance of the MAOs, the discovery of potent and isoform specific inhibitors are pursued by a number of research groups [20–22]. As discussed above, inhibitors specific for the MAO-B isoform are appropriate for Parkinson's disease therapy for the following reasons: (a) MAO-B inhibition conserves central dopamine and enhance dopamine levels after L-dopa therapy, (b) MAO-B inhibition increases the brain levels of β -phenethylamine, which leads to the indirect enhancement of extracellular dopamine concentrations, (c) MAO-B inhibition reduces harmful metabolic by-products of MAO-B in the brain, thereby protecting against neurodegeneration and (d) MAO-B inhibition may prevent the activation of proneurotoxins such as MPTP.

We have recently reported that a series of 3,4-dihydro-2(1*H*)-quinolinone derivatives are high potency MAO-B inhibitors with certain homologues displaying good specificity [23]. For example, the most potent MAO-B inhibitor, 7-(3-bromobenzyloxy)-3,4-dihydro-2(1*H*)-quinolinone (**1a**), exhibits an IC_{50} value of 0.0029 μ M with a 2751-fold selectivity for MAO-B over the MAO-A isoform (Fig. 1). Another compound, 7-(3-chlorobenzyloxy)-3,4-dihydro-2(1*H*)-quinolinone (**1b**) inhibits MAO-B with an IC_{50} of 0.0062 μ M, while displaying an IC_{50} of >100 μ M for MAO-A. Importantly, it was found that substitution on the C7 position of the 3,4-dihydro-2(1*H*)-quinolinone moiety leads to significantly more potent inhibition compared to substitution on C6, and that a benzyloxy substituent on C7 is more favorable than 2-phenylethoxy and 3-phenylpropoxy substitution. Based on the promising potencies and specificities displayed by some of these 3,4-dihydro-2(1*H*)-quinolinones, the present study aims to discover additional homologues with high MAO-B inhibition potencies and specificities, and to further derive structure-activity relationships (SARs).

For this purpose, the current study synthesizes a series of fourteen 3,4-dihydro-2(1*H*)-quinolinone derivatives (Table 1).

As shown, substitution with the benzyloxy, phenylethoxy and 2-phenoxyethoxy moieties on both C6 (compounds **2**) and C7 (compounds **3**) were considered.

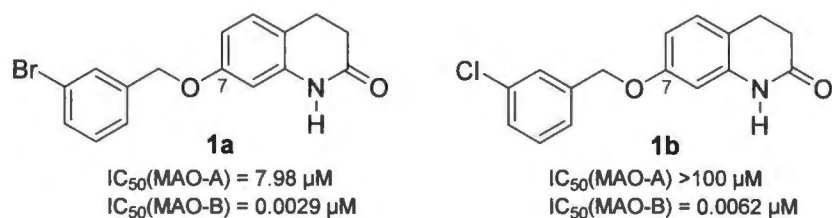


Fig. 1. The structures of 7-(3-bromobenzyloxy)-3,4-dihydro-2(1*H*)-quinolinone (**1a**) and 7-(3-chlorobenzyloxy)-3,4-dihydro-2(1*H*)-quinolinone (**1b**).

Materials and methods

Chemicals and instrumentation

Reagents and solvents required for the chemistry and biology were obtained from Sigma-Aldrich (St. Louis, MO, USA) and were used without further purification.

Kynuramedihydrobromide and insect cell microsomes containing recombinant human MAO-A and MAO-B (5 mg protein/mL) were also obtained from Sigma-Aldrich. ^1H NMR and ^{13}C NMR spectra were recorded with a BrukerAvance III 600 spectrometer (Karlsruhe, Germany) employing DMSO-d_6 as solvent. The chemical shifts are given in parts per million (δ) and were referenced to the residual solvent signal. The spin multiplicities are given as s (singlet), d (doublet), dd (doublet of doublets), t (triplet) or m (multiplet). High resolution mass spectra (HRMS) were recorded with a Bruker micrOTOF-Q II mass spectrometer functioning in atmospheric-pressure chemical ionization (APCI) mode (positive mode). Melting points (mp) were measured with a Büchi B-545 melting point apparatus (Büchi Labortechnik, Flawil, Switzerland) and are uncorrected.

The progress of reactions was monitored with silica gel 60 aluminum coated TLC sheets (Merck, Darmstadt, Germany).

For this purpose the mobile phase consisted of ethyl acetate, and the developed sheets were visualized under an UV-lamp at a wavelength of 254 nm. Fluorescence spectrophotometry was carried out with a Varian Cary Eclipse fluorescence spectrophotometer (Agilent Technologies, Santa Clara, USA) equipped with a microplate reader.

Chemistry

Procedure for the synthesis of 3,4-dihydro-2(1H)-quinolinone derivatives 2a–g and 3a–g

The 3,4-dihydro-2(1H)-quinolinone derivatives were prepared according to a previously reported protocol from the key reagents, 6-hydroxy-3,4-dihydro-2(1H)-quinolinone (**4**) and 7-hydroxy-3,4-dihydro-2(1H)-quinolinone (**5**), which are commercially available (Sigma-Aldrich) [23]. Reagents **4** or **5** (1.50 mmol) was suspended in ethanol (6 mL) containing KOH (1.66 mmol), and the required alkyl bromide (1.50 mmol) was added. The reaction was heated at reflux for 5 h and, upon completion (as judged by TLC), was poured into aqueous NaOH (1%). The precipitate that formed was collected by filtration and crystallized from ethanol.

6-(4-Chlorobenzyloxy)-3,4-dihydro-2(1H)-quinolinone (2a)

The title compound was prepared in a yield of 6%: mp 194.3 °C (ethanol). ¹H NMR (600 MHz, DMSO-*d*₆) δ 9.92 (s, 1H), 7.42 (s, 4H), 6.84 (d, *J* = 2.5 Hz, 1H), 6.80 – 6.72 (m, 2H), 5.01 (s, 2H), 2.80 (t, *J* = 7.6 Hz, 2H), 2.38 (t, *J* = 7.6 Hz, 2H). ¹³C NMR (151 MHz, DMSO-*d*₆) δ 169.93, 153.37, 136.39, 132.37, 132.08, 129.47, 128.47, 124.99, 115.85, 114.52, 113.37, 68.67, 30.37, 25.14. APCI-HRMS *m/z*: calcd for C₁₆H₁₅ClN₂O₂(MH⁺), 288.0786, found 288.0776.

6-(4-Bromobenzyloxy)-3,4-dihydro-2(1H)-quinolinone (2b)

The title compound was prepared in a yield of 4%: mp 185.2 – 212.7 °C (ethanol). ¹H NMR (600 MHz, DMSO-*d*₆) δ 9.92 (s, 1H), 7.56 (d, *J* = 8.3 Hz, 2H), 7.37 (d, *J* = 8.6 Hz, 2H), 6.84 (d, *J* = 2.5 Hz, 1H), 6.80 – 6.72 (m, 2H), 5.00 (s, 2H), 2.80 (t, *J* = 7.5 Hz, 2H), 2.38 (t, *J* = 7.5 Hz, 2H). ¹³C NMR (151 MHz, DMSO-*d*₆) δ 169.91, 153.34, 136.82, 132.08, 131.38, 129.77, 124.98, 120.89, 115.84, 114.51, 113.37, 68.68, 30.36, 25.13. APCI-HRMS *m/z*: calcd for C₁₆H₁₅BrNO₂ (MH⁺), 332.0281, found 332.0260.

6-(3-Methylbenzyloxy)-3,4-dihydro-2(1H)-quinolinone (2c)

The title compound was prepared in a yield of 44%: mp 163.3 °C (ethanol). ¹H NMR (600 MHz, DMSO-*d*₆) δ 9.92 (s, 1H), 7.25 (t, *J* = 7.5 Hz, 1H), 7.22 (s, 1H), 7.19 (d, *J* = 7.6 Hz, 1H), 7.11 (d, *J* = 7.4 Hz, 1H), 6.85 (d, *J* = 2.5 Hz, 1H), 6.80 – 6.73 (m, 2H), 4.97 (s, 2H), 2.81 (t, *J* = 7.5 Hz, 2H), 2.38 (t, *J* = 7.4 Hz, 2H), 2.30 (s, 3H). ¹³C NMR (151 MHz, DMSO-*d*₆) δ 169.79, 153.58, 137.55, 137.20, 131.92, 128.39, 128.31, 128.18, 124.88, 124.72, 115.76, 114.38, 113.24, 69.50, 30.35, 25.11, 21.02. APCI-HRMS *m/z*: calcd for C₁₇H₁₈NO₂ (MH⁺), 268.1332, found 268.1357.

6-(4-Methylbenzyloxy)-3,4-dihydro-2(1H)-quinolinone (2d)

The title compound was prepared in a yield of 37%: mp 173.3 – 177 °C (ethanol). ¹H NMR (600 MHz, DMSO-*d*₆) δ 9.91 (s, 1H), 7.29 (d, *J* = 7.9 Hz, 2H), 7.17 (d, *J* = 7.8 Hz, 2H), 6.84 (d, *J* = 2.5 Hz, 1H), 6.79 – 6.72 (m, 2H), 4.96 (s, 2H), 2.80 (t, *J* = 7.5 Hz, 2H), 2.38 (t, *J* = 7.4 Hz, 2H), 2.28 (s, 3H). ¹³C NMR (151 MHz, DMSO-*d*₆) δ 169.79, 153.55, 136.97, 134.23, 131.88, 128.95, 127.72, 124.85, 115.74, 114.41, 113.29, 69.36, 30.35, 25.11, 20.79. APCI-HRMS *m/z*: calcd for C₁₇H₁₈NO₂ (MH⁺), 268.1332, found 268.1324.

6-[2-(3-Methylphenyl)ethoxy]-3,4-dihydro-2(1H)-quinolinone (2e)

The title compound was prepared in a yield of 6%: mp 135.6 °C (ethanol). ¹H NMR (600 MHz, DMSO-*d*₆) δ 9.90 (s, 1H), 7.17 (t, *J* = 7.5 Hz, 1H), 7.10 (s, 1H), 7.07 (d, *J* = 7.7 Hz, 1H), 7.01 (d, *J* = 7.5 Hz, 1H), 6.79 – 6.72 (m, 2H), 6.70 (dd, *J* = 8.6, 2.7 Hz, 1H), 4.08 (t, *J* = 6.9 Hz, 2H), 2.94 (t, *J* = 6.9 Hz, 2H), 2.80 (t, *J* = 7.6 Hz, 2H), 2.37 (t, *J* = 7.6 Hz, 2H), 2.27 (s, 3H). ¹³C NMR (151 MHz, DMSO-*d*₆) δ 169.84, 153.63, 138.31, 137.36, 131.76, 129.61, 128.23, 126.92, 126.01, 124.91, 115.82, 114.07, 113.01, 68.48, 35.01, 30.38, 25.09, 21.05. APCI-HRMS *m/z*: calcd for C₁₈H₂₀NO₂ (MH⁺), 282.1489, found 282.1473.

6-[2-(4-Methylphenyl)ethoxy]-3,4-dihydro-2(1H)-quinolinone (2f)

The title compound was prepared in a yield of 19%: mp 152.1 °C (ethanol). ¹H NMR (600 MHz, DMSO-*d*₆) δ 9.90 (s, 1H), 7.17 (d, *J* = 7.8 Hz, 2H), 7.09 (d, *J* = 7.7 Hz, 2H), 6.77 – 6.71 (m, 2H), 6.69 (dd, *J* = 8.6, 2.7 Hz, 1H), 4.06 (t, *J* = 6.9 Hz, 2H), 2.92 (t, *J* = 6.9 Hz, 2H), 2.79 (t, *J* = 7.6 Hz, 2H), 2.37 (t, *J* = 7.4 Hz, 2H), 2.25 (s, 3H). ¹³C NMR (151 MHz, DMSO-*d*₆) δ 169.90, 153.67, 135.35, 135.25, 131.75, 128.93, 128.86, 124.94, 115.85, 114.08, 113.00, 68.57, 34.66, 30.39, 25.10, 20.71. APCI-HRMS *m/z*: calcd for C₁₈H₂₀NO₂ (MH⁺), 282.1489, found 282.1484.

6-[2-Phenoxyethoxy]-3,4-dihydro-2(1H)-quinolinone (2g)

The title compound was prepared in a yield of 6%. ¹H NMR (600 MHz, DMSO-*d*₆) δ 9.93 (s, 1H), 7.28 (t, *J* = 7.3 Hz, 2H), 7.01 – 6.88 (m, 3H), 6.82 (s, 1H), 6.79 – 6.72 (m, 2H), 4.29 – 4.24 (m, 2H), 4.24 – 4.18 (m, 2H), 2.81 (t, *J* = 7.7 Hz, 2H), 2.39 (t, *J* = 7.7 Hz, 2H). ¹³C NMR (151 MHz, DMSO-*d*₆) δ 169.85, 158.32, 153.51, 131.97, 129.58, 124.95, 120.76, 115.84, 114.49, 114.13, 113.12, 66.61, 66.24, 30.37, 25.12. APCI-HRMS *m/z*: calcd for C₁₇H₁₈NO₃ (MH⁺), 284.1281, found 284.1273.

7-(4-Chlorobenzoyloxy)-3,4-dihydro-2(1H)-quinolinone (3a)

The title compound was prepared in a yield of 56%: mp 162.4 – 163.3 °C (ethanol). ¹H NMR (600 MHz, CDCl₃) δ 9.06 (s, 1H), 7.33 (s, 4H), 7.02 (d, *J* = 8.2 Hz, 1H), 6.55 (dd, *J* = 8.3, 2.5 Hz, 1H), 6.45 (d, *J* = 2.4 Hz, 1H), 4.97 (s, 2H), 2.87 (t, *J* = 7.5 Hz, 2H), 2.60 (t, *J* = 7.6 Hz, 2H). ¹³C NMR (151 MHz, CDCl₃) δ 172.28, 158.04, 138.27, 135.25, 133.73, 128.73, 128.71, 128.62, 116.21, 108.94, 102.63, 69.30, 30.95, 24.51. APCI-HRMS *m/z*: calcd for C₁₆H₁₅ClNO₂ (MH⁺), 288.0786, found 288.0790.

7-(4-Bromobenzoyloxy)-3,4-dihydro-2(1H)-quinolinone (3b)

The title compound was prepared in a yield of 25%: mp 193.4 – 194.5 °C (ethanol). ¹H NMR (600 MHz, DMSO-*d*₆) δ 10.01 (s, 1H), 7.56 (d, *J* = 8.2 Hz, 2H), 7.36 (d, *J* = 8.3 Hz, 2H), 7.03 (d, *J* = 8.3 Hz, 1H), 6.53 (dd, *J* = 8.3, 2.5 Hz, 1H), 6.48 (d, *J* = 2.5 Hz, 1H), 5.00 (s, 2H), 2.76 (t, *J* = 7.5 Hz, 2H), 2.39 (t, *J* = 7.5 Hz, 2H). ¹³C NMR (151 MHz, DMSO-*d*₆) δ 170.39, 157.35, 139.26, 136.58, 131.38, 129.75, 128.48, 120.93, 116.06, 107.85, 102.18, 68.40, 30.73, 24.04. APCI-HRMS *m/z*: calcd for C₁₆H₁₅BrNO₂ (MH⁺), 332.0281, found 332.0259.

7-(3-Methylbenzoyloxy)-3,4-dihydro-2(1H)-quinolinone (3c)

The title compound was prepared in a yield of 39%: mp 151.3 °C (ethanol). ¹H NMR (600 MHz, DMSO-*d*₆) δ 10.01 (s, 1H), 7.25 (t, *J* = 7.5 Hz, 1H), 7.22 (s, 1H), 7.19 (d, *J* = 7.7 Hz, 1H), 7.12 (d, *J* = 7.4 Hz, 1H), 7.03 (d, *J* = 8.2 Hz, 1H), 6.54 (dd, *J* = 8.2, 2.5 Hz, 1H), 6.50 (d, *J* = 2.5 Hz, 1H), 4.97 (s, 2H), 2.76 (t, *J* = 7.6 Hz, 2H), 2.39 (t, *J* = 7.3 Hz, 2H), 2.30 (s, 3H). ¹³C NMR (151 MHz, DMSO-*d*₆) δ 170.33, 157.59, 139.22, 137.59, 136.97, 128.45, 128.42, 128.34, 128.20, 124.74, 115.83, 107.80, 102.08, 69.22, 30.73, 24.02, 21.01. APCI-HRMS *m/z*: calcd for C₁₇H₁₈NO₂ (MH⁺), 268.1332, found 268.1328.

7-(4-Methylbenzyloxy)-3,4-dihydro-2(1H)-quinolinone (3d)

The title compound was prepared in a yield of 7%: mp 152.1 °C (ethanol). ¹H NMR (600 MHz, DMSO-*d*₆) δ 10.00 (s, 1H), 7.29 (d, *J* = 8.0 Hz, 2H), 7.17 (d, *J* = 7.8 Hz, 2H), 7.02 (d, *J* = 8.2 Hz, 1H), 6.53 (dd, *J* = 8.3, 2.5 Hz, 1H), 6.49 (d, *J* = 2.5 Hz, 1H), 4.96 (s, 2H), 2.75 (t, *J* = 7.5 Hz, 2H), 2.39 (t, *J* = 7.5 Hz, 2H), 2.28 (s, 3H). ¹³C NMR (151 MHz, DMSO-*d*₆) δ 170.32, 157.56, 139.21, 137.04, 134.01, 128.97, 128.40, 127.74, 115.79, 107.85, 102.12, 69.08, 30.73, 24.01, 20.78. APCI-HRMS *m/z*: calcd for C₁₇H₁₈NO₂ (MH⁺), 268.1332, found 268.1318.

7-[2-(4-Methylphenyl)ethoxy]-3,4-dihydro-2(1H)-quinolinone (3e)

The title compound was prepared in a yield of 9%: mp 160 – 161.8 °C (ethanol). ¹H NMR (600 MHz, DMSO-*d*₆) δ 9.96 (s, 1H), 7.17 (d, *J* = 7.8 Hz, 2H), 7.10 (d, *J* = 7.7 Hz, 2H), 7.02 (d, *J* = 8.3 Hz, 1H), 6.47 (dd, *J* = 8.3, 2.5 Hz, 1H), 6.41 (d, *J* = 2.5 Hz, 1H), 4.05 (t, *J* = 6.9 Hz, 2H), 2.93 (t, *J* = 6.9 Hz, 2H), 2.75 (t, *J* = 7.5 Hz, 2H), 2.39 (t, *J* = 7.5 Hz, 2H), 2.25 (s, 3H). ¹³C NMR (151 MHz, DMSO-*d*₆) δ 170.34, 157.63, 139.20, 135.26, 135.18, 128.91, 128.82, 128.47, 115.62, 107.62, 101.65, 68.27, 34.47, 30.75, 24.00, 20.68. APCI-HRMS *m/z*: calcd for C₁₈H₂₀NO₂ (MH⁺), 282.1489, found 282.1480.

7-[2-Phenoxyethoxy]-3,4-dihydro-2(1H)-quinolinone (3f)

The title compound was prepared in a yield of 5%: mp 180 – 186.5 °C (ethanol). ¹H NMR (600 MHz, DMSO-*d*₆) δ 10.01 (s, 1H), 7.28 (t, *J* = 7.9 Hz, 2H), 7.05 (d, *J* = 8.3 Hz, 1H), 7.00 – 6.89 (m, 3H), 6.53 (dd, *J* = 8.3, 2.5 Hz, 1H), 6.47 (d, *J* = 2.5 Hz, 1H), 4.31 – 4.24 (m, 2H), 4.24 – 4.16 (m, 2H), 2.77 (t, *J* = 7.5 Hz, 2H), 2.40 (t, *J* = 7.6 Hz, 2H). ¹³C NMR (151 MHz, DMSO-*d*₆) δ 170.41, 158.32, 157.59, 139.28, 129.61, 128.55, 120.82, 115.98, 114.52, 107.55, 101.91, 66.40, 66.17, 30.76, 24.04. APCI-HRMS *m/z*: calcd for C₁₇H₁₈NO₃ (MH⁺), 284.1281, found 284.1254.

7-[2-(4-Chlorophenoxy)ethoxy]-3,4-dihydro-2(1H)-quinolinone (3g)

The title compound was prepared in a yield of 25%: mp 153.2 °C (ethanol). ¹H NMR (600 MHz, DMSO-*d*₆) δ 10.01 (s, 1H), 7.32 (d, *J* = 9.0 Hz, 2H), 7.05 (d, *J* = 8.2 Hz, 1H), 7.00 (d, *J* = 9.0 Hz, 2H), 6.52 (dd, *J* = 8.3, 2.6 Hz, 1H), 6.46 (d, *J* = 2.5 Hz, 1H), 4.31 – 4.24 (m, 2H), 4.23 – 4.16 (m, 2H), 2.77 (t, *J* = 7.5 Hz, 2H), 2.40 (t, *J* = 7.6 Hz, 2H). ¹³C NMR (151 MHz, DMSO-*d*₆) δ 170.32, 157.51, 157.18, 139.26, 129.29, 128.49, 124.46, 116.30, 115.97, 107.49, 101.87, 66.67, 66.26, 30.72, 24.01. APCI-HRMS *m/z*: calcd for C₁₇H₁₇ClNO₃ (MH⁺), 318.0891, found 318.0875.

Enzymology

Procedure for the measurement of IC₅₀ values for the inhibition of MAO

The protocol for the measurement of IC₅₀ values for the inhibition of the MAOs has been reported in literature [24,25]. In short, the enzyme reactions were carried out to a volume of 200 μ L in 96-well microtiter plates and contained kynuramine (50 μ M), the test inhibitors (0.003–100 μ M), and potassium phosphate buffer (pH 7.4, 100 mM).

Each reaction also contained 4% DMSO as co-solvent, and control reactions, performed in the absence of inhibitor, were included for each inhibitor evaluated. The enzyme reactions were initiated with the addition of recombinant human MAO-A (0.0075 mg protein/mL) or MAO-B (0.015 mg protein/mL) and incubated for 20 min at 37 °C. The reactions were subsequently terminated with the addition of 80 μ L sodium hydroxide (2 N) and the oxidation product of kynuramine, 4-hydroxyquinoline, was quantified by fluorescence spectrophotometry ($\lambda_{\text{ex}} = 310$; $\lambda_{\text{em}} = 400$ nm) [26].

A linear calibration curve was prepared with authentic 4-hydroxyquinoline (0.047–1.56 μ M). The rate data were fitted to the one site competition model of the Prism 5 software package (GraphPad, San Diego, CA, USA) to obtain sigmoidal plots, from which the IC₅₀ values were estimated. All measurements were carried out in triplicate and IC₅₀ values are given as the mean \pm standard deviation (SD).

Procedure for examining the reversibility of inhibition by dialysis

The protocol for investigating the reversibility of MAO inhibition by dialysis has been reported in literature [24,25]. Recombinant human MAO-B (0.03 mg protein/mL) was combined with the test inhibitor (**2b**) and the mixture (0.8 mL) was preincubated for 15 min at 37 °C. These preincubations were carried out in potassium phosphate buffer (100 mM, pH 7.4) containing 5% sucrose.

Employing this buffer also as dialysis buffer, the mixtures were subsequently dialyzed at 4 °C. For this purpose Slide-A-Lyzer dialysis cassettes with a molecular weight cut-off of 10 000 and a sample volume capacity of 0.5–3 mL were used (Thermo Scientific, Waltham, MA, USA). The dialysis buffer was replaced with fresh buffer at 3 h and 7 h after the start of dialysis. After 24 h of dialysis, the reactions were diluted twofold with the addition of kynuramine to give a final substrate concentration of 50 μ M and a final inhibitor concentration of $2 \times IC_{50}$.

The reactions (500 μ L) were incubated for 20 min at 37 °C, and were subsequently terminated with the addition of NaOH (400 μ L of 2 N) and 1000 μ L water. The fluorescence emission of 4-hydroxyquinoline in these reactions was measured as described above, employing a 3.5 mL quartz cuvette (pathlength 10 \times 10 mm). As negative control, MAO-B was preincubated and dialyzed in the absence of inhibitor. As positive control, MAO-B was preincubated and dialyzed in the presence of a concentration equal to $4 \times IC_{50}$ of the irreversible inhibitor, (R)-deprenyl ($IC_{50} = 0.079 \mu$ M) [27]. Also included in the study were undialyzed mixtures of MAO-B and **2b**, which were maintained at 4 °C for 24 h and diluted and assayed as above. All reactions were carried out in triplicate and the residual enzyme rates are given as mean \pm SD.

Procedure for the construction of Lineweaver-Burk plots

The protocol for constructing Lineweaver-Burk plots has been reported in literature [24,25]. For the inhibition of MAO-B by **2b**, six Lineweaver-Burk plots were constructed. The first plot was constructed in the absence of inhibitor, while the remaining five plots were constructed in the presence of the following inhibitor concentrations: $\frac{1}{4} \times IC_{50}$, $\frac{1}{2} \times IC_{50}$, $\frac{3}{4} \times IC_{50}$, $1 \times IC_{50}$ and $1\frac{1}{4} \times IC_{50}$. For each plot, kynuramine served as substrate at eight different concentrations (15–250 μ M).

After addition of the inhibitor and substrate, the enzymatic reactions (500 μ L) were initiated with the addition of MAO-B (0.015 mg/mL). The enzyme reactions and activity measurements were subsequently carried out as described above for the dialysis experiments and the K_i value was estimated by global (shared) fitting of the inhibition data to the Michaelis-Menten equation using the Prism 5 software package. The K_i value may also be estimated from a plot of the slopes of the Lineweaver-Burke plots versus inhibitor concentration (x-axis intercept equals $-K_i$).

Computer modeling

Procedure for docking with CDOCKER

The procedure for docking with CDOCKER has been reported in literature [24,28]. For the docking studies, the Windows-based Discovery Studio 3.1 software package (Accelrys, San Diego, CA, USA) was used and the reported X-ray crystal structures of human MAO-A (PDB code 2Z5X) and human MAO-B (PDB code 2V5Z) served as protein models [29,30]. The protein models were prepared by firstly calculating the pKa values and protonation states of the ionizable amino acids and subsequently adding hydrogen atoms to the models at pH 7.4. The FAD was set to the oxidized state, fixed atom constraints were applied to the protein backbones and the models were energy minimized using the Smart Minimizer algorithm. With the exception of HOH 710, 718 and 739 in MAO-A, and HOH 1155, 1170 and 1351 in the A-chain of MAO-B, all waters and the co-crystallized ligands were removed and docking was carried out with the CDOCKER algorithm. Ten random conformations were generated for each ligand, the heating target temperature was set to 700 K and full potential mode was used.

The docking solutions were finally refined using in situ ligand minimization with the Smart Minimizer algorithm. The illustrations were prepared with PyMol (Schrödinger, New York, NY, USA) [31].

Results and Discussion

Chemistry

The 3,4-dihydro-2(1*H*)-quinolinone derivatives **2a–g** and **3a–g** were synthesized according to the reported protocol (Fig.2) [32,23]. 6-Hydroxy-3,4-dihydro-2(1*H*)-quinolinone (**4**) or 7-hydroxy-3,4-dihydro-2(1*H*)-quinolinone (**5**), which are commercially available, were suspended in ethanol and treated with the required arylalkyl bromide.

Potassium hydroxide served as base. The reaction mixture was heated at reflux for 5 h and poured into aqueous sodium hydroxide (1%). A precipitate was obtained which was recrystallized from ethanol to yield the target 3,4-dihydro-2(1*H*)-quinolinone derivatives in yields of 4–56%. The structures of **2a–g** and **3a–g** were characterized by ¹H NMR, ¹³C NMR and mass spectrometry as given in the supplementary material. On the ¹H NMR spectra, two triplets at approximately 2.8 and 2.4 ppm represent the methylene protons of the 3,4-dihydro-2(1*H*)-quinolinone moiety, while the NH signals are present at 9–10 ppm. On the ¹³C NMR spectra, the signal of the carbonyl carbon is found at approximately 170 ppm. For **2a–g** the proton on C5 are represented by doublets at approximately 6.85 ppm, while the proton on C7 are represented by a signal at approximately 6.70 ppm (doublet of doublets). For **3a–g** the proton on C8 are represented by doublets at approximately 6.45 ppm, while the protons on C5 and C6 are represented by signals at approximately 7.02 ppm (doublet) and 6.55 ppm (doublet of doublets).

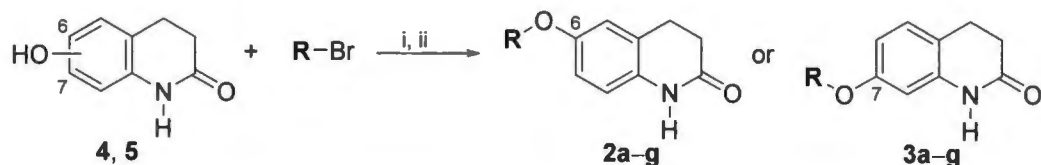


Fig.2. The synthesis of 3,4-dihydro-2(1H)-quinolinone derivatives **2a-g** and **3a-g**. Reagents and conditions: (i) KOH, ethanol, reflux; (ii) recrystallization from ethanol.

IC₅₀ values and SARs for MAO inhibition

The inhibition of the human MAOs by derivatives **2a-g** and **3a-g** was examined under identical experimental conditions as those of the reported 3,4-dihydro-2(1H)-quinolinones [23]. This allows for the direct comparison of IC₅₀ values recorded in this study with those cited in the literature report.

IC₅₀ values were measured by recording the catalytic rates of human MAO-A and MAO-B in the presence of different concentrations of the test inhibitors spanning at least three orders of magnitude (0.0003–100 μM). Sigmoidal dose–response curves (catalytic rate versus logarithm of inhibitor concentration) were constructed in triplicate from which the IC₅₀ values were estimated. The recombinant human MAOs served as enzyme sources and kynuramine was used as substrate for both isoforms. Kynuramine is oxidized by the MAOs to yield 4-hydroxyquinoline, a metabolite which may (after alkalization) be measured at the endpoint of the enzymatic reaction using fluorescence spectrophotometry. Examples of sigmoidal dose–response curves obtained in this study are shown in [fig. 3](#). As shown in [Table 1](#), substitution on both C6 and C7 was considered in order to determine if substitution on C7 of the 3,4-dihydro-2(1H)-quinolinone moiety in all instances lead to significantly more potent inhibition compared to substitution on C6, as proposed in a previous study [23].

This study also explores the effect of *meta* and *para* substitution of the benzyloxy side chain with bromine, chlorine and the methyl group for comparison with compounds **1a** and **1b**, previously reported [23]. The effect of the 2-phenoxyethoxy moiety and methyl substituted 2-phenylethoxy side chains were also investigated. The 2-phenoxyethoxy moiety, in particular has been shown to enhance the MAO-B inhibition potency of caffeine derived inhibitors [33].

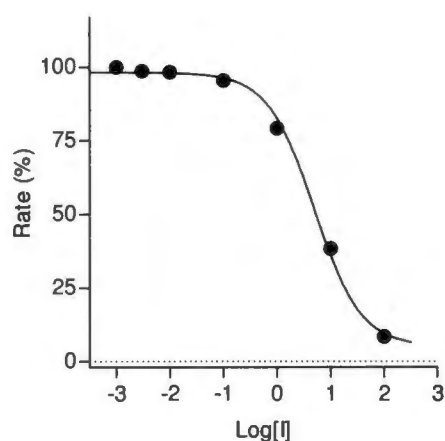
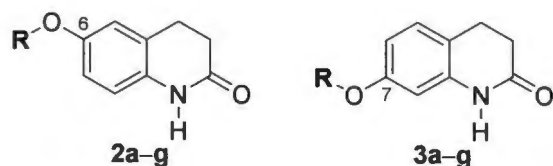


Fig. 3. Sigmoidal dose–response curves for the inhibition of human MAO-B by **2d**.

Table 1. The IC₅₀ values for the inhibition of recombinant human MAO-A and MAO-B by compounds **2a–g** and **3a–g**.



	R	IC ₅₀ (μM) ^a		SI ^b
		MAO-A	MAO-B	
2a	4-ClC ₆ H ₄ CH ₂ –	56.4 ± 20.0	0.017 ± 0.0046	3318
2b	4-BrC ₆ H ₄ CH ₂ –	>100 ^c	0.0054 ± 0.0011	>18519
2c	3-CH ₃ C ₆ H ₄ CH ₂ –	31.0 ± 2.48	0.313 ± 0.028	99
2d	4-CH ₃ C ₆ H ₄ CH ₂ –	>100 ^c	0.098 ± 0.024	>1020
2e	3-CH ₃ C ₆ H ₄ (CH ₂) ₂ –	39.3 ± 2.47	0.198 ± 0.110	198
2f	4-CH ₃ C ₆ H ₄ (CH ₂) ₂ –	>100 ^c	0.025 ± 0.0087	>4000
2g	C ₆ H ₅ O(CH ₂) ₂ –	>100 ^c	0.102 ± 0.0019	>980
3a	4-ClC ₆ H ₄ CH ₂ –	28.9 ± 4.22	0.0014 ± 0.0003	20643
3b	4-BrC ₆ H ₄ CH ₂ –	>100 ^c	0.0025 ± 0.0007	>40000
3c	3-CH ₃ C ₆ H ₄ CH ₂ –	26.4 ± 8.20	0.011 ± 0.00065	2400
3d	4-CH ₃ C ₆ H ₄ CH ₂ –	44.1 ± 5.25	0.018 ± 0.0083	2450
3e	4-CH ₃ C ₆ H ₄ (CH ₂) ₂ –	34.5 ± 13.1	0.047 ± 0.021	734
3f	C ₆ H ₅ O(CH ₂) ₂ –	>100 ^c	0.047 ± 0.0080	>2128
3g	4-ClC ₆ H ₄ O(CH ₂) ₂ –	>100 ^c	0.113 ± 0.065	>885

^a All values are expressed as the mean ± SD of triplicate determinations.

^b The selectivity index is the selectivity for the MAO-B isoform and is given as the ratio IC₅₀(MAO-A)/IC₅₀(MAO-B).

^c No inhibition observed at a concentration of 100 μM.

The IC_{50} values show that among both the C6- and C7-substituted 3,4-dihydro-2(1*H*)-quinolinones high potency MAO-B inhibitors exist. Most notably among these are **2b**, **3a** and **3b** which display IC_{50} values of $<0.006 \mu\text{M}$. The MAO-B inhibition potencies of these compounds are comparable to those of **1a** ($IC_{50} = 0.0029$) and **1b** ($IC_{50} = 0.0062$), and are significantly more potent than the reference MAO-B inhibitors lazabemide ($IC_{50} = 0.091 \mu\text{M}$) and safinamide ($IC_{50} = 0.048 \mu\text{M}$), evaluated under the same experimental conditions [34]. These compounds also display high specificities for the MAO-B enzyme with selectivity index (SI) values $>18,519$. In this regard, **3b** is particularly isoform specific since it possesses an IC_{50} for MAO-A inhibition of $>100 \mu\text{M}$. Similar to the 3,4-dihydro-2(1*H*)-quinolinones studied before, **2a–g** and **3a–g** are relatively weak MAO-A inhibitors with $IC_{50}>26.4 \mu\text{M}$. From the inhibition data, the following SARs may be derived: (a) Similar to the reported study, C7 substitution yields compounds with higher MAO-B inhibition potencies than C6 substitution. For each pair of homologues, the corresponding C7-substituted compounds display more potent inhibition although differences in inhibition potencies are in many instances very small (compare **2b** vs. **3b**; **2d** vs. **3d**; **2g** vs. **3f**). (b) Chlorine and bromine substitution on the *para* position of the benzyloxy ring yields similar MAO-B inhibition than *meta* substitution (compare **1b** vs. **3a**; **1a** vs. **3b**). Methyl substitution on either the *meta* or *para* positions of the benzyloxy ring is, however, less suitable for MAO-B inhibition compared to the halogens (compare **2c/2d** with **2a/2b**; **3c/3d** with **3a/3b**). (c) Substitution with the 2-phenoxyethoxy moiety on both the C6 (**2g**, $IC_{50} = 0.102 \mu\text{M}$) and C7 (**3f**, $IC_{50} = 0.047 \mu\text{M}$) positions of the 3,4-dihydro-2(1*H*)-quinolinone yields good potency MAO-B inhibition. These compounds are particularly specific inhibitors since they display IC_{50} values for MAO-A inhibition of $>100 \mu\text{M}$. Interestingly, chlorine substitution (**3g**, $IC_{50} = 0.113 \mu\text{M}$) of the phenoxy ring significantly reduces MAO-B inhibition potency compared to the unsubstituted homologue **3f**.

(d) Among the 2-phenylethoxy substituted compounds (**2e**, **2f**, **3e**), **2f** ($IC_{50} = 0.025 \mu M$) is the most potent MAO-B inhibitor. The good potency of this compound demonstrates that, with the appropriate substitution pattern, 2-phenylethoxy substitution may yield similar potency MAO-B inhibitors compared to benzyloxy substitution (compare **2f** vs. **2d**).

Reversibility of MAO-B inhibition

Using compound **1a** as model inhibitor, it has been established that 3,4-dihydro-2(1*H*)-quinolinones inhibits MAO-B with a reversible mode of action, although some tight-binding of the inhibitor to the enzyme may occur [23]. Since **1a** is a C7-substituted homologue, the present study investigates the reversibility of MAO-B inhibition by a C6-substituted 3,4-dihydro-2(1*H*)-quinolinone, compound **2b**. Reversibility of inhibition was investigated by dialysis. Compound **2b** (at a concentration of $4 \times IC_{50}$) was preincubated with MAO-B for 15 min and subsequently dialyzed for 24 h. The incubation mixtures were diluted twofold with the addition of kynuramine and the formation of 4-hydroxyquinoline was measured at the endpoint of the enzyme reaction. From the 4-hydroxyquinoline concentrations the residual activities were calculated. Similar dialysis experiments were carried out in the absence of inhibitor (negative control) and presence of the irreversible MAO-B inhibitor, (R)-deprenyl (positive control). The activity (rate of 4-hydroxyquinoline formation) of the negative control represents 100% residual activity. As third control, the residual MAO-B activity of undialyzed mixtures of MAO-B and **2b** was also recorded. As shown in Fig. 4, following inhibition with **2b**, dialysis restores enzyme activity to 100% of the negative control (100%). Following inhibition with (R)-deprenyl, enzyme activity is not restored by dialysis with the residual activity at only 2.4%. In undialyzed mixtures of MAO-B and **2b**, inhibition persists and the activity is recorded at 67%.

Since dialysis is expected to restore enzyme activity to 100% for reversible inhibitors, it may be concluded that **2b** is a reversible MAO-B inhibitor.

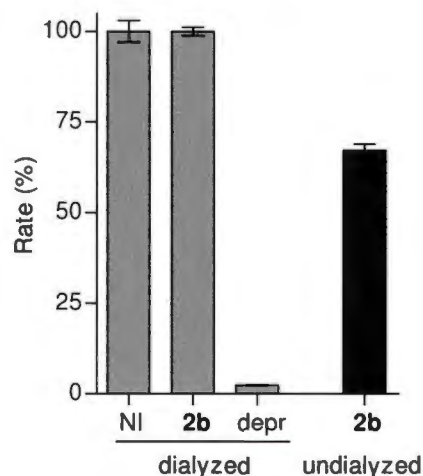


Fig. 4. Compound **2b** inhibits MAO-B with a reversible mode. MAO-B and **2b** (at $4 \times IC_{50}$) was preincubated for 15 min, dialyzed for 24 h and the residual enzyme activity was measured (**2b**-dialyzed). Similar incubation and dialysis of MAO-B in the absence inhibitor (NI dialyzed) and presence of the irreversible inhibitor, (R)-deprenyl (depr dialyzed), were also carried out. The residual activity of undialyzed mixtures of MAO-B with **2b** was also recorded (**2b**-undialyzed).

Lineweaver-Burk plots and competitive inhibition

This study also set out to measure the enzyme-inhibitor dissociation constant (K_i value) for the reversible interaction between **2b** and MAO-B. To measure the K_i value a set of six Lineweaver-Burk plots was constructed using various inhibitor concentrations ($0 \mu\text{M}$, $\frac{1}{4} \times IC_{50}$, $\frac{1}{2} \times IC_{50}$, $\frac{3}{4} \times IC_{50}$, $1 \times IC_{50}$ and $1\frac{1}{4} \times IC_{50}$) and eight concentrations of kynuramine ($15\text{--}250 \mu\text{M}$) for each plot. The set of Lineweaver-Burk plots is shown in Fig. 5. Since the lines are linear and intersect on the y-axis it may be concluded that **2b** is a competitive inhibitor of MAO-B. Global (shared) fitting of the inhibition data directly to the Michaelis-Menten equation yields a K_i value of $0.0026 \pm 0.00024 \mu\text{M}$ ($R^2 = 0.98$).

From a plot of the slopes of the Lineweaver-Burk plots versus inhibitor concentration a similar value ($0.0028\mu\text{M}$) is obtained (x-axis intercept equals $-K_i$).

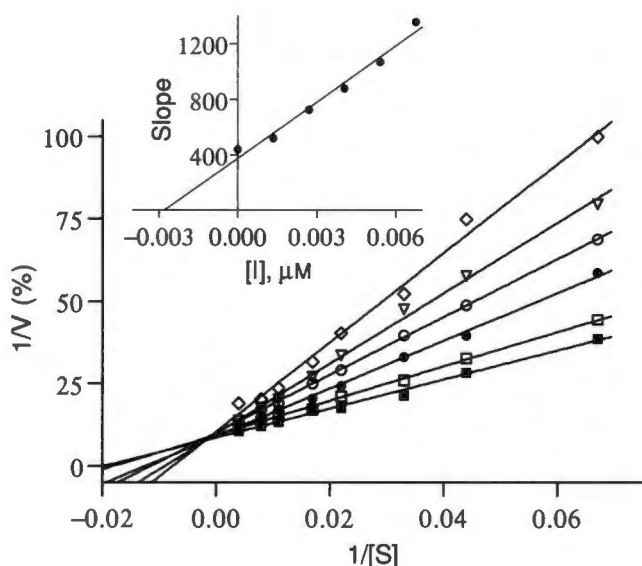


Fig. 5. Lineweaver-Burk plots for the inhibition of MAO-B by **2b**. The inset is a graph of the slopes of the Lineweaver-Burk plots versus inhibitor concentration.

Docking studies

An interesting SAR of MAO-B inhibition by 3,4-dihydro-2(1*H*)-quinolinones is that C7 substitution yields higher potency MAO-B inhibition compared to C6 substitution. In certain instances the differences in MAO-B inhibition are small (e.g. **2b/3b**) while for other homologues (e.g. **2c/3c**) the C7-substituted homologue is significantly more potent than the corresponding C6-substituted homologue. To determine if differing binding modes to MAO-B may be responsible for this SAR, **2c** and **3c** were docked into the MAO-B active site using the CDOCKER docking algorithm of Discovery Studio 3.1 [28]. To propose possible reasons for the weaker MAO-A inhibition of 3,4-dihydro-2(1*H*)-quinolinones, these compounds were also docked into the MAO-A active site. The docking simulations were carried out according to the literature procedure and the reported crystal structures of human MAO-A (PDB code: 2Z5X) [29] and MAO-B (PDB code: 2V5Z) [30] served as protein models [24].

As shown in Fig. 6, **2c** and **3c** exhibit differing binding modes to MAO-B, particularly with respect to the orientation of the 3,4-dihydro-2(1*H*)-quinolinone moiety. Compared to **2c**, the 3,4-dihydro-2(1*H*)-quinolinone moiety of **3c** is rotated by approximately 180 °.

This inversion of orientation allows for the benzyloxy side chain of **3c** to extend into the entrance cavity of the enzyme, similar to **2c**. For **2c**, polar interactions (H-bonding and π - π interaction with Tyr-398) are established in the enzyme's substrate cavity, which are not possible for **3c**. Since **3c** is a more potent MAO-B inhibitor than **2c**, these polar interactions play a lesser role in inhibitor stabilization, and Van der Waals interactions between the benzyloxy side chain and the entrance cavity most likely contribute to a higher degree. This is supported by the observation that **4** and **5**, compounds lacking a C6 or C7 side chain, are very weak MAO-B inhibitors ($IC_{50} > 201 \mu M$) [23]. It may thus be concluded that, although the placements and orientations of these side chains are very similar, for **3c** more productive Van der Waals interactions are possible, perhaps because this compound extends slightly deeper into the entrance cavity enabling it to establish interactions with key residues.

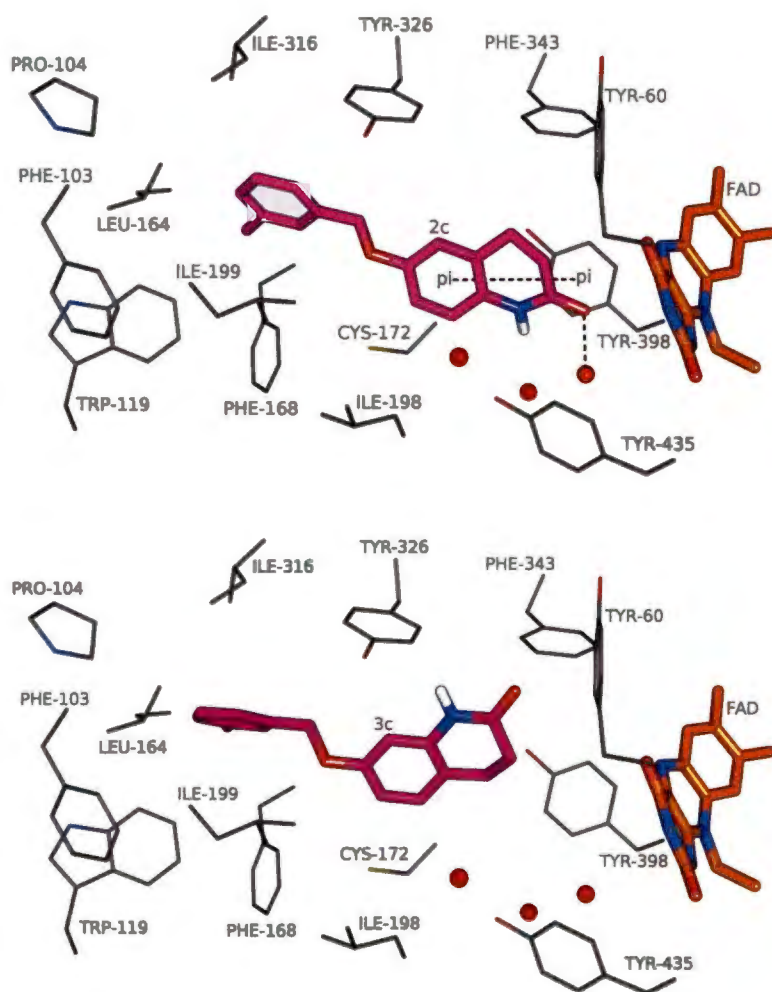


Fig. 6. The proposed binding modes of **2c** and **3c** to MAO-B.

In contrast to MAO-B, compounds **2c** and **3c** exhibit similar binding modes to MAO-A with respect to the orientation of the 3,4-dihydro-2(1*H*)-quinolinone moiety as well as the placement of the benzyloxy phenyl ring (Fig. 7). Both compounds establish polar interactions (H-bonding and π - π interactions) with MAO. The similar binding modes to MAO-A explain their comparable MAO-A inhibition activities. It is noteworthy that **2c** and **3c** bind in folded conformations in MAO-A, while exhibiting extended conformations in MAO-B. In MAO-A restrictions imposed by the side chain of Phe-208 are most likely responsible for the folded conformation. In MAO-B the residue that corresponds to Phe-208 in MAO-A, is Ile-199. For larger inhibitors, the side chain of Ile-199 rotates from the active site cavity, allowing for extension into the entrance cavity.

Larger inhibitors are thus, in general, better accommodated in MAO-B than MAO-A, hence more potent inhibition of MAO-B by the C6- and C7-substituted 3,4-dihydro-2(1*H*)-quinolinones.

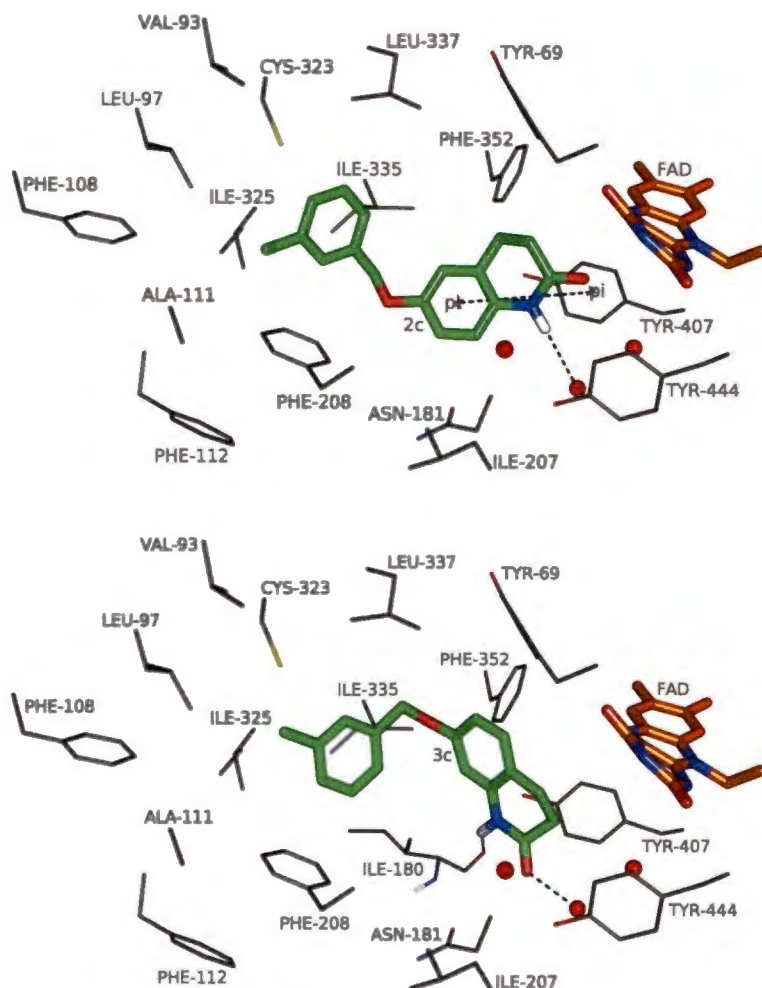


Fig. 7. The proposed binding modes of **2c** and **3c** to MAO-A.

Conclusion

In conclusion, the current study shows that 3,4-dihydro-2(1*H*)-quinolinones, in general, are MAO-B specific inhibitors. Three compounds, **2b**, **3a** and **3b**, were identified with high potency MAO-B inhibition ($IC_{50} < 0.006 \mu M$). Specific MAO-B inhibitors such as these represent potential candidate drugs for the treatment of Parkinson's disease, with a low risk of provoking the side effects associated with MAO-A inhibition (e.g. "cheese effect"). As shown with **2b**, this class acts as reversible and competitive MAO-B inhibitors.

Acknowledgements

The NMR and MS spectra were recorded by André Joubert and Johan Jordaan of the SASOL Centre for Chemistry, North-West University. This work is based on the research supported in part by the Medical Research Council and National Research Foundation of South Africa (Grant specific unique reference numbers (UID) 85642, 96180). The Grantholders acknowledge that opinions, findings and conclusions or recommendations expressed in any publication generated by the NRF supported research are that of the authors, and that the NRF accepts no liability whatsoever in this regard.

Conflict of Interest

The authors declare that they have no conflicts of interest to disclose.

References

1. Youdim MB, Edmondson D, Tipton KF. The therapeutic potential of monoamine oxidase inhibitors. *Nat Rev Neurosci* 2006; 7: 295–309
2. Schwartz TL. A neuroscientific update on monoamine oxidase and its inhibitors. *CNS Spectr* 2013; 18(Suppl 1): 25–32
3. Lum CT, Stahl SM. Opportunities for reversible inhibitors of monoamine oxidase-A (RIMAs) in the treatment of depression. *CNS Spectr* 2012; 17: 107–120
4. Shoulson I, Oakes D, Fahn S, Lang A, Langston JW, LeWitt P, Olanow CW, Penney JB, Tanner C, Kieburtz K, Rudolph A; Parkinson Study Group. Impact of sustained deprenyl (selegiline) in levodopa-treated Parkinson's disease: a randomized placebo-controlled extension of the deprenyl and tocopherolantioxidative therapy of parkinsonism trial. *Ann Neurol* 2002; 51: 604–612
5. Fernandez HH, Chen JJ. Monoamine oxidase-B inhibition in the treatment of Parkinson's disease. *Pharmacotherapy* 2007; 27: 174S–185S
6. Finberg JP, Wang J, Bankiewicz K, Harvey-White J, Kopin IJ, Goldstein DS. Increased striatal dopamine production from L-DOPA following selective inhibition of monoamine oxidase B by R(+)-N-propargyl-1-aminoindan (rasagiline) in the monkey. *J Neural TransmSuppl* 1998; 52: 279–285
7. Da Prada M, Zürcher G, Wüthrich I, Haefely WE. On tyramine, food, beverages and the reversible MAO inhibitor moclobemide. *J Neural TransmSuppl* 1988; 26: 31–56
8. Flockhart DA. Dietary restrictions and drug interactions with monoamine oxidase inhibitors: an update. *J Clin Psychiatry* 2012; 73(Suppl 1): 17–24
9. Finberg JP, Gillman K. Selective inhibitors of monoamine oxidase type B and the "cheese effect". *Int Rev Neurobiol* 2011; 100: 169–190

10. Lasbennes F, Sercombe R, Seylaz J. Monoamine oxidase activity in brain microvessels determined using natural and artificial substrates: relevance to the blood-brain barrier. *J Cereb Blood Flow Metab* 1983; 3: 521–528
11. Finberg JP, Lamensdorf I, Armoni T. Modification of dopamine release by selective inhibitors of MAO-B. *Neurobiology (Bp)* 2000; 8: 137–142
12. Janssen PA, Leysen JE, Megens AA, Awouters FH. Does phenylethylamine act as an endogenous amphetamine in some patients? *Int J Neuropsychopharmacol* 1999; 2: 229–240
13. Chiba K, Trevor A, Castagnoli N Jr. Metabolism of the neurotoxic tertiary amine, MPTP, by brain monoamine oxidase. *BiochemBiophys Res Commun* 1984; 120: 574–578
14. Youdim MB, Bakhle YS. Monoamine oxidase: isoforms and inhibitors in Parkinson's disease and depressive illness. *Br J Pharmacol* 2006; 147(Suppl 1): S287–296
15. Edmondson DE. Hydrogen peroxide produced by mitochondrial monoamine oxidase catalysis: biological implications. *Curr Pharm Des* 2014; 20: 155–160
16. Fowler JS, Volkow ND, Wang GJ, Logan J, Pappas N, Shea C, MacGregor R. Age-related increases in brain monoamine oxidase B in living healthy human subjects. *Neurobiol Aging* 1997; 18: 431–435
17. Maurel A, Hernandez C, Kunduzova O, Bompart G, Cambon C, Parini A, Francés B. Age-dependent increase in hydrogen peroxide production by cardiac monoamine oxidase A in rats. *Am J Physiol Heart CircPhysiol* 2003; 284: H1460–1467
18. Xu S, Adisetiyo H, Tamura S, Grande F, Garofalo A, Roy-Burman P, Neamati N. Dual inhibition of survivin and MAO A synergistically impairs growth of PTEN-negative prostate cancer. *Br J Cancer* 2015; 113: 242–251

19. Wu JB, Shao C, Li X, Li Q, Hu P, Shi C, Li Y, Chen YT, Yin F, Liao CP, Stiles BL, Zhau HE, Shih JC, Chung LW. Monoamine oxidase A mediates prostate tumorigenesis and cancer metastasis. *J Clin Invest* 2014; 124: 2891–2908
20. Carradori S, Silvestri R. New frontiers in selective human MAO-B inhibitors. *J Med Chem* 2015; 58: 6717–6732
21. Carradori S, Petzer JP. Novel monoamine oxidase inhibitors: a patent review (2012 - 2014). *Expert Opin Ther Pat* 2015; 25: 91–110
22. Gnerre C, Catto M, Leonetti F, Weber P, Carrupt PA, Altomare C, Carotti A, Testa B. Inhibition of monoamine oxidases by functionalized coumarin derivatives: biological activities, QSARs, and 3D-QSARs. *J Med Chem* 2000; 43: 4747–4758
23. Meiring L, Petzer JP, Petzer A. Inhibition of monoamine oxidase by 3,4-dihydro-2(1H)-quinolinone derivatives. *Bioorg Med Chem Lett* 2013; 23: 5498–5502
24. Mostert S, Petzer A, Petzer JP. Indanones as high-potency reversible inhibitors of monoamine oxidase. *ChemMedChem* 2015; 10: 862–873
25. Mostert S, Petzer A, Petzer JP. Inhibition of monoamine oxidase by benzoxathiolone analogues. *Bioorg Med Chem Lett* 2016; 26: 1200–1204
26. Novaroli L, Reist M, Favre E, Carotti A, Catto M, Carrupt PA. Human recombinant monoamine oxidase B as reliable and efficient enzyme source for inhibitor screening. *Bioorg Med Chem* 2005; 13: 6212–6217
27. Petzer A, Harvey BH, Wegener G, Petzer JP. Azure B, a metabolite of methylene blue, is a high-potency, reversible inhibitor of monoamine oxidase. *Toxicol Appl Pharmacol* 2012; 258: 403–409
28. Accelrys Discovery Studio 3.1 (2005). Accelrys Software Inc., San Diego, CA, USA. <http://www.accelrys.com>.

29. Son SY, Ma J, Kondou Y, Yoshimura M, Yamashita E, Tsukihara T. Structure of human monoamine oxidase A at 2.2-Å resolution: the control of opening the entry for substrates/inhibitors. *Proc Natl Acad Sci U S A* 2008; 105: 5739–5744
30. Binda C, Wang J, Pisani L, Caccia C, Carotti A, Salvati P, Edmondson DE, Mattevi A. Structures of human monoamine oxidase B complexes with selective noncovalent inhibitors: safinamide and coumarin analogs. *J Med Chem* 2007; 50: 5848–5852
31. DeLano, W.L. (2002) The PyMOL molecular graphics system. DeLano Scientific, San Carlos, USA.
32. Shigematsu N. Studies on the synthetic analgesics. XVI. Synthesis of 1-(2-tert-aminoalkyl)-3, 4-dihydrocarbostyrils. *Chem Pharm Bull* 1961; 9: 970–975
33. Strydom B, Bergh JJ, Petzer JP. The inhibition of monoamine oxidase by 8-(2-phenoxyethoxy)caffeine analogues. *Arzneimittel-Forsch* 2012; 62: 513–518
34. Petzer A, Pienaar A, Petzer JP. The inhibition of monoamine oxidase by esomeprazole. *Arzneimittel-Forsch* 2013; 63: 462–467

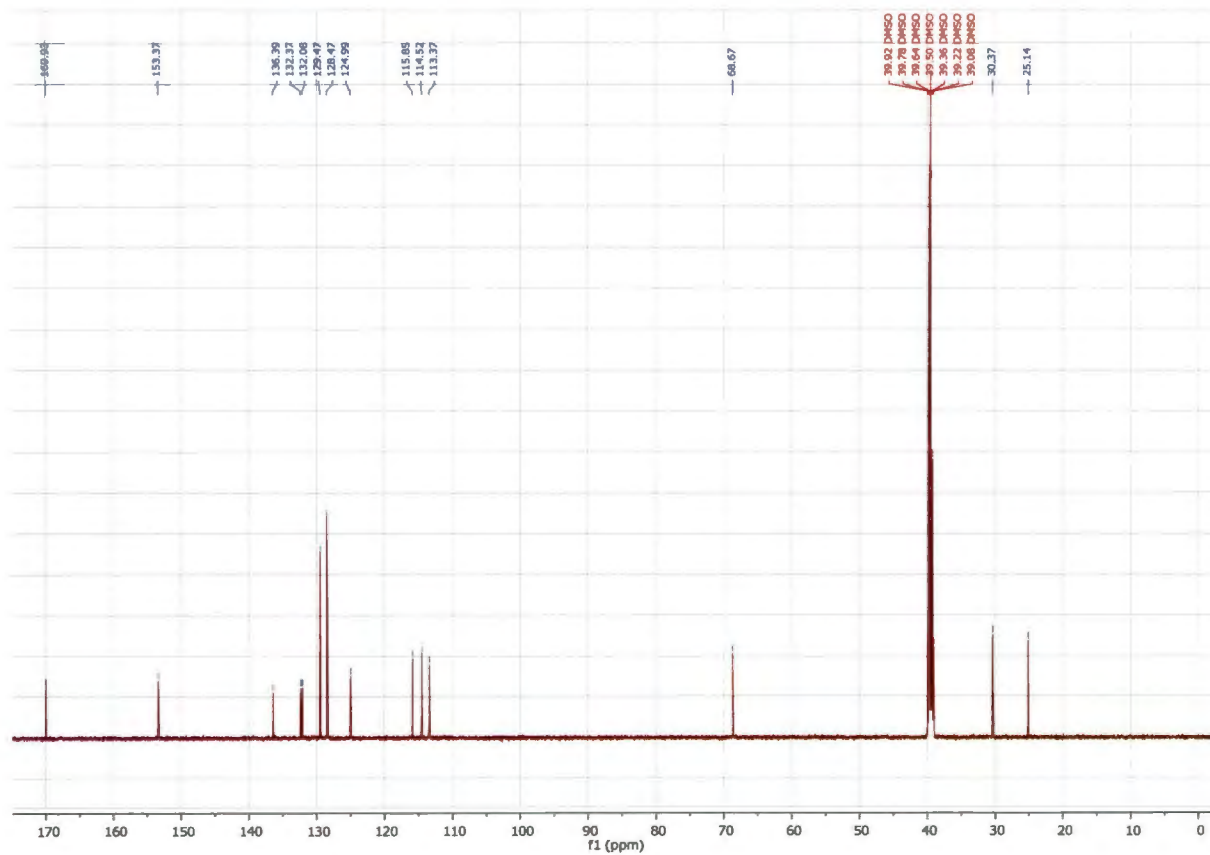
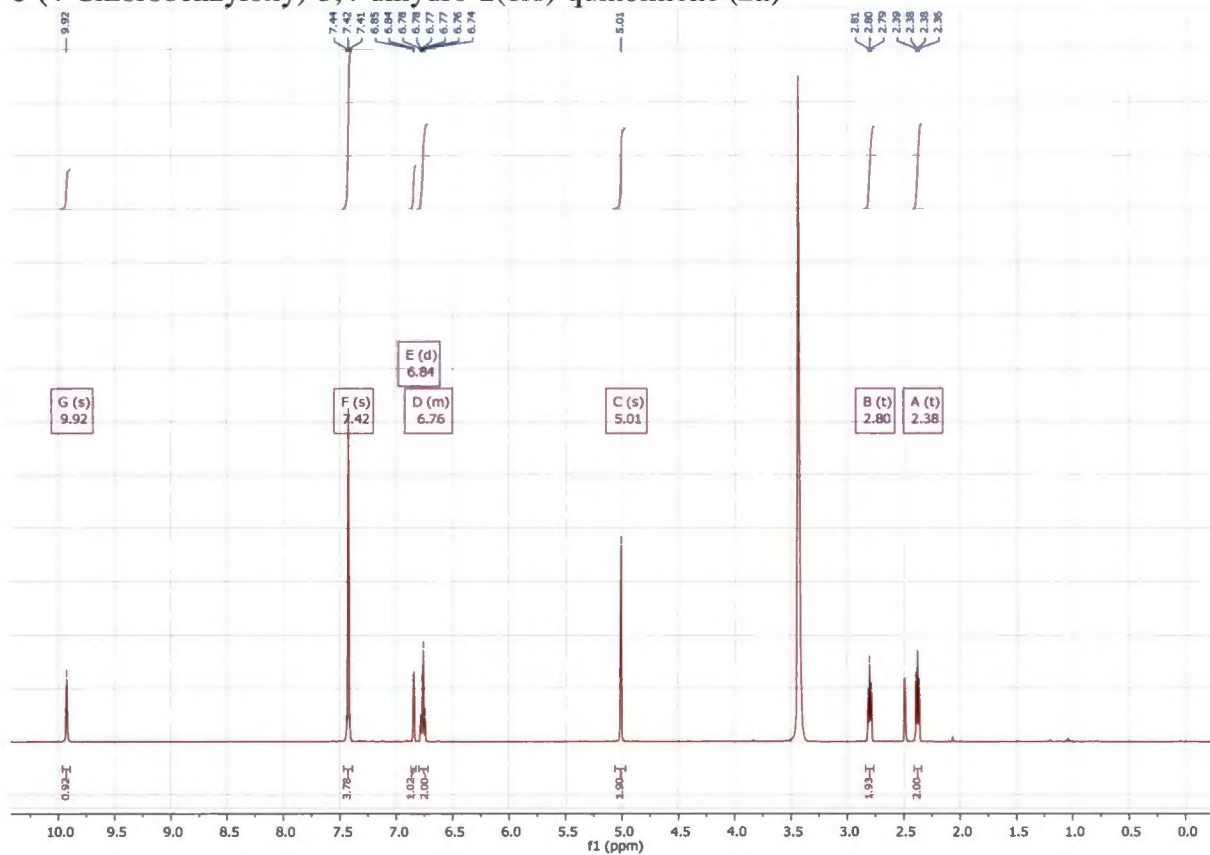
Supplementary Material

C6- and C7-substituted 3,4-dihydro-2(1H)-quinolinones as inhibitors of monoamine oxidase

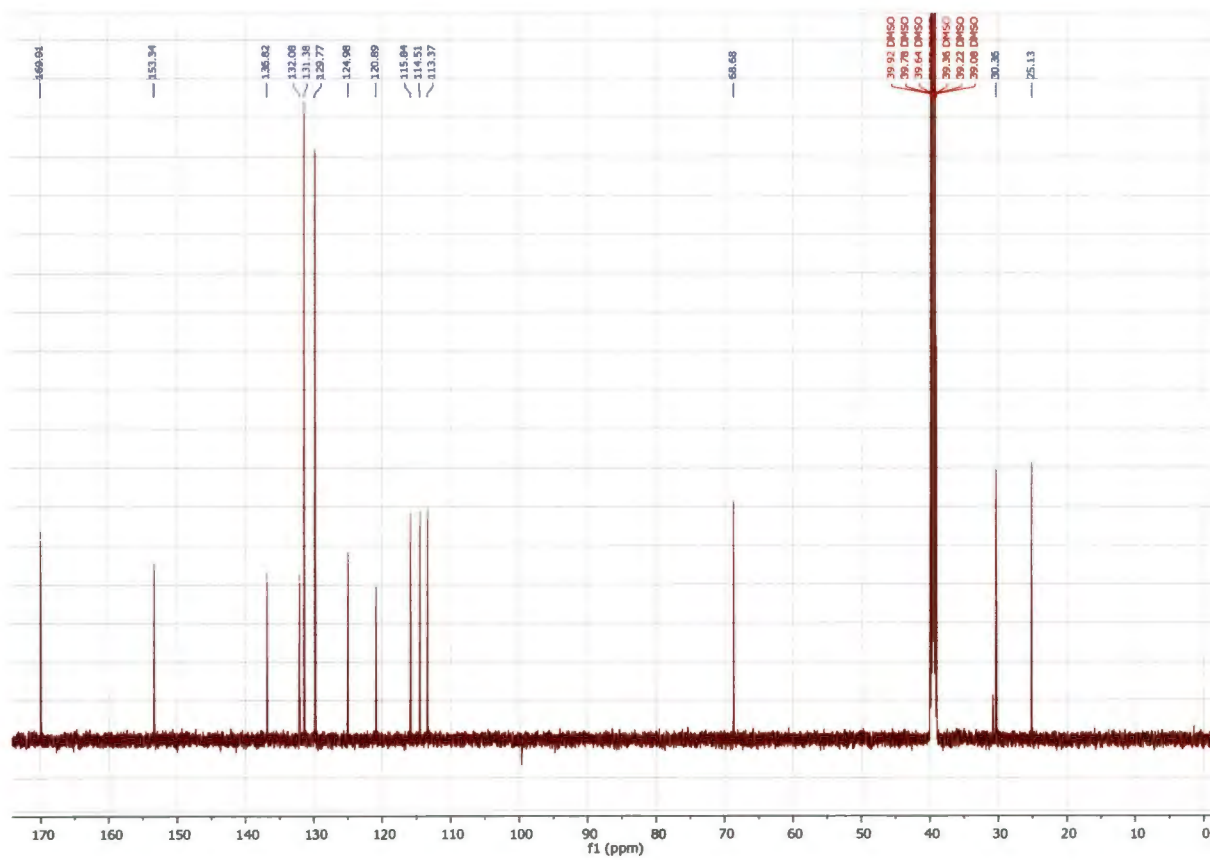
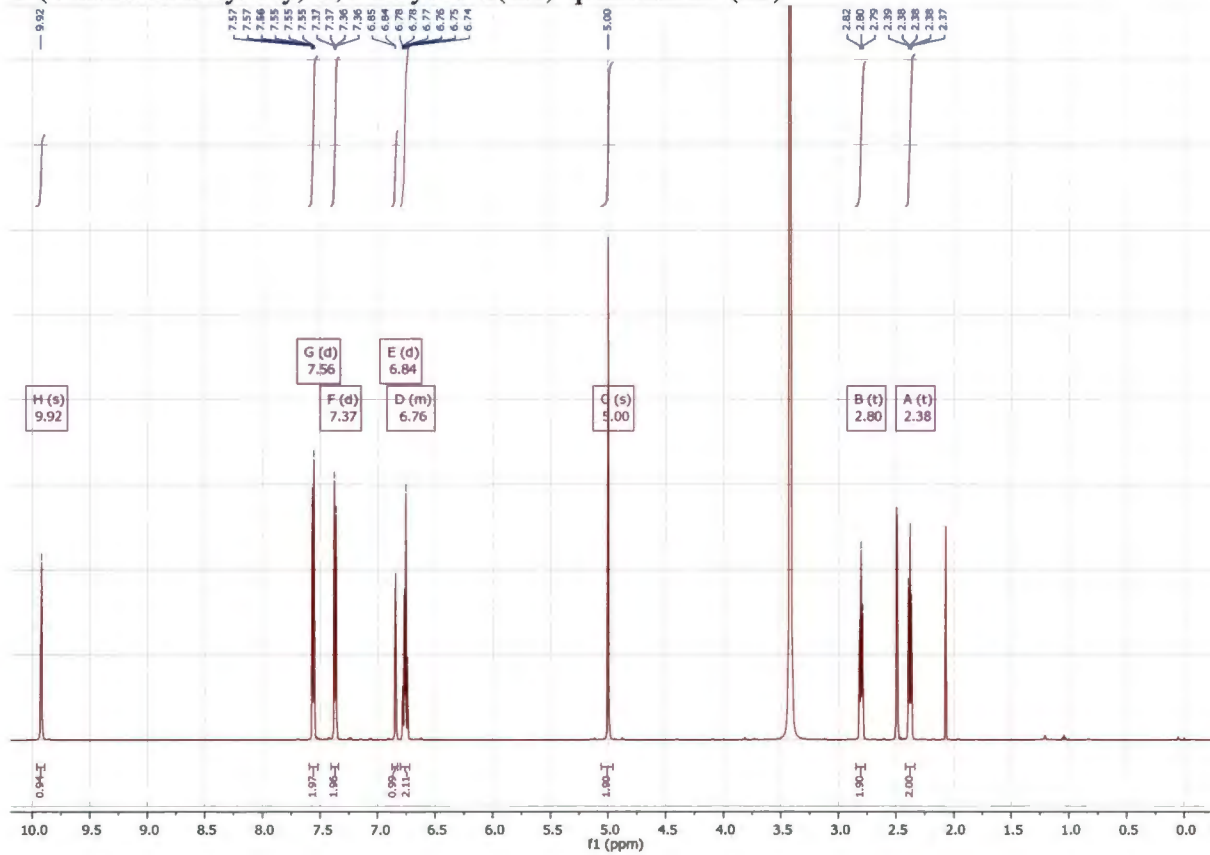
Letitia Meiring, ¹Jacobus P. Petzer,¹ and Anél Petzer^{1,*}

- ¹ *Pharmaceutical Chemistry, School of Pharmacy and Centre of Excellence for Pharmaceutical Sciences, North-West University, Private Bag X6001, Potchefstroom 2520, South Africa*

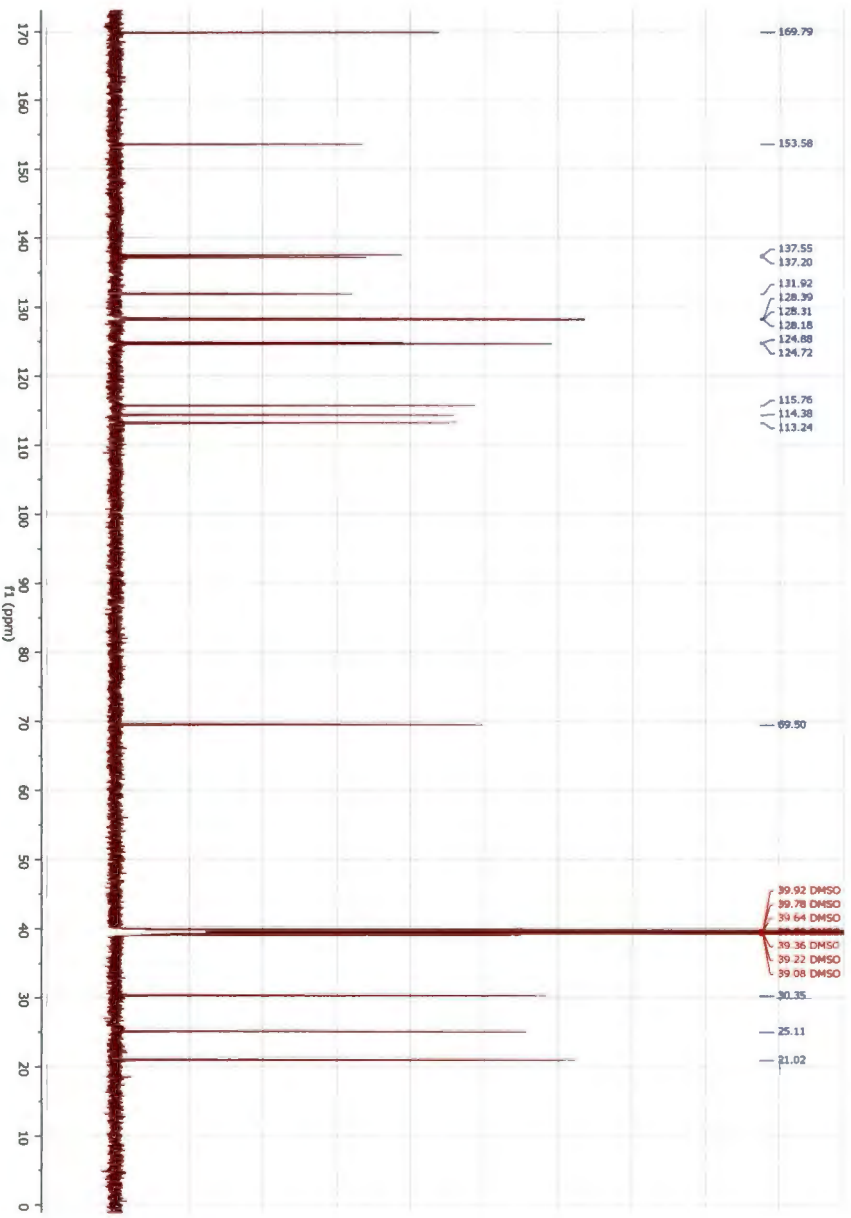
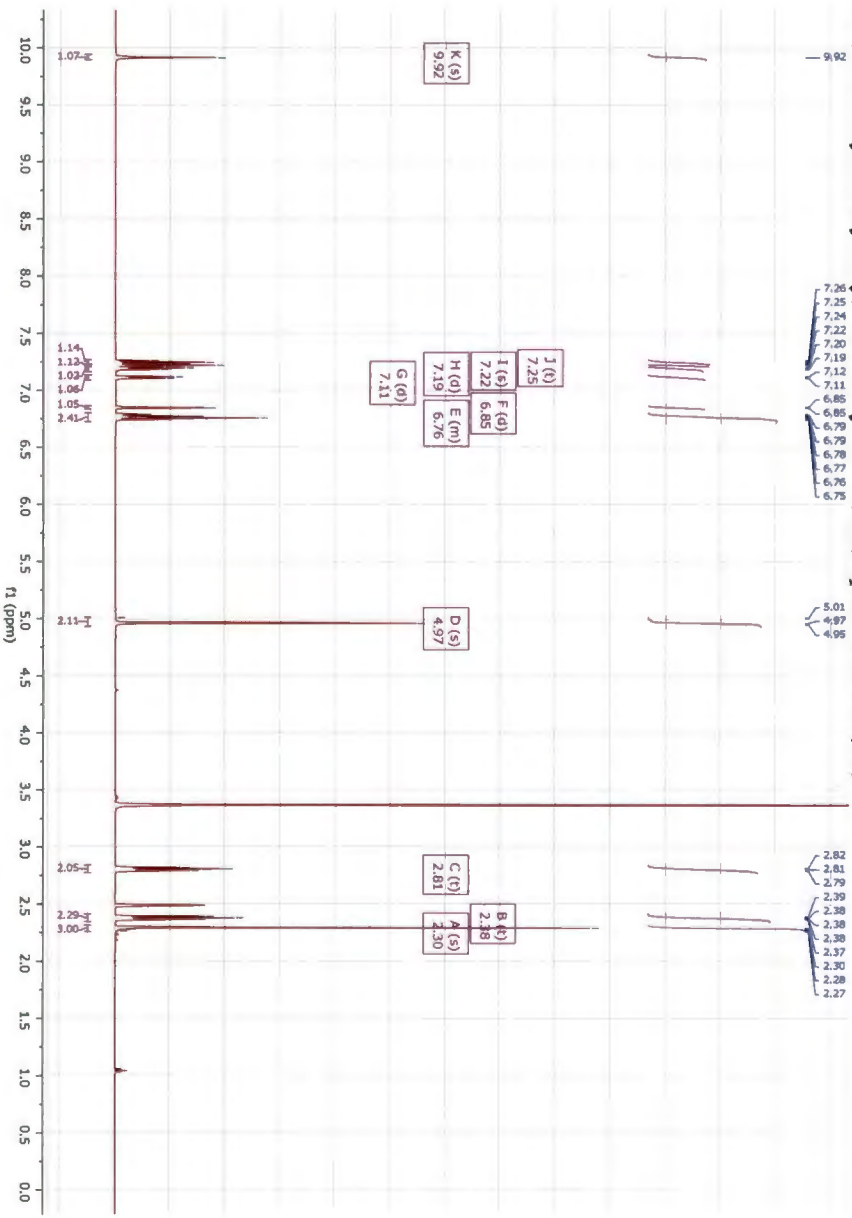
6-(4-Chlorobenzoyloxy)-3,4-dihydro-2(1H)-quinolinone (2a)

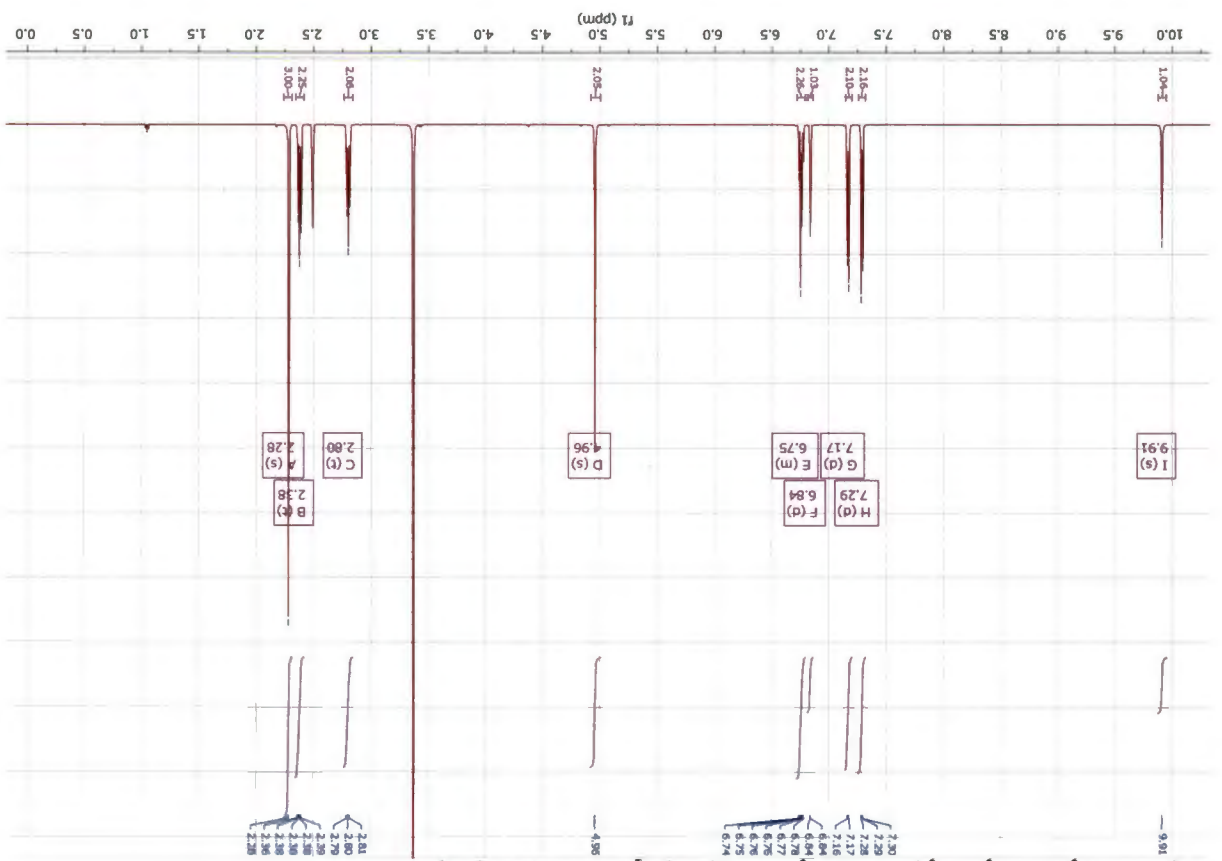
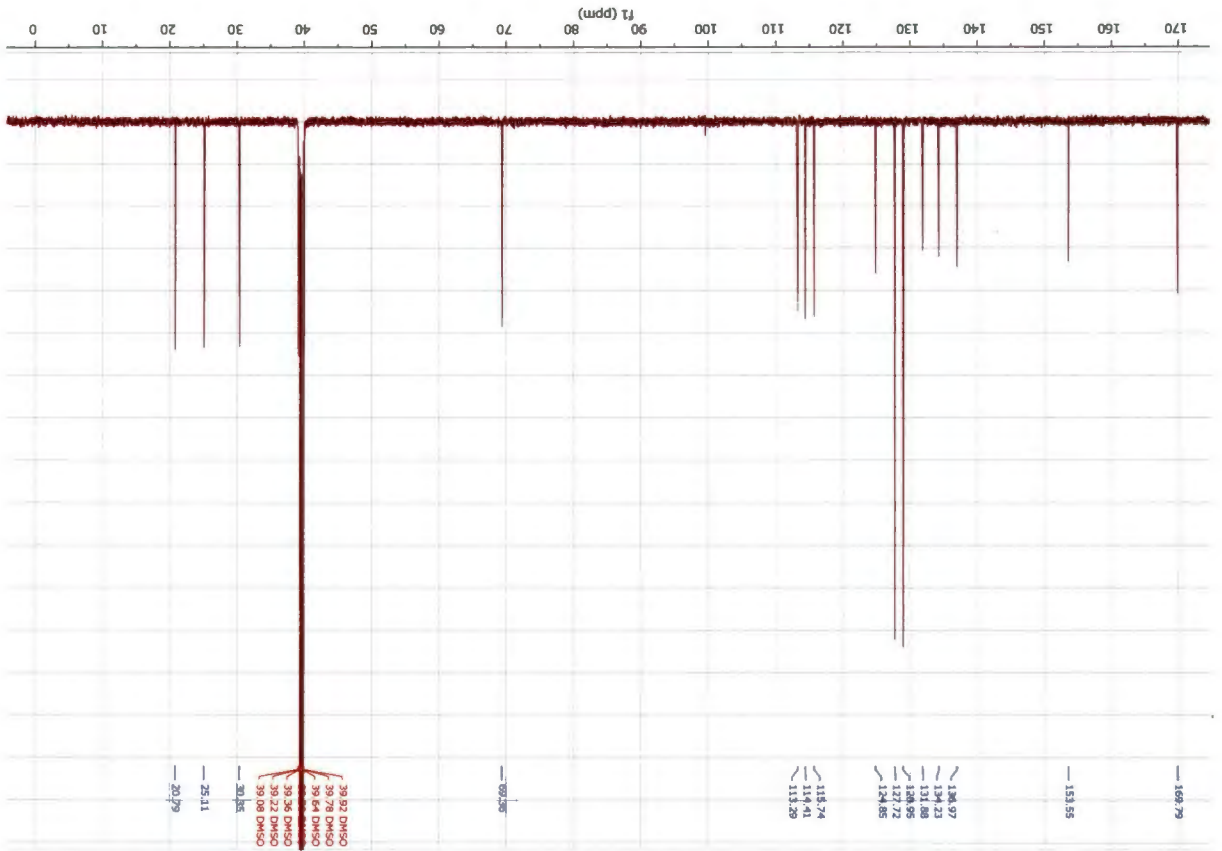


6-(4-Bromobenzoyloxy)-3,4-dihydro-2(1H)-quinolinone (2b)



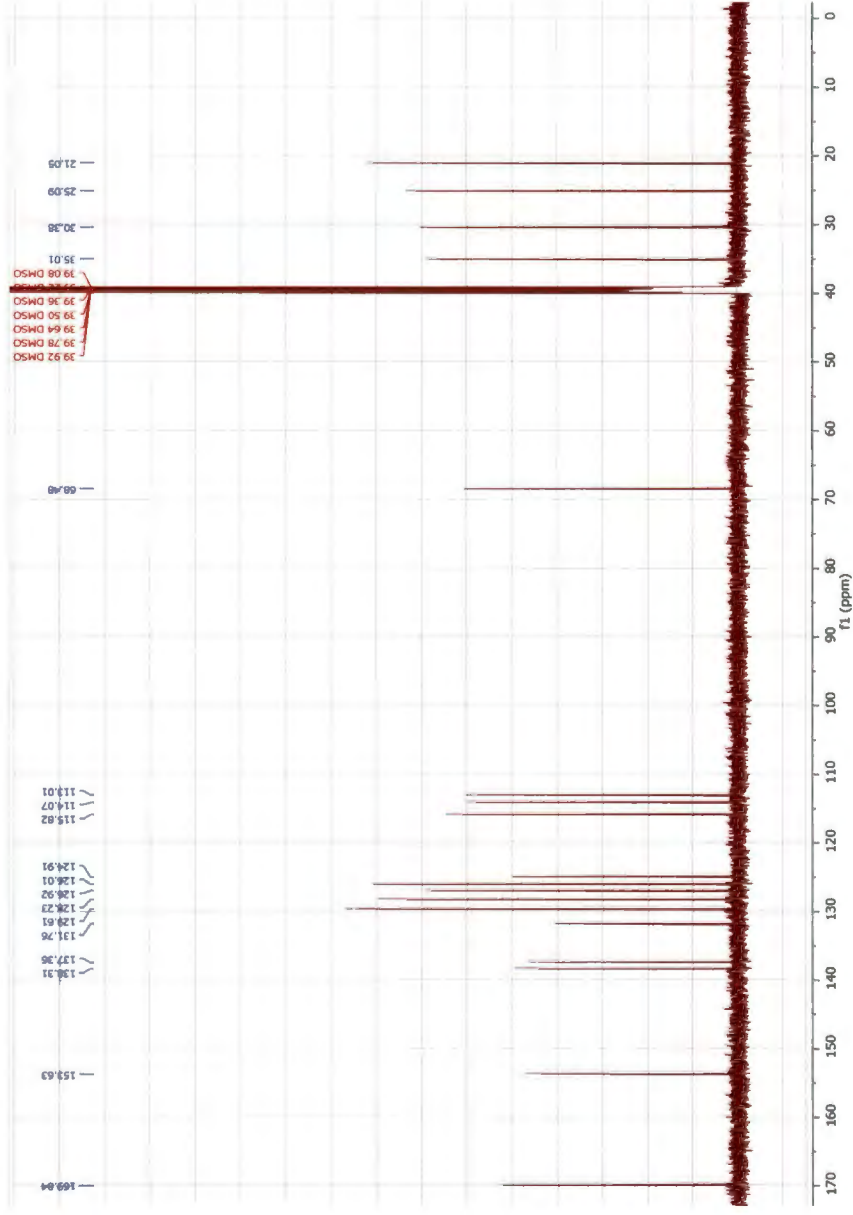
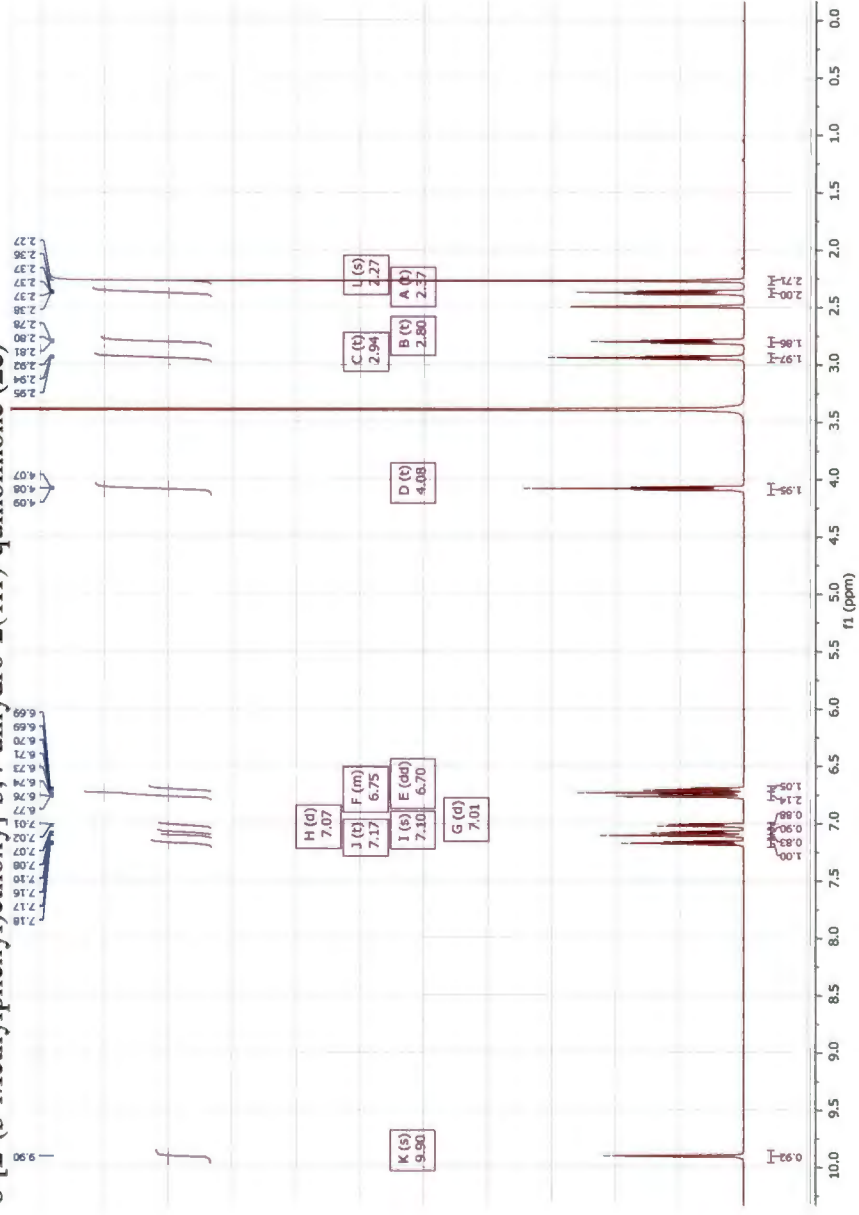
6-(3-Methylbenzyloxy)-3,4-dihydro-2(1H)-quinolinone (2c)



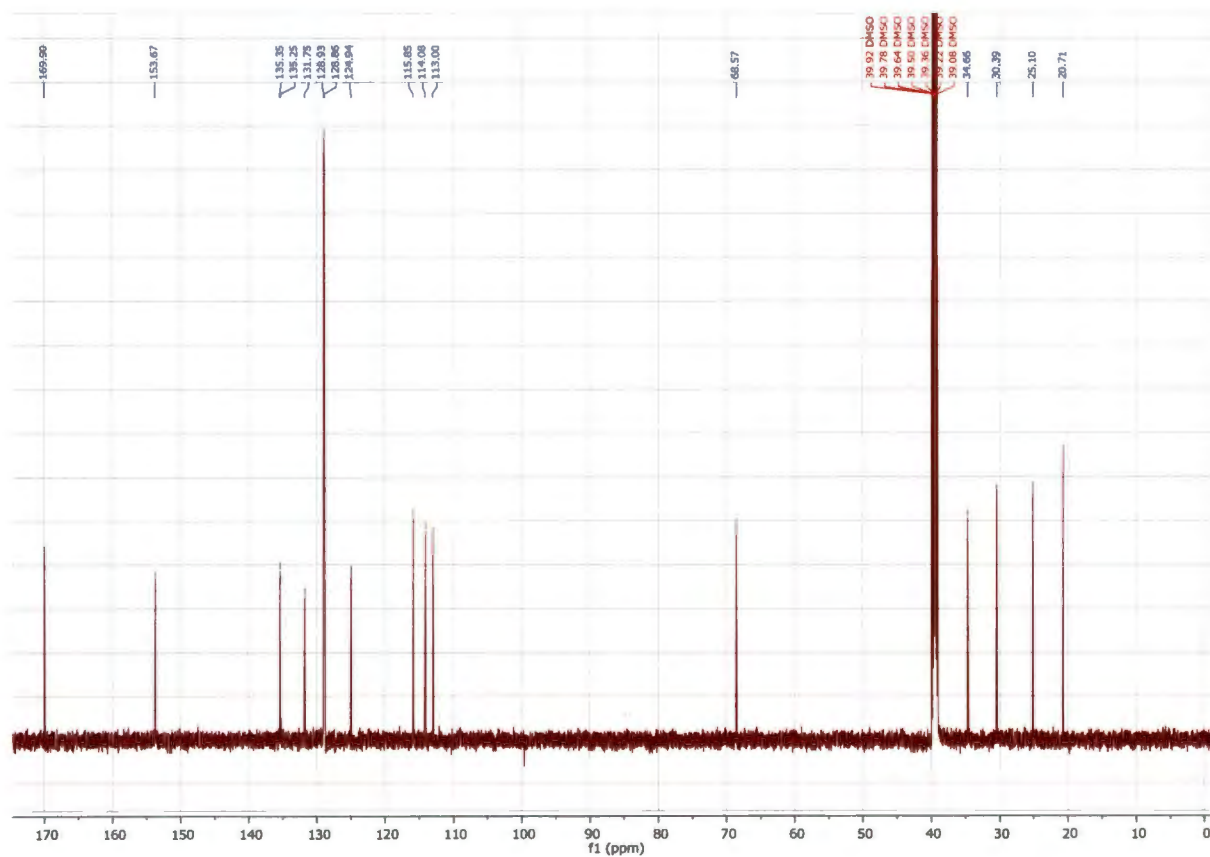
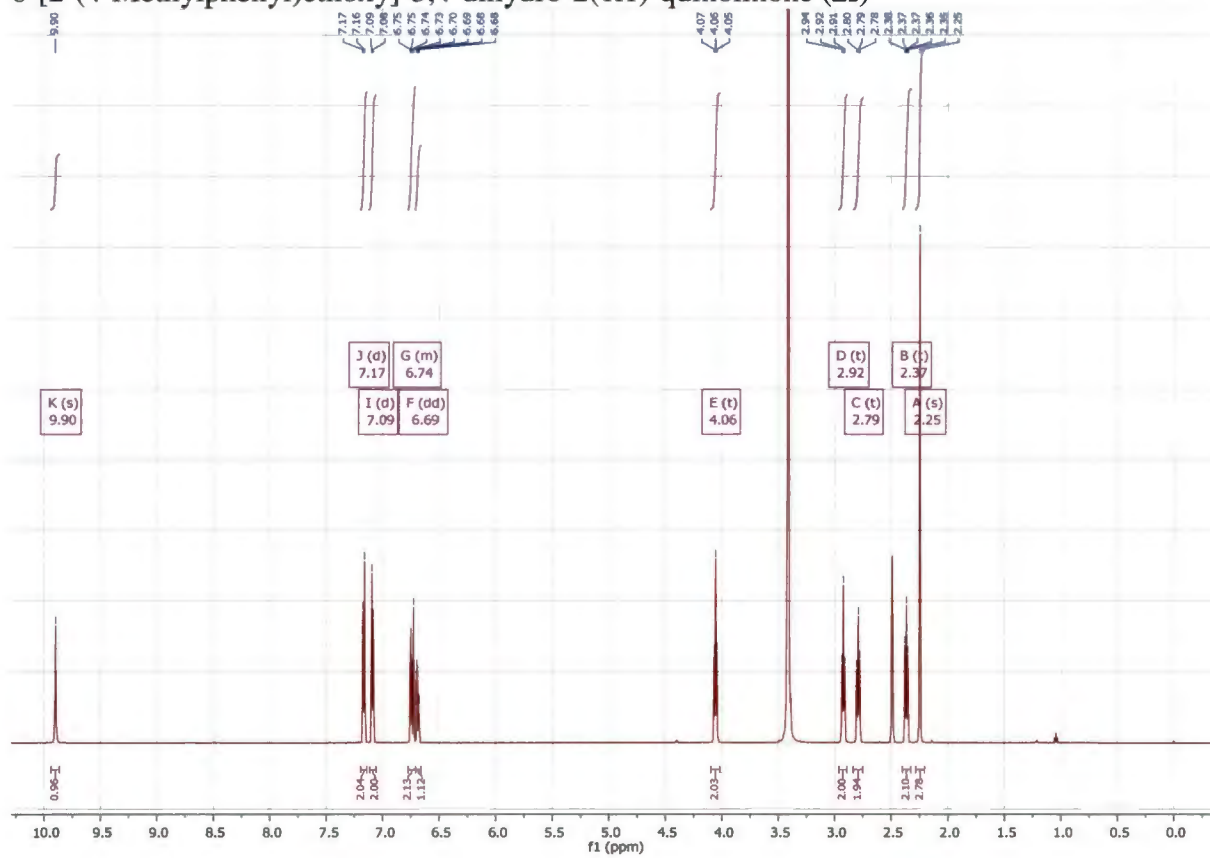


6-(4-Methylbenzyloxy)-3,4-dihydro-2(1H)-quinolinone (2d)

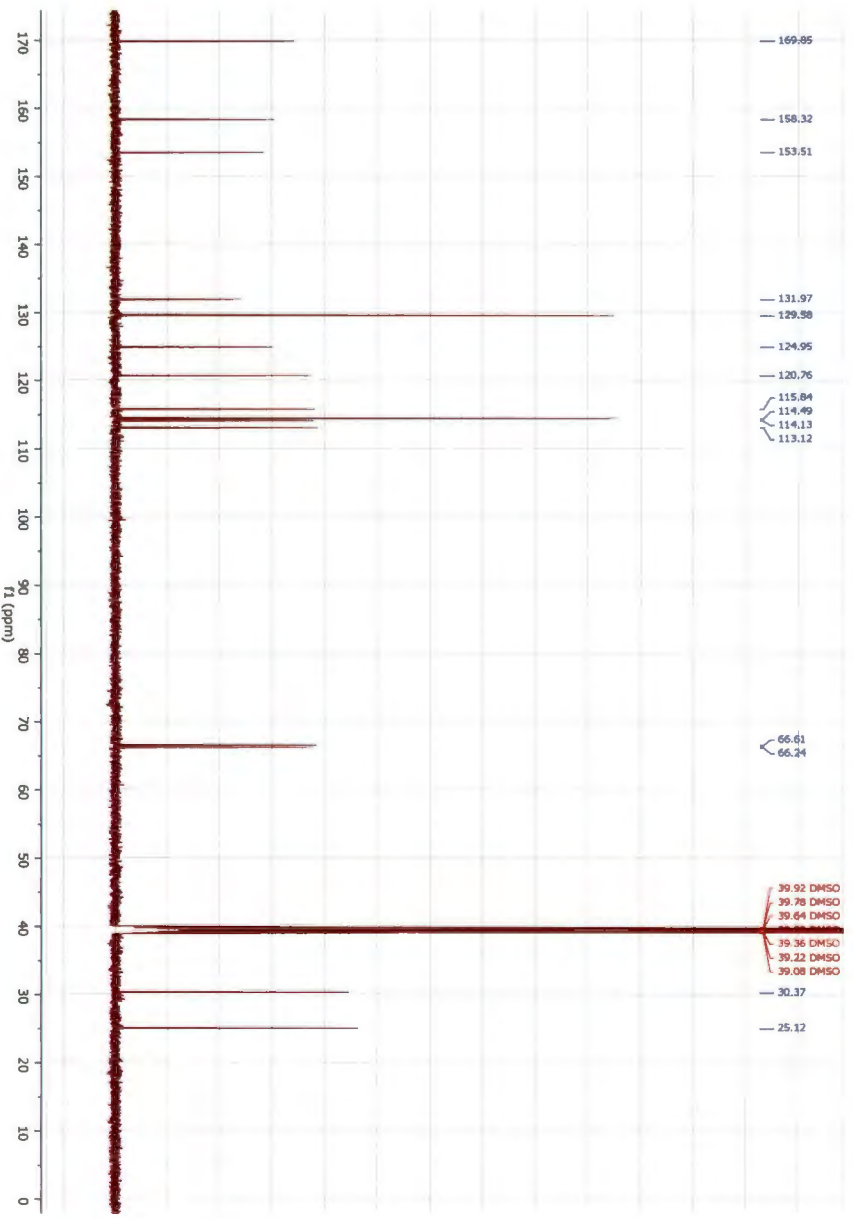
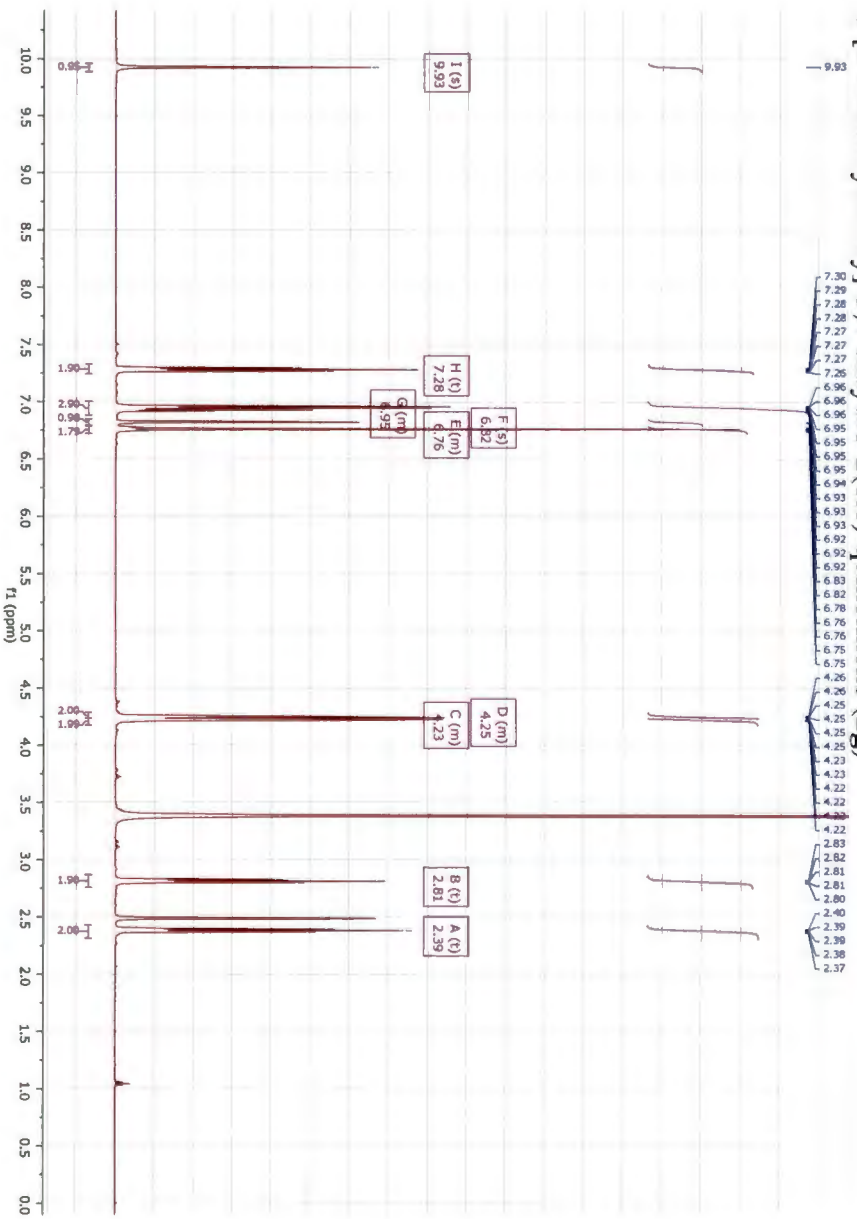
6-[2-(3-Methylphenyl)ethoxy]-3,4-dihydro-2(1H)-quinolinone (2e)



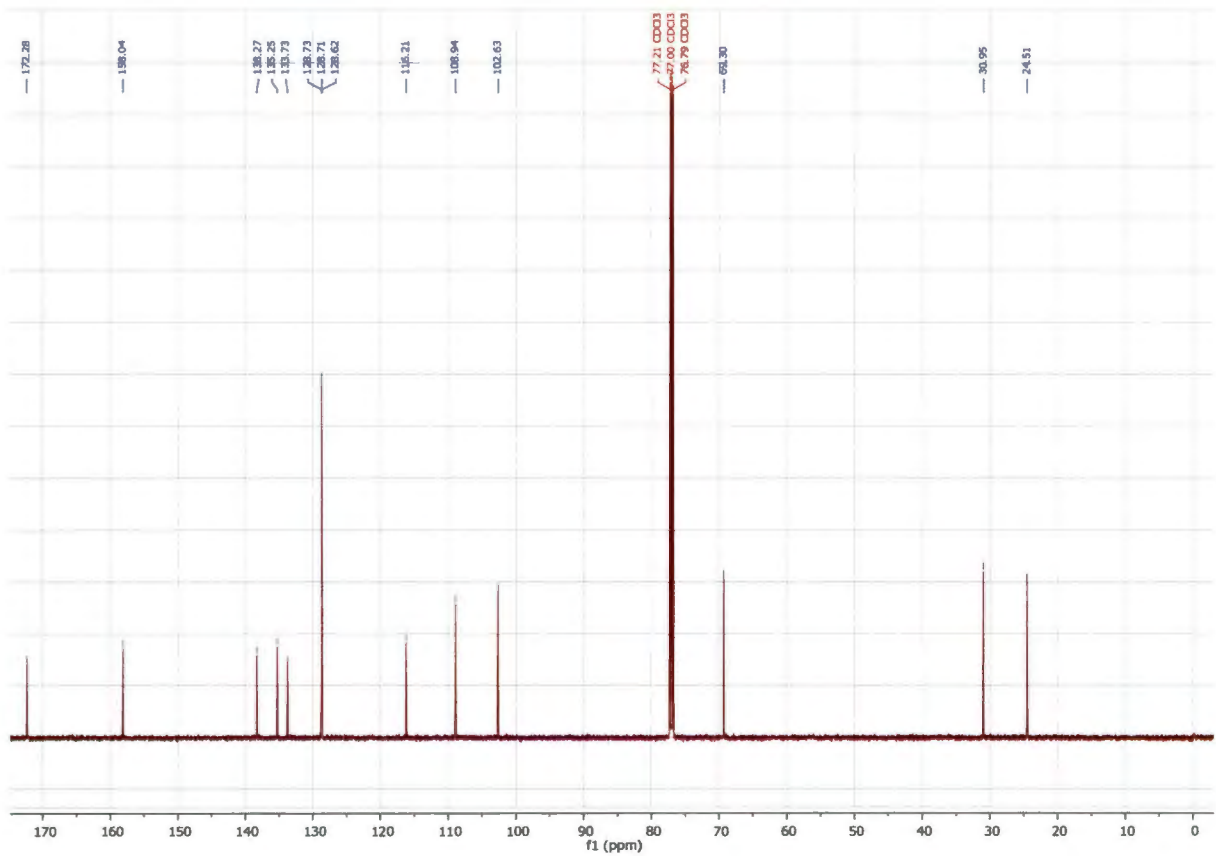
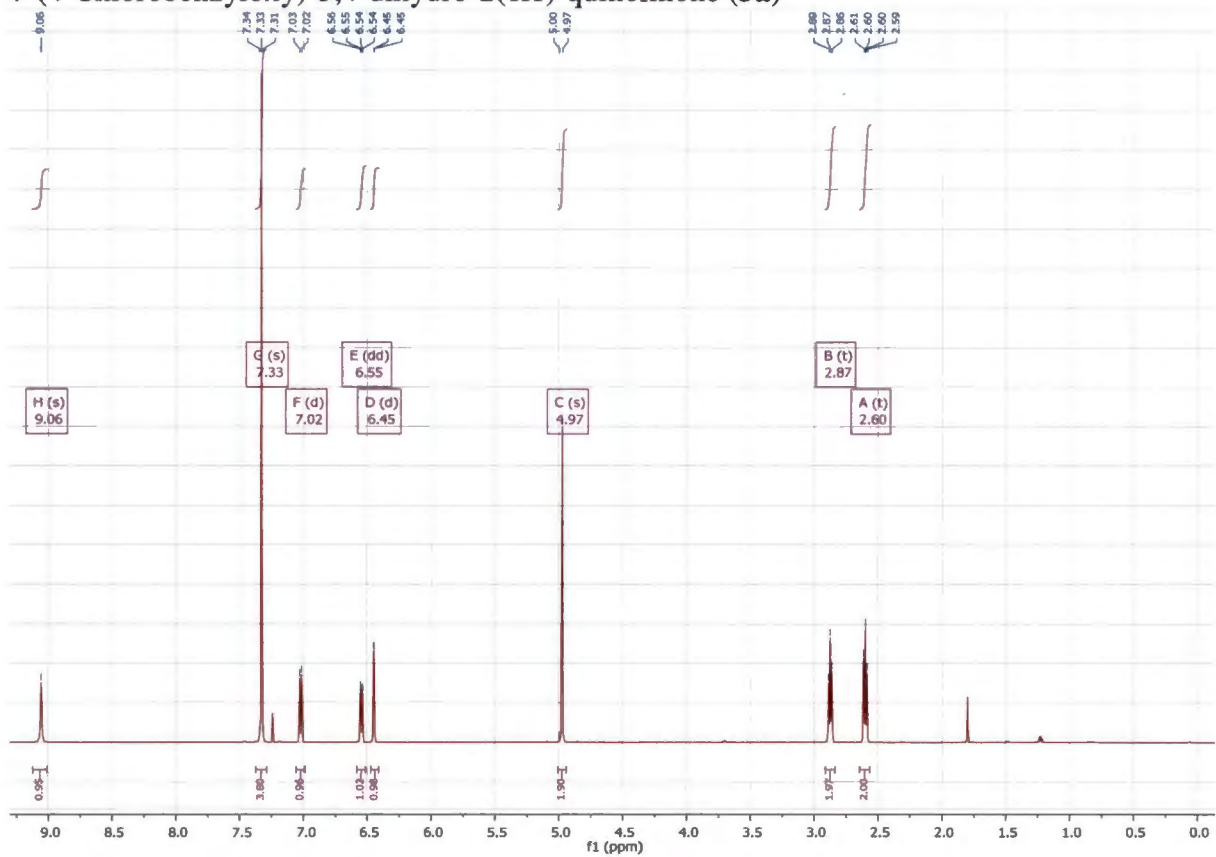
6-[2-(4-Methylphenyl)ethoxy]-3,4-dihydro-2(1H)-quinolinone (2f)



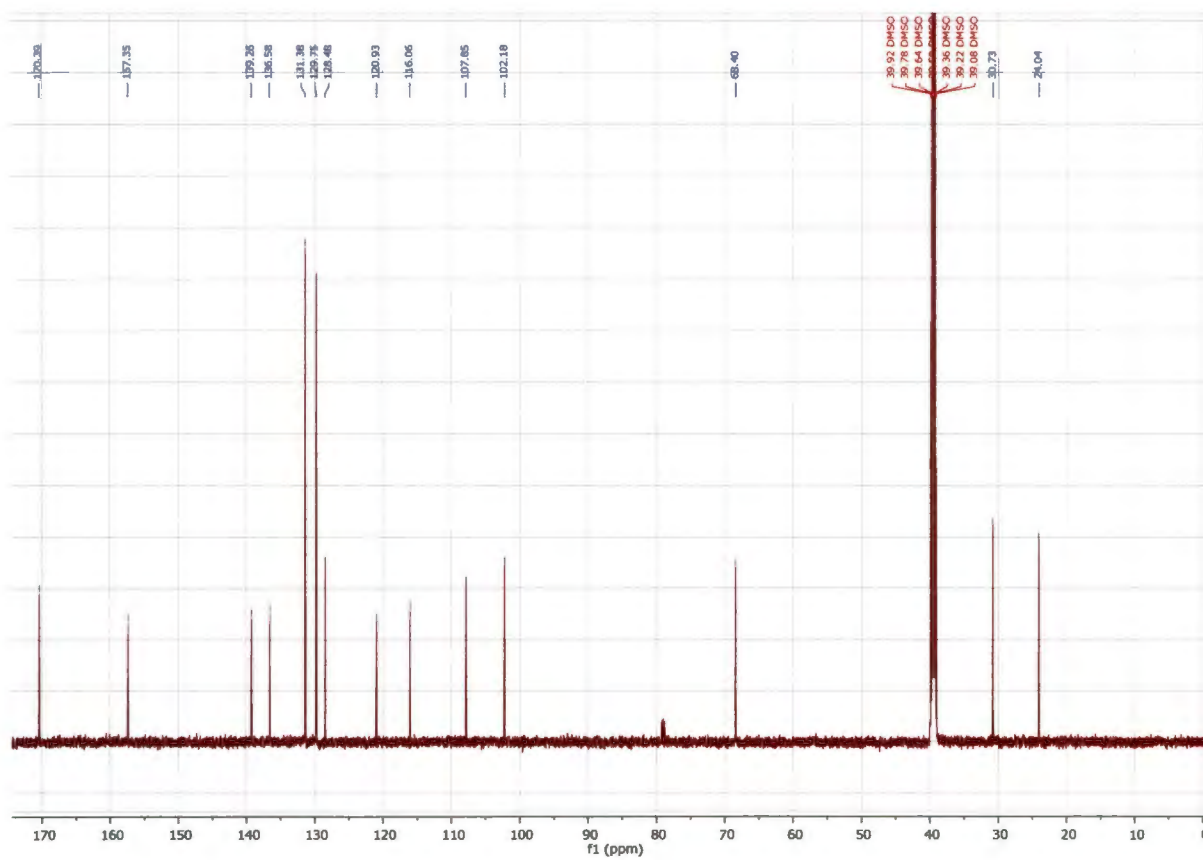
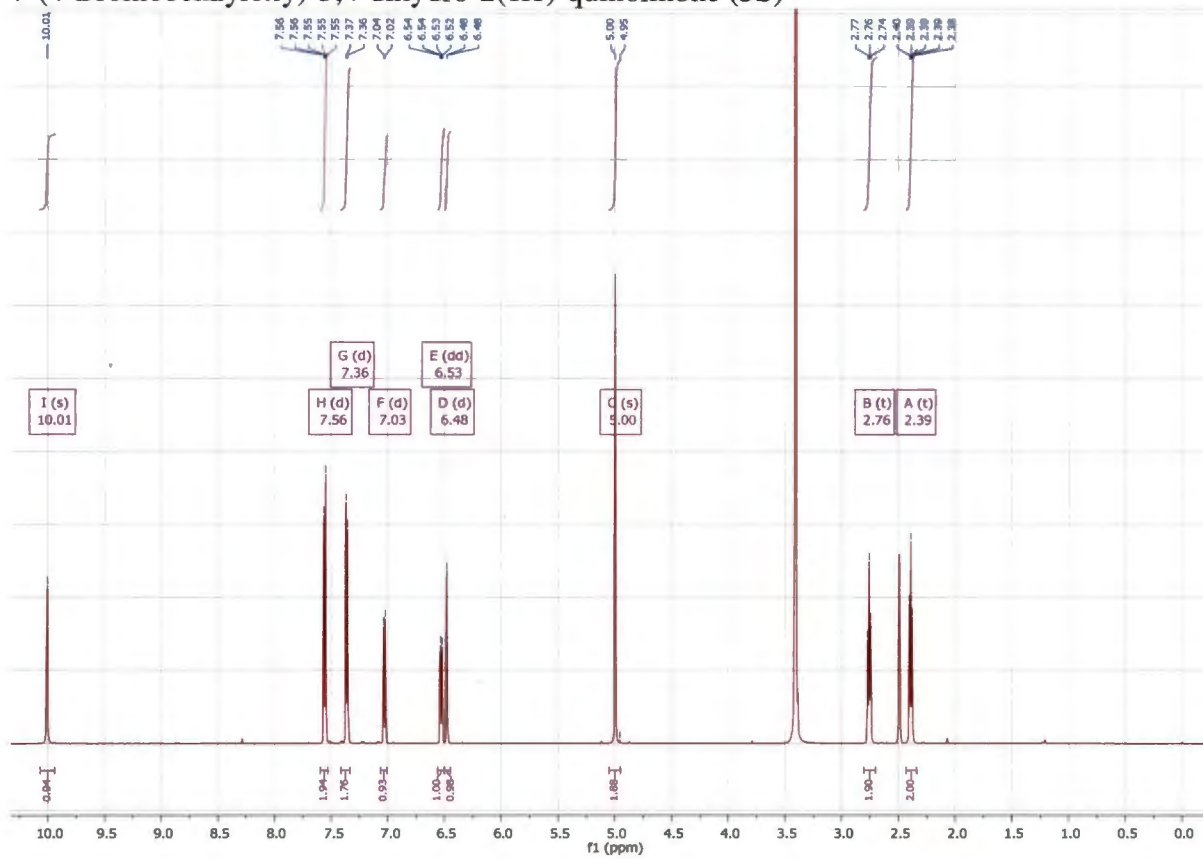
6-[2-Phenoxyethoxy]-3,4-dihydro-2(1H)-quinolinone (2g)



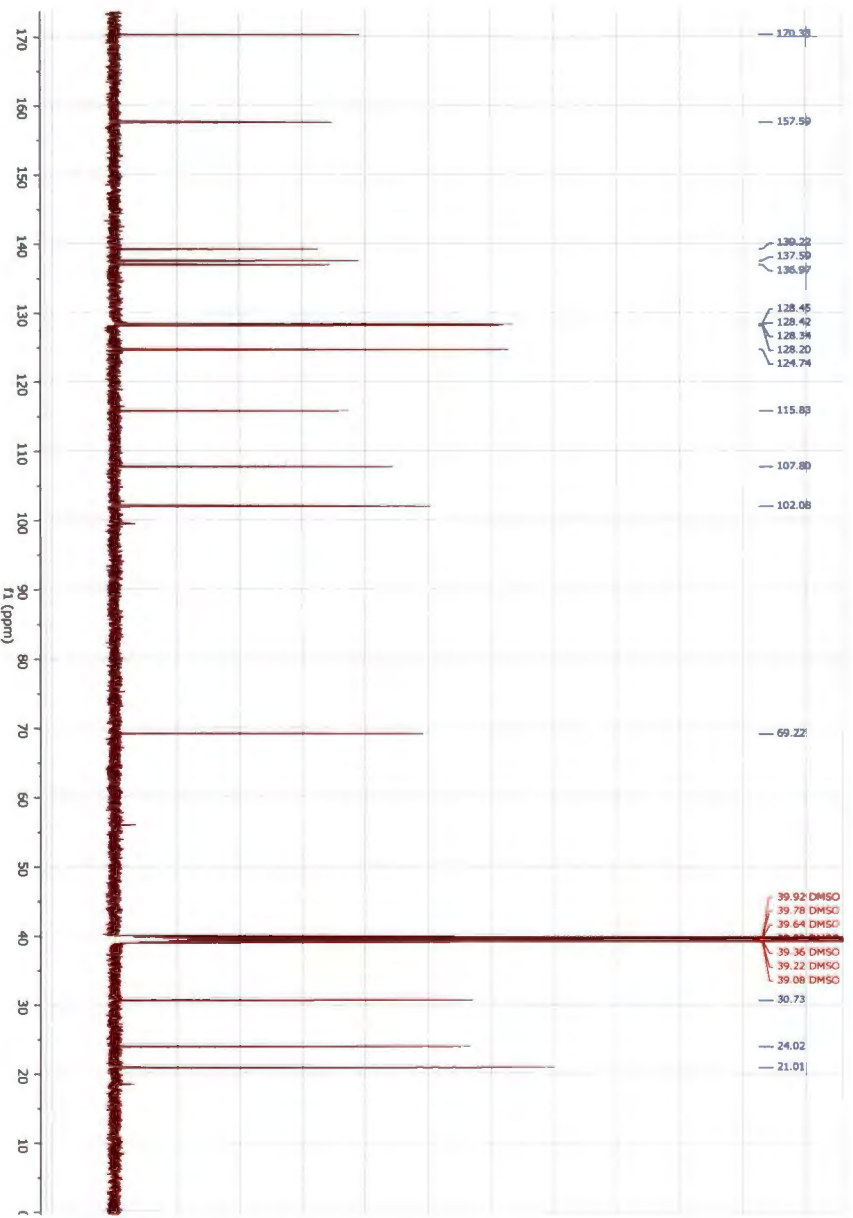
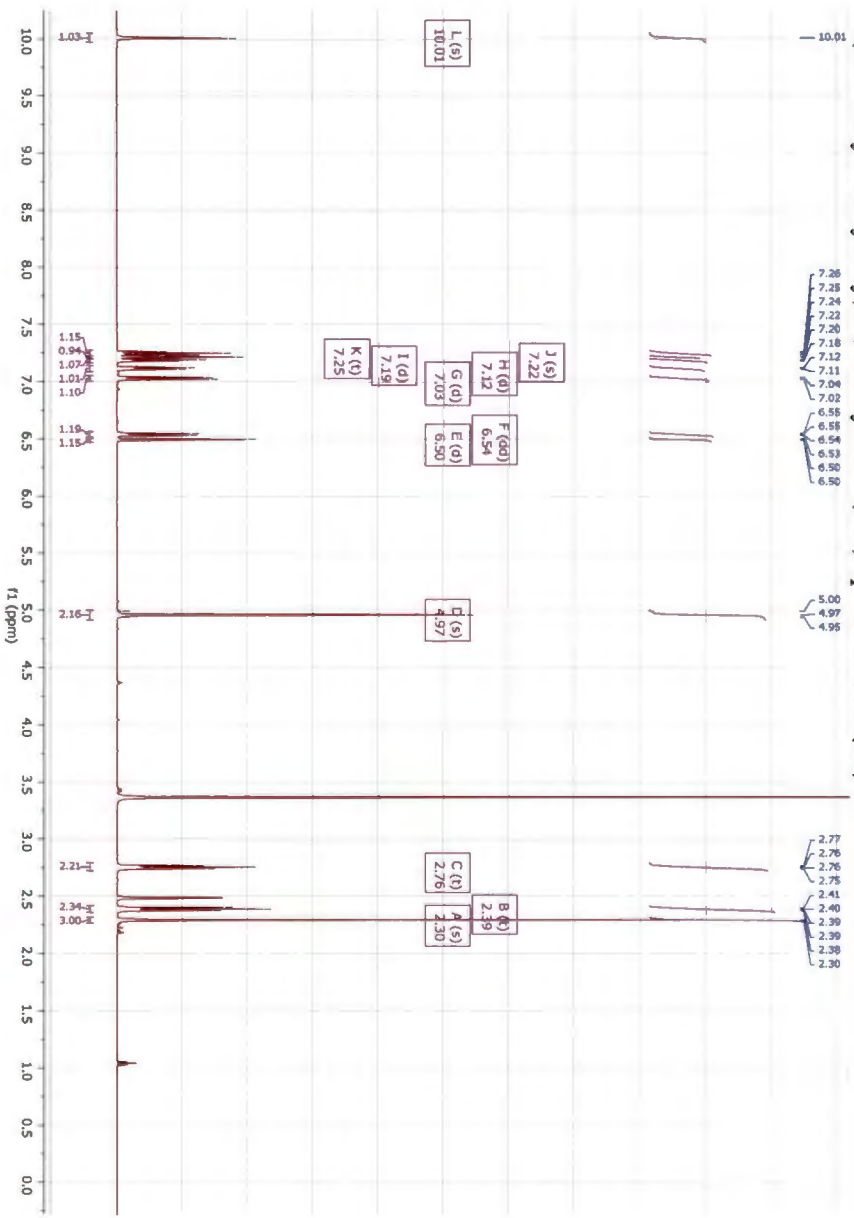
7-(4-Chlorobenzoyloxy)-3,4-dihydro-2(1H)-quinolinone (3a)



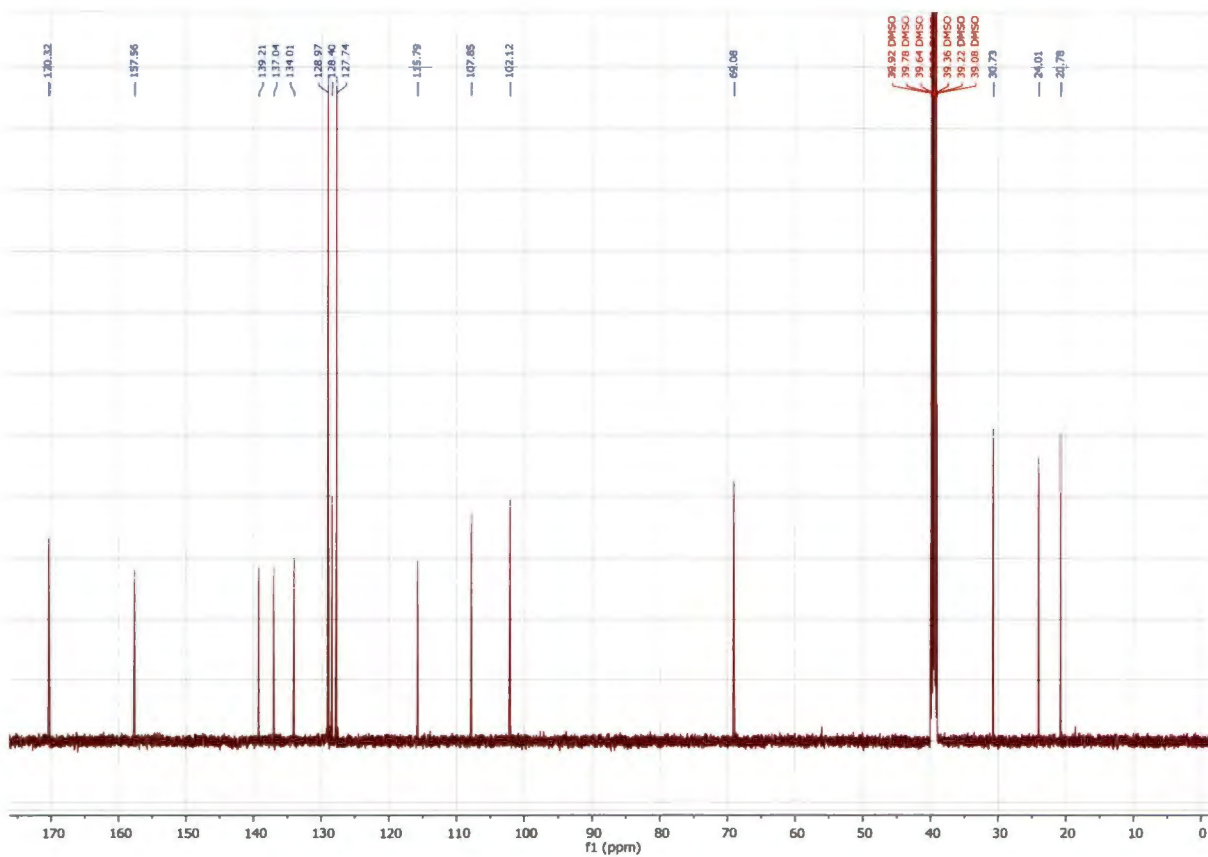
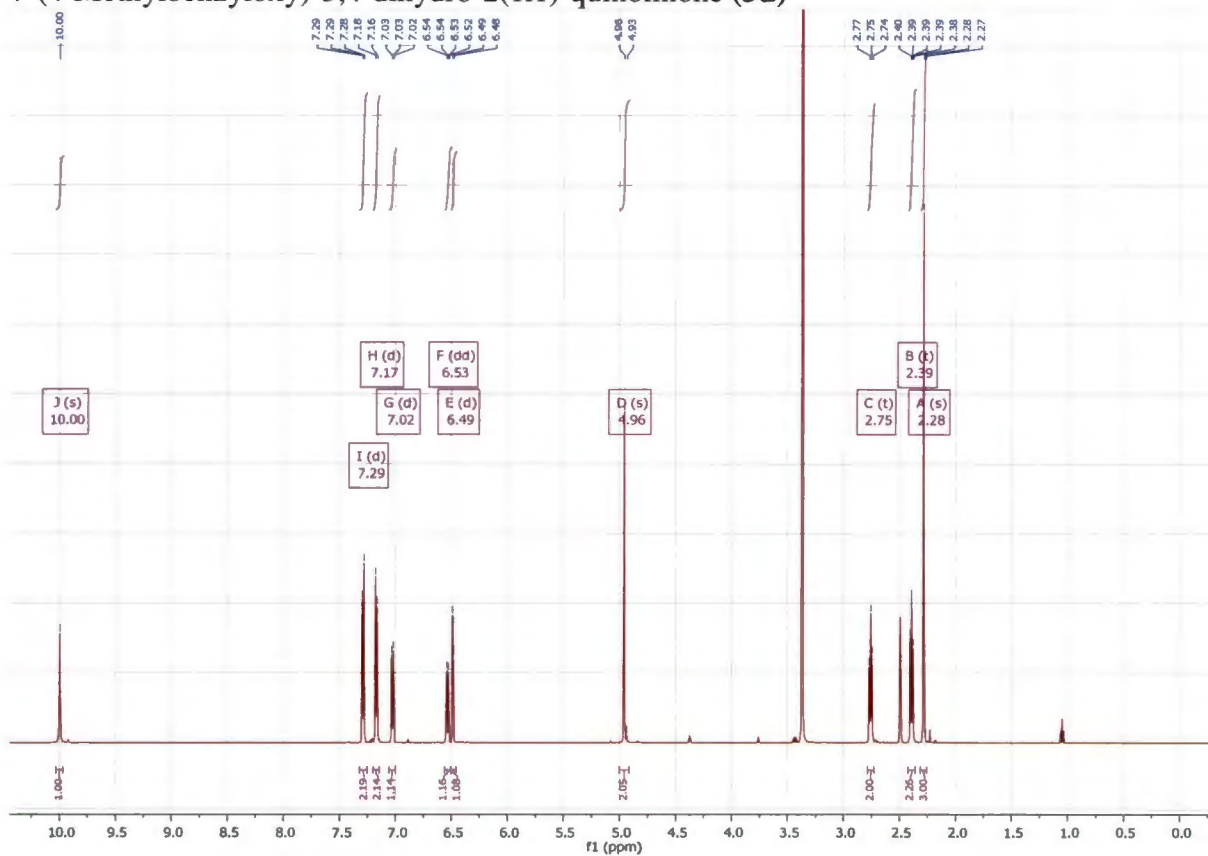
7-(4-Bromobenzyloxy)-3,4-dihydro-2(1H)-quinolinone (**3b**)



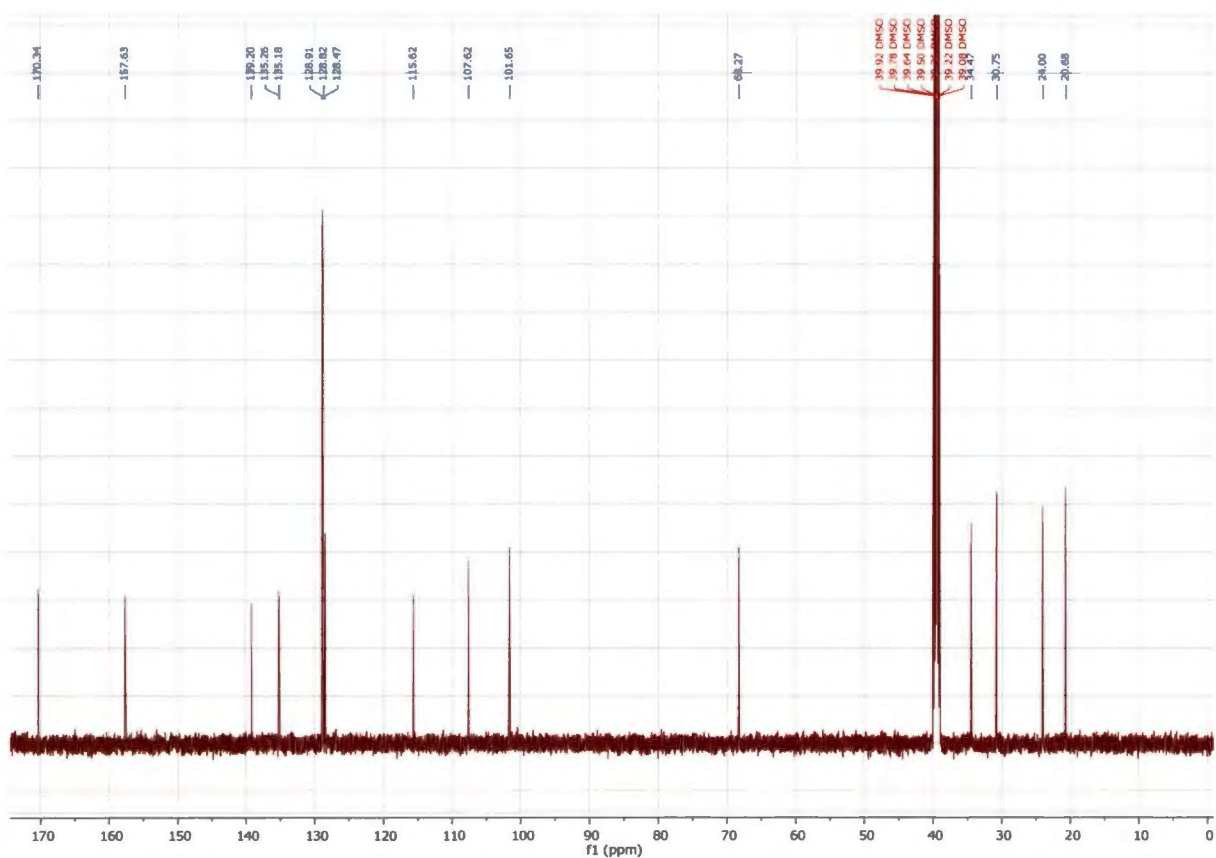
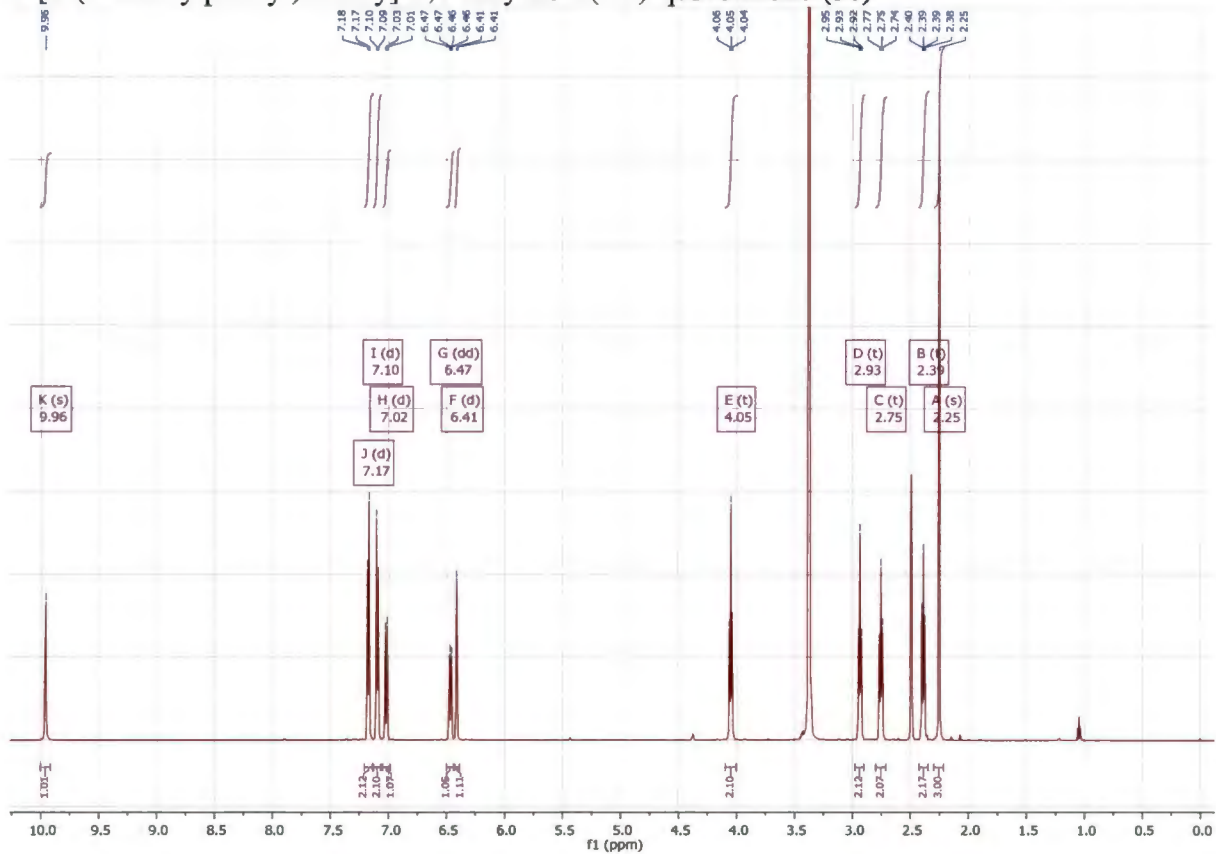
7-(3-Methylbenzyloxy)-3,4-dihydro-2(1H)-quinolinone (3c)



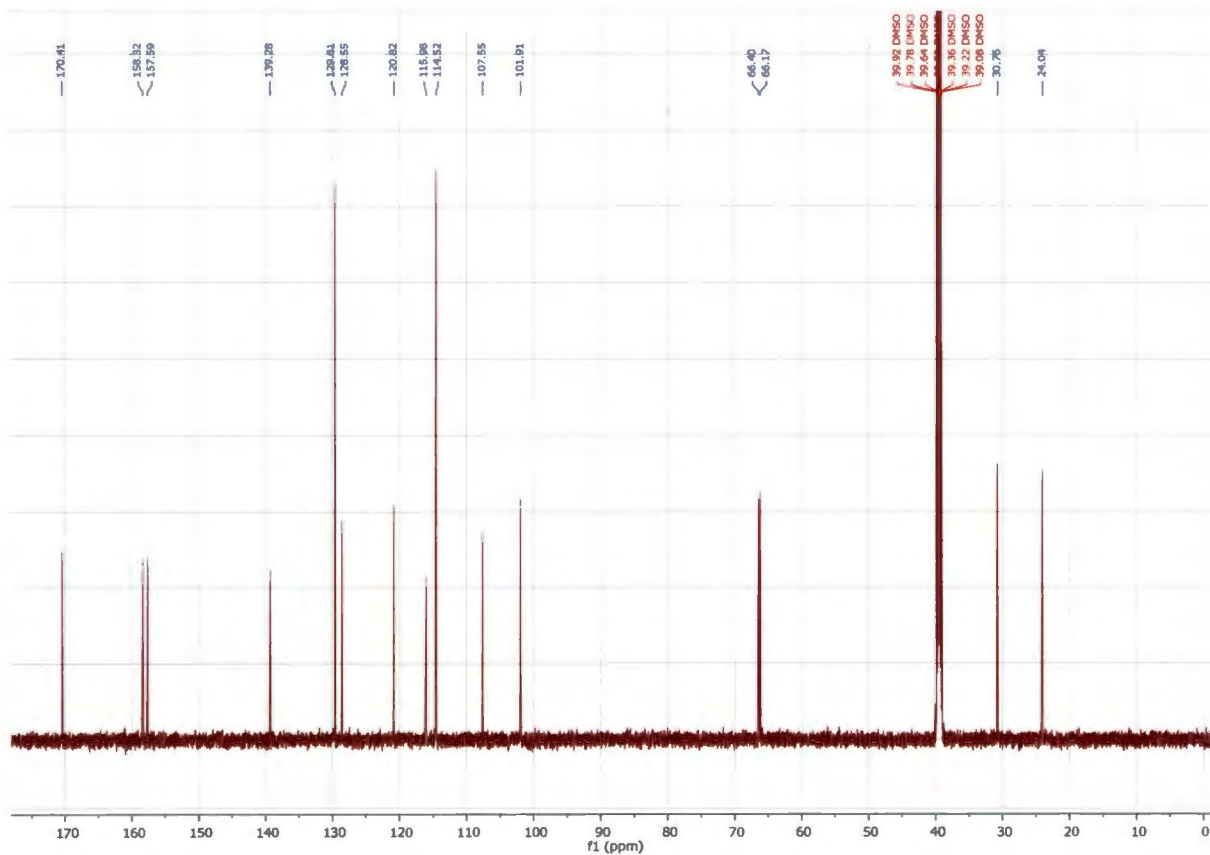
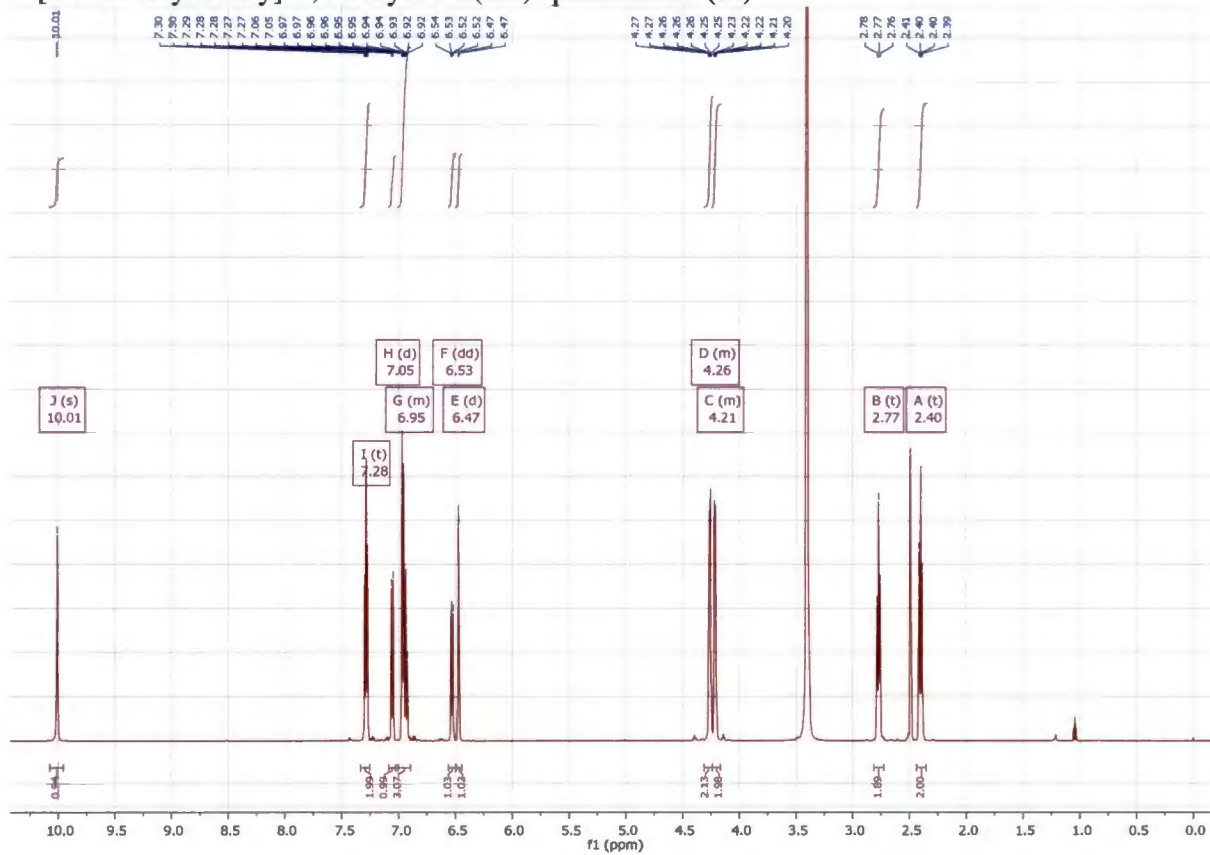
7-(4-Methylbenzyloxy)-3,4-dihydro-2(1H)-quinolinone (**3d**)



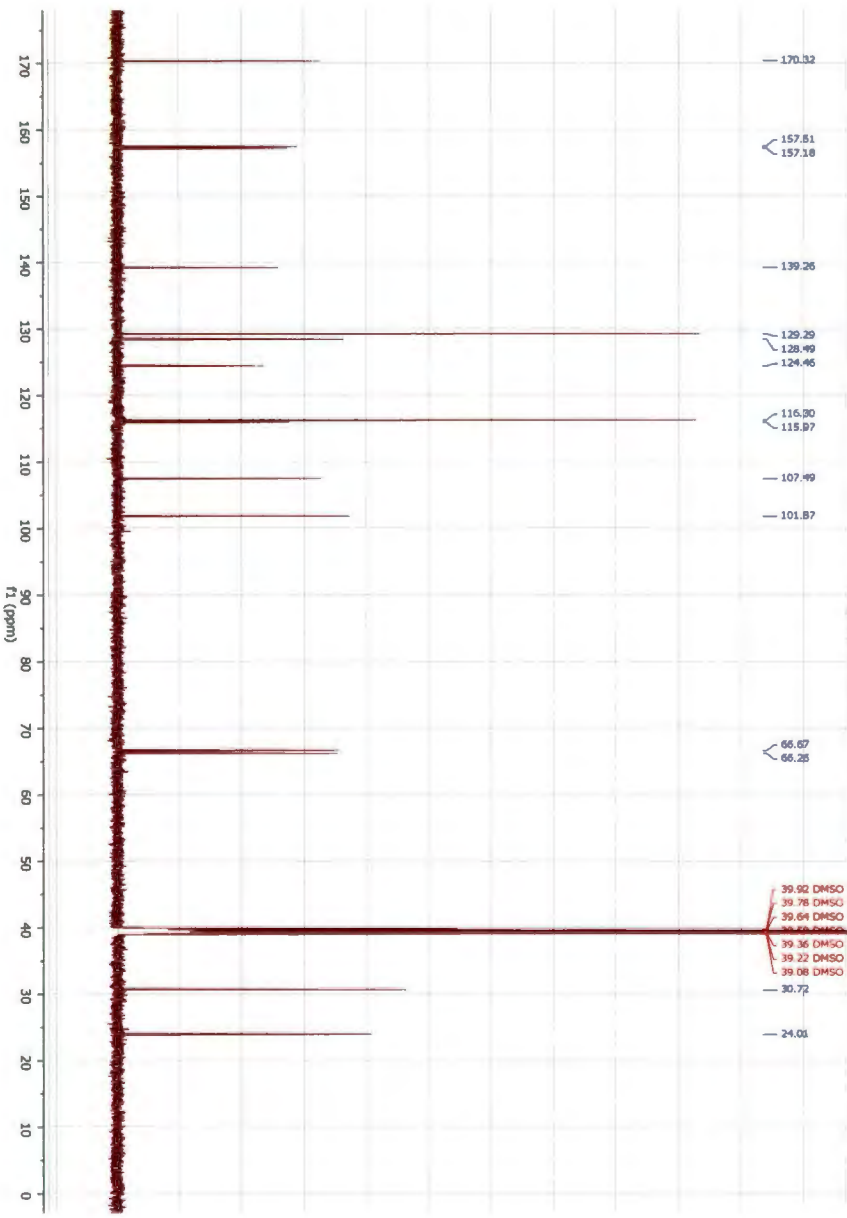
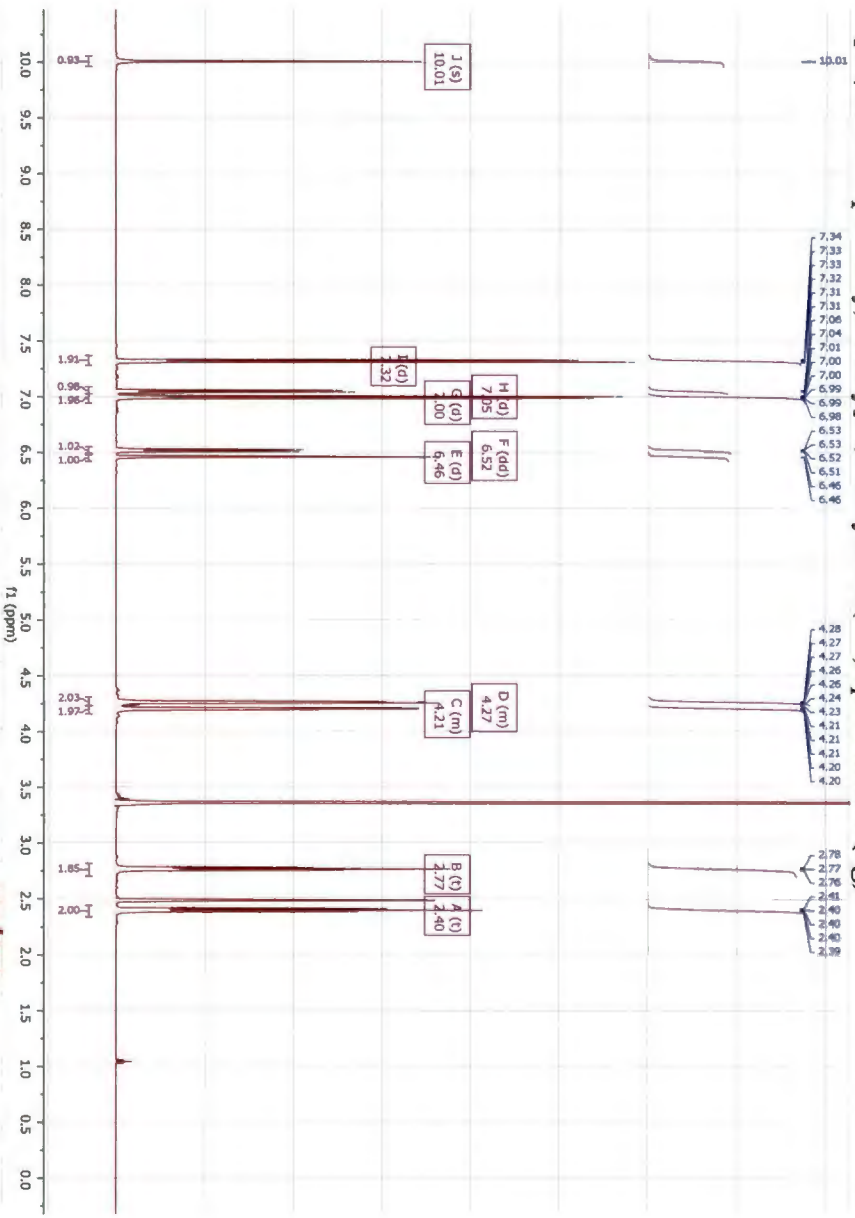
7-[2-(4-Methylphenyl)ethoxy]-3,4-dihydro-2(1H)-quinolinone (**3e**)



7-[2-Phenoxyethoxy]-3,4-dihydro-2(1H)-quinolinone (3f)



7-[2-(4-Chlorophenoxy)ethoxy]-3,4-dihydro-2(1H)-quinolinone (**3g**)



MANUSCRIPT C

The evaluation of 2-phenoxyethoxy-substituted tetralones as inhibitors of monoamine oxidase

Authors' contributions:

- The experimental work, interpretation of results and documentation of this study was carried out by L. Meiring.
- This study was conceptualised and documented with the assistance of J.P Petzer.
- The enzymology section of this study was conducted under the supervision of A. Petzer.

All co-authors provided permission to use this manuscript as part of L. Meiring's Ph.D thesis.

Letitia Meiring,¹ Jacobus P. Petzer,¹ Lesetja J. Legoabe,¹ and Anél Petzer^{1,*}

² *Pharmaceutical Chemistry, School of Pharmacy and Centre of Excellence for Pharmaceutical Sciences, North-West University, Private Bag X6001, Potchefstroom 2520, South Africa*

*Corresponding author: Anél Petzer, Tel.: +27 18 2994464, fax: +27 18 2994243

E-mail address: 12264954@nwu.ac.za

Running title: β -Tetralones as MAO inhibitors

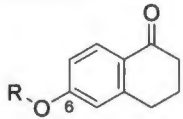
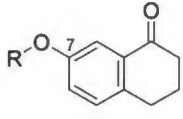
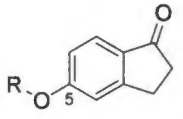
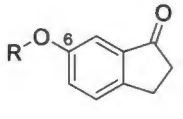
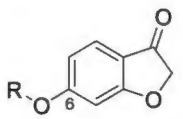
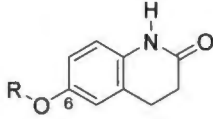
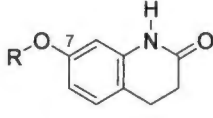
Keywords: monoamine oxidase, MAO, inhibition, reversible, tetralone.

Abstract: Previous studies have shown that α -tetralone (3,4-dihydro-2*H*-naphthalen-1-one) derivatives are highly potent monoamine oxidase (MAO) inhibitors with substitution on both the C6- and C7-positions yielding active compounds. Although α -tetralones are selective for the MAO-B isoform, this class of compounds also inhibits MAO-A with IC_{50} values <2.25 μ M. The present study investigates the possibility that the regioisomer, β -tetralone (3,4-dihydro-1*H*-naphthalen-2-one), may also act as a suitable scaffold for MAO inhibitor design. β -Tetralone derivatives, however, proved to be difficult to synthesise and purify, and after numerous experiments one derivative, 7-(2-phenoxyethoxy)-3,4-dihydronaphthalen-2(1*H*)-one (**17**), was obtained. For comparison, the C6- and C7-substituted α -tetralone homologues of this compound (**18** and **19**, respectively) were also synthesised. Interestingly **17** was found to be a weak inhibitor of human MAO-A ($IC_{50} = 56.2$ μ M) compared to the reported α -tetralones as well as to compounds **18** ($IC_{50} = 1.96$ μ M) and **19** ($IC_{50} = 1.81$ μ M). Compound **17**, however, was a potent human MAO-B inhibitor ($IC_{50} = 0.033$ μ M). It was also established that **17** is a reversible and competitive MAO-B inhibitor ($K_i = 0.128$ μ M). It may thus be concluded that, in contrast to the α -tetralones reported to date, **17** is a more selective MAO-B inhibitor. Selective MAO-B inhibitors are considered useful agents for the treatment of Parkinson's disease and are being investigated for slowing the progression of Alzheimer's disease.

The monoamine oxidase (MAO) enzymes consist of two distinctive isoforms, MAO-A and MAO-B (Youdim & Bahkle, 2006). These enzymes are present in all mammals and metabolise amine-containing neurotransmitters and compounds derived from the diet. Because of the key roles that they play in neurotransmitter metabolism, the MAOs are targets for several disease states, both in the central nervous system and in the peripheral tissues (Ramsay *et al.*, 2012; Ramsay *et al.*, 2013). Although similar in their amino acid sequences and structures of their active sites, MAO-A and MAO-B have different substrate specificities and also display different tissue distribution (Shih *et al.*, 1999; Son *et al.*, 2008). As a result, inhibitors of the two isoforms are employed for treatment of different disorders. MAO-A inhibitors are, for example, established therapy for depressive illness and act by blocking central serotonin metabolism (Lum and Stahl, 2012). MAO-B inhibitors are used in the treatment of Parkinson's disease where they reduce the MAO-B-catalysed metabolism of dopamine (Youdim *et al.*, 2006; Finberg, 2014). MAO-B inhibitors are also under investigation for Alzheimer's disease therapy and, in this regard, may act by a number of mechanisms (Naoi and Maruyama, 2010; Cai, 2014). Evidence suggests that MAO-A inhibitors may represent potential therapy for age-dependent cardiac cellular degeneration (Maurel *et al.*, 2003) and advanced prostate cancer (Flamand *et al.*, 2010). MAO-B inhibitors in particular have been advocated as potential neuroprotective agents by reducing MAO-generated hydrogen peroxide formation in the brain (Youdim & Bahkle, 2006). For neuroprotection in disorders associated with ageing such as Parkinson's disease, MAO-B is the relevant isoform since MAO-B activity increases in the brain with age, while MAO-A activity remains unchanged (Fowler *et al.*, 1997).

Interest in the pharmacology and potential new clinical applications of MAO inhibitors are thus substantial and a number of research efforts are aimed at discovering new chemical classes of MAO inhibitors, and deriving structure-activity relationships of known classes in inhibitors (Carradori and Silvestri, 2015; Carradori and Petzer, 2015). Tetralones play an important role in synthetic organic chemistry and are often used as starting materials for the synthesis of heterocyclic compounds, active pharmaceutical ingredients and natural products and their derivatives (Carreño *et al.*, 2006). The tetralone moiety is also frequently encountered in compounds displaying pharmacological activities (Manvar *et al.*, 2015). In this regard, recent reports that C6- and C7-substituted α -tetralone derivatives (**1** and **2**) are potent inhibitors of human MAO are of particular interest (Legoabe *et al.*, 2014; Legoabe *et al.*, 2015). As shown in table 1, the α -tetralone derivatives inhibit both MAO isoforms with specificity for MAO-B. Other chemical classes closely related to α -tetralone have also been reported to potently inhibit the MAOs. These include 1-indanone (**3** and **4**), 3-coumaranone (**5**) and 3,4-dihydro-2(1*H*)-quinolinone (**6** and **7**) derivatives (Mostert *et al.*, 2015; Van Dyk *et al.*, 2015; Meiring *et al.*, 2013). For all of these derivatives substitution occur on the phenyl ring with an alkyloxy group such as the benzyloxy, 2-phenylethoxy, 3-phenylpropoxy and 2-phenoxyethoxy groups. This substitution is crucial for inhibitory activity as the hydroxy-substituted parent compounds (**8–14**) display weak MAO inhibition (Table 2). In the present study we investigate the possibility that the regioisomer of α -tetralone, β -tetralone (3,4-dihydro-1*H*-naphthalen-2-one), may also represent a useful scaffold for MAO inhibitor design (Fig. 1). Based on the close similarity with other moieties successfully used in experimental MAO inhibitors, such as those in table 1, it is anticipated that β -tetralone-derived compounds would act as MAO inhibitors.

Table 1. The reported IC₅₀ values for the inhibition of recombinant human MAO-A and MAO-B by α -tetralone (1 and 2), 1-indanone (3 and 4), 3-coumaranone (5) and 3,4-dihydro-2(1*H*)-quinolinone derivatives (6 and 7) derivatives (R = alkyl/arylalkyl substituent).

		IC ₅₀ range (μ M)	
		MAO-A	MAO-B
1		0.024–2.25 ^a	0.0045–0.078 ^a
2		0.010–1.26 ^b	0.00089–0.047 ^b
3		0.504–10.75 ^c	0.015–0.298 ^c
4		0.032–1.348 ^c	0.001–0.03 ^c
5		0.586–(>100) ^d	0.004–1.05 ^d
6		12.4–50.6 ^e	0.086–4.01 ^e
7		7.98–(>100) ^e	0.0029–0.191 ^e

^a Values obtained from reference (Legoabe *et al.*, 2014).

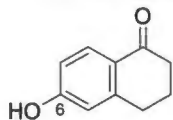
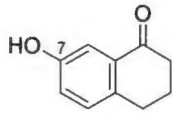
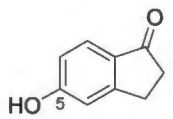
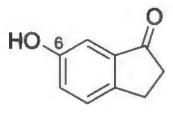
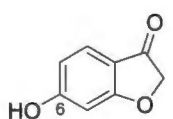
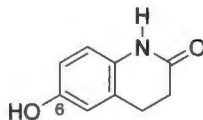
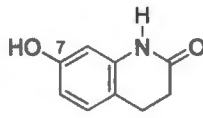
^b Values obtained from reference (Legoabe *et al.*, 2015).

^c Values obtained from reference (Mostert *et al.*, 2015).

^d Values obtained from reference (Van Dyk *et al.*, 2015).

^e Values obtained from reference (Meiring *et al.*, 2013).

Table 2. The reported IC₅₀ values for the inhibition of recombinant human MAO-A and MAO-B by hydroxy-substituted α -tetralones, 1-indanones, 3-coumaranone and 3,4-dihydro-2(1*H*)-quinolinones.

		IC ₅₀ (μ M)	
		MAO-A	MAO-B
8		43.8 ^a (51.6 \pm 0.256) ^b	66.4 ^a (108 \pm 3.81) ^b
9		39.4 ^c (42.0 \pm 4.63) ^b	187 ^c (85.1 \pm 12.3) ^b
10		61.7 ^d	>100 ^d
11		64.7 ^d	85.4 ^d
12		>100 ^e	12.0 ^e
13		161 ^f	201 ^f
14		183 ^f	>100 ^f

^a Values obtained from reference (Legoabe *et al.*, 2014).

^b Determined in the current study [mean \pm standard deviation (SD)].

^c Values obtained from reference (Legoabe *et al.*, 2015).

^d Values obtained from reference (Mostert *et al.*, 2015).

^e Values obtained from reference (Van Dyk *et al.*, 2015).

^f Values obtained from reference (Meiring *et al.*, 2013).

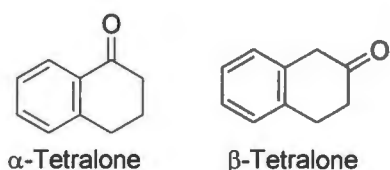


Fig. 1. The structures of α -tetralone and β -tetralone.

For this study, β -tetralone will be substituted on the C7-position with alkyloxy groups. This selection was based on the commercial availability of 7-methoxy-2-tetralone (**15**) in sufficient quantities to allow for the synthetic modification thereof.

To synthesise the β -tetralone derivatives a similar approach was followed as that reported for the synthesis of substituted α -tetralone derivatives (Fig. 2) (Legoabe *et al.*, 2014; Legoabe *et al.*, 2015). The key starting material, 7-methoxy-2-tetralone (**15**) was treated with aluminum trichloride (AlCl_3 , anhydrous) in toluene to yield 7-hydroxy-2-tetralone (**16**). 7-Hydroxy-2-tetralone (**16**), in turn, was reacted with the selected alkyl bromide in acetone, with K_2CO_3 serving as base. These reactions were carried out at reflux temperature for 6 h. The workup consisted of filtration of the reaction through a pad of celite, and purification of the product with silica gel column chromatography (ethyl acetate/petroleum ether 40:60). C7-Substituted ethers of β -tetralone, however, proved to be difficult to synthesise and after reacting 7-hydroxy-2-tetralone (**16**) with benzyl bromide (including 4-chlorobenzyl bromide), 2-phenylethyl bromide, 3-phenylpropyl bromide, cyclohexylmethyl bromide and 2-bromoethyl phenyl ether, only the latter reaction yielded significant amounts (>1%) of product [7-(2-phenoxyethoxy)-3,4-dihydronaphthalen-2(1*H*)-one (**17**)] with acceptable purity (Fig. 3). The reaction of 2-bromoethyl phenyl ether with 6-hydroxy-1-tetralone (**8**) and 7-hydroxy-1-tetralone (**9**), however, proceeded with moderate yields (34–49%), and high purity products were obtained without the requirement of column chromatography. Compounds **18** and **19** thus synthesised were purified by recrystallisation from ethanol.

6-Hydroxy-1-tetralone (**8**) and 7-hydroxy-1-tetralone (**9**) were synthesised from the methoxy homologues, **20** and **21**, as described previously (Legoabe *et al.*, 2014; Legoabe *et al.*, 2015). The structures of the tetralones were characterised by ^1H NMR, ^{13}C NMR and mass spectrometry, and the physical data are given in the supplementary material.

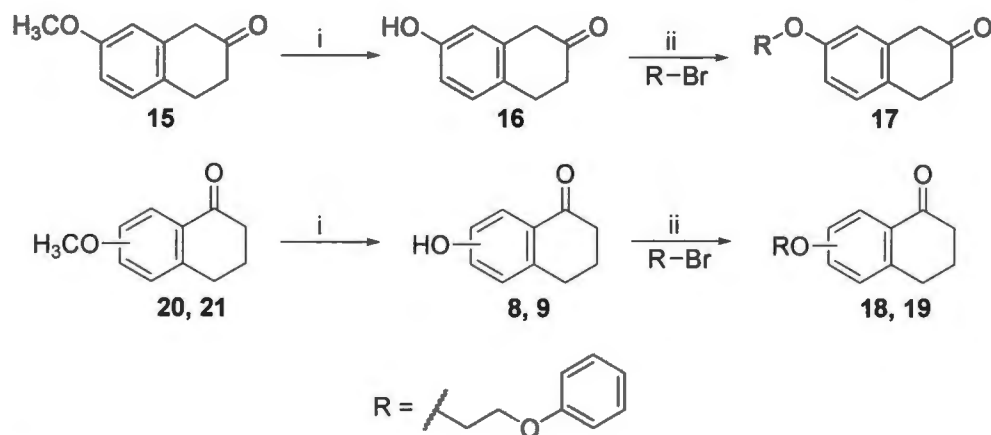


Fig. 2. Synthetic pathway to C6- or C7-substituted ethers of α -tetralone and β -tetralone. Reagents and conditions: (i) AlCl_3 , toluene; reflux; (ii) acetone, K_2CO_3 , reflux.

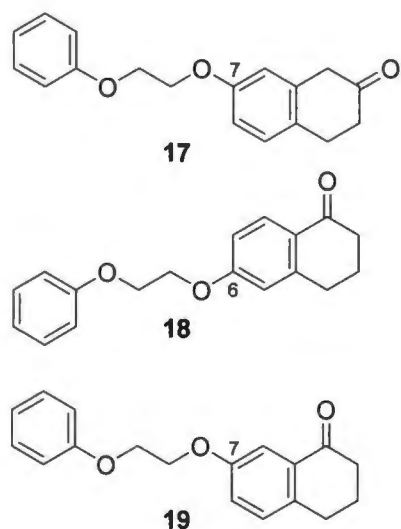
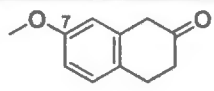
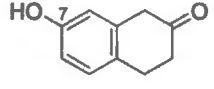
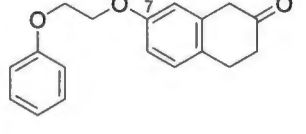
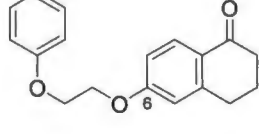
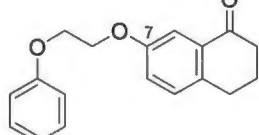


Fig. 3. The structures of tetralone derivatives **17–19**.

The MAO inhibition properties of the 2-phenoxyethoxy-substituted tetralones, compounds **17–19**, were characterised with the aim of comparing their inhibition potencies.

The MAO inhibition potencies of the starting material, 7-methoxy-2-tetralone (**15**), and intermediate, 7-hydroxy-2-tetralone (**16**), in the synthesis of **17** were also measured for comparison. The MAO inhibition properties of 6-hydroxy-1-tetralone (**8**) and 7-hydroxy-1-tetralone (**9**) have been reported (Table 2) (Legoabe *et al.*, 2014; Legoabe *et al.*, 2015). Since the inhibition data given in tables 1 and 2 were recorded under identical conditions as this study, direct comparison of the IC₅₀ values are possible. For the inhibition studies, recombinant human MAO-A and MAO-B were used as enzyme sources with kynuramine serving as substrate for both isoforms. The formation of 4-hydroxyquinoline, the ultimate product of kynuramine oxidation by MAO, were measured by fluorescence spectrophotometry (Mostert *et al.*, 2015). After measuring the rate of kynuramine oxidation in the absence and presence of the test inhibitor (at concentrations spanning at least 3 orders of magnitude) sigmoidal dose-response were constructed from which IC₅₀ values were estimated (Fig. 4). These values are given in table 3.

Table 3. The measured IC_{50} values for the inhibition of recombinant human MAO-A and MAO-B by tetralone derivatives **17–19** as well as by 7-methoxy-2-tetralone (**15**) and 7-hydroxy-2-tetralone (**16**).

		IC_{50} (μM) ^a		SI ^b
		MAO-A	MAO-B	
15		38.1 ± 1.00	59.8 ± 1.28	0.64
16		70.5 ± 1.83	>100 ^c	–
17		56.2 ± 3.44	0.033 ± 0.004	1703
18		1.96 ± 0.72	0.022 ± 0.0013	89
19		1.81 ± 0.326	0.0043 ± 0.0012	421

^a All values are expressed as the mean \pm SD of triplicate determinations.

^b The selectivity index is the selectivity for the MAO-B isoform and is given as the ratio of IC_{50} (MAO-A)/ IC_{50} (MAO-B).

^c No inhibition observed at maximum tested concentration of 100 μM .

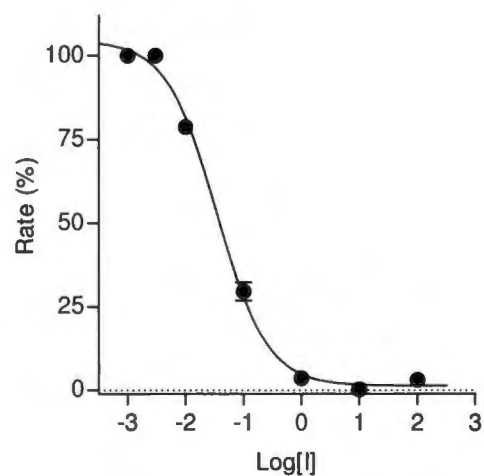


Fig. 4. The sigmoidal dose-response curves for the inhibition of MAO-B by **17**. Data were measured in triplicate and data points are given as mean \pm standard deviation (SD).

As anticipated, the C7-substituted β -tetralone ether, compound **17**, proved to be a potent MAO-B inhibitor with an IC_{50} value of 0.033 μ M. The inhibition potency of this compound is therefore in the same range as that of the reference MAO-B inhibitors lazabemide (IC_{50} = 0.091 μ M) and safinamide (IC_{50} = 0.048 μ M) (Petzer *et al.*, 2013). Based on this comparison, **17** may thus be regarded as a potent MAO-B inhibitor. The C6- and C7-substituted α -tetralone ethers, **18** and **19**, also inhibited MAO-B with good potencies and displayed IC_{50} values of 0.022 and 0.0043 μ M. The α -tetralone compound **19** is thus a significantly more potent MAO-B inhibitor than **17**.

The results also show that the C7-substituted α -tetralone ethers, **18** (IC_{50} = 1.96 μ M) and **19** (IC_{50} = 1.81 μ M), are significantly more potent MAO-A inhibitors than β -tetralone homologue **17** (IC_{50} = 56.2 μ M). According to the selectivity index values ($SI > 89$), all of these compounds are, however, selective MAO-B inhibitors with **17** ($SI = 1703$) being the most selective. The molecular basis for the lower MAO-A and MAO-B inhibition potencies of **17** compared to **18** and **19** is not apparent and will be investigated with molecular docking below. As anticipated, the 2-phenoxyethoxy substituent is required for MAO-A and MAO-B inhibition since 7-hydroxy-2-tetralone (**16**) is a very weak inhibitor of both MAO isoforms.

Employing dialysis, the reversibility of MAO-B inhibition by **17** was investigated. Since **17** proved to be a weak MAO-A inhibitor, the reversibility of MAO-A inhibition was not examined. For comparison the reversibility of MAO-B inhibition by **18** and **19** were also investigated. Interestingly, previous reports suggest that MAO-B inhibition by selected C7-substituted α -tetralone ethers is not completely reversible and these compounds may exhibit tight-binding to the enzyme. To investigate reversibility, the test inhibitors (at concentrations of $4 \times IC_{50}$) were incubated with MAO-B for 15 min and subsequently dialysed for 24 h.

The mixtures were diluted twofold with the addition of kynuramine and the residual activities were measured. As controls, similar dialysis experiments were carried out in the presence of the irreversible MAO-B inhibitor, (R)-deprenyl (positive control), as well as in the absence of inhibitor (negative control signifying 100% residual activity). The residual MAO-B activity of undialysed mixtures of MAO-B and the test inhibitors were also recorded for comparison. The results show that the test compounds, **17–19**, are reversible MAO-B inhibitors since dialysis restores enzyme activity to levels of 64–149% of the negative control (Fig. 5). Inhibition, however, persists in undialysed mixtures of MAO-B and the test inhibitors with the enzyme activities at 16–48%. As expected, dialysis does not restore MAO-B activity after inactivation with (R)-deprenyl (5%).

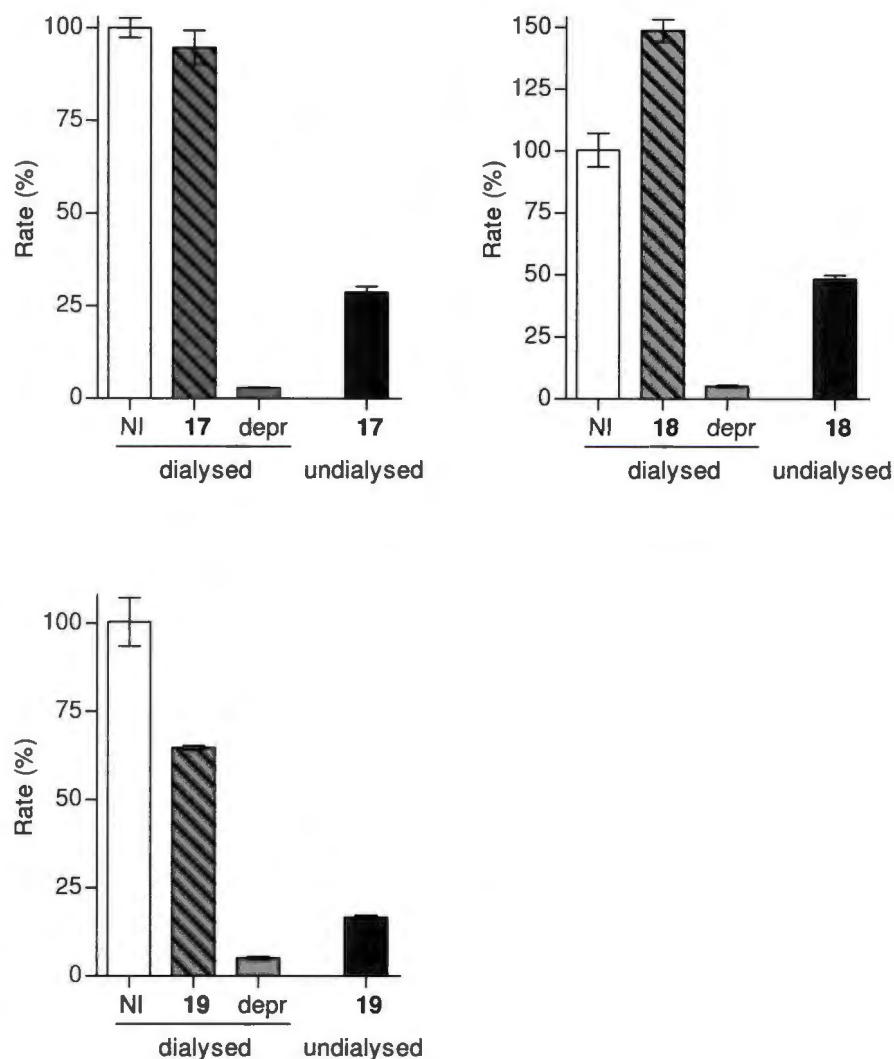


Fig. 5. Compounds **17–19** inhibit MAO-B reversibly. MAO-B and the test inhibitors (at $4 \times IC_{50}$) were preincubated for 15 min, dialysed for 24 h and the residual enzyme activity was measured (**17–19** dialysed). Similar incubation and dialysis of MAO-B in the absence inhibitor (NI dialysed) and presence of the irreversible inhibitor, (R)-deprenyl (depr dialysed), were also carried out. The residual activities of undialysed mixtures of MAO-B with the test inhibitors were also recorded (**17–19** undialysed).

Since **17** is a reversible MAO-B inhibitor, the enzyme-inhibitor dissociation constant (K_i value) was measured. For this purpose a set of six Lineweaver-Burk plots was constructed using the following inhibitor concentrations: $0 \mu\text{M}$, $\frac{1}{4} \times IC_{50}$, $\frac{1}{2} \times IC_{50}$, $\frac{3}{4} \times IC_{50}$, $1 \times IC_{50}$ and $1\frac{1}{4} \times IC_{50}$. For each plot eight concentrations of kynramine ($15\text{--}250 \mu\text{M}$) were used.

The set of Lineweaver-Burk plots is given in Fig. 6 and is indicative of competitive inhibition since the linear lines intersect on the y-axis. Global (shared) fitting of the inhibition data directly to the Michaelis-Menten equation gave a K_i value of $0.128 \pm 0.032 \mu\text{M}$ ($R^2 = 0.98$). This value is similar to that ($0.056 \mu\text{M}$) obtained from a plot of the slopes of the Lineweaver-Burk plots versus inhibitor concentration where the x-axis intercept equals $-K_i$.

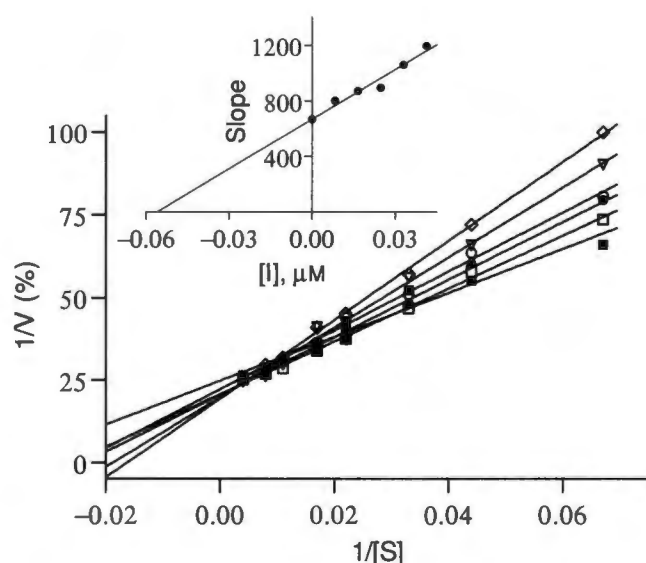


Fig. 6. Lineweaver-Burk plots for the inhibition of MAO-B by **17**. The inset is a graph of the slopes of the Lineweaver-Burk plots versus inhibitor concentration.

To determine possible binding modes and key interactions of **17–19**, the inhibitors were docked into the MAO active sites using the CDOCKER docking algorithm of Discovery Studio 3.1 (Accelrys). For this purpose the literature procedure was followed (Mostert *et al.*, 2015). As enzyme models, the crystal structures of human MAO-A (PDB code: 2Z5X) (Son *et al.*, 2008) and MAO-B (PDB code: 2V5Z) (Binda *et al.*, 2007) were employed. As shown in Fig. 7, compounds **17–19** bind in the MAO-B active site with the tetralone moieties located in the substrate cavity, in proximity to the flavin adenine dinucleotide (FAD) cofactor.

The 2-phenoxyethoxy side chains of these inhibitors project into the entrance cavity of MAO-B (the space beyond Ile-199). These binding orientations are similar to those observed for related compounds, such as 7-(3-chlorobenzoyloxy)-4-formylcoumarin (**22**), in crystallographic studies (Fig. 8) (Binda *et al.*, 2007).

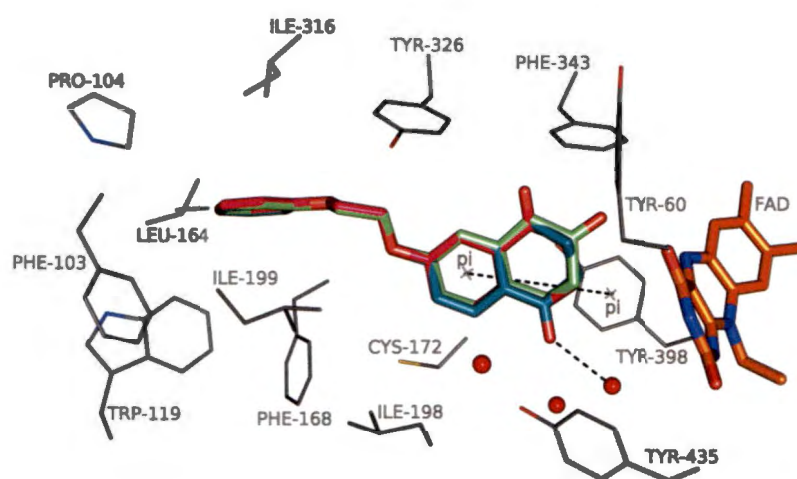


Fig. 7. The docked binding orientations of **17–19** in MAO-B. Key: **17** (light green); **18** (dark green); **19** (magenta).

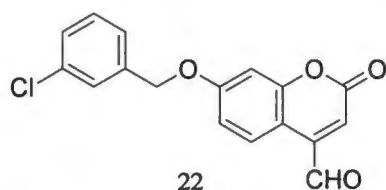


Fig. 8. The structure of 7-(3-chlorobenzoyloxy)-4-formylcoumarin (**22**).

Most noteworthy is that the binding orientations of **17–19** are virtually super imposable, which may explain the finding that these compounds are all highly potent MAO-B inhibitors ($IC_{50} < 0.033 \mu M$).

The principal difference in binding is that, for **18**, the carbonyl oxygen projects towards residues Tyr-398 and Tyr-435 and establishes hydrogen bonding with a water molecule.

For compounds **17** and **19**, the carbonyl oxygen project towards the space lined by Phe-343 and hydrogen bonding is not observed. Since **17–19** are all potent MAO-B inhibitors, hydrogen bonding appears to be of lesser importance and for inhibitor stabilisation, and Van der Waals and π – π -interactions (with Tyr-398) most likely play leading roles. Since the entrance cavity is reported to be a lipophilic space, Van der Waals interactions with the 2-phenoxyethoxy side chains are probably important stabilising interactions (Binda *et al.*, 2002).

Similar to MAO-B, **17–19** binds in MAO-A with the tetralone moieties in proximity to the FAD (Fig. 9). In MAO-A, the positioning of the inhibitors, however, differ notably from each other, particularly with regards to placement of the tetralone moieties. Thus only **18** forms π – π -interactions with Tyr-407, and only **17** and **18** undergoes hydrogen bonding with Tyr-444. Although it would be speculative to correlate a specific interaction with enhanced inhibition potency, the observation that, in MAO-A, the inhibitors are differently placed and thus undergo different interactions may explain their wide range of MAO-A inhibition potencies (IC_{50} = 1.81–56.2 μ M). An explanation for the higher MAO-B inhibition potencies (compared to MAO-A), however, is not apparent from the docking studies. Because of limitations imposed by the MAO-A active site, particularly Phe-208, larger inhibitors such as **17–19** studied here, are reported to be better accommodated in MAO-B, and such compounds often are MAO-B selective inhibitors (Hubálek *et al.*, 2005). In MAO-B the residue corresponding to Phe-208 in MAO-A is Ile-199. In contrast to Phe-208, the side chain of Ile-199 may rotate from the MAO-B active site cavity to allow to larger inhibitors to extend into the entrance cavity.

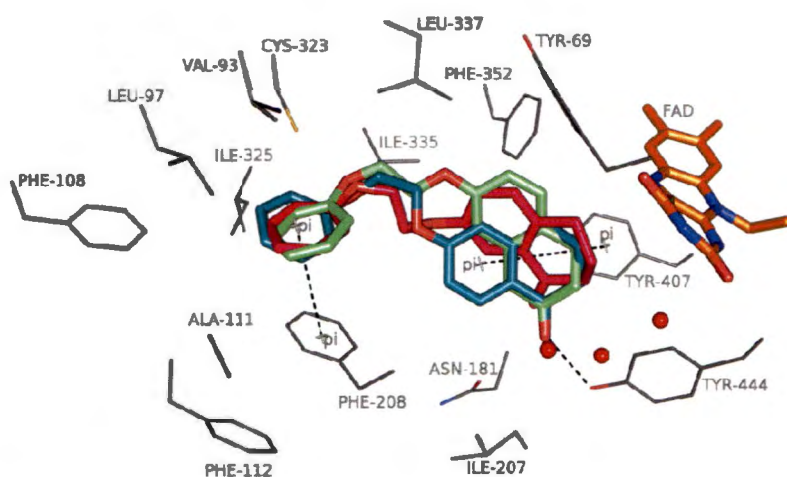


Fig. 9. The docked binding orientations of **17–19** in MAO-A. Key: **17** (light green); **18** (dark green); **19** (magenta).

In conclusion, the present study shows that β -tetralone **17** is a potent and selective MAO-B inhibitor. It is also established that this compound inhibits MAO-B reversibly. Although the α -tetralone homologues **18** and **19** are more potent MAO-B inhibitors, compound **17** displays better isoform selectivity.

For the design of therapies for disorders such as Parkinson's and Alzheimer's diseases, where selective MAO-B inhibition is relevant, **17** may thus represent a suitable lead. The validity of C7-substituted β -tetralone ethers for MAO-B inhibition is thus established.

Acknowledgements

The NMR and MS spectra were recorded by André Joubert and Johan Jordaan of the SASOL Centre for Chemistry, North-West University. This work is based on the research supported in part by the Medical Research Council and National Research Foundation of South Africa (Grant specific unique reference numbers (UID) 85642, 96180). The Grantholders acknowledge that opinions, findings and conclusions or recommendations expressed in any publication generated by the NRF supported research are that of the authors, and that the NRF accepts no liability whatsoever in this regard.

Conflict of Interest

The authors have no conflicts of interest to declare

References

1. Youdim, M.B.H. & Bakhle, Y.S. (2006) 'Monoamine oxidase: Isoforms and inhibitors in Parkinson's disease and depressive illness', *British journal of pharmacology*, 147(S1), pp. S287–S296
2. Ramsay, R.R. (2012) 'Monoamine oxidases: the biochemistry of the proteins as targets in medicinal chemistry and drug discovery', *Current topics in medicinal chemistry*, 12(20), pp. 2189–2209.
3. Ramsay, R.R. (2013) 'Inhibitor design for monoamine oxidases', *Current pharmaceutical design*, 19(14), pp. 2529–2539.
4. Shih, J.C., Chen, K., & Ridd, M.J. (1999) 'Monoamine oxidase: from genes to behavior', *Annual review of neuroscience*, 22, pp. 197–217.
5. Son, S., Ma, J., Kondou, Y., Yoshimura, M., Yamashita, E. & Tsukihara, T. (2008) 'Structure of human monoamine oxidase A at 2.2-Å resolution: The control of opening the entry for substrates/inhibitors', *The national academy of sciences of the United States of America*, 105, pp. 5739–5744.
6. Lum, C.T. & Stahl, S.M. (2012) 'Opportunities for reversible inhibitors of monoamine oxidase-A (RIMAs) in the treatment of depression', *CNS Spectrums*, 17(3), pp. 107–120.
7. Youdim, M.B.H., Edmondson, D. & Tipton, K.F. (2006), 'The therapeutic potential of monoamine oxidase inhibitors', *Nature reviews. Neuroscience*, 7, pp. 295–309.
8. Finberg, J.P. (2014) 'Update on the pharmacology of selective inhibitors of MAO-A and MAO-B: focus on modulation of CNS monoamine neurotransmitter release', *Pharmacology & Therapeutics*, 143(2), pp, 133–152.
9. Naoi, M. & Maruyama, W. (2010) 'Monoamine oxidase inhibitors as neuroprotective agents in age-dependent neurodegenerative disorders', *Current pharmaceutical design*, 16(25), pp. 2799–2817.

10. Cai, Z. (2014) 'Monoamine oxidase inhibitors: promising therapeutic agents for Alzheimer's disease (Review)', *Molecular medicine reports*, 9(5), pp. 1533–1541.
11. Maurel, A., Hernandez, C., Kunduzova, O., Bompart, G., Cambon, C., Parini, A. & Francés, B. (2003) 'Age-dependent increase in hydrogen peroxide production by cardiac monoamine oxidase A in rats', *Am J Physiol Heart Circ Physiol*, 284(4), pp. H1460–H1467.
12. Flamand, V., Zhao, H. & Peehl, D.M. (2010) 'Targeting monoamine oxidase A in advanced prostate cancer', *Journal of cancer research and clinical oncology*, 136(11), pp. 1761–1771.
13. Fowler, J.S., Volkow, N.D. & Wang, G.J. (1997) 'Age-related increases in brain monoamine oxidase B in living healthy human subjects', *Neurobiology of aging*, 18(4), pp. 431–435.
14. Carradori, S. & Silvestri, R. (2015) 'New frontiers in selective human MAO-B inhibitors', *Journal of medicinal chemistry*, 58, pp. 6717–6732.
15. Carradori, S. & Petzer, J.P. (2015) 'Novel monoamine oxidase inhibitors: a patent review (2012 - 2014)', *Expert opinion on therapeutic patents*, 25, pp. 91–110.
16. Carreño, M.C., Gonzalez-López, M., Latorre, A. & Urbano, A. (2006) 'General synthesis of 8-aryl-2-tetralones', *The journal of organic chemistry*, 71(13), pp. 4956–4964.
17. Manvar, D., Fernandes Tde, A., Domingos, J.L., Baljinnyam, E., Basu, A., Junior, E.F., Costa, P.R. & Kaushik-Basu, N. (2015) 'Synthesis and biological evaluation of α -aryl- α -tetralone derivatives as hepatitis C virus inhibitors', *European journal of medicinal chemistry*, 93, pp. 51–54.

18. Legoabe, L.J., Petzer, A. & Petzer, J.P. (2014) ' α -Tetralone derivatives as inhibitors of monoamine oxidase', *Bioorganic & medicinal chemistry letters*, 24(12), pp. 2758–2763.
19. Legoabe, L.J., Petzer, A. & Petzer, J.P. (2015) 'The synthesis and evaluation of C7-substituted α -tetralone derivatives as inhibitors of monoamine oxidase', *Chemical biology & drug design*, 86(4), pp. 895–904.
20. Mostert, S., Petzer, A. & Petzer, J.P. (2015) 'Indanones as high-potency reversible inhibitors of monoamine oxidase', *ChemMedChem*, 10(5), pp. 862–873.
21. Van Dyk, A.S., Petzer, J.P., Petzer, A. & Legoabe, L.J. (2015) '3-Coumaranone derivatives as inhibitors of monoamine oxidase', *Journal of drug design, development and therapy*, 9, pp. 5479–5489.
22. Meiring, L., Petzer, J.P. & Petzer, A. (2013) 'Inhibition of monoamine oxidase by 3,4-dihydro-2(1H)-quinolinone derivatives', *Bioorganic & medicinal chemistry letters*, 23(20), pp. 5498–5502.
23. Petzer, A., Pienaar, A. & Petzer JP. (2013) 'The inhibition of monoamine oxidase by esomeprazole', *Drug research*, 63(9), pp. 462–467.
24. Accelrys Discovery Studio 3.1 (2005). Accelrys Software Inc., San Diego, CA, USA. <http://www.accelrys.com>.
25. Binda, C., Wang, J., Pisani, L., Caccia, C., Carotti, A., Salvati, P., Edmondson, D.E. & Mattevi, A. (2007) 'Structures of human monoamine oxidase B complexes with selective noncovalent inhibitors: safinamide and coumarin analogues', *Journal of medicinal chemistry*, 50, pp. 5848–5852.
26. Binda, C., Mattevi, A. & Edmondson, D.E. (2002) 'Structure-function relationships in flavoenzyme-dependent amine oxidations: a comparison of polyamine oxidase and monoamine oxidase', *Journal of biological chemistry*, 277(27), pp. 23973–23976.

27. Hubálek, F., Binda, C., Khalil, A., Li, M., Mattevi, A., Castagnoli, N. & Edmondson, D.E. (2005) 'Demonstration of isoleucine 199 as a structural determinant for the selective inhibition of human monoamine oxidase B by specific reversible inhibitors', *Journal of biological chemistry*, 280, pp. 15761–15766.

Supplementary Material

The evaluation of 2-phenoxyethoxy-substituted tetralones as inhibitors of monoamine oxidase

Letitia Meiring,¹ Jacobus P. Petzer,¹ Lesetja J. Legoabe,¹ and Anél Petzer^{1,*}

¹ *Pharmaceutical Chemistry, School of Pharmacy and Centre of Excellence for Pharmaceutical Sciences, North-West University, Private Bag X6001, Potchefstroom 2520, South Africa*

1. Materials and methods

Chemicals, solvents and biological agents: All reagents and solvents for the synthetic chemistry and enzymology were obtained from Sigma-Aldrich and were used without further purification. This included the MAO substrate, kynuramine. 2HBr, and insect cell microsomes containing recombinant human MAO-A and MAO-B (5 mg protein/mL). NMR spectroscopy: ¹H NMR and ¹³C NMR spectra were recorded with a Bruker Avance III 600 spectrometer in CDCl₃. The chemical shifts are reported in parts per million (δ) and were referenced to the residual solvent signal at 7.26 ppm (¹H NMR) and 77.0 ppm (¹³C NMR). The following notations were used to indicate spin multiplicities: s (singlet), d (doublet), dd (doublet of doublets), t (triplet) or m (multiplet). Mass spectrometry: High resolution mass spectra (HRMS) were recorded with a Bruker micrOTOF-Q II mass spectrometer functioning in atmospheric-pressure chemical ionisation (APCI) mode (positive mode). Melting points (mp): Melting points (mp) were measured with a Buchi B-545 melting point apparatus and are uncorrected. Thin-layer chromatography (TLC): Reaction progress was monitored with silica gel 60 aluminium coated TLC sheets (Merck). The sheets were developed in a mobile phase consisting of ethyl acetate:petroleum ether (40:60), and visualised under an UV-lamp at a wavelength of 254 nm and/or by staining with iodine vapour.

Fluorescence spectrophotometry: The fluorescence emission of 4-hydroxyquinoline was measured with a Varian Cary Eclipse fluorescence spectrophotometer.

2. Synthesis of 7-(2-phenoxyethoxy)-3,4-dihydronaphthalen-2(1H)-one (17)

While in an atmosphere of nitrogen, 7-methoxy-2-tetralone (**15**) (28.4 mmol) was added to a suspension of anhydrous aluminum trichloride (AlCl_3 , anhydrous) (71 mmol) in toluene (125 mL) at room temperature. The mixture was heated (110 °C) under reflux, for 2 h. The reaction was cautiously quenched with ice water (125 mL). The reaction was extracted to ethyl acetate (150 mL \times 3) and the combined ethyl acetate phases were subsequently washed with water (150 mL \times 3). The ethyl acetate phase was dried over MgSO_4 (5 g), filtered and removed by rotary evaporation to yield a beige-orange solid residue. The product was recrystallised from toluene (28 mL) at room temperature (for 14 h) to yield 7-hydroxy-2-tetralone (**16**). Crystallised 7-hydroxy-2-tetralone (**16**) appeared as light beige crystals. **16**: yield of 41%; mp 111–114.6 °C (toluene).

7-Hydroxy-2-tetralone (**16**) (1.85 mmol) was suspended in acetone (15 mL) containing K_2CO_3 (3.70 mmol). The reaction was treated with 2-bromoethyl phenyl ether (2.35 mmol) and heated (85 °C) under reflux for 6 h. The reaction progress was monitored using silica gel TLC with ethyl acetate:petroleum ether (40:60) as mobile phase. The workup consisted of filtration of the reaction through a pad of celite, and the crude was purified with silica gel column chromatography using ethyl acetate:petroleum ether (40:60) as mobile phase, to yield 7-(2-phenoxyethoxy)-3,4-dihydronaphthalen-2(1H)-one (**17**) (Legoabe *et al.*, 2014; Legoabe *et al.*, 2015).

Compound **17** was prepared in a yield of 0.65%. ^1H NMR (600 MHz, CDCl_3) δ 2.53 (t, 2H, $J = 6.7$ Hz), 2.99 (t, 2H, $J = 6.7$ Hz), 3.54 (s, 2H), 4.22 – 4.38 (m, 4H), 6.71 (d, 1H, $J = 2.6$ Hz), 6.80 (dd, 1H, $J = 2.6, 8.3$ Hz), 6.93 – 7.00 (m, 3H), 7.13 (d, 1H, $J = 8.3$ Hz), 7.25 – 7.33 (m, 2H). ^{13}C NMR (151 MHz, CDCl_3) δ 27.5, 38.5, 45.2, 66.4, 66.7, 113.1, 114.4, 114.6, 121.1, 128.6, 129.2, 129.5, 134.5, 157.6, 158.5, 210.6.

3. Synthesis of compounds **18** and **19**

6-Methoxy-1-tetralone (**20**) or 7-methoxy-1-tetralone (**21**) (28.4 mmol) was added to a suspension of anhydrous aluminum trichloride (AlCl_3 , anhydrous) (71 mmol) in toluene (125 mL) at room temperature. The mixture was heated (85 °C) under reflux for 2 h. The reaction was cautiously quenched with ice water (125 mL). The reaction was extracted to ethyl acetate (150 mL \times 3) and the combined ethyl acetate phases were washed with water (150 mL \times 3). The ethyl acetate phase was dried over MgSO_4 (5 g), filtered and removed by rotary evaporation. The product was recrystallised from ethyl acetate (28 mL) at room temperature to yield 6-hydroxy-1-tetralone (**8**) and 7-hydroxy-1-tetralone (**9**). **8**: yield of 49%; mp 155.5–156.6 °C (ethylacetate). **9**: yield of 34%; mp 154–167 °C (ethylacetate).

6-Hydroxy-1-tetralone (**8**) or 7-hydroxy-1-tetralone (**9**) (1.85 mmol) was suspended in acetone (15 mL) containing K_2CO_3 (3.70 mmol). The reaction was treated with 2-bromoethyl phenyl ether (2.35 mmol) and heated (85 °C) under reflux for 6 h. The reaction progress was monitored using silica gel TLC with ethyl acetate:petroleum ether (40:60) as mobile phase. The acetone was removed by rotary evaporation and the solid residue was suspended in water (35 mL). The suspension was extracted with 35 mL of ethyl acetate and the ethyl acetate phase was washed with water (35 mL). The ethyl acetate phase was dried over MgSO_4 , filtered and removed by rotary evaporation.

The product was recrystallised from boiling ethanol (10 mL) at room temperature to yield compounds **18** and **19** (Legoabe *et al.*, 2014; Legoabe *et al.*, 2015).

Compound **18** was prepared in a yield of 6.32%. ^1H NMR (600 MHz, DMSO- d_6) δ 2.58 (s, 0.4H), 3.00 (s, 1.7H), 3.02 (t, 2H, $J = 6.4$ Hz), 3.40 (t, 2H, $J = 6.1$ Hz), 4.78 – 4.85 (m, 2H), 4.86 – 4.95 (m, 2H), 7.40 – 7.51 (m, 5H), 7.79 (d, 2H, $J = 7.7$ Hz), 8.32 (d, 1H, $J = 9.6$ Hz). ^{13}C NMR (151 MHz, DMSO) δ 23.0, 29.3, 38.4, 66.1, 66.7, 113.3, 113.7, 114.5, 120.9, 125.9, 128.8, 129.6, 147.3, 158.2, 162.2, 196.2; APCI-HRMS m/z : calcd for $\text{C}_{18}\text{H}_{19}\text{O}_3$ (MH^+), 283.1334, found 283.1346.

Compound **19** was prepared in a yield of 14.9%. mp 116.1 °C. ^1H NMR (600 MHz, DMSO- d_6) δ 2.57 (s, 0.4H), 2.99 (s, 1.6H), 3.07 (d, 2H, $J = 5.7$ Hz), 3.36 (t, 2H, $J = 6.0$ Hz), 4.75 – 4.87 (m, 4H), 7.44 (t, 1H, $J = 7.3$ Hz), 7.45- 7.50 (m, 2H), 7.68 (dd, 1H, $J = 2.8, 8.4$ Hz), 7.75 – 7.82 (m, 3H), 7.88 (d, 1H, $J = 2.8$). ^{13}C NMR (151 MHz, DMSO) δ 23.1, 28.1, 38.5, 66.2, 66.6, 109.7, 114.5, 120.8, 121.5, 129.6, 130.5, 133.0, 137.4, 156.9, 158.3, 197.4; APCI-HRMS m/z : calcd for $\text{C}_{18}\text{H}_{19}\text{O}_3$ (MH^+), 283.1334, found 283.1328.

4. Measurement of IC_{50} values for the inhibition of MAO

The protocol for the measurement of IC_{50} values for the inhibition of MAO-A and MAO-B has been reported in literature (Mostert *et al.*, 2015; Mostert *et al.*, 2016). For this purpose the recombinant human MAO-A and MAO-B enzymes were used. Enzyme reactions: The enzyme reactions were carried out in white 96-well microtiter plates (Eppendorf) to a final volume of 200 μL . Potassium phosphate buffer at pH 7.4 (100 mM, made isotonic with KCl) served as reaction medium. The reactions contained kynuramine (50 μM) and the test inhibitors at concentrations of 0.003–100 μM .

Stock solutions of kynuramine were prepared in the reaction buffer while stock solutions of the test inhibitors were prepared in DMSO. The inhibitors were added to the reactions to yield a final concentration of 4% DMSO.

For each inhibitor evaluated, control reactions carried out in the absence of inhibitor (but still containing 4% DMSO) were included. The enzyme reactions were initiated with the addition of MAO-A (0.0075 mg protein/mL) or MAO-B (0.015 mg protein/mL) and incubated for 20 min at 37 °C in a convection oven. Measurement and data analysis: At endpoint, the reactions were terminated with the addition of 80 µL sodium hydroxide (2 N) and the fluorescence of 4-hydroxyquinoline, the oxidation product of kynuramine, was measured ($\lambda_{\text{ex}} = 310$; $\lambda_{\text{em}} = 400$ nm) (Navoroli *et al.*, 2005). To quantify 4-hydroxyquinoline, a linear calibration curve was constructed with authentic 4-hydroxyquinoline (0.047–1.56 µM). The rate of 4-hydroxyquinoline formation was fitted to the one site competition model of the Prism 5 software package (GraphPad) to obtain sigmoidal plots from which the IC₅₀ values were estimated. All enzyme reactions were carried out in triplicate and IC₅₀ values are given as the mean ± standard deviation (SD).

5. Investigation of reversibility of inhibition by dialysis

The protocol for investigating the reversibility of MAO inhibition by dialysis has been reported in literature (Mostert *et al.*, 2015; Mostert *et al.*, 2016). For dialysis, Slide-A-Lyzer® dialysis cassettes (Thermo Scientific) with a molecular weight cut-off of 10 000 and a sample volume capacity of 0.5–3 mL were used. Preincubation: Recombinant human MAO-B (0.03 mg/mL) and the test compounds (17–19) were firstly preincubated for 15 min at 37 °C. The volume of these preincubations was 0.8 mL and potassium phosphate buffer (100 mM, pH 7.4) containing 5% sucrose, served as solvent.

Stock solutions of the test compounds were prepared in DMSO and added to the preincubations to yield 4% DMSO and an inhibitor concentration of $4 \times \text{IC}_{50}$. Dialysis: These mixtures were subsequently dialysed at 4 °C in 80 mL of dialysis buffer, which consisted of potassium phosphate buffer (100 mM, pH 7.4) containing 5% sucrose.

The dialysis buffer was replaced with fresh buffer at 3 h and 7 h after the start of dialysis.

Assay: Following 24 h of dialysis, the reactions were diluted 2-fold (into 1.5 mL microcentrifuge tubes) with the addition of kynuramine (dissolved in potassium phosphate buffer, 100 mM, pH 7.4, made isotonic with KCl). This yielded a final concentration of kynuramine of 50 μM . The final concentration of the test inhibitor in these reactions was $2 \times \text{IC}_{50}$, and the final volume of the reactions was 500 μL . The reactions were incubated for 20 min at 37 °C in a water bath and were terminated with the addition of NaOH (400 μL of 2 N) and 1000 μL water. Measurement and data analysis: The fluorescence of 4-hydroxyquinoline in these samples was measured ($\lambda_{\text{ex}} = 310$; $\lambda_{\text{em}} = 400$ nm) employing a 3.5 mL quartz cuvette (pathlength 10 \times 10 mm) (Navoroli *et al.*, 2005). To quantify 4-hydroxyquinoline, a linear calibration curve was constructed with authentic 4-hydroxyquinoline (0.047–1.56 μM).

Controls: MAO-B was similarly pre-incubated and dialysed in the absence of inhibitor (negative control) as well as in the presence of the irreversible inhibitor, (R)-deprenyl (positive control). The concentration of (R)-deprenyl in the preincubations was $4 \times \text{IC}_{50}$ ($\text{IC}_{50} = 0.079$ μM) (Petzer *et al.*, 2012). Undialysed mixtures: For comparison, undialysed mixtures of MAO-B and the test inhibitors were maintained at 4 °C for 24 h and diluted and assayed as above. All reactions were carried out in triplicate and the residual enzyme catalytic rates are expressed as mean \pm SD.

6. Construction of Lineweaver-Burk plots

To illustrate that compound **17** acts as a competitive MAO-B inhibitor, a set of six Lineweaver-Burk plots was constructed. The first plot was constructed in the absence of inhibitor, while the remaining five plots were constructed in the presence of the following concentrations of **17**: $\frac{1}{4} \times IC_{50}$, $\frac{1}{2} \times IC_{50}$, $\frac{3}{4} \times IC_{50}$, $1 \times IC_{50}$ and $1\frac{1}{4} \times IC_{50}$. For each plot, kynuramine was used at concentrations of 15–250 μ M.

The enzyme reactions were carried out to a volume of 500 μ L in 1.5 mL microcentrifuge tubes and the concentration of MAO-B was 0.015 mg protein/mL. All enzyme reactions and activity measurements were carried out as described above for the dialysis experiments. The K_i value was estimated by global (shared) fitting of the inhibition data directly to the Michaelis-Menten equation using the Prism 5 software package. For comparison, the K_i value was also estimated from a plot of the slopes of the Lineweaver-Burke plots versus inhibitor concentration (x-axis intercept equals $-K_i$).

7. Protocol for docking with CDOCKER

Docking of the test inhibitors in the MAO active sites was carried out with the Windows-based Discovery Studio 3.1 software package ([Accelrys](#)). Unless otherwise specified, the default settings of Discovery Studio were used for all calculations. As protein models, the reported X-ray crystal structures of human MAO-A (PDB code 2Z5X) ([Son et al., 2008](#)) and human MAO-B (PDB code 2V5Z) ([Binda et al., 2007](#)) were obtained from the Brookhaven Protein Data Bank. The pKa values and protonation states of the ionisable amino acids were firstly calculated and hydrogen atoms were added at pH 7.4 to the protein models. When necessary, the valences of the FAD cofactors and co-crystallised ligands were corrected, and the FAD cofactors were set to the oxidised state.

The protein models were automatically typed with the Momany and Rone CHARMM forcefield and a fixed atom constraint was applied to the backbone. The models were subsequently energy minimised using the Smart Minimizer algorithm (maximum steps, 50000) and the implicit generalized Born solvation model with molecular volume. The co-crystallised ligands and backbone constraints were removed from the models and the binding sites were identified from an analysis of the protein cavities.

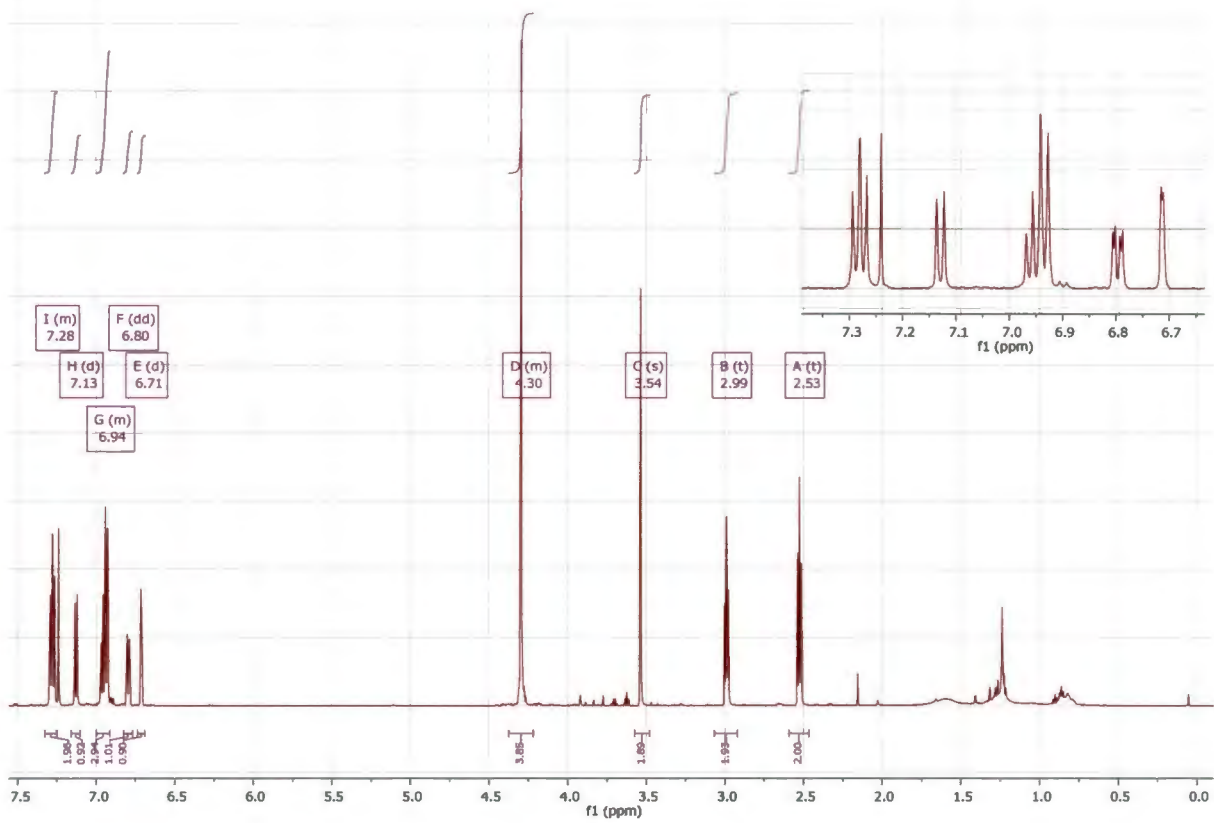
With the exception of HOH 710, 718 and 739 in the MAO-A active site, and HOH 1155, 1170 and 1351 in the A-chain of the MAO-B active site, all waters of the models were subsequently deleted. These active site waters in the MAOs are considered to be conserved and were thus retained. The structures of the ligands to be docked were drawn in Discovery Studio, the geometries were briefly optimised using a Dreiding-like forcefield (5000 iterations) and the structures were prepared for docking with the Prepare Ligands protocol. Atom potential types and partial charges were subsequently assigned to the ligands with the Momany and Rone CHARMM forcefield. Docking was carried out with the CDOCKER algorithm. Ten random conformations were generated for each ligand, the heating target temperature was set to 700 K and full potential mode was used. The docking solutions were finally refined using in situ ligand minimisation with the Smart Minimizer algorithm and the illustrations were prepared with PyMol ([DeLano, 2002](#)).

8. References

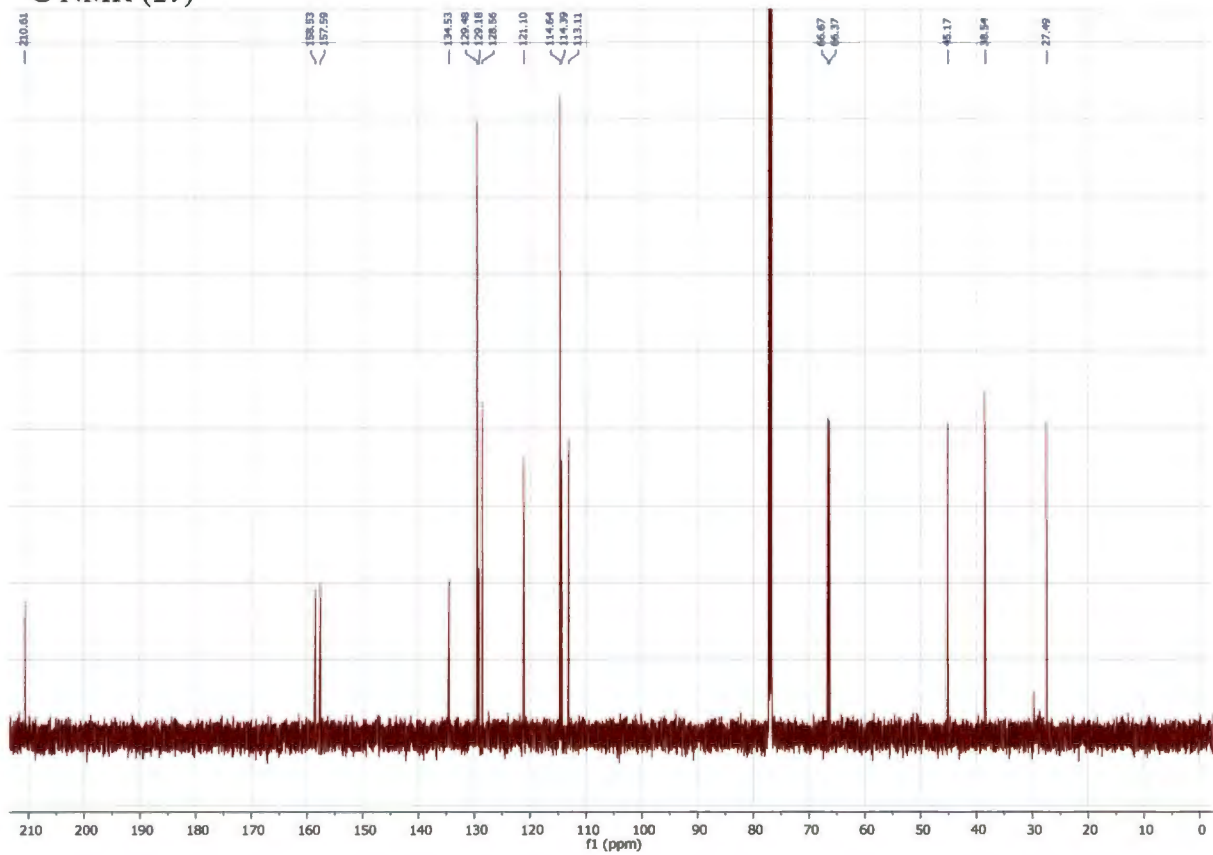
1. Legoabe, L.J., Petzer, A. & Petzer, J.P. (2014) ' α -Tetralone derivatives as inhibitors of monoamine oxidase', *Bioorganic & medicinal chemistry letters*, 24(12), pp. 2758–2763.
2. Legoabe, L.J., Petzer, A. & Petzer, J.P. (2015) 'The synthesis and evaluation of C7-substituted α -tetralone derivatives as inhibitors of monoamine oxidase', *Chemical biology & drug design*, 86(4), pp. 895–904.
3. Mostert, S., Petzer, A. & Petzer, J.P. (2015) 'Indanones as high-potency reversible inhibitors of monoamine oxidase', *ChemMedChem*, 10(5), pp. 862–873.
4. Mostert, S., Petzer, A. & Petzer, J.P. (2016) 'Inhibition of monoamine oxidase by benzoxathiolone analogues', *Bioorganic & medicinal chemistry letters*, 26(4), pp. 1200–1204.
5. Novaroli, L., Reist, M., Favre, E., Carotti, A., Catto, M. & Carrupt, P.A. (2005) 'Human recombinant monoamine oxidase B as reliable and efficient enzyme source for inhibitor screening', *Bioorganic & medicinal chemistry*, 13(22), pp. 6212–6217.
6. Petzer, A., Harvey, B.H., Wegener, G. & Petzer, J.P. (2012) 'Azure B, a metabolite of methylene blue, is a high-potency, reversible inhibitor of monoamine oxidase' *Toxicology and applied pharmacology*, 258(3), pp. 403–409.
7. Son, S., Ma, J., Kondou, Y., Yoshimura, M., Yamashita, E. & Tsukihara, T. (2008) 'Structure of human monoamine oxidase A at 2.2-Å resolution: The control of opening the entry for substrates/inhibitors', *The national academy of sciences of the United States of America*, 105, pp. 5739–5744.
8. Accelrys Discovery Studio 3.1 (2005). Accelrys Software Inc., San Diego, CA, USA. <http://www.accelrys.com>.

9. Binda, C., Wang, J., Pisani, L., Caccia, C., Carotti, A., Salvati, P., Edmonson, D.E. & Mattevi, A. (2007) 'Structures of human monoamine oxidase B complexes with selective noncovalent inhibitors: safinamide and coumarin analogues', *Journal of medicinal chemistry*, 50, pp. 5848–5852.
10. DeLano, W.L. (2002) The PyMOL molecular graphics system. DeLano Scientific, San Carlos, USA.

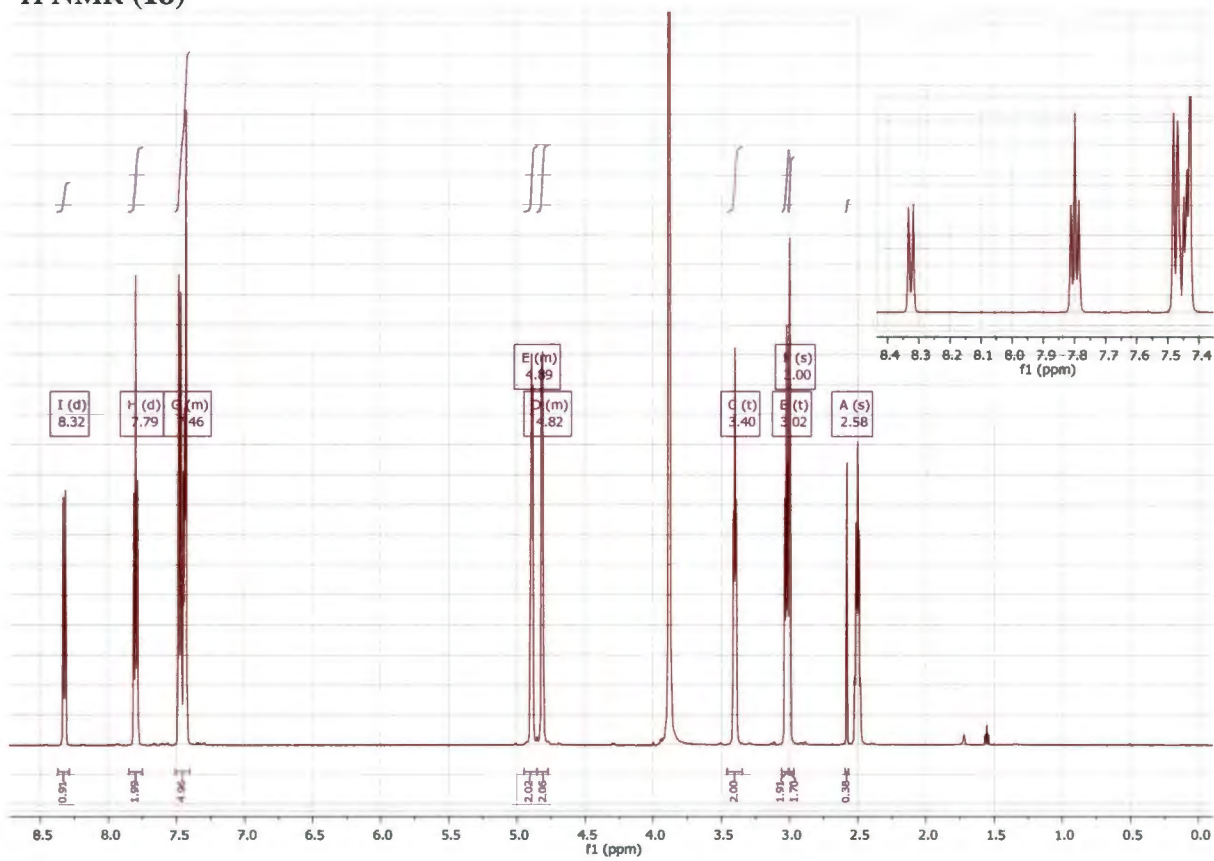
¹H NMR (17)



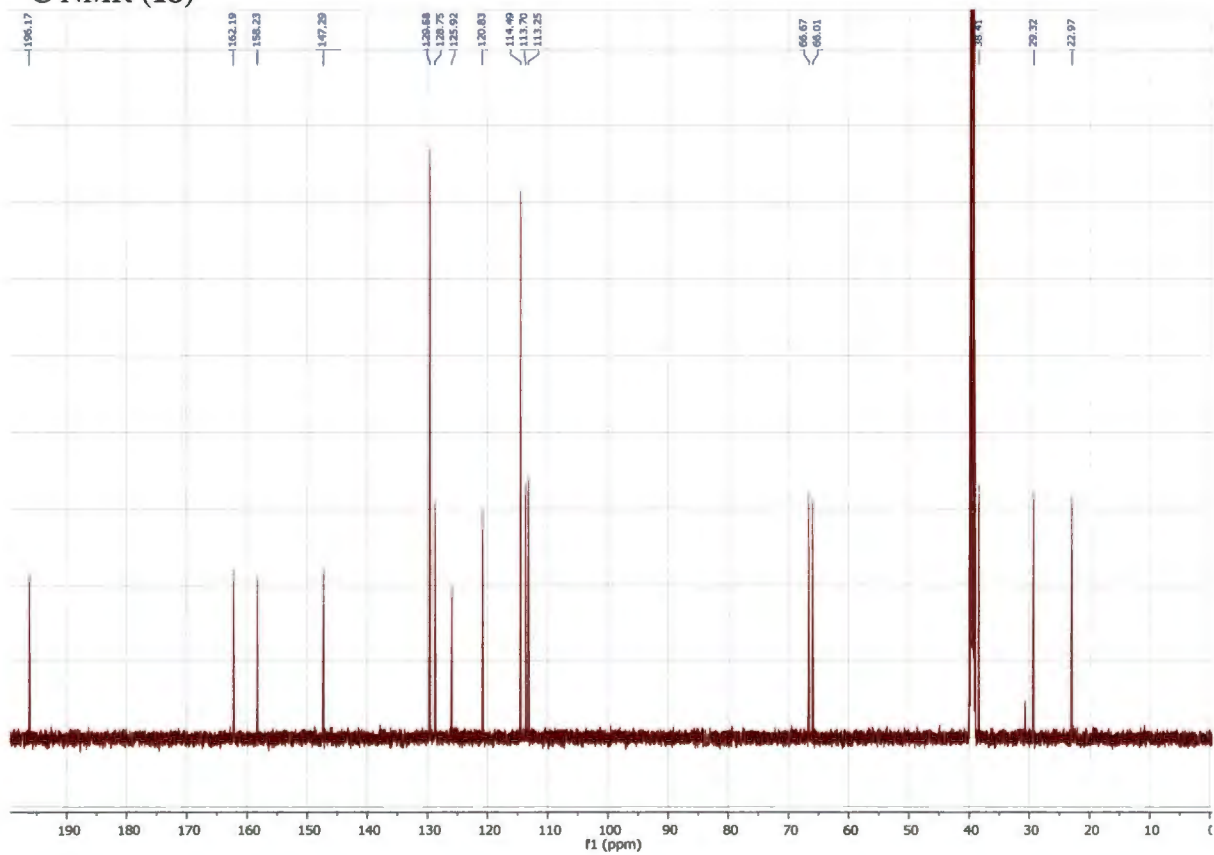
¹³C NMR (17)



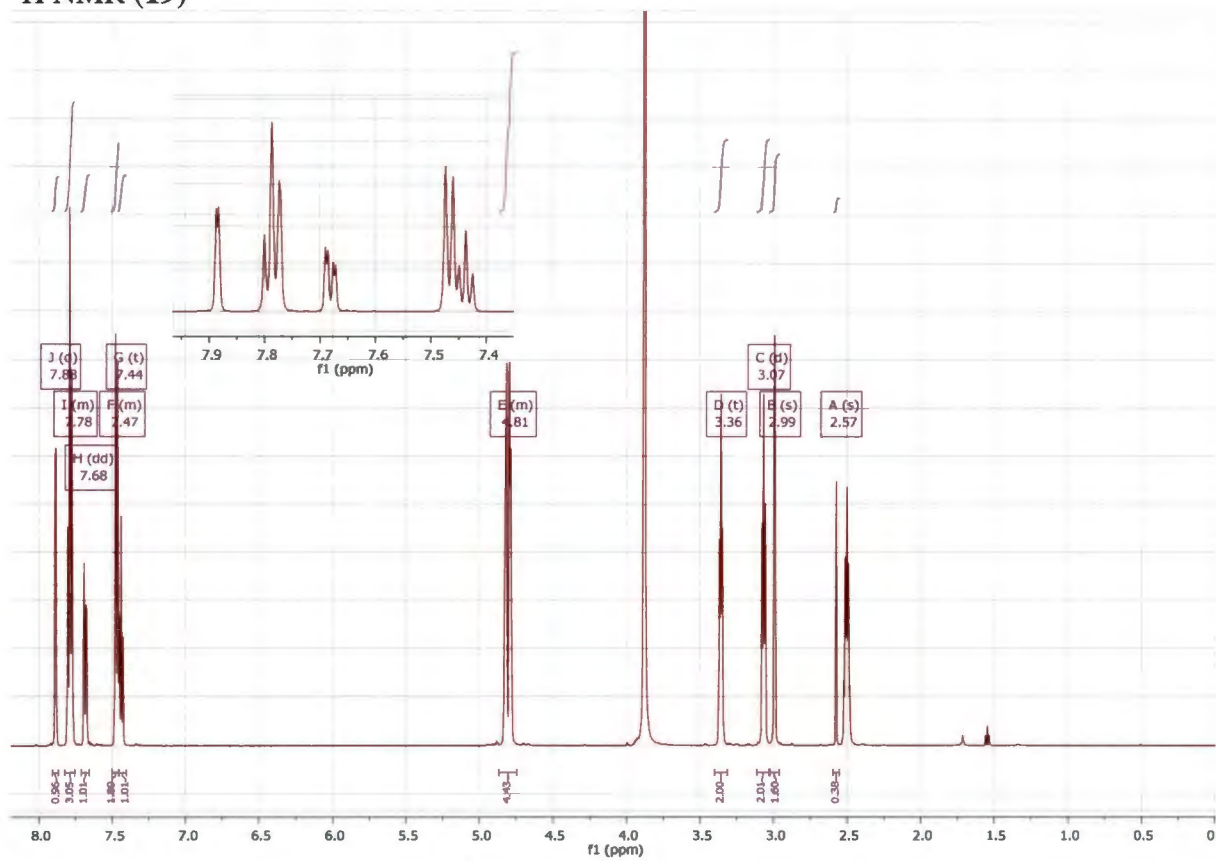
¹H NMR (18)



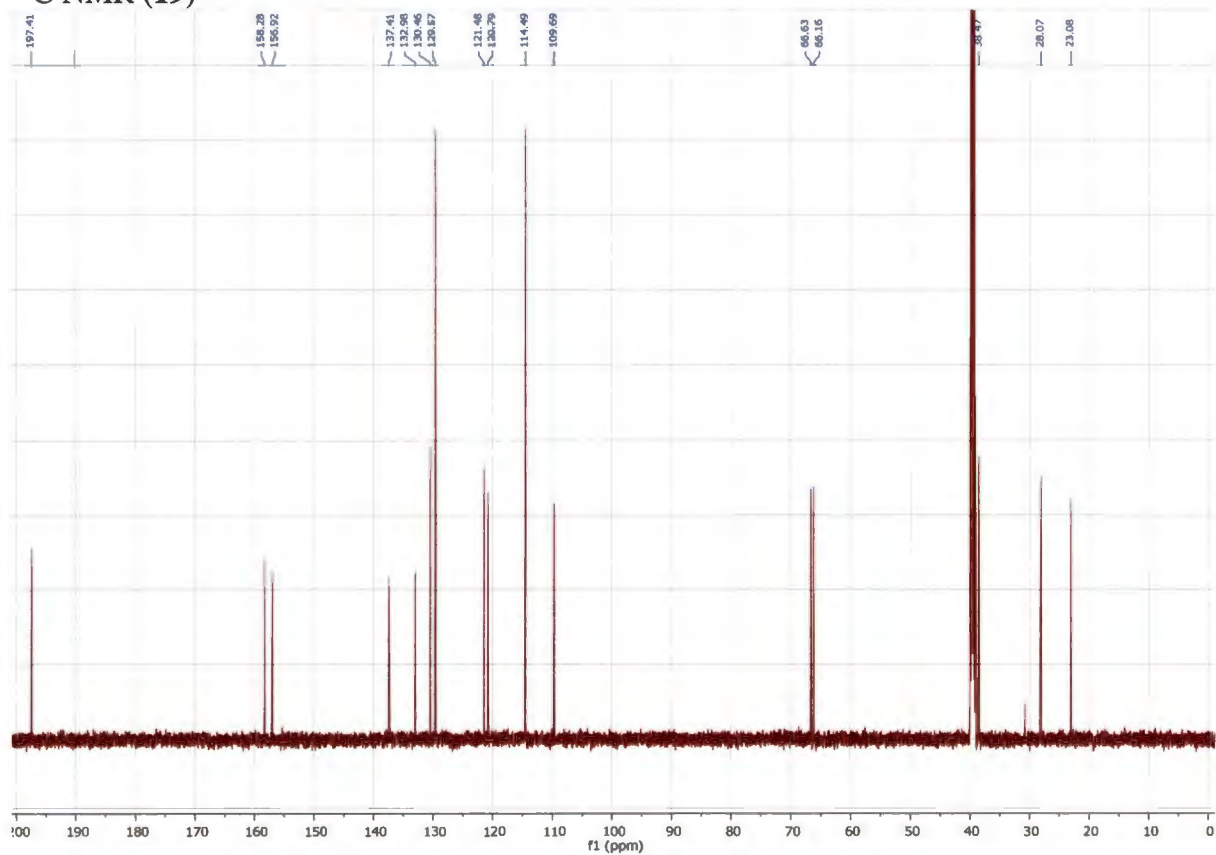
¹³C NMR (18)



¹H NMR (19)



¹³C NMR (19)



MANUSCRIPT D

The evaluation of N-propargylamine-2-aminotetralin as an irreversible inhibitor of monoamine oxidase

Authors' contributions:

- The experimental work, interpretation of results and documentation of this study was carried out by L. Meiring.
- This study was conceptualised and documented with the assistance of J.P Petzer.
- The enzymology section of this study was conducted under the supervision of A. Petzer.

All co-authors provided permission to use this manuscript as part of L. Meiring's Ph.D thesis.

Letitia Meiring,¹Jacobus P. Petzer,¹Lesetja J. Legoabe,¹ and Anél Petzer^{1,*}

- ^{1.} *Pharmaceutical Chemistry, School of Pharmacy and Centre of Excellence for Pharmaceutical Sciences, North-West University, Private Bag X6001, Potchefstroom 2520, South Africa*

*Corresponding author: AnélPetzer, Tel.: +27 18 2994464, fax: +27 18 2994243

E-mail address: 12264954@nwu.ac.za

Running title: N-propargylamine-2-aminotetralin, an irreversible MAO inhibitor

Keywords: monoamine oxidase, MAO, inhibition, irreversible, propargylamine, selegiline, (R)-deprenyl, rasagiline, 2-PAT.

Abstract: Monoamine oxidase B (MAO-B) inhibitors are established therapy for Parkinson's disease and act, in part, by blocking the MAO-catalysed metabolism of dopamine in the brain. Two propargylamine-containing MAO-B inhibitors, selegiline [(R)-deprenyl] and rasagiline, are currently used in the clinic for this purpose. These compounds are mechanism-based inactivators and, after oxidative activation, form covalent N(5) adducts with the FAD co-factor. An important consideration is that selegiline and rasagiline display specificity for MAO-B over the MAO-A isoform thus reducing the risk of tyramine-induced changes in blood-pressure. In the interest of discovering new propargylamine MAO inhibitors, the present study synthesises racemic N-propargylamine-2-aminotetralin (2-PAT), a compound that may be considered as both a six-membered ring analogue of rasagiline and a semi-rigid N-desmethyl ring-closed analogue of selegiline. The in vitro human MAO inhibition properties of this compound were measured and compared to those of rasagiline, selegiline and N-methyl-N-propargylamine-2-aminotetralin (2-MPAT), the latter a known MAO inhibitor and close structural analogue of 2-PAT. The results show that 2-PAT is a 20-fold more potent inhibitor of MAO-A ($IC_{50} = 0.721 \mu M$) compared to MAO-B ($IC_{50} = 14.6 \mu M$). Interestingly, dialysis studies found that 2-PAT is a reversible MAO-A inhibitor, while acting as an inactivator of MAO-B. Since reversible MAO-A inhibitors are much less liable to potentiate tyramine-induced side effects than MAO-A inactivators, it is reasonable to suggest that 2-PAT could be an useful and safe therapeutic agent for disorders such as Parkinson's disease and depression.

Parkinson's disease is a progressive disorder which involves the degeneration of specific neuronal pathways in the central nervous system. In Parkinson's disease, the dopamine-containing neurons of the nigrostriatal pathway are thus destroyed, resulting in a deficiency of dopamine at the nerve terminals in the corpus striatum (Olanow *et al.*, 2009). Replacing the lost dopamine with L-3,4-dihydroxyphenylalanine (L-dopa), the direct metabolic precursor of dopamine, remains the most valuable approach for the treatment of the symptomatic Parkinson's disease (Carlsson, 2002). L-Dopa is, however, extensively metabolised in the periphery which reduces its therapeutic efficiency. For this reason, L-dopa is often co-administered with inhibitors of key L-dopa metabolising enzymes such as dopa decarboxylase and catechol-O-methyl transferase (Perdosa & Timmermann, 2013; Talati *et al.*, 2009). The inhibition of these enzymes in the peripheral tissues increases the availability of L-dopa for uptake into the brain and allows for the effective L-dopa dose to be reduced (Fahn *et al.*, 2004). This approach thus decreases the occurrence of adverse effects as a result of large L-dopa dosages. The efficacy of L-dopa may also be enhanced by inhibiting the metabolism of dopamine with monoamine oxidase (MAO) type B inhibitors (Youdim *et al.*, 2006). The inhibition of MAO-B in the brain conserves central dopamine and, when co-administered with L-dopa, further enhances the levels of central dopamine derived from L-dopa (Shoulson *et al.*, 2002; Fernandez & Chen, 2007; Finberg *et al.*, 1998). MAO-B inhibitors are thus established therapy in Parkinson's disease and as monotherapy in early Parkinson's disease may delay the need for L-dopa therapy (Pålhagen *et al.*, 1998). Two MAO-B inhibitors, (R)-deprenyl (also known as selegiline) and rasagiline, are registered for the treatment of Parkinson's disease (Fig. 1) (Youdim *et al.*, 2006). These are irreversible MAO-B inhibitors containing the propargylamine functional group.

Reversible MAO-B inhibitors such as safinamide, which has completed phase III development for the management of Parkinson's disease, are also under consideration as future medications (Borgohain *et al.*, 2014; Dézsi and Vécsei, 2014).

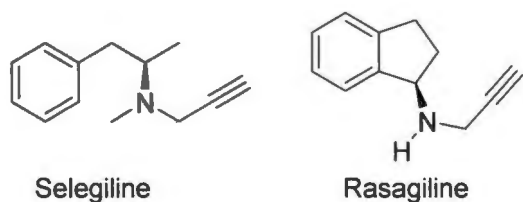


Fig. 1. The structures of the irreversible MAO-B inhibitors, selegiline and rasagiline.

Two isoforms of MAO are expressed in mammals, MAO-A and MAO-B (Youdim & Bakhle, 2006). Although both isoforms metabolise dopamine in the brain, only MAO-B inhibitors are used for the treatment of Parkinson's disease (Youdim *et al.*, 2006). This is mainly due to potentially fatal adverse effects that may occur when MAO-A inhibitors are combined with tyramine-containing food such as cheese and wine. MAO-A inhibitors prevent the metabolism of tyramine in the gastrointestinal mucosa and hepatic tissues leading to high systemic concentrations of tyramine and an elevation in blood-pressure (Da Prada *et al.*, 1988; Flockhart, 2012). This sympathomimetic response may be further exacerbated when MAO-A inhibitors and L-dopa are combined, hence the avoidance of MAO-A inhibitors in Parkinson's disease therapy (Teychenne *et al.*, 1975). With appropriate dietary restrictions MAO-A inhibitors are, however, used for the treatment of major depressive disorder (Schwartz, 2013; Lum & Stahl, 2012). In depression MAO-A inhibitors act by inhibiting the central metabolism of serotonin and norepinephrine, thereby enhancing neurotransmission mediated by these neurotransmitters (Youdim *et al.*, 2006).

MAO-A inhibitors that have been used for the treatment of depression include phenelzine, isocarboxazid, tranylcypromine and iproniazid (Fig. 2) (Youdim *et al.*, 2006; Finberg, 2014). These are irreversible mechanism-based MAO inhibitors and, after oxidation by the enzyme, form covalent adducts with the flavin adenine dinucleotide (FAD) co-factor of MAO (Edmondson *et al.*, 2004; Binda *et al.*, 2004; Binda *et al.*, 2005; Milczek *et al.*, 2008). Reversible inhibitors such as moclobemide and toloxatone have also been used in the therapy of depression.

In contrast to irreversible MAO-A inhibitors, reversible inhibitors are safer and better-tolerated and are not associated with tyramine-induced changes in blood-pressure (Bonnet, 2003; Provost *et al.*, 1992). This is presumably because with reversible inhibition, the increasing amounts of tyramine compete with and displace the reversible inhibitor from MAO-A thus allowing for normal metabolism to occur. This limits the amount of tyramine that reaches the systemic circulation. MAO-B inhibitors have also recently found application in depression therapy. A transdermal delivery system of selegiline has been developed and reported to be effective in the treatment of major depressive disorder in clinical trials (Pae *et al.*, 2014). With this formulation selegiline does not inhibit MAO-A in the gastrointestinal and hepatic systems, and thus the risk of tyramine-induced adverse effects is low.

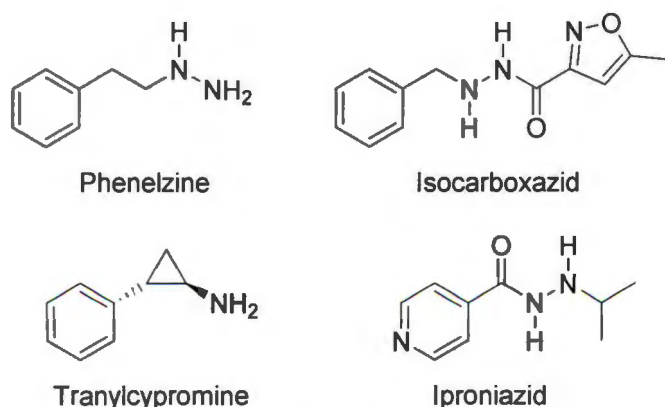


Fig. 2. The structures of the irreversible MAO inhibitors, phenelzine, isocarboxazid, tranylcypromine and iproniazid.

In spite of the risks associated with their use, irreversible inhibitors of the MAOs are an important class of therapeutic agents. Irreversible MAO inhibitors used in the clinic are mechanism-based inhibitors and contain the following functional groups: propargylamine [e.g. (R)-deprenyl, rasagiline], cyclopropylamine (e.g. tranylcypromine), hydrazine (e.g. phenelzine, isocarboxazid), haloallylamine (mofegiline) and N-(2-aminoethyl)carboxamide (e.g. lazabemide) (Fig. 3).

Mechanism-based inhibitors, also known as suicide inhibitors, are metabolised by the MAOs to reactive intermediates which form covalent adducts with the FAD co-factor at the N(5) and C(4a) positions of the isoalloxazine ring (Edmondson *et al.*, 2004; Binda *et al.*, 2004; Binda *et al.*, 2005; Milczek *et al.*, 2008). Motivated by the academic challenge of designing and discovering high potency and isoform-specific MAO inhibitors that may be useful therapeutic agents, the present study synthesises N-propargylamine-2-aminotetralin (2-PAT), and evaluates the racemic mixture as an *in vitro* inhibitor of the human MAOs (Fig. 4). This compound may be considered as both a six-membered ring analogue of rasagiline and a semi-rigid N-desmethyl ring-closed analogue of selegiline. Even though structurally very similar to rasagiline, the MAO inhibition properties of 2-PAT may be very different. For example, literature reports that N-methylation of rasagiline significantly affects the inactivation kinetics, inhibition potency and isoform selectivity (Hubálek *et al.*, 2004). Furthermore, the MAOs are much less sensitive to inhibition by the *S*-enantiomer of rasagiline. The N-methyl analogue of 2-PAT, N-methyl-N-propargylamine-2-aminotetralin (2-MPAT), has been studied. *In vitro* inhibition of rat brain MAO-A and MAO-B found that the enantiomeric pure forms as well as the racemate are potent inhibitors of both MAO isoforms (Table 1) (Hazelhoff *et al.*, 1985). The (+)-enantiomer, however displays highest MAO-B inhibition and best isoform selectivity (over MAO-A).

An earlier study also found that racemic 2-MPAT is a selective inhibitor of MAO-B when using rat liver MAO (Tipton *et al.*, 1982). Via washing of mitochondria it was shown that 2-MPAT inhibits rat liver MAO irreversibly.

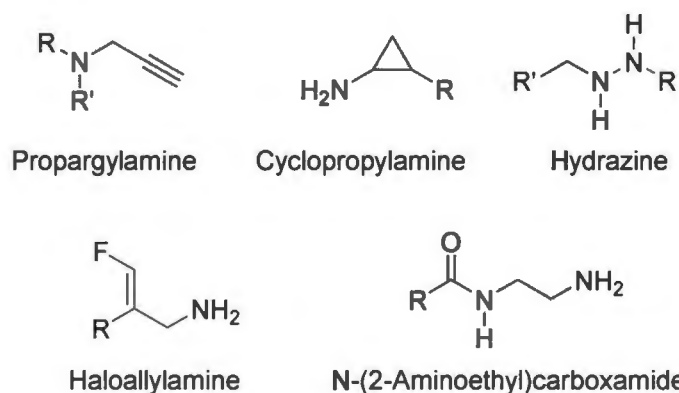


Fig 3. Functional groups responsible for mechanism-based inhibition of the MAOs: propargylamine, cyclopropylamine, hydrazine, haloallylamine and N-(2-aminoethyl)carboxamide.

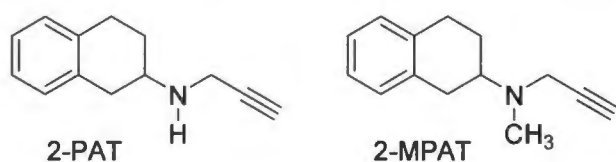


Fig. 4. The structures of N-propargylamine-2-aminotetralin (2-PAT) and N-methyl-N-propargylamine-2-aminotetralin (2-MPAT).

Table 1. The reported IC_{50} values for the inhibition of rat brain MAO-A and MAO-B by 2-MPAT.

	IC_{50} (μM) ^a		SI ^b
	MAO-A	MAO-B	
(±)2-MPAT	0.051	0.041	1.2
(+)2-MPAT	0.140	0.016	8.8
(-)2-MPAT	0.046	0.088	0.5

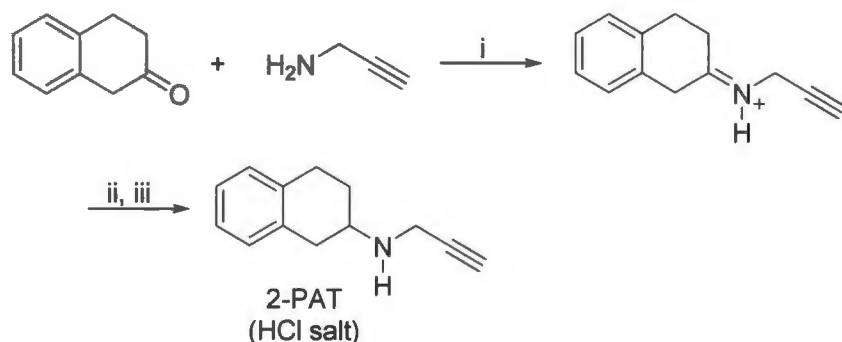
^a Values obtained from reference (Hazelhoff *et al.*, 1985).

^b The selectivity index (SI) equals the ratio of $IC_{50}(\text{MAO-A})/IC_{50}(\text{MAO-B})$.

A number of synthetic approaches are possible for the synthesis of propargylamine derivatives. Rasagiline and derivatives thereof are synthesised by alkylation of 1-aminoindan with propargyl chloride or propargyl bromide in the presence of base, usually potassium carbonate (Guozhen *et al.*, 2014).

In the present study we have explored an alternative route for the synthesis of 2-PAT (Scheme 1). Commercially available β -tetralone (1 equiv.) and propargylamine (5 equiv.) were firstly dehydrated in a Dean-Stark trap in the presence of *p*-toluenesulfonic acid (0.056 equiv.) (Zhuang *et al.*, 1993). After reduction with sodium cyanoborohydride (NaCNBH₄) and a workup that involves acidification with HCl, washing with diethyl ether and extraction to dichloromethane the hydrochloric acid salt of 2-PAT was obtained in low yield as a powder (7.9%). Curiously this salt is soluble in water, dichloromethane, chloroform, methanol and weakly in acetone while being insoluble in most other organic solvents (e.g. diethyl ether, ethyl acetate). Both the ¹H and ¹³C NMR spectra, recorded in CDCl₃ and CD₃OD, corresponded with the proposed structure. In CD₃OD the most characteristic ¹³C signals included the CH₂ (79 ppm) and the acetylenic carbons [55(CH) and 75(C) ppm] of the propargyl group. On the ¹H NMR spectrum the propargyl CH₂ (3.30–3.23 ppm) was observed to correlate with the carbon signal at 79 ppm while the acetylenic CH (3.72–3.62 ppm) correlates with the carbon signal at 55 ppm. In CDCl₃ the exchangeable NH (10 ppm) was visible as a broad singlet, integrating for 2 protons as expected for the HCl salt. Interestingly on the FT-IR spectrum a characteristic absorption band at 2100 cm⁻¹ for the terminal alkyne (due to stretching vibrations) was absent. This absorption band also was not observed for propargyl amine or the free base of 2-PAT (prepared with Na₂CO₃), while reported to be present at low intensity at 2100 cm⁻¹ in the FT-IR spectrum of rasagiline free base (Başköse *et al.*, 2012). The carbonyl stretch vibration of β -tetralone at 1711 cm⁻¹, however, was absent in the IR spectra of both the hydrochloric acid salt and free base of 2-PAT.

The mass spectrum for hydrochloric acid salt of 2-PAT yielded a mother ion $[MH^+]$ of 186.1274, in close agreement with the calculated value.



Scheme 1. Synthetic pathway to 2-PAT. Reagents and conditions: (i) p-toluenesulfonic acid, benzene, Dean-Stark trap; (ii) NaCNBH₄, methanol, N₂, rt; (iii) 10% HCl.

The MAO inhibition properties of 2-PAT was investigated *in vitro* using recombinant human MAO-A and MAO-B (Novaroli *et al.*, 2005). To measure MAO catalytic rates, kynuramine served as substrate for both isoforms and is oxidised to 4-hydroxyquinoline as the ultimate product. After alkalisation of the enzyme reactions at endpoint (after 20 min incubation), 4-hydroxyquinoline was quantified by fluorescence spectrophotometry (Mostert *et al.*, 2015). By thus measuring the rate of kynuramine oxidation in the absence and presence of 2-PAT (at concentrations of 0.003–100 μ M) sigmoidal dose-response curves were constructed in triplicate from which IC₅₀ values were estimated (Fig. 5). The results show that 2-PAT inhibits MAO-A with an IC₅₀ value of $0.721 \pm 0.030 \mu$ M while MAO-B is inhibited an IC₅₀ value of $14.6 \pm 0.282 \mu$ M (Table 2). Based on IC₅₀ values, 2-PAT is therefore 20-fold more potent as an inhibitor of MAO-A compared to MAO-B. For comparison, the propargylamine MAO inhibitors, clorgyline, pargyline and selegiline inhibits the human MAOs with IC₅₀ values of 0.0026 (MAO-A), 13 (MAO-A) and 0.079 (MAO-B) μ M, respectively, under identical conditions (Strydom *et al.*, 2012; Petzer *et al.*, 2012). Compared to clorgyline and selegiline, the MAO inhibition potencies of 2-PAT is therefore modest.

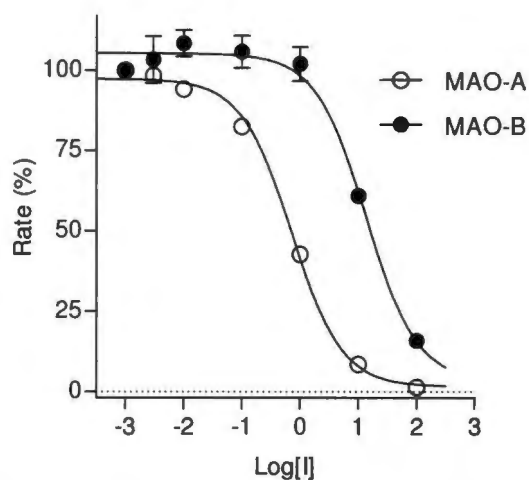


Fig. 5. The sigmoidal dose-response curves of the inhibition of MAO-A and MAO-B by 2-PAT. Rates were measured in triplicate and are shown as mean \pm standard deviation (SD).

Table 2. The IC_{50} values for the inhibition of recombinant human MAO-A and MAO-B by 2-PAT and reference inhibitors.

	IC_{50} (μM) ^a		SI ^b
	MAO-A	MAO-B	
(\pm)2-PAT	0.721 \pm 0.030	14.6 \pm 0.282	0.05
Pargyline	15.6 \pm 0.424	0.782 \pm 0.035	20
Selegiline	29.7 \pm 1.44	0.095 \pm 0.013	313

^a All values are expressed as the mean \pm standard deviation (SD) of triplicate determinations.

^b Ratio of $IC_{50}(\text{MAO-A})/IC_{50}(\text{MAO-B})$.

To verify that 2-PAT acts indeed irreversibly as expected for propargylamine derived MAO inhibitors, the reversibility of inhibition was investigated using dialysis (Mostert *et al.*, 2015). For this purpose 2-PAT (at a concentration of $4 \times IC_{50}$) was incubated with MAO-A and MAO-B for 15 min and the mixture was subsequently dialysed for 24 h.

As negative controls similar incubations of the enzymes were carried out in absence of inhibitor, while as positive controls MAO-A and MAO-B were incubated in the presence of the irreversible inhibitors, pargyline and selegiline, respectively, with the inhibitor concentrations also at $4 \times IC_{50}$. After dialysis, the mixtures were diluted twofold with the addition of kynuramine and the formation 4-hydroxyquinoline was measured at an endpoint of 20 min. The MAO activities of the negative control samples signified 100% residual activity. For comparison, the residual activities of undialysed mixtures of MAO-A and MAO-B and 2-PAT were also measured. The results of these studies show that for MAO-A, inhibition by 2-PAT is reversed by dialysis with the enzyme activity recovering to 102% (Fig. 6). In contrast, enzyme activity is not recovered by dialysis when MAO-A is inhibited by pargyline, with the residual activity at 0.9%. Inhibition persisted in undialysed mixtures of MAO-A and 2-PAT with the residual activity at 46%. Since dialysis clearly restores enzyme activity it may be concluded that 2-PAT is a reversible inhibitor of human MAO-A. For MAO-B, dialysis however does not reverse inhibition by 2-PAT with the residual activity at only 7.5%. This is similar to the residual MAO-B activity after inhibition with selegiline (3.9%) and subsequent dialysis. The almost complete inhibition observed with 2-PAT and selegiline, which cannot be reversed by dialysis, is evidence that these compounds are irreversible human MAO-B inhibitors. Complete inhibition (0.3%) is also observed in undialysed mixtures of MAO-B and 2-PAT.

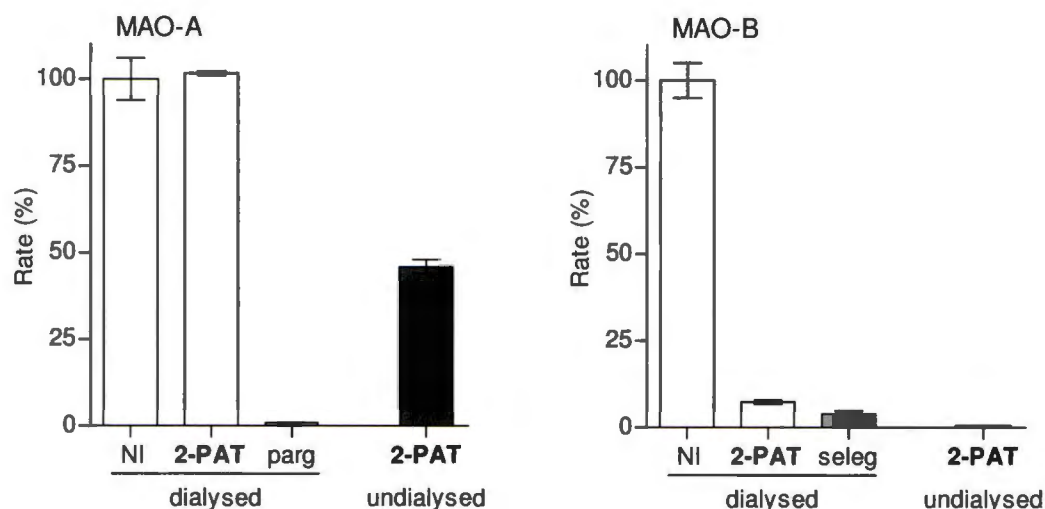


Fig. 6 2-PAT is a reversible MAO-A inhibitor and an irreversible MAO-B inhibitor. The MAO enzymes and 2-PAT (at a concentration of $4 \times IC_{50}$) were incubated for 15 min, dialysed for 24 h and the residual enzyme activity was measured (2-PAT dialysed). Similar incubation and dialysis of the MAOs in the absence (NI dialysed) and presence of the irreversible inhibitors, pargyline (parg dialysed) and selegiline (seleg dialysed) were also carried out. The residual MAO activity of undialysed mixtures of the MAOs with 2-PAT was also recorded (2-PAT undialysed).

To further investigate the reversible interaction between 2-PAT and MAO-A, the enzyme-inhibitor dissociation constant (K_i value) was measured. For this purpose six Lineweaver-Burk (double-reciprocal) plots was constructed employing the following six inhibitor concentrations: $0 \mu\text{M}$, $\frac{1}{4} \times IC_{50}$, $\frac{1}{2} \times IC_{50}$, $\frac{3}{4} \times IC_{50}$, $1 \times IC_{50}$ and $1\frac{1}{4} \times IC_{50}$. For each plot eight concentrations of kynramine ($15\text{--}250 \mu\text{M}$) were used. The set of Lineweaver-Burk plots is shown in Fig. 7. Since the lines are linear and intersect on the y-axis, it may be concluded that the inhibition of MAO-A by 2-PAT is competitive. From global (shared) fitting of the inhibition data directly to the Michaelis-Menten equation, a K_i value of $0.941 \pm 0.079 \mu\text{M}$ ($R^2 = 0.99$) is estimated. A similar value of ($1.32 \mu\text{M}$) is obtained by graphing the slopes of the Lineweaver-Burk plots versus inhibitor concentration (x-axis intercept equals $-K_i$).

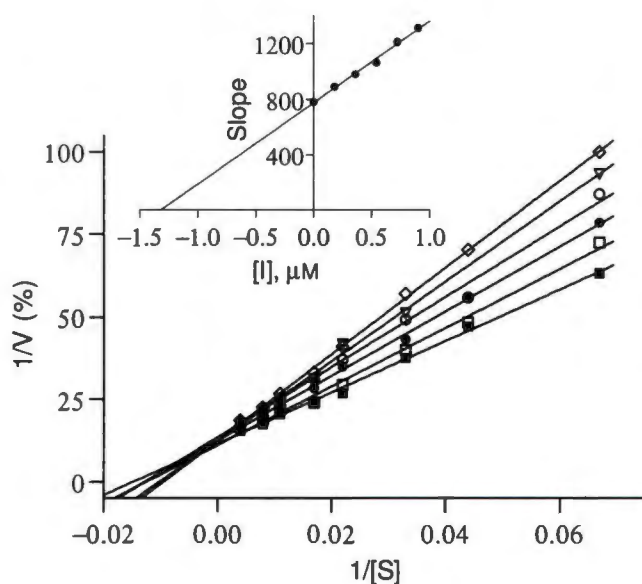


Fig.7. Lineweaver-Burk plots for the inhibition of human MAO-A by 2-PAT. The inset is a graph of the slopes of the Lineweaver-Burk plots versus inhibitor concentration.

An attempt was made to gain insight into the interactions between the MAOs and 2-PAT on the molecular level. For the reversible interaction between 2-PAT and the MAOs, both enantiomers of the inhibitor were docked into the active sites of the enzymes using the CDOCKER docking algorithm of Discovery Studio 3.1 (Accelrys). For this purpose the literature protocol was followed (Mostert *et al.*, 2015) and the reported crystal structure of human MAO-A (PDB code: 2Z5X) and human MAO-B (PDB code: 1S2Q) served as enzyme models (Son *et al.*, 2008, Binda *et al.*, 2004). As shown in Fig. 8, 2-PAT fits in both MAO-A and MAO-B active site cavities. In this respect 2-PAT binds in proximity to the FAD cofactor for both isoforms, and in MAO-B, is thus situated in the substrate cavity. The enantiomers of 2-PAT exhibit similar binding orientations to the respective MAO isoforms.

Interestingly, the propargylamine group of 2-PAT is directed towards the FAD in MAO-A, while being directed towards the entrance of the active site in MAO-B. Based on the reversibility of MAO-A inhibition and irreversibility of MAO-B inhibition by 2-PAT, this is contrary to what is expected. For an irreversible inhibitor, the propargylamine is expected to bind close to the FAD where it may act as a suicide substrate. This inconsistency between the experimental results and docking study suggests that 2-PAT may bind with several orientations to the MAOs, and for MAO-B not all orientations lead to mechanism-based inactivation. This point of view is supported by the observation that 2-PAT is a relatively small molecule compared to the active site cavities of the MAOs.

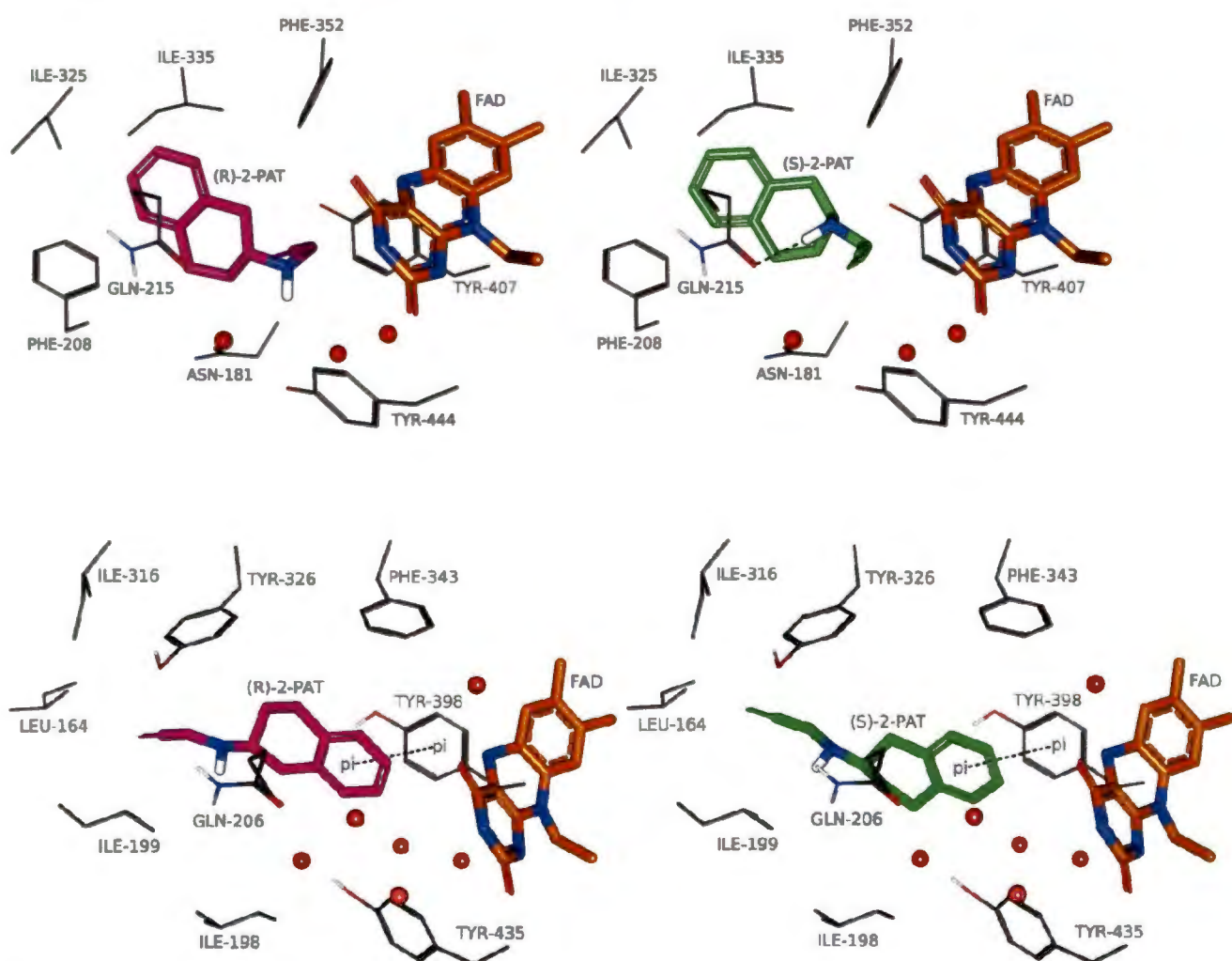


Fig. 8. The proposed reversible interactions between 2-PAT and MAO-A (top) and MAO-B (bottom).

The results in Fig. 9 shows that, in MAO-A, both enantiomers of rasagiline bind with the propargylamine group directed towards the FAD. In MAO-B, orientations with the propargylamine group directed towards the FAD as well as in the opposite direction, were recorded. This further underscores the proposal that small molecule inhibitors may adopt different binding orientations in the relatively large MAO active sites, and for propargylamines, not all orientations lead to inactivation. Key interactions of 2-PAT and rasagiline in the MAOs include hydrogen bonding to Gln-215 (MAO-A), Gln-206, Tyr-398 and water molecules (MAO-B). π - π interactions with Tyr-398 in MAO-B is another important interaction, particularly where 2-PAT and rasagiline binds with the propargylamine group directed towards the FAD.

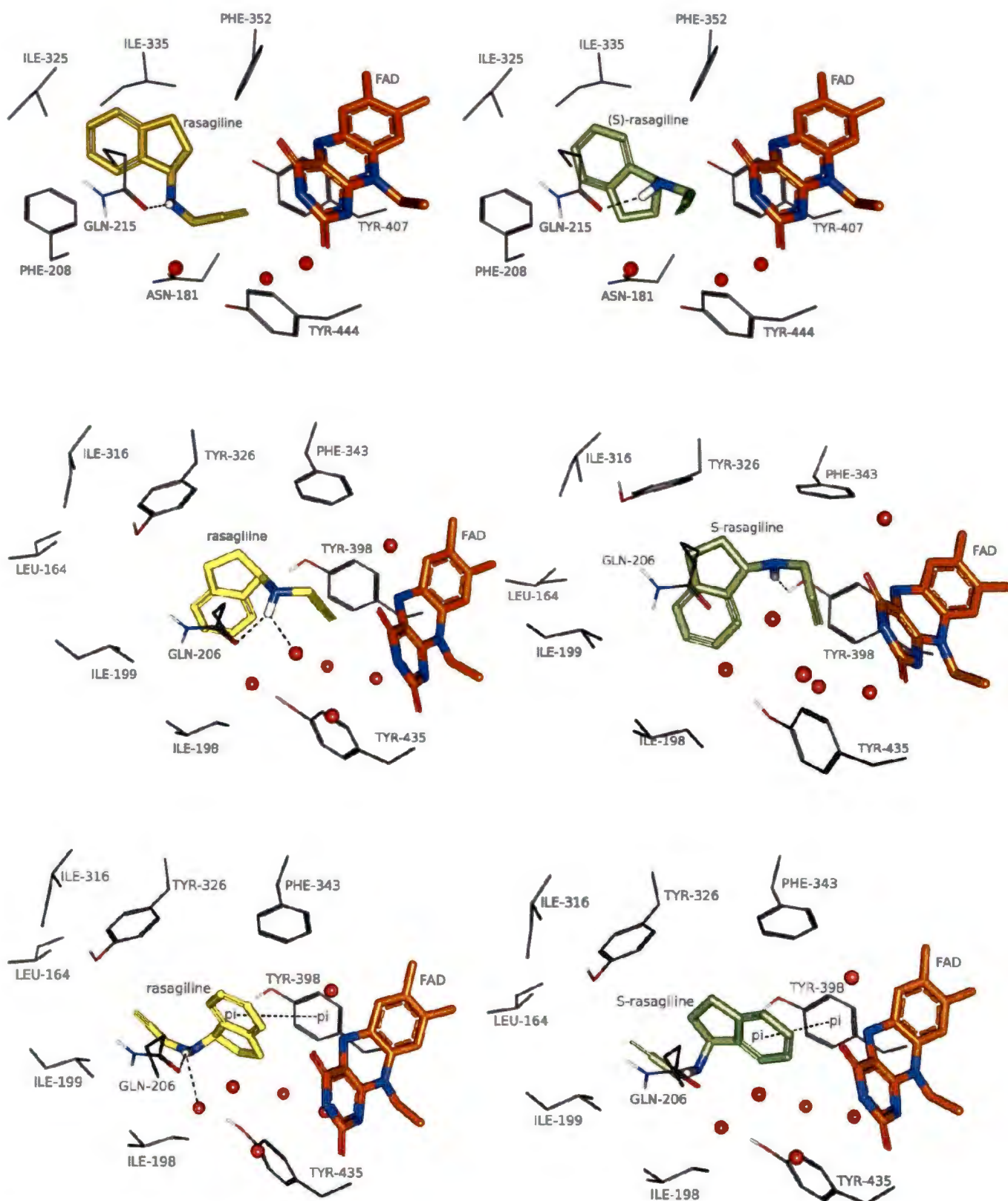


Fig. 9. The proposed reversible interactions of rasagiline and its S-enantiomer with MAO-A (top) and MAO-B (middle and bottom).

In conclusion, this study shows that racemic 2-PAT is mechanism-based inactivator of human MAO-B while acting as a reversible inhibitor of human MAO-A. In this regard 2-PAT may be considered as a relatively potent MAO-A inhibitor with an IC_{50} value of 0.721 μ M. Since 2-PAT is approximately fivefold more potent than tolloxatone ($IC_{50} = 3.92 \mu$ M), a clinically used antidepressant and reversible MAO-A inhibitor, the MAO-A inhibition of 2-PAT may thus be clinically relevant (Petzer *et al.*, 2013). Based on its reversibility of MAO-A inhibition, 2-PAT is unlikely to potentiate tyramine-induced side effects as expected for MAO-A inactivators. Although not nearly as potent as selegiline as a MAO-B inhibitor (based on IC_{50}), 2-PAT would still be expected to produce effective MAO-B inhibition *in vivo* since inhibition is time-dependent and thus cumulative upon chronic dosage regimen. This is the case for pargyline, an effective MAO inhibitor *in vivo* while displaying a modest IC_{50} *in vitro*. Based on these considerations 2-PAT could be useful and safe therapeutic agent for disorders such as Parkinson's disease, particularly where depression is a comorbidity of Parkinson's disease. In a follow-up study the MAO inhibition properties of the individual enantiomers of 2-PAT needs to be investigated in order to determine if either of the pure enantiomers provides enhanced benefits compared to the racemate. A protocol for the synthesis of 2-PAT with improved yields is, however, required for such studies.

Acknowledgements

The NMR and MS spectra were recorded by André Joubert and Johan Jordaan of the SASOL Centre for Chemistry, North-West University. This work is based on the research supported in part by the Medical Research Council and National Research Foundation of South Africa (Grant specific unique reference numbers (UID) 85642, 96180). The Grantholders acknowledge that opinions, findings and conclusions or recommendations expressed in any publication generated by the NRF supported research are that of the authors, and that the NRF accepts no liability whatsoever in this regard.

Conflict of Interest

The authors have no conflicts of interest to declare

References

1. Olanow, C.W., Stern, M.B. & Sethi, K. (2009) 'The scientific and clinical basis for the treatment of Parkinson disease', *Neurology*, 72(21 Suppl 4), pp. S1–S136.
2. Carlsson, A. (2002) 'Treatment of Parkinson's with L-dopa. The early discovery phase and a comment on current problems', *Journal of neural transmission*, 109(5–6), pp. 777–787.
3. Pedrosa, D.J. & Timmermann, L. (2013) 'Review: management of Parkinson's disease', *Neuropsychiatric disease and treatment*, 9, pp. 321–340.
4. Talati, R., Baker, W.L., Patel, A.A., Reinhart, K. & Coleman, C.I. (2009) 'Adding a dopamine agonist to preexisting levodopa therapy vs. levodopa therapy alone in advanced Parkinson's disease: a meta analysis', *International journal of clinical practice*, 63(4), pp. 613–623.
5. Fahn, S., Oakes, D. & Shoulson, I. (2004) 'Levodopa and the progression of Parkinson's disease', *New England journal of medicine*, 351(24), pp. 2498–2508.
6. Youdim, M.B.H., Edmondson, D. & Tipton, K.F. (2006), 'The therapeutic potential of monoamine oxidase inhibitors', *Nature reviews. Neuroscience*, 7, pp. 295–309.
7. Shoulson, I., Oakes, D. & Fahn, S. (2002) 'Impact of sustained deprenyl (selegiline) in levodopa-treated Parkinson's disease: a randomized placebo-controlled extension of the deprenyl and tocopherolantioxidative therapy of parkinsonism trial', *Annals of neurology*, 51(5), pp. 604–612.
8. Fernandez, H.H. & Chen, J.J. (2007) 'Monoamine oxidase B inhibition in the treatment of Parkinson's disease', *Pharmacotherapy*, 27, pp. S174–S185.

9. Finberg, J.P., Wang, J., Bankiewicz, K., Harvey-White, J., Kopin, I.J. & Goldstein, D.S. (1998) 'Increased striatal dopamine production from L-dopa following selective inhibition of monoamine oxidase B by R(+)-N-propargyl-1-aminoindan (rasagiline) in the monkey' *Journal of neural transmission supplementa*, 52, pp. 279–285.
10. Pålhagen, S., Heinonen, E.H. & Hägglund, J. (1998) 'Selegiline delays the onset of disability in de novo parkinsonian patients. Swedish Parkinson Study Group', *Neurology*, 51(2), pp. 520–525.
11. Borgohain, R., Szasz, J., Stanzione, P., Meshram, C., Bhatt, M., Chirilineau, D., Stocchi, F., Lucini, V., Giuliani, R., Forrest, E., Rice, P. & Anand, R. (2014) 'Randomized trial of safinamide add-on to levodopa in Parkinson's disease with motor fluctuations', *Movement disorders*, 29(2), pp. 229–237.
12. Dézsi, L. & Vécsei, L. (2014) 'Safinamide for the treatment of Parkinson's disease', *Expert opinion on investigational drugs*, 23(5), pp. 729–742.
13. Youdim, M.B.H. & Bakhle, Y.S. (2006) 'Monoamine oxidase: Isoforms and inhibitors in Parkinson's disease and depressive illness', *British journal of pharmacology*, 147(S1), pp. S287–S296.
14. Da Prada, M., Zürcher, G., Wüthrich, I. & Haefely W.E. (1988) 'On tyramine, food, beverages and the reversible MAO inhibitor moclobemide', *Journal of neural transmission supplementa*, 26, pp. 31–56.
15. Flockhart, D.A. (2012) 'Dietary restrictions and drug interactions with monoamine oxidase inhibitors: an update', *Journal of clinical psychiatry*, 73(Suppl1), pp. S17–S24.
16. Teychenne, P.F., Calne, D.B., Lewis, P.J. & Findley, L.J. (1975) 'Interactions of levodopa with inhibitors of monoamine oxidase and L-aromatic amino acid decarboxylase', *Clinical pharmacology and therapeutic*, 18(3), pp. 273–237.

17. Schwartz, T.L. (2013) 'A neuroscientific update on monoamine oxidase and its inhibitors' *CNS Spectrums*, 18(Suppl1), pp. 25–32;
18. Lum, C.T. & Stahl, S.M. (2012) 'Opportunities for reversible inhibitors of monoamine oxidase-A (RIMAs) in the treatment of depression', *CNS Spectrums*, 17(3), pp. 107–120.
19. Finberg, J.P. (2014) 'Update on the pharmacology of selective inhibitors of MAO-A and MAO-B: focus on modulation of CNS monoamine neurotransmitter release', *Pharmacology & Therapeutics*, 143(2), pp, 133–152.
20. Edmondson, D.E., Binda, C. & Mattevi, A. (2004a) 'The FAD binding sites of human monoamine oxidases A and B', *Neurotoxicology*, 25, pp. 63–72.
21. Edmondson, D.E., Mattevi, A., Binda, C., Li, M. & Hubálek, F. (2004b) 'Structure and mechanism of monoamine oxidase', *Current medicinal chemistry*, 11, pp. 1983–1993.
22. Binda, C., Hubálek, F., Li, M., Herzig, Y., Sterling, J., Edmondson, D.E. & Mattevi, A. (2004) 'Crystal structures of monoamine oxidase B in complex with four inhibitors of the N-propargylaminoindan class', *Journal of medicinal chemistry*, 47(7), pp. 1767–1774.
23. Binda, C., Hubálek, F., Li, M., Herzig, Y., Sterling, J., Edmondson, D.E. & Mattevi, A. (2005) 'Binding of rasagiline-related inhibitors to human monoamine oxidases: a kinetic and crystallographic analysis', *Journal of medicinal chemistry*. 48(26), pp. 8148–8154.
24. Milczek, E.M., Bonivento, D., Binda, C., Mattevi, A., McDonald, I.A. & Edmondson, D.E. (2008) 'Structural and mechanistic studies of mofegiline inhibition of recombinant human monoamine oxidase B', *Journal of medicinal chemistry*, 51(24), pp. 8019–8026.

25. Bonnet, U. (2003) 'Moclobemide: therapeutic use and clinical studies', *CNS drug reviews*, 9(1), pp. 97–140.
26. Provost, J.C., Funck-Brentano, C., Rovei, V., D'Estanque, J., Ego, D. & Jaillon, P. (1992) 'Pharmacokinetic and pharmacodynamic interaction between toloxatone, a new reversible monoamine oxidase-A inhibitor, and oral tyramine in healthy subjects' *Clinical pharmacology and therapeutic*, 52(4), pp. 384–393.
27. Pae, C.U., Patkar, A.A., Jang, S., Portland, K.B., Jung, S. & Nelson, J.C. (2014) 'Efficacy and safety of selegiline transdermal system (STS) for the atypical subtype of major depressive disorder: pooled analysis of 5 short-term, placebo-controlled trials', *CNS spectrums*, 19(4), pp. 324–329.
28. Hubálek, F., Binda, C., Li, M., Herzig, Y., Sterling, J., Youdim, M.B., Mattevi, A. & Edmondson, D.E. (2004) 'Inactivation of purified human recombinant monoamine oxidases A and B by rasagiline and its analogues', *Journal of medicinal chemistry*, 47(7), pp. 1760–1766.
29. Hazelhoff, B., De Vries, J.B., Dijkstra, D., de Jong, W. & Horn, A.S. (1985) 'The neuropharmacological profile of N-methyl-N-propargyl-2-aminotetralin: a potent monoamine oxidase inhibitor', *Naunyn-Schmiedeberg's archives of pharmacology*, 330(1), pp. 50–58.
30. Tipton, K.F., McCrodden, J.M., Kalir, A.S. & Youdim, M.B. (1982) 'Inhibition of rat liver monoamine oxidase by alpha-methyl- and N-propargyl-amine derivatives', *Biochemical pharmacology*, 31(7), pp. 1251–1255.
31. Ma, G., Xu, Z., Zhang, P., Liu, J., Hao, X., Ouyang, J., Liang, P., You, S. & Jia, X. (2014) 'A novel synthesis of rasagiline via a chemoenzymatic dynamic kinetic resolution' *Organic process research and development*, 18(10), pp 1169–1174.

32. Zhuang, Z.P., Kung, M.P. & Kung, H.F. (1993) 'Synthesis of (R,S)-trans-8-hydroxy-2-[N-n-propyl-N-(3'-iodo-2'-propenyl)amino]tetral in (trans-8-OH-PIPAT): a new 5-HT_{1A} receptor ligand', *Journal of medicinal chemistry*, 36(21), pp. 3161–3165.
33. Başköse, U.C., Bayarı, S.H., Sağlam, S. & Özışık, H. (2012) 'Theoretical investigation of the anti-Parkinson drug rasagiline and its salts: conformations and infrared spectra' *Central European journal of chemistry*, Volume 10, Issue 2, pp 395–406.
34. Novaroli, L., Reist, M., Favre, E., Carotti, A., Catto, M. & Carrupt, P.A. (2005) 'Human recombinant monoamine oxidase B as reliable and efficient enzyme source for inhibitor screening', *Bioorganic & medicinal chemistry*, 13(22), pp. 6212–6217.
35. Mostert, S., Petzer, A. & Petzer, J.P. (2015) 'Indanones as high-potency reversible inhibitors of monoamine oxidase', *ChemMedChem*, 10(5), pp. 862–873.
36. Strydom, B., Bergh, J.J. & Petzer, J.P. (2012) '8-Aryl- and alkyloxycaffeine analogues as inhibitors of monoamine oxidase', *European journal of medicinal chemistry*, 46(8), pp. 3474–3485.
37. Petzer, A., Harvey, B.H., Wegener, G. & Petzer, J.P. (2012) 'Azure B, a metabolite of methylene blue, is a high-potency, reversible inhibitor of monoamine oxidase' *Toxicology and applied pharmacology*, 258(3), pp. 403–409.
38. Accelrys Discovery Studio 3.1 (2005). Accelrys Software Inc., San Diego, CA, USA. <http://www.accelrys.com>.
39. Son, S., Ma, J., Kondou, Y., Yoshimura, M., Yamashita, E. & Tsukihara, T. (2008) 'Structure of human monoamine oxidase A at 2.2-Å resolution: The control of opening the entry for substrates/inhibitors', *The national academy of sciences of the United States of America*, 105, pp. 5739–5744.

40. Petzer, A., Pienaar, A. & Petzer, J.P. (2013) 'The inhibition of monoamine oxidase by esomeprazole', *Drug research*, 63(9), pp. 462–467.

Supplementary Material

The evaluation of N-propargylamine-2-aminotetralin as an irreversible inhibitor of monoamine oxidase

Letitia Meiring,¹Jacobus P. Petzer,¹Lesetja J. Legoabe,¹ and Anél Petzer^{1,*}

^{2.} *Pharmaceutical Chemistry, School of Pharmacy and Centre of Excellence for Pharmaceutical Sciences, North-West University, Private Bag X6001, Potchefstroom 2520, South Africa*

1. Materials and methods

Chemistry: All starting materials and reagents were obtained from Sigma-Aldrich (unless otherwise noted) and were used without further purification. Proton (¹H) and carbon (¹³C) NMR spectra were recorded on a 600 MHz spectrometer employing chloroform-*d* or methanol-*d*₄ as NMR solvents. Chemical shifts are reported in parts per million (δ) downfield from the signal of tetramethylsilane and were referenced to the residual solvent signal at 7.26 ppm (¹H NMR) and 77.0 ppm (¹³C NMR) for chloroform-*d* and 3.31 ppm (¹H NMR) and 49.00 ppm (¹³C NMR) for methanol-*d*₄. Spin multiplicities are given as s (singlet), d (doublet), t (triplet), qd (quartet of doublets) or m (multiplet). High resolution mass spectra (HRMS) were recorded on a Bruker micrOTOF-Q II mass spectrometer in atmospheric-pressure chemical ionization (APCI) mode (positive mode). Melting points (mp) were determined with a Buchi B-545 melting point apparatus and are uncorrected. Thin layer chromatography (TLC) was carried out using silica gel 60 (Merck) with UV₂₅₄ fluorescent indicator, employing a mobile phase of ethyl acetate:petroleum ether (40:60). The developed sheets were visualised by staining with iodine vapour.

Biology: All solvents and chemicals used for the biology were obtained from Sigma-Aldrich (unless otherwise noted). These include microsomes from insect cells containing recombinant human MAO-A and MAO-B (5 mg/mL), kynuraminedihydrobromide, selegiline hydrochloride and pargyline hydrochloride. Fluorescence spectrophotometry was carried out with a Varian Cary Eclipse fluorescence spectrophotometer.

2. Synthesis of the hydrochloric acid salt of N-propargylamine-2-aminotetralin (2-PAT)

β -Tetralone (5 mmol) and propargylamine (25 mmol) were dissolved in 40 mL benzene and p-toluenesulfonic acid (0.282 mmol) was added. The mixture was heated under reflux for 2 h while water was separated with a Dean-Stark distilling trap. The reaction solvent was evaporated in vacuo and the residue, a dark orange oil, was dissolved in 11 mL methanol. Under an atmosphere of nitrogen, NaCNBH₄ (3.06 mmol) was added and the reaction was stirred for 30 min at room temperature. Water (11 mL) was added and the reaction was subsequently acidified with HCl (10%) to a pH of 1 and extracted to diethyl ether (3 × 30 mL). The pH of the aqueous phase was adjusted to 8–9 with the addition of solid NaHCO₃, and extracted to dichloromethane (3 × 30 mL). The dichloromethane phases were combined and evaporated in vacuo to yield a light yellow solid, which was suspended and washed in boiling ethyl acetate (40 mL). The resulting cream coloured solid was collected by filtration and appeared pure by TLC (Zhuang *et al*, 1993).

Yield of 7.9%; mp 127.5 °C; APCI-HRMS m/z: calcd for C₁₃H₁₆N (MH⁺), 186.1277, found 186.1274.

¹H NMR (600 MHz, Methanol-*d*₄) δ 7.19 – 7.08 (m, 4H), 4.10 (d, *J* = 2.6 Hz, 2H), 3.72 – 3.62 (m, 1H), 3.30 – 3.23 (m, 2H), 3.04 – 2.87 (m, 3H), 2.39 – 2.29 (m, 1H), 1.93 – 1.82 (m, 1H); ¹³C NMR (151 MHz, Methanol-*d*₄) δ 135.86, 132.89, 130.23, 129.74, 127.86, 127.43, 79.14, 74.76, 55.12, 34.95, 32.84, 28.21, 26.91.

¹H NMR (600 MHz, Chloroform-*d*) δ 10.07 (s, 2H), 7.17 – 7.00 (m, 4H), 3.96 (qd, *J* = 16.9, 2.6 Hz, 2H), 3.80 – 3.68 (m, 1H), 3.35 – 3.17 (m, 2H), 3.04 – 2.82 (m, 2H), 2.54 (t, *J* = 2.6 Hz, 1H), 2.52 – 2.44 (m, 1H), 2.12 (qd, *J* = 12.0, 5.8 Hz, 1H); ¹³C NMR (151 MHz, Chloroform-*d*) δ 134.48, 131.87, 129.24, 128.69, 126.70, 126.27, 78.08, 72.90, 52.86, 33.40, 31.86, 27.67, 25.84.

3. Procedure for the measurement of IC₅₀ values

The procedure for the measurement of IC₅₀ values for the inhibition of MAO-A and MAO-B has been detailed in the literature (Mostert *et al.*, 2015; Mostert *et al.*, 2016). For these studies the recombinant human enzymes and kynuramine served as enzyme sources and substrate, respectively. MAO oxidises kynuramine to ultimately yield 4-hydroxyquinoline, which may be measured by fluorescence spectrophotometry ($\lambda_{\text{ex}} = 310 \text{ nm}$; $\lambda_{\text{em}} = 400 \text{ nm}$). After recording the catalytic rates of the MAOs in the presence of different concentrations of the test inhibitors (0.003–100 μM), sigmoidal dose-response plots were constructed. From these the IC₅₀ values were determined. All measurements were conducted in triplicate and the IC₅₀ values are given as the mean \pm standard deviation (SD).

4. Recovery of enzyme activity after dialysis

The procedure for the dialysis studies has been detailed in the literature (Mostert *et al.*, 2015; Mostert *et al.*, 2016). The MAO enzymes and the test inhibitors were combined and preincubated for 15 min at 37 °C. The concentrations of the inhibitors were fourfold the IC₅₀ value for the inhibition of the relevant MAO. The mixtures were dialysed at 4 °C for 24 h, during which the dialysis buffer was replaced twice, and diluted twofold with the addition of kynuramine. The residual enzyme catalytic rates were subsequently determined by measuring the formation of 4-hydroxyquinoline.

As positive and negative controls, respectively, MAO-A and MAO-B were similarly preincubated and dialysed in the presence of the irreversible inhibitors, pargyline and selegiline, and in the absence of inhibitor. The enzyme activities of undialysed mixtures of the MAOs and the test inhibitors, which were maintained at 4 °C for 24 h, were also recorded. Dialysis and rate measurements were carried out in triplicate and the residual enzyme catalytic rates are given as mean ± SD.

5. The construction of Lineweaver-Burk plots and calculation of K_i value

The reversible interaction of 2-PAT with MAO-A was investigated by constructing a set of six Lineweaver-Burk plots. The procedure for the construction of Lineweaver-Burk plots has been reported in the literature (Mostert *et al.*, 2015; Mostert *et al.*, 2016). The first plot was constructed in the absence of inhibitor while the remaining five plots were constructed in the presence of the following concentrations of 2-PAT: $\frac{1}{4} \times \text{IC}_{50}$, $\frac{1}{2} \times \text{IC}_{50}$, $\frac{3}{4} \times \text{IC}_{50}$, $1 \times \text{IC}_{50}$ and $1\frac{1}{4} \times \text{IC}_{50}$. For each plot the substrate, kynuramine, was used at eight different concentrations (15–250 μM).

After incubation of the reactions containing the substrate, inhibitor and enzyme (0.015 mg/mL), the MAO-generated 4-hydroxyquinoline was quantified by fluorescence spectrophotometry. The K_i value for the inhibition of MAO-A was estimated from plots of the slopes of the Lineweaver-Burke plots versus inhibitor concentration (x-axis intercept equals $-K_i$) as well as by global (shared) fitting of the inhibition data to the Michaelis-Menten equation.

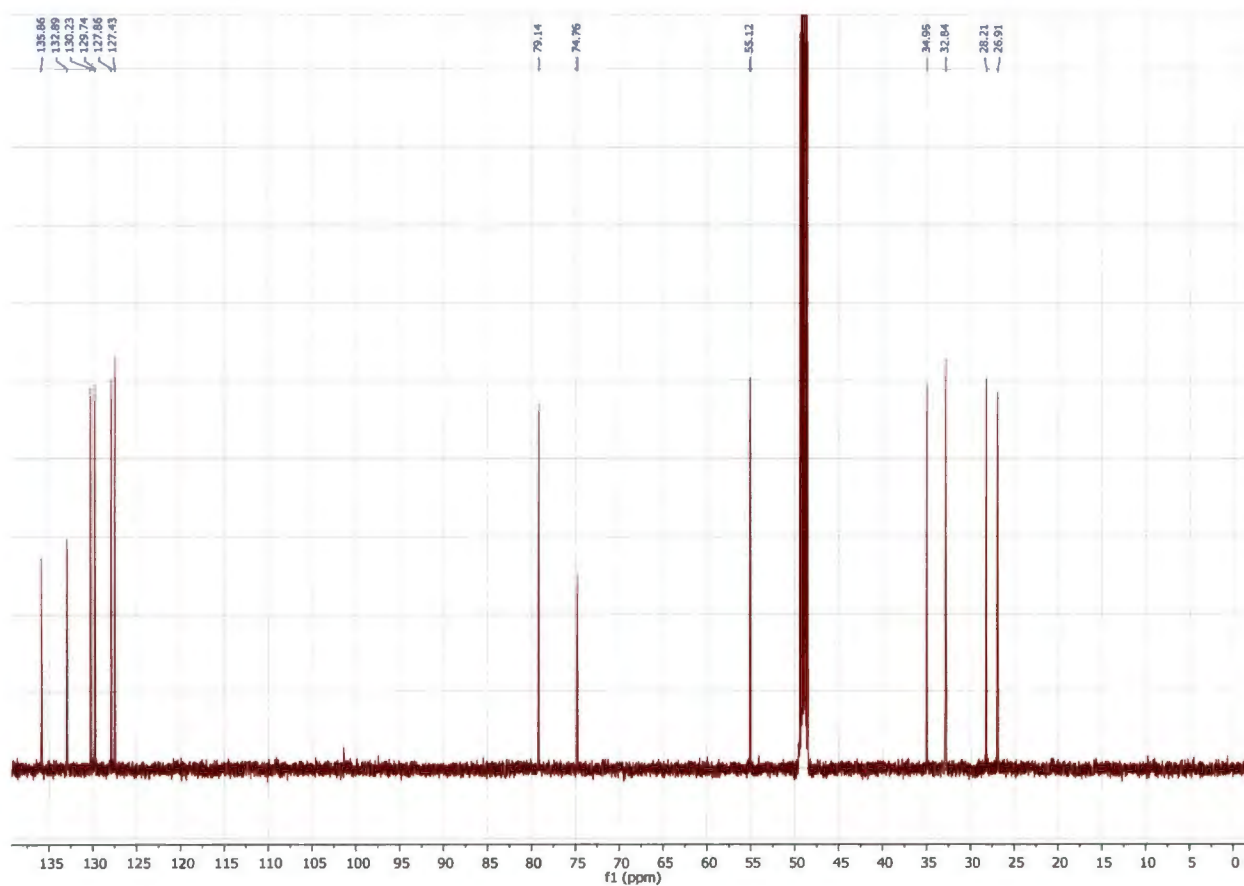
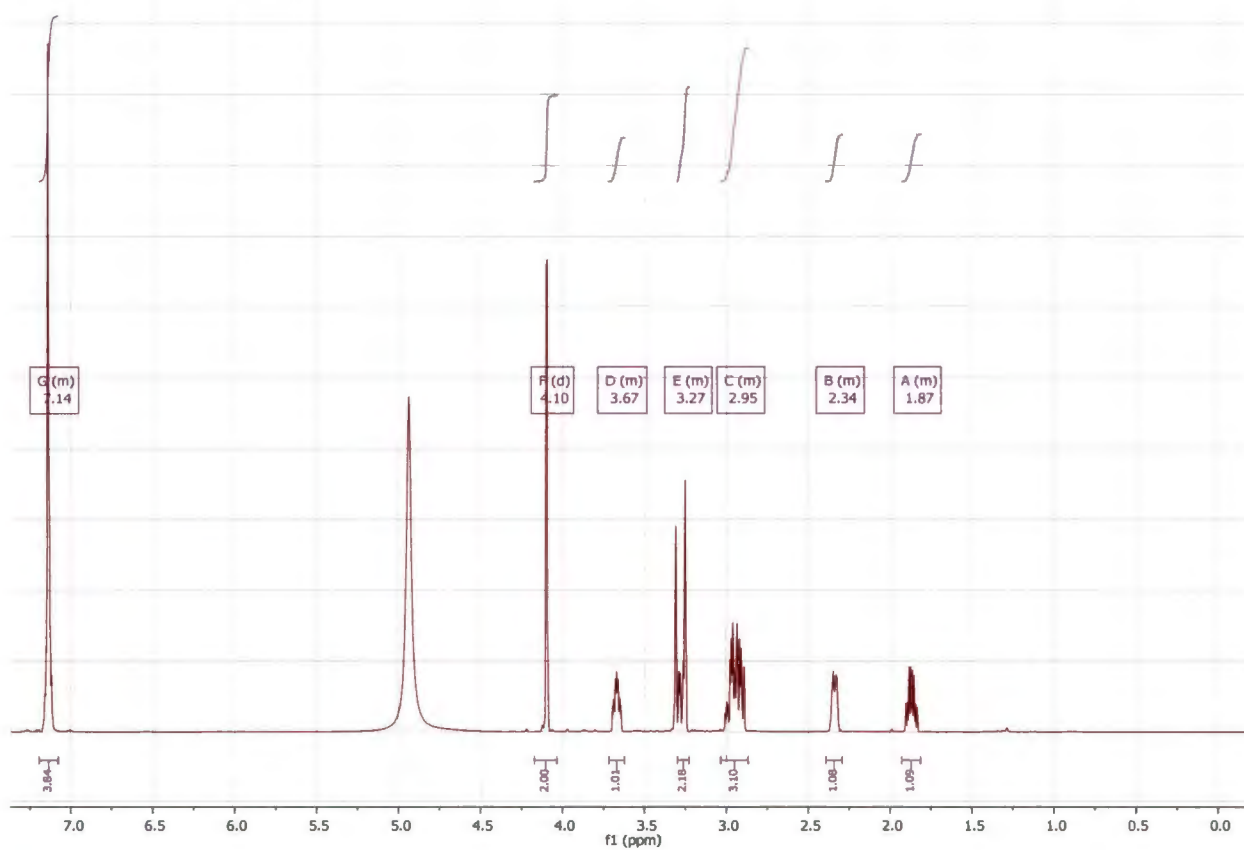
6. Procedure for molecular docking and dynamics simulations

The procedure for docking inhibitors into the MAO active sites has been reported in literature (Mostert *et al.*, 2015). The Windows-based Discovery Studio 3.1 software package (Accelrys) was used for these studies and the reported X-ray crystal structures of human MAO-A (PDB code 2Z5X) (Son *et al.*, 2008) and human MAO-B (PDB code 1S2Q) (Binda *et al.*, 2004) served as protein models. Preparation of the protein models included the calculation of pKa values and protonation states of the ionisable amino acids to which hydrogen atoms were subsequently added at pH 7.4. After verifying that the FAD is in the oxidised state, a fixed atom constraint was applied to the protein backbones. The protein models were energy minimised using the Smart Minimizer algorithm and the co-crystallised ligands and waters were removed. Only three waters in each model were retained: HOH 710, 718 and 739 in the MAO-A active site, and HOH 1155, 1170 and 1351 in the A-chain of the MAO-B active site. The test ligands were drawn in Discovery Studio and docking was performed with the CDOCKER algorithm. For this purpose full potential mode was used, ten random conformations were generated for each ligand and the heating target temperature was set to 700 K. After docking, the ligand orientations and interactions were further refined using in situ ligand minimisation with the Smart Minimizer algorithm. The illustrations were prepared with PyMol (DeLano, 2002).

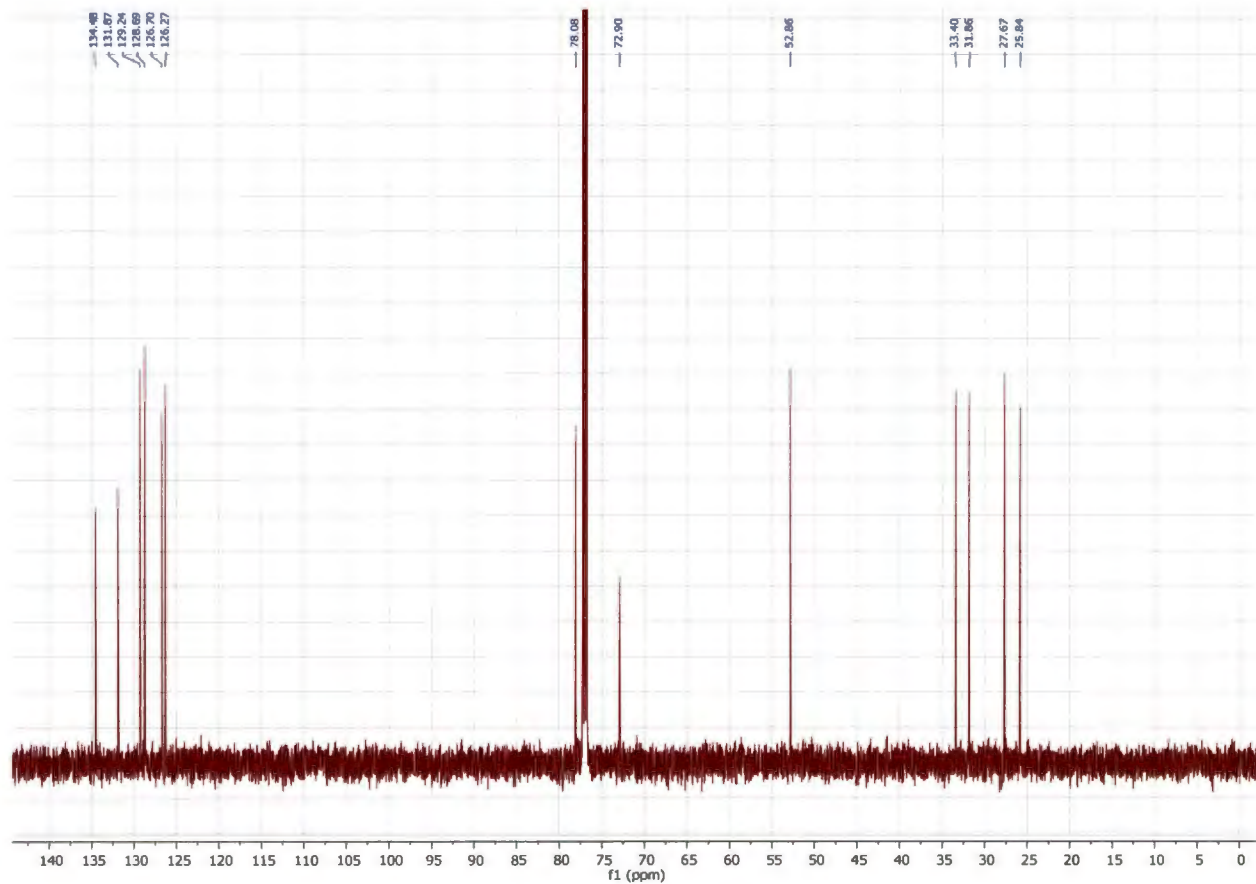
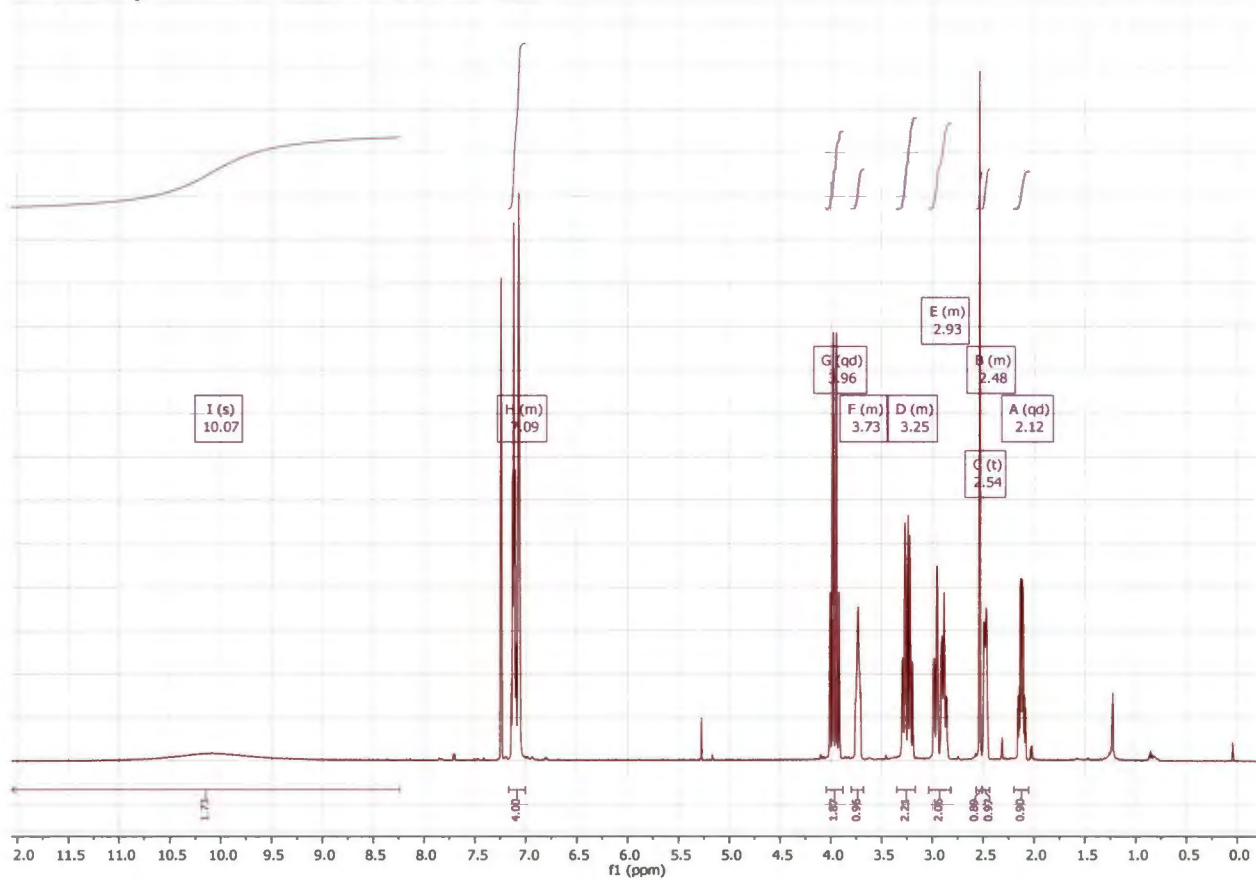
7. References

1. Zhuang, Z.P., Kung, M.P. & Kung, H.F. (1993) 'Synthesis of (R,S)-trans-8-hydroxy-2-[N-n-propyl-N-(3'-iodo-2'-propenyl)amino]tetral in (trans-8-OH-PIPAT): a new 5-HT_{1A} receptor ligand', *Journal of medicinal chemistry*, 36(21), pp. 3161–3165.
2. Mostert, S., Petzer, A. & Petzer, J.P. (2015) 'Indanones as high-potency reversible inhibitors of monoamine oxidase', *ChemMedChem*, 10(5), pp. 862–873.
3. Mostert, S., Petzer, A. & Petzer, J.P. (2016) 'Inhibition of monoamine oxidase by benzoxathiolone analogues', *Bioorganic & medicinal chemistry letters*, 26(4), pp. 1200–1204.
4. Accelrys Discovery Studio 3.1 (2005). Accelrys Software Inc., San Diego, CA, USA. <http://www.accelrys.com>.
5. Son, S., Ma, J., Kondou, Y., Yoshimura, M., Yamashita, E. & Tsukihara, T. (2008) 'Structure of human monoamine oxidase A at 2.2-Å resolution: The control of opening the entry for substrates/inhibitors', *The national academy of sciences of the United States of America*, 105, pp. 5739–5744.
6. Binda, C., Hubálek, F., Li, M., Herzig, Y., Sterling, J., Edmondson, D.E. & Mattevi, A. (2004) 'Crystal structures of monoamine oxidase B in complex with four inhibitors of the N-propargylaminoindan class', *Journal of medicinal chemistry*, 47(7), pp. 1767–1774.
7. DeLano, W.L. (2002) The PyMOL molecular graphics system. DeLano Scientific, San Carlos, USA.

2-PAT (hydrochloric acid salt) (CD₃OD)



2-PAT (hydrochloric acid salt) (CDCl₃)



CHAPTER 7

CONCLUSION

Introduction: In the current study three chemical classes were synthesised and evaluated as recombinant human MAO inhibitors. These include (1) C6- and C7-substituted 3,4-dihydro-2(1*H*)-quinolinones, (2) 2-phenoxyethoxy-substituted tetralones and (3) N-propargylamine-2-aminotetralin (2-PAT).

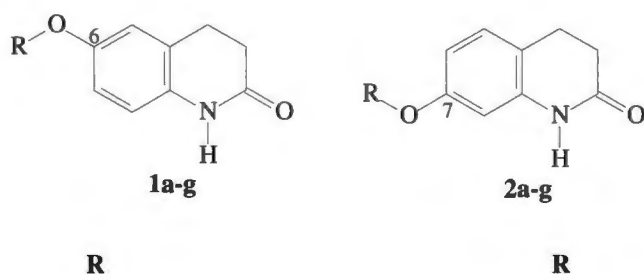
MAO consists of two isoenzymes, MAO-A and MAO-B. The MAOs are mitochondrial bound FAD containing enzymes. MAO-A is mainly present in the placenta and gastrointestinal tract, whilst MAO-B is the main form in the basal ganglia, blood platelets and liver. MAO-A is responsible for the deactivation of catecholamines in circulation as well as vasopressors such as tyramine ingested in the diet. MAO-A inhibitors inhibit the oxidation of serotonin and noradrenaline in the central nervous system, making these drugs useful in the treatment of depression. Side effects of MAO-A inhibitors include the cheese reaction, which occur with the irreversible inhibition of MAO-A (Youdim *et al.*, 2006).

Since DA is mainly oxidised by MAO-B in the basal ganglia of the midbrain, inhibitors of MAO-B are useful in the treatment of PD. The oxidation of DA is associated with the formation of by-products such as hydrogen peroxide and aldehydes, which may lead to oxidative stress and neurotoxicity if not inactivated or cleared (Fernandez & Chen, 2007). Hydrogen peroxide and aldehydes produced by the MAO catalytic cycle may contribute to neurodegeneration in PD. By preventing the formation of these potentially neurotoxic metabolic by-products, MAO-B inhibitors may act as neuroprotective agents. MAO-B inhibitors may also slow the depletion of DA stores and elevate the levels of endogenous DA (Youdim *et al.*, 2006). This analysis shows that MAO-B inhibitors are valuable as symptomatic and potentially neuroprotective agents for the treatment of PD.

Selection of compounds: Quinolinone and β -tetralone derivatives are structurally related to chemical classes which have been reported to inhibit the MAOs. These chemical classes include α -tetralones, 1-indanones and 3-coumaranones (Meiring *et al.*, 2013; Legoabe *et al.*, 2014; Legoabe *et al.*, 2015).

In this study a series of fourteen 3,4-dihydro-2(1*H*)-quinolinone derivatives were synthesised (**1a–g** and **2a–g**) by substitution of 3,4-dihydro-2(1*H*)-quinolinone on C6 and C7 with a variety of substituents (Table 7.1). A second series of three β -tetralone derivatives were also synthesised: 6-(2-phenoxyethoxy)-3,4-dihydronaphthalen-1(2*H*)-one (**10**), 7-(2-phenoxyethoxy)-3,4-dihydronaphthalen-1(2*H*)-one (**11**) and 7-(2-phenoxyethoxy)-3,4-dihydronaphthalen-2(1*H*)-one (**12**) (Figure 7.1).

Table 7.1. The structures of the C6- and C7-substituted quinolinones (**1a–g** and **2a–g**) that were synthesised in this study.



1a	4-ClC ₆ H ₄ CH ₂ -	2a	4-ClC ₆ H ₄ CH ₂ -
1b	4-BrC ₆ H ₄ CH ₂ -	2b	4-BrC ₆ H ₄ CH ₂ -
1c	3-CH ₃ C ₆ H ₄ CH ₂ -	2c	3-CH ₃ C ₆ H ₄ CH ₂ -
1d	4-CH ₃ C ₆ H ₄ CH ₂ -	2d	4-CH ₃ C ₆ H ₄ CH ₂ -
1e	3-CH ₃ C ₆ H ₄ (CH ₂) ₂ -	2e	4-CH ₃ C ₆ H ₄ (CH ₂) ₂ -
1f	4-CH ₃ C ₆ H ₄ (CH ₂) ₂ -	2f	C ₆ H ₅ O(CH ₂) ₂ -
1g	C ₆ H ₅ O(CH ₂) ₂ -	2g	4-ClC ₆ H ₄ O(CH ₂) ₂ -

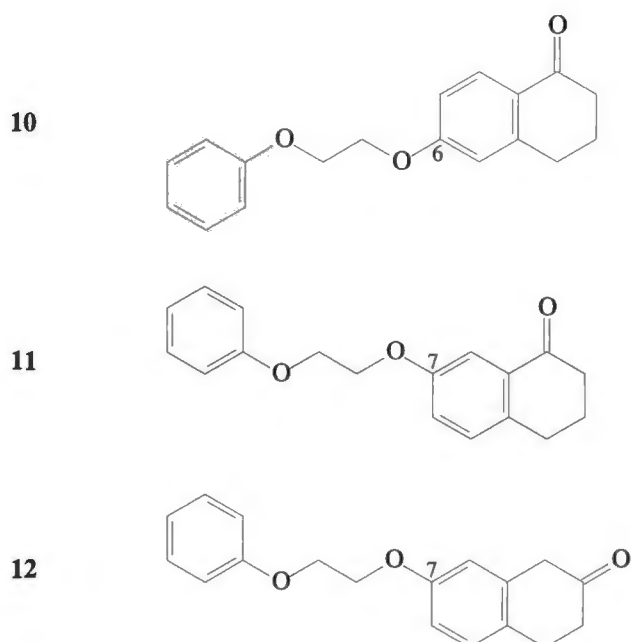


Figure 7.1: The structures of 6-(2-phenoxyethoxy)-3,4-dihydronaphthalen-1(2*H*)-one (**10**), 7-(2-phenoxyethoxy)-3,4-dihydronaphthalen-1(2*H*)-one (**11**) and 7-(2-phenoxyethoxy)-3,4-dihydronaphthalen-2(1*H*)-one (**12**).

Finally, 2-PAT, structurally very similar to rasagiline and the previously studied 2-MPAT, was also synthesised and evaluated as a MAO inhibitor. This study was motivated by the academic challenge of designing and discovering high potency and isoform-specific MAO inhibitors that may be useful therapeutic agents in PD.

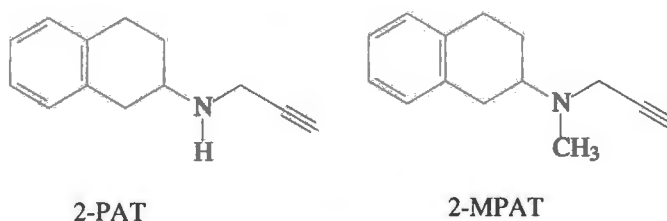


Figure 7.2: The structures of N-propargylamine-2-aminotetralin (2-PAT) and N-methyl-N-propargylamine-2-aminotetralin (2-MPAT).

Synthesis: The C6- and C7-substituted 3,4-dihydro-2(1*H*)-quinolinone and 2-phenoxyethoxy tetralone derivatives were synthesised by reacting 6- or 7-hydroxy-3,4-dihydro-2(1*H*)-quinolinone and 6- or 7-hydroxytetralone, respectively, with an appropriate alkyl bromide in the presence of base (Shigematzu, 1961; Meiring *et al.*, 2013; Legoabe *et al.*, 2014; Legoabe *et al.*, 2015).

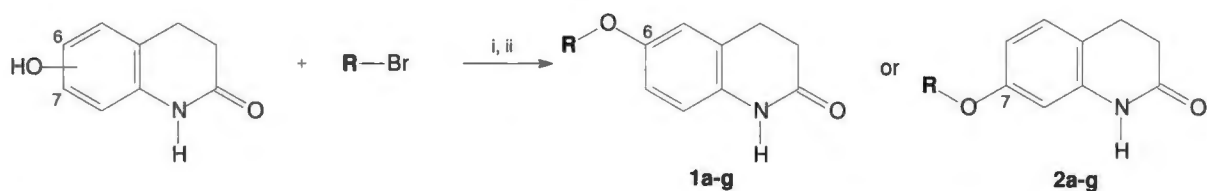


Figure 7.3: The synthesis of 3,4-dihydro-2(1*H*)-quinolinone derivatives **1a-g** and **2a-g**. Reagents and conditions: (i) KOH, ethanol, reflux; (ii) recrystallisation from ethanol.

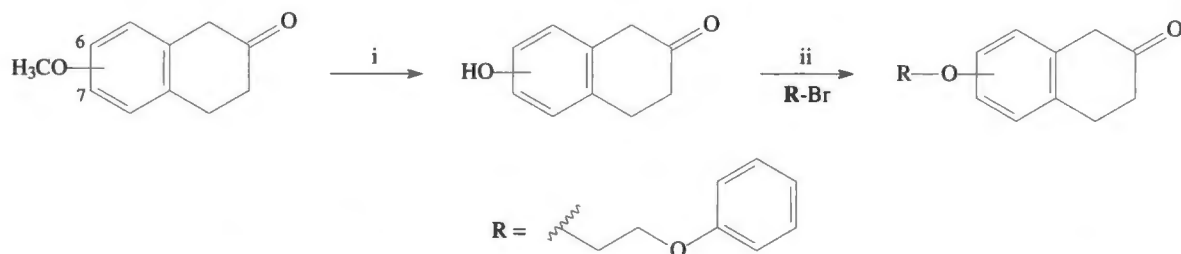


Figure 7.4: The synthesis of C6- or C7-substituted ethers of β -tetralone. Reagents and conditions: (i) AlCl_3 , toluene; reflux; (ii) acetone, K_2CO_3 , reflux.

2-PAT was synthesised by dehydrating commercially available β -tetralone and propargylamine in the presence of *p*-toluenesulfonic acid. After reduction with sodium cyanoborohydride (NaCNBH_4) and a workup that involves acidification with HCl, washing with diethyl ether and extraction to dichloromethane the hydrochloric acid salt of 2-PAT was obtained in low yield (Zhuang *et al.*, 1993).

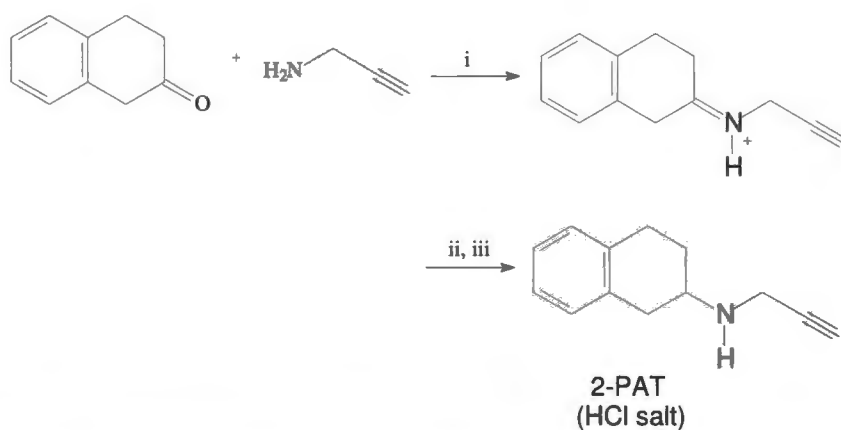


Figure 7.5: The synthesis of 2-PAT. Reagents and conditions: (i) p-toluenesulfonic acid, benzene, Dean-Stark trap; (ii) NaCNBH₄, methanol, N₂, rt; (iii) 10% HCl.

Enzymology: The synthesised compounds were evaluated as inhibitors of the recombinant human MAO-A and MAO-B enzymes, which are commercially available (Novaroli *et al.*, 2005). To measure MAO activities, the MAO-A/B mixed substrate, kynuramine, was employed. Kynuramine is oxidised by the MAO enzymes to yield 4-hydroxyquinoline. Since 4-hydroxyquinoline is fluorescent, the formation of 4-hydroxyquinoline was measured by fluorescence spectrophotometry. Sigmoidal dose-response curves were constructed and the inhibition potencies, the corresponding IC₅₀ values, were calculated (Mostert *et al.*, 2015; Mostert *et al.*, 2016).

To determine the reversibility of inhibition of MAO by selected derivatives, dialysis was employed. For reversible inhibition, sets of Lineweaver-Burk plots were constructed to determine the modes of inhibition. Finally, the inhibitors were docked into the MAO active sites using the CDocker docking algorithm of Discovery Studio 3.1 (Accelrys). This was done to gain insight into the interactions between the enzyme and selected inhibitors (Mostert *et al.*, 2015; Mostert *et al.*, 2016; Silverman, 1995; Son *et al.*, 2008; Binda *et al.*, 2004).

The results of the first study document that the 3,4-dihydro-2(1*H*)-quinolinone derivatives are MAO-B specific with high inhibition potencies. Most notably among these are 6-(4-bromobenzyloxy)-3,4-dihydro-2(1*H*)-quinolinone (**1b**), 7-(4-chlorobenzyloxy)-3,4-dihydro-2(1*H*)-quinolinone (**2a**) and 7-(4-bromobenzyloxy)-3,4-dihydro-2(1*H*)-quinolinone (**2b**) which display IC₅₀ values <0.006 μM. The most potent inhibitor, **2a**, displayed an IC₅₀ value of 0.0014 μM, and is significantly more potent than the reference MAO-B inhibitors lazabemide (IC₅₀ = 0.091 μM) and safinamide (IC₅₀ = 0.048 μM) (evaluated under the same experimental conditions). The 3,4-dihydro-2(1*H*)-quinolinone derivatives also display high specificities for the MAO-B enzyme with selectivities for MAO-B ranging from 99 to 40,000-fold.

Based on dialysis experiments, it was concluded that **1b** is a reversible MAO-B inhibitor. The Lineweaver-Burk plots constructed for the inhibition of MAO-B by **1b** were linear and intersected on the y-axis, indicating that this compound is a competitive MAO-B inhibitor.

An analysis of the Lineweaver-Burk plots indicated that **1b** inhibits MAO-B with a K_i value of 2.8 nM. An analysis of the structure-activity relationships for MAO-B inhibition by 3,4-dihydro-2(1*H*)-quinolinones shows that C7 substitution yields compounds with higher MAO-B inhibition potencies than C6 substitution. For each pair of homologues, the corresponding C7-substituted compounds display more potent inhibition although differences in inhibition potencies are in many instances very small.

The results for the second study document that the β-tetralone derivative, 7-(2-phenoxyethoxy)-3,4-dihydronaphthalen-2(1*H*)-one (**12**), is a weak inhibitor of human MAO-A (IC₅₀ = 56.2 μM) compared to the corresponding α-tetralone derivatives, 6-(2-phenoxyethoxy)-3,4-dihydronaphthalen-1(2*H*)-one (**10**) (IC₅₀ = 1.96 μM) and 7-(2-phenoxyethoxy)-3,4-dihydronaphthalen-1(2*H*)-one (**11**) (IC₅₀ = 1.81 μM). Compound **12**, however, was a potent human MAO-B inhibitor (IC₅₀ = 0.033 μM). It was also established that **12** is a reversible and competitive MAO-B inhibitor (K_i = 0.128 μM). This is the first report of the MAO inhibition properties of a β-tetralone derivative.

The results for the final study shows that 2-PAT is a 20-fold more potent inhibitor of MAO-A (IC₅₀ = 0.721 μM) compared to MAO-B (IC₅₀ = 14.6 μM) and 2-PAT is approximately fivefold more potent than toloxatone (IC₅₀ = 3.92 μM), a clinically used antidepressant and reversible MAO-A inhibitor.

Interestingly, dialysis studies found that 2-PAT is a reversible MAO-A inhibitor, while acting as an inactivator of MAO-B. This is the first report that a propargylamine compound acts as reversible inhibitor of one MAO isoform, while inhibiting the other irreversibly.

Conclusion: In conclusion, the first study shows that 3,4-dihydro-2(1*H*)-quinolinones are MAO-B specific inhibitors with compounds, **1b**, **2a** and **2b** showing high potency MAO-B inhibition ($IC_{50} < 0.006 \mu M$). The second study shows for the first time that a β -tetralone derivative, compound **12**, is a potent and selective MAO-B inhibitor. It was also established that this compound inhibits MAO-B reversibly. Although the α -tetralone homologues **10** and **11** are more potent MAO-B inhibitors, compound **12** displays better isoform selectivity. It may thus be concluded that, in contrast to the α -tetralones reported to date, **12** is a more selective MAO-B inhibitor. Specific MAO-B inhibitors such as these represent leads for the design of therapeutic agents for PD with lower risk for MAO-A related side effects.

The final study found that 2-PAT is a potent reversible MAO-A inhibitor, which may be clinically relevant since this compound is approximately fivefold more potent than toloxatone ($IC_{50} = 3.92 \mu M$). 2-PAT is unlikely to potentiate tyramine-induced side effects as seen with MAO-A inactivators, since 2-PAT is a reversible inhibitor of MAO-A. Although not as potent as current MAO-B inhibitors such as selegiline, 2-PAT would still be expected to inhibit MAO-B *in vivo* since inhibition is time-dependent and thus cumulative with a chronic dosage regimen. Based on the above considerations, 2-PAT could be a safe and useful agent for the treatment of PD, specifically where depression is a comorbidity of PD.

This study therefore concludes that the objectives given in Chapter 1 have been achieved and the hypotheses proven. 3,4-Dihydro-2(1*H*)-quinolinones and β -tetralones are suitable scaffolds for the design of MAO-B inhibitors and appropriate substitution yields highly potent MAO-B inhibitors. Such compounds are thus suitable leads for the design of antiparkinsonian therapies. 2-PAT possesses an interesting MAO inhibition profile that may be a useful in the treatment of PD.

Accelrys Discovery Studio 3.1. (2005) Accelrys Software Inc., San Diego, CA, USA.
<http://www.accelrys.com>.

Binda, C., Hubalek, F., Li, M., Herzig, Y., Sterling, J., Edmondson, D.E. & Mattevi, A. (2004) 'Crystal structures of monoamine oxidase B in complex with four inhibitors of the N-propargylaminoindan class', *Journal of medicinal chemistry*, 47, pp. 1767–1774.

Fernandez, H.H. & Chen, J.J. (2007) 'Monoamine oxidase B inhibition in the treatment of Parkinson's disease', *Pharmacotherapy*, 27, pp. S174–S185.

Legoabe, L.J., Petzer, A. & Petzer, J.P. (2014) ' α -Tetralone derivatives as inhibitors of monoamine oxidase', *Bioorganic & medicinal chemistry letters*, 24(12), pp. 2758–2763.

Legoabe, L.J., Petzer, A. & Petzer, J.P. (2015) 'The synthesis and evaluation of C7-substituted α -tetralone derivatives as inhibitors of monoamine oxidase', *Chemical biology & drug design*, 86(4), pp. 895–904.

Meiring, L., Petzer, J.P. & Petzer, A. (2013) 'Inhibition of monoamine oxidase by 3,4-dihydro-2(1H)-quinolinone derivatives', *Bioorganic & medicinal chemistry letters*, 23(20), pp. 5498–5502.

Mostert, S., Petzer, A. & Petzer, J.P. (2015) 'Indanones as high-potency reversible inhibitors of monoamine oxidase', *ChemMedChem*, 10(5), pp. 862–873.

Mostert S, Petzer A, Petzer JP. (2016) 'Inhibition of monoamine oxidase by benzoxathiolone analogues', *Bioorganic & medicinal chemistry letters*, 26, pp. 1200–1204.

Novaroli, L., Reist, M., Favre, E., Carotti, A., Catto, M. & Carrupt, P.A. (2005) 'Human recombinant monoamine oxidase B as reliable and efficient enzyme source for inhibitor screening', *Bioorganic and medicinal chemistry*, 13, pp. 6212.

Shigematsu, N. (1961) 'Studies of the synthetic analgesics XVI', *Chemical and pharmaceutical bulletin*, 9, pp. 970.

Silverman, R.B. (1995) 'Mechanism-based enzyme inactivators', *Methods in enzymology*, 249, pp. 240–283.

Son, S., Ma, J., Kondou, Y., Yoshimura, M., Yamashita, E. & Tsukihara, T. (2008) 'Structure of human monoamine oxidase A at 2.2-Å resolution: The control of opening the entry for substrates/inhibitors', *The national academy of sciences of the United States of America*, 105, pp. 5739–5744.

Youdim, M.B.H., Edmondson, D. & Tipton, K.F. (2006), 'The therapeutic potential of monoamine oxidase inhibitors', *Nature reviews. Neuroscience*, 7, pp. 295–309.

Zhuang, Z.P., Kung, M.P. & Kung, H.F. (1993) 'Synthesis of (R,S)-trans-8-hydroxy-2-[N-n-propyl-N-(3'-iodo-2'-propenyl)amino]tetral in (trans-8-OH-PIPAT): a new 5-HT_{1A} receptor ligand', *Journal of medicinal chemistry*, 36(21), pp. 3161–3165.

ADDENDUM A

Author guidelines: Mini-Reviews in Medicinal Chemistry

INSTRUCTIONS FOR AUTHORS

ONLINE MANUSCRIPT SUBMISSION:

An online submission and tracking service *via* Internet facilitates a speedy and cost-effective submission of manuscripts. The full manuscript has to be submitted online *via* Bentham's Content Management System (CMS) at [bsp-cms.eurekaselect.com / View Submission Instructions](http://bsp-cms.eurekaselect.com/View_Submission_Instructions)

Manuscripts must be submitted by one of the authors of the manuscript, and should not be submitted by anyone on their behalf. The principal/corresponding author will be required to submit a Copyright Letter along with the manuscript, on behalf of all the co-authors (if any). The author(s) will confirm that the manuscript (or any part of it) has not been published previously or is not under consideration for publication elsewhere. Furthermore, any illustration, structure or table that has been published elsewhere must be reported, and copyright permission for reproduction must be obtained.

For all online submissions, please provide soft copies of all the materials (main text in MS Word or Tex/LaTeX), figures / illustrations in TIFF, PDF or JPEG, and chemical structures drawn in ChemDraw (CDX) / ISISDraw (TGF) as separate files, while a PDF version of the entire manuscript must also be included, embedded with all the figures / illustrations / tables / chemical structures etc.

It is advisable that the document files related to a manuscript submission should always have the name of the corresponding author as part of the file name, i.e., "Cilli MS text.doc", "Cilli MS Figure 1" *etc.*

It is imperative that before submission, authors should carefully proofread the files for special characters, mathematical symbols, Greek letters, equations, tables, references and images, to ensure that they appear in proper format.

References, figures, tables, chemical structures etc. should be referred to in the text at the appropriate place where they have been first discussed. Figure legends/captions should also be provided.

A successful electronic submission of a manuscript will be followed by a system-generated acknowledgement to the principal/corresponding author. Any queries therein should be addressed to info@benthamscience.org

Conference Proceedings:

For proposals to publish conference proceedings in this journal, please contact us at email: proceedings@benthamscience.org

Editorial Policies:

The editorial policies of Bentham Science Publishers on publication ethics, peer-review, plagiarism, copyrights/ licenses, errata/corrections and article retraction/ withdrawal can be viewed at [Editorial Policy](#)

MANUSCRIPTS PUBLISHED:

The Journal publishes peer reviewed mini-review articles written in English. Single topic/thematic issues may also be considered for publication.

Single Topic Issues:

These peer-reviewed issues will be restricted to invited or uninvited review/mini-review articles. A Single Topic Issue Editor will offer a short perspective and co-ordinate the solicitation of manuscripts between 3-5 (for a mini-thematic issue) to 6-10 (for full-length thematic issue) from leading scientists. Authors interested in editing a single topic issue in an emerging topic of medicinal chemistry may submit their proposal to the Editor-in-Chief at mrmc@benthamscience.org for consideration.

MANUSCRIPT LENGTH:

Full-Length Reviews:

Full-length reviews should be 8000-40000 words excluding figures, structures, photographs, schemes, tables *etc.*

Mini-Reviews:

Mini-reviews should be 3000- 6000 words excluding figures, structures, photographs, schemes, tables *etc.*

Book Reviews:

Publishers are invited to first contact the reviews editor/editor-in-chief stating the title of the e-book, date of publication and e-book summary by email mrmc@benthamscience.org

There is no restriction on the number of figures, tables or additional files e.g. video clips, animation and datasets, that can be included with each article online. Authors should include all relevant supporting data with each article (Refer to Supplementary Material section).

MANUSCRIPT PREPARATION:

The manuscript should be written in English in a clear, direct and active style. All pages must be numbered sequentially, facilitating in the reviewing and editing of the manuscript.

MICROSOFT WORD TEMPLATE:

It is advisable that authors prepare their manuscript using the template available on the Web, which will assist in preparation of the manuscript according to Journal's Format. [Download the Template.](#)

Our contracted service provider [Eureka Science](#) can, if needed, provide professional assistance to authors for the improvement of English language and figures in manuscripts.

MANUSCRIPT SECTIONS FOR PAPERS:

Manuscripts for review articles submitted to the journal may be divided into the following sections:

- Copyright Letter
- Title
- Title Page
- Structured Abstract
- Graphical Abstract
- Keywords

- Text Organization
- Conclusion
- List of Abbreviations (if any)
- Conflict of Interest
- Acknowledgements
- References
- Appendices
- Figures/Illustrations (if any)
- Chemical Structures (if any)
- Tables (if any)
- Supportive/Supplementary Material (if any)

Copyright Letter:

It is mandatory that a signed copyright letter also be submitted along with the manuscript by the author to whom correspondence is to be addressed, delineating the scope of the submitted article declaring the potential competing interests, acknowledging contributions from authors and funding agencies, and certifying that the paper is prepared according to the '*Instructions for Authors*'. All inconsistencies in the text and in the reference section, and any typographical errors must be carefully checked and corrected before the submission of the manuscript. The article should not contain any such material or information that may be unlawful, defamatory, fabricated, plagiarized, or which would, if published, in any way whatsoever, violate the terms and conditions as laid down in the copyright agreement.

The authors acknowledge that the publishers have the legal right to take appropriate action against the authors for any such violation of the terms and conditions as laid down in the copyright agreement. [Download the Copyright letter](#)

Title:

The title of the article should be precise and brief and must not be more than 120 characters. Authors should avoid the use of non-standard abbreviations. The title must be written in title case except for articles, conjunctions and prepositions.

Authors should also provide a short 'running title'. Title, running title, byline, correspondent footnote and keywords should be written as presented in original manuscripts.

Title Page:

Title page should include paper title, author(s) full name and affiliation, corresponding author(s) names complete affiliation/address, along with phone, fax and email.

Structured Abstract:

The abstract of an article should be its clear, concise and accurate summary, having no more than 250 words, and including the explicit sub-headings (as in-line or run-in headings in bold). Use of abbreviations should be avoided and the references should not be cited in the abstract. Ideally, each abstract should include the following sub-headings, but these may vary according to requirements of the article.

- Background
- Objective
- Method
- Results
- Conclusion

Graphical Abstract:

A graphic should be included when possible with each manuscript for use in the Table of Contents (TOC). This must be submitted separately as an electronic file (preferred file types are EPS, PDF, TIFF, Microsoft Word, PowerPoint and CDX etc.). A graphical abstract, not exceeding 30 words along with the illustration, helps to summarize the contents of the manuscript in a concise pictorial form.

It is meant as an aid for the rapid viewing of the journals' contents and to help capture the readers' attention. The graphical abstract may feature a key structure, reaction, equation, etc. that the manuscript elucidates upon. It will be listed along with the manuscript title, authors' names and affiliations in the contents page, typeset within an area of 5 cm by 17 cm, but it will not appear in the article PDF file or in print.

Graphical Abstracts should be submitted as a separate file (must clearly mention graphical abstract within the file) online *via* Bentham's Content Management System by selecting the option "supplementary material".

Keywords:

Provide 6 to 8 keywords in alphabetical order.

Text Organization:

The main text should begin on a separate page and should be divided into separate sections. The manuscript should be divided into title page, abstract and the main text. The text may be subdivided further according to the areas to be discussed, which should be followed by the Acknowledgements and Reference sections. The Review Article should mention any previous important recent and old reviews in the field and contain a comprehensive discussion starting with the general background of the field. It should then go on to discuss the salient features of recent developments. The authors should avoid presenting material which has already been published in a previous review. The authors are advised to present and discuss their observations in brief. The manuscript style must be uniform throughout the text and 10 pt Times New Roman fonts should be used. The full term for an abbreviation should precede its first appearance in the text unless it is a standard unit of measurement. The reference numbers should be given in square brackets in the text. Italics should be used for Binomial names of organisms (Genus and Species), for emphasis and for unfamiliar words or phrases. Non-assimilated words from Latin or other languages should also be italicized e.g. *per se*, *et al.* etc.

Authentication of Cell Lines:

The NIH acknowledges the misidentification and/or cross-contamination of cell cultures e.g. HeLa cells being used in a research study as a serious problem. In order to ensure validation of the work and proper utilization of resources.

It is a prerequisite that correct reagents be used in studies dealing with established human (tumor) cell lines that have been cultured for more than 4 years up to the date of submission of the manuscript. Cell lines such as short-term cultures of human tumors, murine cell lines (as a catalog of DNA profiles is not yet available) and tumor cell lines established in the course of the study that is being submitted are presently exempt from this rule. To minimize the risk of working with misidentified and/or contaminated cell lines, tests such as isoenzyme analysis, karyotyping/cytogenetic analysis and, more recently, molecular techniques of DNA profiling may be carried out to authenticate cell cultures. These tests may help confirm or establish the identify profile for a cell line. Bentham Science recommends that all cell lines be authenticated prior to submitting a paper for review. Authors are therefore required to provide authentication of the origin and identity of the cells by performing cell profiling either in their own laboratory or by outsourcing an approved laboratory or cell bank.

Authentication is required when a new line is established or acquired, before freezing a cell line, if the performance of the line is not consistent or results are unexpected, if using more than one cell line, and before publication of the study.

The cell lines profile should be cross-checked with the profile of the donor tissue of other continuous cell lines such as provided by the authentic data bank such as www.dsmz.de/fp/cgi-bin/str.html, ATCC® etc.

Greek Symbols and Special Characters:

Greek symbols and special characters often undergo formatting changes and get corrupted or lost during preparation of manuscript for publication. To ensure that all special characters used are embedded in the text, these special characters should be inserted as a symbol but should not be a result of any format styling (*Symbol* font face) otherwise they will be lost during conversion to PDF/XML.

Authors are encouraged to consult reporting guidelines. These guidelines provide a set of recommendations comprising a list of items relevant to their specific research design. Chemical equations, chemical names, mathematical usage, unit of measurements, chemical and physical quantity & units must conform to SI and Chemical Abstracts or IUPAC.

All kinds of measurements should be reported only in International System of Units (SI).

Conclusion:

A small paragraph summarizing the contents of the article, presenting the final outcome of the research or proposing further study on the subject, may be given at the end of the article under the Conclusion section.

List of Abbreviations:

If abbreviations are used in the text either they should be defined in the text where first used, or a list of abbreviations can be provided.

Conflict of Interest:

Financial contributions to the work being reported must be clearly acknowledged, as should any potential conflict of interest under the heading 'Conflict of Interest'. Authors must list the source(s) of funding for the study, for each author, and for the manuscript preparation.

Acknowledgements:

All individuals listed as authors must have contributed substantially to the design, performance, analysis, or reporting of the work and are required to indicate their specific contribution. Anyone (individual/company/institution) who has substantially contributed to the study for important intellectual content, or who was involved in the article's drafting the manuscript or revising must also be acknowledged.

Guest or honorary authorship based solely on position (e.g. research supervisor, departmental head) is discouraged.

References:

References must be listed in the ACS Style only. All references should be numbered sequentially [in square brackets] in the text and listed in the same numerical order in the reference section. The reference numbers must be finalized and the bibliography must be fully formatted before submission.

See below few examples of references listed in the ACS Style:

Journal Reference:

- [1] Bard, M.; Woods, R.A.; Bartón, D.H.; Corrie, J.E.; Widdowson, D.A. Sterol mutants of *Saccharomyces cerevisiae*: chromatographic analyses. *Lipids*, 1977,12(8), 645-654.
- [2] Zhang, W.; Brombosz, S.M.; Mendoza, J.L.; Moore, J.S. A high-yield, one-step synthesis of o-phenylene ethynylene cyclic trimer *via* precipitation-driven alkyne metathesis. *J. Org. Chem.*, 2005, 70, 10198-10201.

Book Reference:

- [3] Crabtree, R.H. *The Organometallic Chemistry of the Transition Metals*, 3rd ed.; Wiley & Sons: New York, 2001.

Book Chapter Reference:

- [4] Wheeler, D.M.S.; Wheeler, M.M. Stereoselective Syntheses of Doxorubicin and Related Compounds In: *Studies in Natural Products Chemistry*; Atta-ur-Rahman, Ed. Elsevier Science B. V: Amsterdam, 1994; Vol. 14, pp. 3-46.

Conference Proceedings:

- [5] Jakeman, D.L.; Withers, S.G.E. In: *Carbohydrate Bioengineering: Interdisciplinary Approaches* In: Proceedings of the 4th Carbohydrate Bioengineering Meeting, Stockholm, Sweden, June 10-13, 2001; Teeri, T.T.; Svensson, B.; Gilbert, H.J.; Feizi, T., Eds. Royal Society of Chemistry: Cambridge, UK, 2002; pp. 3-8.

URL (WebPage):

- [6] National Library of Medicine. Specialized Information Services: Toxicology and Environmental Health. sis.nlm.nih.gov/Tox/ToxMain.html (Accessed May 23, 2004).

Patent:

- [7] Hoch, J.A.; Huang, S. Screening methods for the identification of novel antibiotics. U.S. Patent 6,043,045, March 28, 2000.

Thesis:

- [8] Mackel, H. *Capturing the Spectra of Silicon Solar Cells*. PhD Thesis, The Australian National University: Canberra, December 2004.

E-citations:

- [9] Citations for articles/material published exclusively online or in open access (free-to-view), must contain the exact Web addresses (URLs) at the end of the reference(s), except those posted on an author's Web site unless editorially essential, e.g. 'Reference: Available from: URL'.

Some important points to remember:

- All references must be complete and accurate.
- All authors must be cited and there should be no use of the phrase *et al.*
- Online citations should include the date of access.
- Journal abbreviations should follow the *Index Medicus/MEDLINE*.
- Special care should be taken of the punctuation convention as described in the above-mentioned examples.
- Superscript in the in-text citations and reference section should be avoided.
- Abstracts, unpublished data and personal communications (which can only be included if prior permission has been obtained) should not be given in the reference section but they may be mentioned in the text and details provided as footnotes.
- The authors are encouraged to use a recent version of EndNote (version 5 and above) or Reference Manager (version 10) when formatting their reference list, as this allows references to be automatically extracted.

Appendices:

In case there is a need to present lengthy, but essential methodological details, appendices must be used, which can be a part of the article. An appendix must not exceed three pages (Times New Roman, 12 point fonts, 900 max. words per page). The information should be provided in a condensed form, ruling out the need of full sentences. A single appendix should be titled APPENDIX, while more than one can be titled APPENDIX A, APPENDIX B, and so on.

Figures/Illustrations (if any):

All authors must strictly follow the guidelines below for preparing illustrations for publication in *Mini-Reviews in Medicinal Chemistry*. If the figures are found to be sub-standard, then the manuscripts will be rejected and the authors offered the option of figure improvement professionally by Eureka Science. The costs for such improvement will be charged to the authors.

Illustrations should be provided as separate files, embedded in the text file, and must be numbered consecutively in the order of their appearance. Each figure should include only a single illustration which should be cropped to minimize the amount of space occupied by the illustration.

If a figure is in separate parts, all parts of the figure must be provided in a single composite illustration file.

Photographs should be provided with a scale bar if appropriate, as well as high-resolution component files.

Scaling/Resolution:

Line Art image type is normally an image based on lines and text. It does not contain tonal or shaded areas. The preferred file format should be TIFF or EPS, with the color mode being Monochrome 1-bit or RGB, in a resolution of 900-1200 dpi.

Halftone image type is a continuous tone photograph containing no text. It should have the preferred file format TIFF, with color mode being RGB or Grayscale, in a resolution of 300 dpi.

Combination image type is an image containing halftone, text or line art elements. It should have the preferred file format TIFF, with color mode being RGB or Grayscale, in a resolution of 500-900 dpi.

Formats:

For illustrations, the following file formats are acceptable:

- Illustrator
- EPS (preferred format for diagrams)
- PDF (also especially suitable for diagrams)
- PNG (preferred format for photos or images)
- Microsoft Word (version 5 and above; figures must be a single page)
- PowerPoint (figures must be a single page)
- TIFF

- JPEG (conversion should be done using the original file)
- BMP
- CDX (ChemDraw)
- TGF (ISISDraw)

Bentham Science does not process figures submitted in GIF format.

If the large size of TIFF or EPS figures acts as an obstacle to online submission, authors may find that conversion to JPEG format before submission results in significantly reduced file size and upload time, while retaining acceptable quality. JPEG is a 'lossy' format, however. In order to maintain acceptable image quality, it is recommended that JPEG files are saved at High or Maximum quality.

Files should not be compressed with tools such as Zipit or Stuffit prior to submission as these tools will in any case produce negligible file-size savings for JPEGs and TIFFs, which are already compressed.

Please do not:

1. Supply embedded graphics in your word processor (spreadsheet, presentation) document.
2. Supply files that are optimized for screen use (like GIF, BMP, PICT, WPG); the resolution is too low.
3. Supply files that are too low in resolution.
4. Submit graphics that are disproportionately large for the content.

Image Conversion Tools:

There are many software packages, many of them freeware or shareware, capable of converting to and from different graphics formats, including PNG.

Good general tools for image conversion include GraphicConverter on the Macintosh, PaintShop Pro, for Windows, and ImageMagick, which is available on Macintosh, Windows and UNIX platforms.

Note that bitmap images (*e.g.* screenshots) should not be converted to EPS, since this will result in a much larger file size than the equivalent JPEG, TIFF, PNG or BMP, with no increase in quality.

EPS should only be used for images produced by vector-drawing applications such as Adobe Illustrator or CorelDraw. Most vector-drawing applications can be saved in, or exported as, EPS format. In case the images have been originally prepared in an Office application, such as Word or PowerPoint, then the original Office files should be directly uploaded to the site, instead of being converted to JPEG or another format that may be of low quality.

Color Figures/Illustrations:

- Color figures publication in the journal: The cost for each individual page of color figures is US\$ 995.
- Color figures should be supplied in CMYK not RGB colors.

Chemical Structures:

Chemical structures **MUST** be prepared in ChemDraw/CDX and provided as separate file.

Structure Drawing Preferences:

[As according to the ACS style sheet]

Drawing Settings:

Chain angle	120°
Bond spacing	18% of width
Fixed length	14.4 pt (0.500cm, 0.2in)
Bold width	2.0 pt (0.071cm, 0.0278in)
Line width	0.6 pt (0.021cm, 0.0084in)
Margin width	1.6 pt (0.096cm)
Hash spacing	2.5 pt (0.088cm, 0.0347in)

Text settings:

Font	Times New Roman
Size	8 pt

Under the Preference Choose:

Units	points
Tolerances	3 pixels

Under Page Setup Use:

Paper	US letter
Scale	100%

Tables:

- Data Tables should be submitted in Microsoft Word table format.
- Each table should include a title/caption being explanatory in itself with respect to the details discussed in the table. Detailed legends may then follow.
- Table number in bold font *i.e.* Table 1, should follow a title. The title should be in small case with the first letter in caps. A full stop should be placed at the end of the title.
- Tables should be embedded in the text exactly according to their appropriate placement in the submitted manuscript.
- Columns and rows of data should be made visibly distinct by ensuring that the borders of each cell are displayed as black lines.
- Tables should be numbered in Arabic numerals sequentially in order of their citation in the body of the text.
- If a reference is cited in both the table and text, please insert a lettered footnote in the table to refer to the numbered reference in the text.
- Tabular data provided as additional files can be submitted as an Excel spreadsheet.

Supportive/Supplementary Material:

We do encourage to append supportive material, for example a PowerPoint file containing a talk about the study, a PowerPoint file containing additional screenshots, a Word, RTF, or PDF document showing the original instrument(s) used, a video, or the original data (SAS/SPSS files, Excel files, Access Db files etc.) provided it is inevitable or endorsed by the journal's Editor.

Published/reproduced material should not be included unless you have obtained written permission from the copyright holder, which must be forwarded to the Editorial Office in case of acceptance of your article for publication.

Supportive/Supplementary material intended for publication must be numbered and referred to in the manuscript but should not be a part of the submitted paper. In-text citations as well as a section with the heading "Supportive/Supplementary Material" before the "References" section should be provided. Here, list all Supportive/Supplementary Material and include a brief caption line for each file describing its contents.

Any additional files will be linked to the final published article in the form supplied by the author, but will not be displayed within the paper. They will be made available in exactly the same form as originally provided only on our Web site. Please also make sure that each additional file is a single table, figure or movie (please do not upload linked worksheets or PDF files larger than one sheet). Supportive/ Supplementary material must be provided in a single zipped file not larger than 4 MB.

Authors must clearly indicate if these files are not for publication but meant for the reviewers'/editors' perusal only.

PERMISSION FOR REPRODUCTION:

Bentham Science has collaborated with the Copyright Clearance Center to meet our customer's licensing, besides rights & permission needs.

The Copyright Clearance Center's RightsLink[®] service makes it faster and easier to secure permission from Bentham Science's journal titles. Simply visit [Journals by Title](#) and locate the desired content. Then go to the article's abstract and click on "Rights and Permissions" to open the RightsLink's page. If you are unable to locate the content you wish to use or you are unable to secure the rights you are seeking, please e-mail us at permissions@benthamscience.org

Published/reproduced material should not be included unless written permission has been obtained from the copyright holder, which should be forwarded to the Editorial Office in case of acceptance of the article for publication.

AUTHORS AND INSTITUTIONAL AFFILIATIONS:

The names of the authors should be provided according to the previous citations or as the authors would want them to be published along with the institutional affiliations, current address, telephone, cell & fax numbers and the email address. Email address must be provided with an asterisk in front of the name of the principal author. The corresponding author(s) should be designated and their complete address, business telephone and fax numbers and e-mail address must be stated to receive correspondence and galley proofs.

REVIEWING AND PROMPTNESS OF PUBLICATION:

All manuscripts submitted for publication will be immediately subjected to peer-reviewing, usually in consultation with the members of the Editorial Advisory Board and a number of external referees. Authors may, however, provide in their Copyright Letter the contact details (including e-mail addresses) of four potential peer reviewers for their paper. Any peer reviewers suggested should not have recently published with any of the authors of the submitted manuscript and should not be members of the same research institution.

All peer-reviewing will be conducted *via* the Internet to facilitate rapid reviewing of the submitted manuscripts. Every possible effort will be made to assess the manuscripts quickly with the decision being conveyed to the authors in due course.

PAGE CHARGES:

No page charges will be levied to authors for the publication of their article.

LANGUAGE AND EDITING:

Manuscripts submitted containing language inconsistencies will not be published. Authors must seek professional assistance for correction of grammatical, scientific and typographical errors. Professional team available at Eureka Science may assist you in the English language editing of your article. Please contact Eureka Science for a language editing quote at e-mail: info@eureka-science.com stating the total number of words of the article to be edited.

언어 및 편집:

영문 오타가 많은 원고는 출판되지 않을 것입니다. 영문 오타를 없애겠다는 조건으로 받은 원고는 영어 편집 전문회사인 유럽 공동 기술개발 기구로부터 가격 견적서가 보내 질 것입니다. 영어 작문에 어려움이 있는 비영어권 국가의 저자들은 원고를 학술지에 제출하기 전에 영어 편집회사와 접촉할 것을 권합니다. 영어 편집 견적서를 받기 위해서 교정될 원고의 단어수를 적은 메일을 유럽 공동 기술개발 기구 메일인 info@eureka-science.com 로 보내시기 바랍니다.

语言和编辑:

含有很多英文印刷错误的提交稿将不予发表。接受发表的稿件其英文写作应是正确的；专业的语言编辑公司（尤里卡科学，可对稿件的英文润色提供报价。建议非英语国家且英文写作欠佳的作者在投稿前先与语言编辑公司联系。请与尤里卡科学联系 info@eureka-science.com。

EDITION ET LANGUE:

Les manuscrits soumis avec plusieurs erreurs typographiques en Anglais ne seront pas publiés en l'état. Les manuscrits sont acceptés pour publication à la condition que l'anglais utilisé soit corrigé après la soumission et seront envoyés pour examen à Eureka Science, une société d'édition de langue professionnelle. Les auteurs en provenance de pays où la langue est différente de l'anglais et qui ont de médiocres compétences en anglais écrit, sont priés de contacter la société d'édition de langue avant de soumettre leur manuscrit à la revue. Merci de contacter Eureka Science à info@eureka-science.com pour un devis en indiquant le nombre total de mot de l'article à éditer.

PROOF CORRECTIONS:

Authors will receive page proofs of their accepted paper before publications. To avoid delays in publication, proofs should be checked immediately for typographical errors and returned within 48 hours. Major changes are not acceptable at the proof stage.

If unable to send corrections within 48 hours due to some reason, the author(s) must at least send an acknowledgement on receiving the galley proofs or the article will be published exactly as received and the publishers will not be responsible for any error occurring in the published manuscript in this regard.

The corresponding author will be solely responsible for ensuring that the revised version of the manuscript incorporating all the submitted corrections receives the approval of all the co-authors of the manuscript.

REPRINTS:

Printed reprints and e-prints may be ordered from the Publisher prior to publication of the article. First named authors may also order a personal online subscription of the journal at 50% off the normal subscription rate by contacting the subscription department at e-mail: subscriptions@benthamscience.org.

OPEN ACCESS PLUS:

Bentham Science also offers authors the choice of “Open Access Plus” publication of articles at a fee of US\$ 2,900 per article. This paid service allows for articles to be disseminated to a much wider audience, on the terms of the Creative Commons CC BY-NC-ND (Attribution-NonCommercial-NoDerivs) Licence (<http://creativecommons.org/licenses/by-nc-nd/4.0/>). Authors are asked to indicate whether or not they wish to pay to have their article made more widely available on this “Open Access Plus” basis. Where an author does not opt-in to this paid service, then the author’s article will be published only on Bentham Science’s standard subscription-based access, at no additional cost to the author.

Authors who select the “Quick Track” publication option (see below) and also wish to have their article made available on an “Open Access Plus” basis will be entitled to a 50% discount on the “Open Access Plus” publication fee.

For more information please contact us at e-mail: openaccess@benthamscience.org

FEATURED ARTICLE:

Authors may opt to publicize their article(s) published with Bentham Science by highlighting their title(s) both at the journal's Homepage and the issue Contents page at a cost of US\$ 600.

REVIEWING AND PROMPTNESS OF PUBLICATION:

All manuscripts submitted for publication will be immediately subjected to peer-reviewing, usually in consultation with the members of the Editorial Advisory Board and a number of external referees. Authors may, however, provide in their Copyright Letter the contact details (including e-mail addresses) of four potential peer reviewers for their paper. Any peer reviewers suggested should not have recently published with any of the authors of the submitted manuscript and should not be members of the same research institution.

All peer-reviewing will be conducted *via* the Internet to facilitate rapid reviewing of the submitted manuscripts. Every possible effort will be made to assess the manuscripts quickly with the decision being conveyed to the authors in due course.

QUICK TRACK Publication:

For this journal an optional fast publication fee-based service called QUICK TRACK is available to authors for their submitted manuscripts.

QUICK TRACK allows online publication within 2 weeks of receipt of the final approved galley proofs from the authors. Similarly the manuscript can be published in the next forthcoming PRINT issue of the journal. The total publication time, from date of first receipt of manuscript to its online publication is 10 weeks, subject to its acceptance by the referees and modification (if any) by the authors within one week.

Authors who have availed QUICK TRACK services in a BSP journal will be entitled for an exclusive 30% discount if they again wish to avail the same services in any Bentham journal.

For more information please contact the Editorial Office by e-mail at mrmc@benthamscience.org.

COPYRIGHT:

Authors who publish in Bentham Science print & online journals will transfer copyright to their work to *Bentham Science Publishers*. Submission of a manuscript to the respective journals implies that all authors have read and agreed to the content of the Copyright Letter or the Terms and Conditions. It is a condition of publication that manuscripts submitted to this journal have not been published and will not be simultaneously submitted or published elsewhere.

Plagiarism is strictly forbidden, and by submitting the article for publication the authors agree that the publishers have the legal right to take appropriate action against the authors, if plagiarism or fabricated information is discovered. By submitting a manuscript the authors agree that the copyright of their article is transferred to the publishers if and when the article is accepted for publication. Once submitted to the journal, the author will not withdraw their manuscript at any stage prior to publication.

SELF-ARCHIVING

By signing the Copyright Letter the authors retain the rights of self-archiving. Following are the important features of self-archiving policy of Bentham Science journals:

1. Authors can deposit the first draft of a submitted article on their personal websites, their institution's repositories or any non-commercial repository for personal use, internal institutional use or for permitted scholarly posting.
2. Authors may deposit the ACCEPTED VERSION of the peer-reviewed article on their personal websites, their institution's repository or any non-commercial repository such as PMC, arXiv after 12 MONTHS of publication on the journal website. In addition, an acknowledgement must be given to the original source of publication and a link should be inserted to the published article on the journal's/publisher's website.
3. If the research is funded by NIH, Wellcome Trust or any other Open Access Mandate, authors are allowed the archiving of published version of manuscripts in an institutional repository after the mandatory embargo period. Authors should first contact the Editorial Office of the journal for information about depositing a copy of the manuscript to a repository. Consistent with the copyright agreement, Bentham Science does not allow archiving of FINAL PUBLISHED VERSION of manuscripts.
4. The link to the original source of publication should be provided by inserting the DOI number of the article in the following sentence: "The published manuscript is available at EurekaSelect via [http://www.eurekaselect.com/openurl/content.php?genre=article&doi= \[insert DOI\]](http://www.eurekaselect.com/openurl/content.php?genre=article&doi=[insert DOI])
5. There is no embargo on the archiving of articles published under the OPEN ACCESS PLUS category. Authors are allowed deposition of such articles on institutional, non-commercial repositories and personal websites immediately after publication on the journal website.

PLAGIARISM PREVENTION:

Bentham Science Publishers uses the iThenticate software to detect instances of overlapping and similar text in submitted manuscripts. iThenticate software checks content against a database of periodicals, the Internet, and a comprehensive article database. It generates a similarity report, highlighting the percentage overlap between the uploaded article and the published material. Any instance of content overlap is further scrutinized for suspected plagiarism according to the publisher's Editorial Policies.

Bentham Science allows an overall similarity of 20% for a manuscript to be considered for publication. The similarity percentage is further checked keeping the following important points in view:

Low Text Similarity:

The text of every submitted manuscript is checked using the Content Tracking mode in iThenticate. The Content Tracking mode ensures that manuscripts with an overall low percentage similarity (but which may have a higher similarity from a single source) are not overlooked. The acceptable limit for similarity of text from asingle source is 5%. If the similarity level is above 5%, the manuscript is returned to the author for paraphrasing the text and citing the original source of the copied material.

It is important to mention that the text taken from different sources with an overall low similarity percentage will be considered as a plagiarized content if the majority of the article is a combination of copied material.

High Text Similarity:

There may be some manuscripts with an overall low similarity percentage, but a higher percentage from a single source. A manuscript may have less than 20% overall similarity but there may be 15 % similar text taken from a single article. The similarity index in such cases is higher than the approved limit for a single source. Authors are advised to thoroughly rephrase the similar text and properly cite the original source to avoid plagiarism and copyright violation.

Types of Plagiarism:

We all know that scholarly manuscripts are written after thorough review of previously published articles. It is therefore not easy to draw a clear boundary between legitimate representation and plagiarism. However, the following important features can assist in identifying different kinds of plagiarized content. These are:

- Reproduction of others words, sentences, ideas or findings as one's own without proper acknowledgement.
- Text recycling, also known as self-plagiarism. It is an author's use of a previous publication in another paper without proper citation and acknowledgement of the original source.
- Paraphrasing poorly: Copying complete paragraphs and modifying a few words without changing the structure of original sentences or changing the sentence structure but not the words.
- Verbatim copying of text without putting quotation marks and not acknowledging the work of the original author.
- Properly citing a work but poorly paraphrasing the original text is considered as unintentional plagiarism. Similarly, manuscripts with language somewhere between paraphrasing and quoting are not acceptable. Authors should either paraphrase properly or quote and in both cases, cite the original source.
- Higher similarity in the abstract, introduction, materials and methods, and discussion and conclusion sections indicates that the manuscript may contain plagiarized text. Authors can easily explain these parts of the manuscript in many ways. However, technical terms and sometimes standard procedures cannot be rephrased; therefore Editors must review these sections carefully before making a decision.

Plagiarism in Published Manuscripts:

Published manuscripts which are found to contain plagiarized text are retracted from the journal website after careful investigation and approval by the Editor-in-Chief of the journal. A 'Retraction Note' as well as a link to the original article is published on the electronic version of the plagiarized manuscript and an addendum with retraction notification in the journal concerned.

E-PUB AHEAD OF SCHEDULE:

Bentham Science Publishers are pleased to offer electronic publication of accepted papers prior to scheduled publication. These peer-reviewed papers can be cited using the date of access and the unique DOI number. Any final changes in manuscripts will be made at the time of print publication and will be reflected in the final electronic version of the issue. Articles ahead of schedule may be ordered by pay-per-view at the relevant links by each article stated *via* the E-Pub Ahead of Schedule

Disclaimer:

Articles appearing in E-Pub Ahead-of-Schedule sections have been peer-reviewed and accepted for publication in this journal and posted online before scheduled publication.

Articles appearing here may contain statements, opinions, and information that have errors in facts, figures, or interpretation. Accordingly, *Bentham Science Publishers*, the editors and authors and their respective employees are not responsible or liable for the use of any such inaccurate or misleading data, opinion or information contained of articles in the E-Pub Ahead-of-Schedule.

ADDENDUM B

Author guidelines: Drug Research

Drug Research accepts manuscripts in English covering drug research and development as well as the latest scientific findings on substances and/or products already marketed. The journal accepts manuscripts from the following areas: analytics, bioavailability, biochemistry, chemistry, clinical pharmacology, drug interactions, efficacy testing, experimental pharmacology, pharmacodynamics, pharmacokinetics, teratology, toxicology as well as questions relating to drug formulation, mathematical and statistical methods for the evaluation of results from industrial investigations as well as clinical trials. Translational medicine aspects are key features of the journal. Please note that bioequivalence studies will no longer be accepted. When submitted, manuscripts must not have been published elsewhere or be under simultaneous consideration by another journal. The aim of the journal is to disseminate new and reliable experimental data from across the field of drug research to researchers, scientists and doctors worldwide. N.B.: Incorrect English can result in the immediate rejection of your manuscript whereas correct English will help a speedy publication process. It is in your own interest to ensure that your paper has been read by a native speaker of English; alternatively, you should use a copy-editing service like “American Journal Experts” if you have concerns about the English in your manuscript.

These types of manuscripts will be accepted:

Original Articles Reviews Commentaries Controversies Opinion Papers Short Communications Letters Clinical Trials.

The Journal supports trial registration. All trials reported must be registered at an official registry recognised by the International Committee of Medical Journal Editors, such as ClinicalTrials.gov (www.clinicaltrials.gov) or any of the primary registries on the World Health Organization’s International Clinical Trial Registry Platform (www.who.int/ictrp).
Conflict of Interest Please state the conflicts of interest of all authors. During the online submission process, you will be asked to declare your conflicts of interest. Failure to do so or an incomplete declaration may result in non-publication.

Ethics

The journal is very concerned about ethical standards. Please provide proof that the terms of the latest version of the “World Medical Association Declaration of Helsinki - Ethical Principles for Medical Research Involving Human Subjects” have been adhered to or provide approval of your local ethics committee. The same applies to animals. Please provide proof that experiments involving animals were carried out in compliance with the “Guide for the Care and Use of Laboratory animals” published by the National Academy of Sciences or else provide approval of your local ethics committee.

Manuscript Submission

All manuscripts must be submitted exclusively via online submission at <http://mc.manuscriptcentral.com/drugres>

Submissions of hardcopy manuscripts will not be accepted. Please include tables and figures as separate files, they should not be integrated into the main document, but a list with the legends of the figures and tables should be included there. Provide graphic files with sufficient resolution: coloured and black-white bitmaps: 300 dpi; diagrams and line drawings: 600 dpi minimum. Figures should be serially numbered with Arabic numerals. There should be a clear mark in the manuscript indicating where the figure should be inserted. Authors are responsible for the correctness of the manuscripts and the list of references. All measurements must be in Systeme International (SI) units.

A. Original Articles

Original papers should deal with investigations and results of high scientific value which have not been published previously.

1. Original papers should not exceed 6 printed pages, i.e. 15 typewritten double-spaced manuscript pages of 30 lines of 60 letters each, including references, tables, figures and legends. Please do not use more than one blank space between words and sentences.

2. Preparation of manuscripts

Authors are asked to follow the outline set below: Page 1: a) title, b) short running title (limit: 40 characters), c) name of the author (no titles or academic grades) and address of the institute(s) where the investigations have been carried out. Should the address of the author at the time of publication differ from the one stated in the paper, the current address should be stated in a footnote, d) complete mailing address of corresponding author including telephone and telefax numbers and e-mail addresses.

Page 2: a) a concise and comprehensive abstract detailing the key elements of the submitted paper (e.g. the background, the methods, the results and the major conclusion).

The abstract should contain no more than 250 words with no abbreviations, b) keywords (3–6 without repeating words in the title): Page 3 and onwards: a) introduction also indicating the aim of the study, b) materials and methods, c) results: double presentation of data in the form of text, tables or figures should be avoided, d) discussion and conclusions, e) list of references, f) legends of tables and figures. Do include your acknowledgements in the main document. 3. References a) Text: Citations and references should be numbered consecutively using square brackets in the order in which they are cited in the text, followed by any in tables or legends. Please do not number references under alphabetical order of authors. Do not use footnotes and hyperlinks. If authors are mentioned in the text, only the first author should be given followed by “*et al.*” whenever the reference has three or more authors. Example: “ ...protein concentrations were determined according to Lowry *et al.* [1].” b) List of References: References should be given as plain text. Do not use fields in MS Word, as these are difficult to process later. The references should be listed in numbered order according to the sequence they appear in the text. Preferably, all authors or groups of authors of each publication should be mentioned.

The name of the author(s) should be followed by the full title of the paper, name of the journal in which it has been published (abbreviations according to “Index Medicus”), year of publication, volume, first and last page. Abstracts and supplements have to be indicated. Chapters from books have to be cited as follows: author(s), title of chapter, title of book, editor(s), place of publication, publisher, year of publication, first and last page of the chapter. See also the recommendations of the International Committee of Medical Journal Editors (www.icmje.org). Examples: 1 Park HY, Lim H, Pyo H, Kwon YS. Downregulation of matrix metalloproteinase-13 by the root extract of *Caythula officinalis* Kuan and its constituents in IL-1 β -treated chondrocytes. *Planta Med* 2011; 75: 1528–1530 2 Kerner W, Pfeiffer EF. The artificial pancreas. In: Samols E (ed). *The endocrine pancreas*. New York: Raven Press, 1991: 441–456.

B. Reviews

Reviews deal with previous research on a certain topic and serve to summarize current findings on the topic so far. The structure of the review will vary from an original paper according to the nature of the review, but please adhere to the guidelines concerning references. Please aim at no more than 20 type-written pages and 100 references.

C. Commentaries

They usually follow the article that they discuss, have no special structure and are usually invited. They could also deal with an actual topic such as pivotal new scientific findings in the field. Commentaries should not exceed 6 type-written pages, with a maximum of 20 references. Please adhere to the reference guidelines outlined above.

D. Opinion Papers, Controversies

The structure of these papers will vary from an original paper according to the nature of the topic and argument. Opinion papers present the authors' comprehensive views on current developments in the area and discuss perspectives for the future. Controversies describe a relevant ongoing scientific dispute from an unbiased point of view. They should not exceed 10 type-written pages, with a maximum of 40 references. Please adhere to the guidelines concerning references outlined above.

E. Short Communications

Short Communications are completed projects of smaller scope and should contain new clinical and experimental data of immediate interest. 1. They should not exceed 2 printed pages (i.e. 6 type-written double-spaced pages in manuscript 30 lines of 60 letters each) and may include 1 table and 1 figure. The list of references at the end of the paper should not exceed 10 citations. 2. The guidelines for the structure of Short Communications are the same as for Original Articles with the following exceptions: a) no keywords and b) no titles of the papers in the list of references.

F. Letters

This section has been introduced to encourage authors to engage in a free exchange of ideas. The opinions presented do not necessarily reflect the opinions of the Editors.

Page Charges

The publisher will impose a page charge of 160 € per printed page (including 19% VAT) starting with the tenth page.

Reproduction of Color Figures

The journal's fee for color reproduction amounts to € 440 for the first color figure and € 80 for any further figure (including 19% VAT).

Proofs and Reprints as PDF File Galley proofs will be sent to the corresponding author as a PDF file. At this stage of the production process, only minor corrections (typos, obvious errors in the production process) are accepted. All other alterations will trigger a de-novo submission. The corresponding author receives a PDF file of the published article free of charge.

Copyright

The publisher holds the copyright to all material appearing in the journal. A Copyright Transfer Agreement will be sent to the corresponding author together with the galley proofs. The agreement must be completed and returned to the publishers before the article can be published. If material taken from foreign sources (including figures, etc.) is included in a manuscript submitted to the Journal it must be indicated as such by citation of the original source and, whenever necessary, permission for reproduction must be obtained from the respective publishing company.

Editor-in-Chief: Martin Wehling, MD Professor of Medicine Institute of Experimental and Clinical Pharmacology and Toxicology Medical Faculty Mannheim University of Heidelberg Maybachstr. 14 68169 Mannheim Germany E-mail: drugresearch@thieme.de